



Fakultät für Medizin

Institut für Strahlenbiologie

Characterisation of murine mesenchymal stem cells during ageing and radiation exposure

Yashodhara Ingawale

Vollständiger Abdruck der von der Fakultät für Medizin der Technischen Universität München zur Erlangung des akademischen Grades eines

Doctor of Philosophy (Ph.D.)

genehmigten Dissertation.

Vorsitzende/r: Prof. Dr. Claus Zimmer

Betreuer/in: Prof. Dr. Michael J. Atkinson

Prüfer der Dissertation:

1. Prof. Dr. Peter J. Nelson
2. Priv.-Doz. Dr. Natalia S. Pellegata

Die Dissertation wurde am 03.06.2016 bei der Fakultät für Medizin der Technischen Universität München eingereicht und durch die Fakultät für Medizin am 12.08.2016 angenommen.

Contents

1	Abstract	5
2	Introduction	7
2.1	Ionizing radiation, stem cells and therapeutic consequences	7
2.2	Stem cells	7
2.2.1	Factors regulating stemness properties	9
2.2.2	Stem cell therapy	10
2.3	Mesenchymal stem cells	11
2.3.1	History and origin	11
2.3.2	Criteria used to characterise the MSCs	12
2.3.3	Functional assays to characterise the MSCs	14
2.3.4	Transcriptional control and phenotypical markers of MSC differentiation	14
2.3.5	Functions of MSCs	15
2.3.6	Therapeutic uses and clinical applications of MSCs	16
2.3.7	Risks and challenges involved in the use of MSCs for therapeutic purposes	16
2.4	Retinoblastoma gene and its haploinsufficiency	18
2.5	Ionizing radiation	18
2.5.1	Effect of ionizing radiation on biological systems	19
2.6	Stem cells and ionizing radiation	20
2.6.1	Possible harmful effects of ionizing radiation on MSCs	21
2.7	Hypothesis	22
3	Materials	24
3.1	Mice	24
3.2	Cell culture	24
3.2.1	Standard media and supplements for MSC culturing and differentiation	24
3.2.2	Medium and serum mixtures for testing mMSC growth	24
3.2.3	Cell lines	25
3.3	Enzymes	25
3.4	Antibodies and Isotype Controls	26
3.5	Solutions and buffers	27
3.6	Chemicals and reagents	28
3.7	Consumables	31
3.8	Equipment	32

3.9	Commercially available kits	34
3.10	Molecular weight and length standards	34
3.11	PCR array	35
3.12	Microbiological work	35
3.13	Calibrator cDNA and reference DNA	35
3.14	Software	35
3.15	Primers	36
3.15.1	Genotyping	36
3.15.2	Real-Time PCR	36
4	Methods	40
4.1	Mice	40
4.1.1	FVB/N <i>Rb1</i> ^{+/-} mice	40
4.1.2	B6C3F1 mouse bone marrow	40
4.2	Cell culture	40
4.2.1	Cultivation of primary murine mesenchymal stem cells	40
4.2.2	Subculturing of mMSCs	41
4.2.3	Cell counting	42
4.2.4	Freezing and thawing of mMSCs	42
4.3	PrestoBlue® cell viability assay	42
4.4	Flow cytometry analysis of the cell cycle	43
4.5	Irradiation	43
4.6	Molecular biology techniques	44
4.6.1	Mice genotyping	44
4.6.2	DNA isolation	44
4.6.3	RNA isolation	44
4.6.4	Nucleic acid concentration measurement	45
4.6.5	PCR	45
4.6.6	Agarose gel preparation and electrophoresis	46
4.6.7	Reverse transcription	47
4.6.8	Real-Time Polymerase Chain Reaction (Real-Time PCR)	47
4.7	Histochemical stainings	51
4.7.1	Differentiation assays and stainings	51
4.7.2	Giemsa staining	52
4.7.3	Senescence associated beta-galactosidase staining (SA- β -gal staining)	53
4.8	Surface marker expression analysis of mMSCs	53
4.8.1	Surface marker analysis by immunocytochemistry	53
4.8.2	Surface marker analysis by flow cytometry	55
4.9	Clonogenic survival assay	56
4.10	Apoptosis assay	57
4.11	Differentiation potential of mMSCs after exposure to ionizing radiation	58
4.11.1	Differentiation of mMSCs in presence of lineage inducing growth medium after ionizing radiation exposure	58

4.11.2 Differentiation of mMSCs in absence of lineage inducing growth medium after ionizing radiation exposure	58
4.12 Quantification of adipocytes in bone marrow tissue sections from whole body irradiated mice	60
4.13 LB medium and LB agar plates for E. Coli growth	61
4.14 Identification <i>Pou5f1</i> transcripts of mMSC	61
4.14.1 Purification of Real-Time PCR products	61
4.14.2 Amplification and separation of purified Real-Time PCR products	61
4.14.3 TOPO® TA cloning	62
4.14.4 Colony screening	63
4.14.5 Continuing the colony and extraction of Real-Time PCR products	63
4.14.6 Sequencing	64
4.14.7 Product purification after cycle sequencing reaction	64
4.14.8 Nucleotide blast alignment	65
4.15 Statistical analysis	65
5 Results	67
5.1 Establishment and long-term maintenance of <i>in vitro</i> mesenchymal stem cell culture from mice of different genotypes	67
5.1.1 Determination of the mouse genotypes	67
5.1.2 Identification of the optimal environment for long-term <i>in vitro</i> culturing of mMSCs	68
5.1.3 Selection of an appropriate proteolytic enzyme for subculturing the mMSCs	69
5.2 Properties of <i>in vitro</i> cultured mMSCs	69
5.2.1 Trilineage differentiation potential of mMSCs	70
5.2.2 Surface marker expression of <i>in vitro</i> cultured mMSCs	71
5.3 Effects of oxygen concentration on <i>in vitro</i> cultured mMSCs	75
5.3.1 Colony forming ability of mMSCs under hypoxic and normoxic conditions	75
5.3.2 Cell cycle analysis of mMSCs growing in hypoxic and normoxic conditions	75
5.4 Expression analysis of stemness marker genes in <i>in vitro</i> cultured mMSCs	79
5.5 Telomere length measurement of <i>in vitro</i> cultured mMSCs	81
5.5.1 Effect of oxygen concentration on telomere length in mMSCs	81
5.5.2 Effect of retinoblastoma gene status on telomere length in mMSCs	81
5.6 Identification of <i>Pou5f1</i> Real-Time PCR products in mMSCs	82
5.7 <i>In vitro</i> ageing of mMSCs	85
5.8 Characterisation of <i>in vitro</i> cultured mMSCs after exposure to ionizing radiation	92
5.8.1 Effect of ionizing radiation on <i>in vitro</i> ageing of mMSCs	92
5.8.2 Effect of ionizing radiation on clonogenic survival of mMSCs: hypoxic and normoxic conditions	95
5.8.3 Effect of ionizing radiation on senescence in mMSCs: hypoxic and normoxic conditions	96
5.8.4 Effect of ionizing radiation on apoptosis in mMSCs: hypoxic condition	98
5.8.5 Effect of ionizing radiation on differentiation ability of mMSCs	100
5.8.6 Effect of ionizing radiation on the expression of lineage specific genes in MSCs	103

5.8.7	Effect of ionizing radiation on expression profile of stemness and pluripotency marker genes in MSCs	107
5.8.8	Quantification of adipocytes in the bone marrow sections of whole body irradiated mice	109
6	Discussion	111
6.1	Hypoxia promotes long-term <i>in vitro</i> growth and survival of mMSCs	112
6.2	Reduced clonogenicity of mMSCs in higher oxygen tension is potentiated by ionizing radiation	113
6.3	Ionizing radiation sensitises mMSCs towards high oxygen concentration-induced senescence	114
6.4	Murine mesenchymal stem cells are resistant towards ionizing radiation initiated apoptosis	116
6.5	Murine mesenchymal stem cells retain their induced multilineage differentiation ability but undergo ionizing radiation-induced adipogenesis after γ -irradiation treatment	117
6.6	Ionizing radiation affects the gene expression profile of mMSCs	118
6.7	Conclusions	120
	Bibliography	122
	Abbreviations	137
	Appendices	140
A	Identification of the suitable nutrient mixture for <i>in vitro</i> culturing of mMSCs	141
B	List of RT ² profiler genes with their corresponding fold change in mMSCs as compared to osteoblasts	143
C	List of Genes	148
	List of Figures	153
	List of Tables	155
	Acknowledgements	156
	Curriculum Vitae	157

Chapter 1

Abstract

Mesenchymal stem cells are becoming widely used in clinical settings to treat a variety of diseases. The promise of mesenchymal stem cells in stem cell therapy lies in their multilineage differentiation potential, relatively simple isolation from different tissue sources, ease of *ex vivo* expansion and their range of functional abilities including immunomodulatory properties, migration to the site of injury, support of haematopoiesis and promotion of angiogenesis. Their use has raised concerns regarding the long-term safety and efficacy of mesenchymal stem cell therapy, especially if these cells have been previously exposed to stress factors. For their safe and effective use it is therefore necessary to understand the effect of stress on the biology of mesenchymal stem cells.

Every living organism is exposed to ionizing radiation present in the environment. In addition, the exposure to ionizing radiation from medical applications is growing at an alarming rate. Therefore, the likelihood that a mesenchymal stem cell donor has been previously exposed to ionizing radiation is high. Ionizing radiation is known to generate genotoxic damage and oxidative stress in biological systems. This can be compounded by oxidative stress induced by respiration. After their isolation mesenchymal stem cells are traditionally cultured under atmospheric oxygen concentration during their pre-therapy expansion. This abnormally high atmospheric oxygen concentration can cause oxidative damage to the cells that are normally present in the relatively hypoxic stem cell niche. Therefore, to study the effects of damage caused by ionizing radiation and atmospheric oxygen mesenchymal stem cells were isolated from the mouse bone marrow, cultured *in vitro* under hypoxic (2% O₂) or normoxic (21% O₂) conditions, and then treated with medically-relevant doses of ionizing radiation. The effects were assessed in terms of typical stem cell features; for example long-term growth, clonogenicity and lineage potency. It was observed that hypoxia promotes both sustainable *in vitro* growth and survival of murine mesenchymal stem cells. The mesenchymal stem cells maintained their telomeric integrity *in vitro* under hypoxic and normoxic conditions. On the other hand, the impaired growth of murine mesenchymal stem cells at the higher oxygen tension was accompanied by reduced clonogenicity and increased senescence. These effects of normoxia on clonogenicity and senescence in murine mesenchymal stem cells were potentiated by exposure to ionizing radiation. Hypoxic murine mesenchymal stem cells were found to be more resistant towards ionizing radiation-induced apoptosis. Increased ionizing radiation-induced adipogenesis was also observed in irradiated hypoxic cultures even in the absence of a lineage inducing growth medium. This suggests that damage induced by both ionizing radiation and high oxygen tension can independently and synergistically affect the essential mesenchymal stem cells properties. This study

provides a new insight into the effects of ionizing radiation and oxygen on the inherent stemness of mesenchymal stem cells. The results obtained in this study will help to recognise the possible concerns related to the therapeutic efficiency of the stress exposed mesenchymal stem cells.

Chapter 2

Introduction

2.1 Ionizing radiation, stem cells and therapeutic consequences

Ionizing radiation is known to evoke cellular and genotoxic stress in biological systems. The effects of ionizing radiation range from macromolecular damage within a cell to impairment of the local microenvironment resulting in disruption of tissue homeostasis and ultimately cause detriment to the organism (reviewed by [1]). Sources of ionizing radiation are natural background radiation and artificial ionizing radiation sources. Artificial sources are mainly derived from medical exposure that typically involve imaging procedures employing low dose ionizing radiation, and from the radiotherapy of malignant tumours requiring high dose exposure [2–4].

Stem Cells (SCs) are present throughout embryonic development and adult life of both plants [5] and animals (reviewed by [6]). With their long lifespan, SCs are exposed to numerous environmental carcinogens and stressors such as ionizing radiation during their life time. The long lifespan and self-renewal ability of the SCs increases their risk of accumulating genetic damages induced by exogenous carcinogens (reviewed by [7]). In addition, their unlimited proliferative capacity can cause propagation of some of this impairment to their differentiated progenies (reviewed by [1]). The response of SCs to ionizing radiation-generated genotoxic stress can vary depending on their origin and biology [8–10]. Nevertheless, continuous aggregation of mutations is suggested to provoke malignant transformation of the SCs, tremendously increasing the risk of cancer (reviewed by [1]). Ionizing radiation can also kill cells directly [4, 11]. Further, exposure to ionizing radiation can affect the stemness properties such as proliferation or lineage potency, and can disrupt the stemness regulatory mechanisms by altering the onset of ageing and senescence in the culture [8, 9, 12]. Collectively these events can bring about an exhaustion of the stem cell pool.

2.2 Stem cells

Stem cells are undifferentiated cells that have the potential to divide constantly to regenerate themselves and to produce committed precursor cells that can subsequently divide and differentiate into mature differentiated cells with specialised functions. Stem cells display two important properties, namely self-renewal and potency (fig. 1).

Self-renewal is a process by which a SC divides symmetrically or asymmetrically to generate one

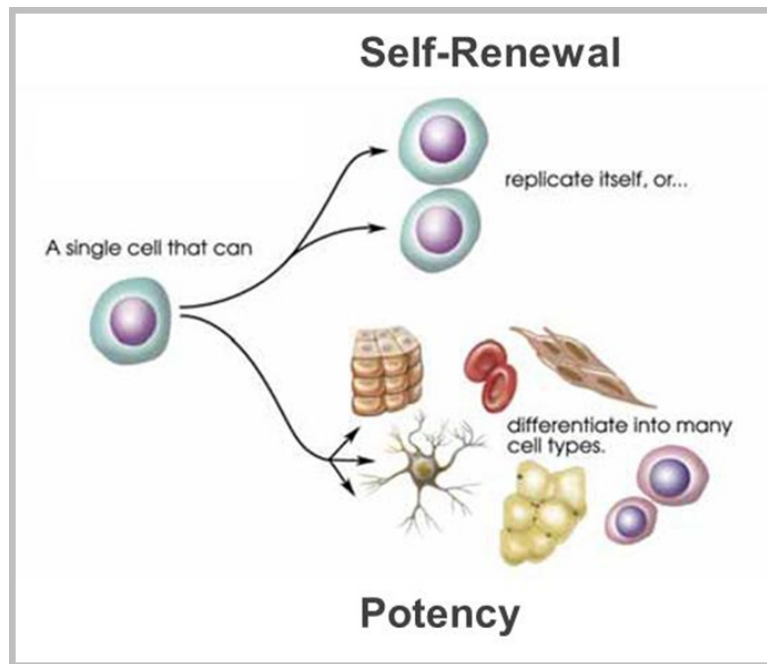


Figure 1: Stem cell. A typical stem cell displays the two important properties of self-renewal and potency. Self-renewal refers to the ability of a stem cell to be able to replicate itself while the potency is the ability to differentiate into various kinds of specialised cells (modified from [13]).

or two daughter stem cell(s). This renewal process is required to conserve the SC pool, therefore the daughter SCs have a developmental potential similar to the original (mother) stem cell. It can also maintain the required numbers of differentiated progenies by means of asymmetric cell division where one daughter cell is similar to that of original SC whilst the second is a differentiated progeny [14]. The second key property of a stem cell refers to SC potency which is the ability of a SC to form various types of specialised cells. Based on their source the SCs are generally divided into two types: Embryonic Stem Cells (ESCs) and Adult Stem Cells (ASCs) (reviewed by [6]).

i. Embryonic Stem Cells (ESCs)

The cells found in inner cell mass during the blastocyst phase of embryonic development are pluripotent and when cultured they are called embryonic stem cells. These cells, under appropriate culture conditions, maintain their pluripotency *in vitro* [15]. Pluripotency is defined as the ability of a cell to differentiate into the cells of three germ layers as endoderm, mesoderm and ectoderm. ESCs have an ability for unlimited proliferation and a capacity to generate all the types of foetal and adult cells except extra-embryonic tissues such as the placenta [15].

ii. Adult Stem Cells (ASCs)

Adult stem cells are found throughout the body of in adult tissues and organs. These cells are in an undifferentiated state, and possess multi-potency which means they are able to develop into multiple cell types. The main task of ASCs is to replenish or regenerate the ageing, damaged or dead cells of an organ, thereby contributing to tissue maintenance (reviewed by [6]). Usually, ASCs are characterised by their source tissues or organs, and are able to produce the cell types of their originating tissue. Adult stem cells can be found in bone marrow such as haematopoietic

stem cells or mesenchymal stem cells, in brain as neural stem cells, in skin such as epidermal stem cells and melanocyte stem cells (reviewed by [6]).

2.2.1 Factors regulating stemness properties

Several extrinsic and intrinsic factors are responsible for inducing, maintaining and regulating the stemness characteristics. Extrinsic factors present in the microenvironment such as self-renewal promoting fibroblast growth factor 2 [16], members of the transforming growth factor beta superfamily including the bone morphogenetic proteins that maintain self-renewal and control differentiation towards the mesodermal lineage [17–19] and components of the Wnt signalling pathway which is involved in proliferation and differentiation [20, 21] are the key players in the regulation of SC pluripotency.

Intrinsic factors normally involve cell specific transcription factors and epigenetic regulators that coordinate to control gene expressions. Epigenetic regulation is achieved by DNA methylation, chromatin remodelling, modification of histone proteins, polycomb group repressive complexes and non-protein-coding RNAs [22–25]. The regulation of the undifferentiated state and lineage commitment of the ESC by epigenetic mechanisms are mediated in part by the polycomb group repressive complexes and promotor DNA methylation [22, 24]. Stem cells such as cardiac progenitor cells [23] and skeletal muscle stem cell [25] are also shown to be under control of epigenetic regulators to determine their cellular fate.

It has been shown that a restricted set of intrinsic transcription factors, including Oct-4 (or POU class 5 homeobox 1-Pou5f1) [26], SRY (sex determining region Y)-box 2 (Sox2) [26], Kruppel-like factor 4 (Klf4) [26], c-Myc [26] and Nanog homeobox (Nanog) are required to generate induced Pluripotent Stem Cell (iPSC) by reprogramming the adult cells [27–29]. Pou5f1, Sox2 and Nanog are the three pivotal transcription factors that have essential roles in stem cell regulatory circuitry, maintaining an undifferentiated state and self-renewal of SCs as they have been shown to share a substantial portion of their target genes and collaborate together to form auto regulatory and feed-forward loops [30].

Pou5f1 is a POU family transcription factor and is important for conserving the pluripotency of an embryonic stem cell [31]. It has been shown to regulate expression of a set of genes including human chorionic gonadotropin genes and forkhead box family genes [32, 33]. It plays an important regulatory role in the initial cell fate decisions of mammalian development and in its absence pluripotent cells may revert back to the trophoblast lineage both *in vivo* and *in vitro* [31]. Pou5f1 is also expressed in several human ASCs such as breast epithelial, pancreatic, mesenchymal, human kidney, liver and gastric SC [34].

Sox2 is a member of the SRY-related HMG box gene family. In early embryonic development it is required in the lineage stages leading to epiblast formation and when it is absent trophectoderm formation results [35]. Sox2 is required for the formation of extraembryonic ectoderm [35]. Sox2 expression was also observed in various ASCs, for example, the SC from testes, glandular stomach and lens [36].

Nanog is an essential molecule regulating the pluripotency of ESCs. It is a homo-domain containing protein necessary to block pluripotent cell differentiation into extraembryonic endoderm lineage. Nanog is found to regulate the expression of both Pou5f1 and Sox2 [31]. In ASCs such as

human Mesenchymal Stem Cells (hMSCs), both *Nanog* and *Pou5f1* are responsible for maintaining the self-renewal capacity and undifferentiated state [37].

Klf4 is a part of the ESCs transcriptional network and belongs to the Kruppel-like factor family of conserved zinc finger transcription factors [38]. It plays a role in self-renewal and pluripotency of the ESCs. It has been demonstrated that *Klf4* functions upstream of *Nanog* and binds to its promoter region to control *Nanog* expression [38]. *Klf4* expression decreases rapidly during ESC differentiation [17].

Other important transcription factors are *Nestin* and *Bmi1* polycomb ring finger oncogene (*Bmi1*). *Nestin* (*Nes*) is a class V intermediate filament protein. It is a typical marker of multipotent neural stem cells and shown to be necessary for their self-renewal and survival [39]. *Nestin* was found to be expressed on distinct cell types within rat and human pancreatic islets and ducts which have an extended capacity for *in vitro* proliferation and were able to differentiate into pancreatic endocrine, exocrine and hepatic phenotypes [40]. Very recently *Nestin* was described as a cancer stem cell marker of neurogenic tumours and tumours of both epithelial/mesenchymal origins [41].

Bmi1 is a member of the polycomb group gene family which is fundamental for the normal development of an organism. *Bmi1* protein was found to perform a role in self-renewal of haematopoietic and neural stem cells by repressing senescence [42].

The potency and self-renewal abilities of the SCs are governed by tightly controlled regulatory mechanisms [30, 43]. These regulatory mechanisms involve complex interaction between various molecular (extrinsic and intrinsic) and environmental players (reviewed by [44]). With their constant communication between each other and the surrounding transcription factors are the molecular bases of this regulatory circuitry [30, 43].

2.2.2 Stem cell therapy

Stem Cell Therapy (SC Therapy) involves the use of SCs for therapeutic purposes to prevent and cure diseases. The era of regenerative therapy began with the first successful bone marrow transplant involving identical twins by Dr. E. Donnall Thomas in 1956 [45]. It took almost 40 years before the isolation and growth of human ESCs (hESCs) in the lab [46]. With isolation of hESCs the notion of SC therapy gained its momentum for tissue regeneration and repair. In addition to tissue regeneration SC therapy theoretically provides the possibility of manipulating stem cell regulators to change the stem cell fate to form a specialised cell type for repair [14].

The unlimited proliferative potential and potency of ESCs make them a highly desirable candidate for stem cell and regenerative therapy. Human ESCs are mainly obtained from pre-implantation blastocyst [46]. Some of the first human ESC lines were derived from embryos produced by *in vitro* fertilisation. However, the use of human embryos in scientific research created many ethical problems and major controversies [47]. Alternatively, ESCs can be produced by the process of nuclear transfer, known as cloning, where a somatic cell nucleus is transferred into an enucleated oocyte leading to normal embryonic development [48]. However, generating cloned human embryos for the research purposes is even more controversial. Therefore, ESC therapy remains a highly controversial issue. It also involves eminent risk of developing teratomas by implanting the SC which are still in an undifferentiated state. Besides, the limited ESC lines currently available are generic and not matched to any individuals; hence, the product derived from these cells can be rejected by the

patients [49].

In the light of the problems faced by ESC therapy, the discovery of iPSCs came as a major breakthrough. These are pluripotent stem cells derived from embryonic and adult cells by reprogramming the differentiated cells with key transcription factors [26]. The major advantage of iPSCs over ESCs is they can be obtained from a variety of adult cells without the use of human embryos. Induced pluripotent stem cells have unlimited proliferative potential like ESCs [26]. Plus, they can be obtained by reprogramming a patient's own cells, creating a possibility of personalized stem cell therapy (reviewed by [50]). Although iPSCs show many similarities to ES cells in-depth analyses have revealed many differences such as different epigenetic signature (reviewed by [50]). If transplanted these cells, like ESCs, pose the risk of teratoma formation. Induced pluripotent stem cells are exposed to culture adaptations that can affect their genomic stability and even the optimum culturing protocol for iPSCs is still missing (reviewed by [50]). This emphasises that there are many obstacles still to overcome before iPSCs can be safely used in SC therapy.

Adult Stem Cells provide a reliable alternative to the use of ESCs or iPSCs in SC therapy. The benefits of ASCs include nearly negligible risk of teratoma formation due to limited potency and easier isolation of the cells from the patient [51, 52]. This provides the option of autologous transplantation, similar to iPSCs, without causing immunological rejection. Adult stem cells display unlimited proliferative potential giving the possibility of *ex vivo* expansion [52]. Despite these benefits the effective use of ASCs in SC therapy still faces major challenges as ASCs are also prone to culture induced changes in their morphological, proliferative and differentiation properties [53]. Plus, having unlimited self-renewal ability a risk of malignant transformation always exists [54, 55].

2.3 Mesenchymal stem cells

2.3.1 History and origin

Mesenchymal Stem Cells (MSCs) are multipotent adult stem cells and are progenitors of a variety of cells of the mesodermal lineages (fig. 2) [56–59].

Fridenstein et al. proved that the formation of bone in transplants of bone marrow was related to a small population of non-haematopoietic bone marrow cells [60, 61]. They successfully demonstrated that the cells associated with the formation of a bone can be distinguished from other cells by their adherence to the charged culture flask surface [60, 61]. When bone marrow cell suspensions are cultured at low density distinct colonies were formed. These cells were termed Colony-Forming Unit-Fibroblastic (CFU-F) due to the fibroblast like appearance of the cells present in those colonies [62]. This led to the hypothesis that the bone marrow stroma might contain a stem cell of non-haematopoietic lineage which was initially called a Stromal Stem Cell by Owen et al. [63] and an Osteogenic Stem Cell by Fridenstein [61]. The actual term Mesenchymal Stem Cell was later coined by Arnold Caplan in 1991 [64]. He successfully demonstrated the *in vitro* differentiation of cells obtained from embryonic chick limbs into both osteoblasts and chondrocytes [64]. In 1999, Pittenger et al. effectively isolated cells with MSC properties from bone marrow aspirates of volunteer donors. They were able to stimulate these cells to differentiate exclusively into adipocytes, chondrocytes and osteocytes thereby proving their mesenchymal multipotency *in vitro* [56].

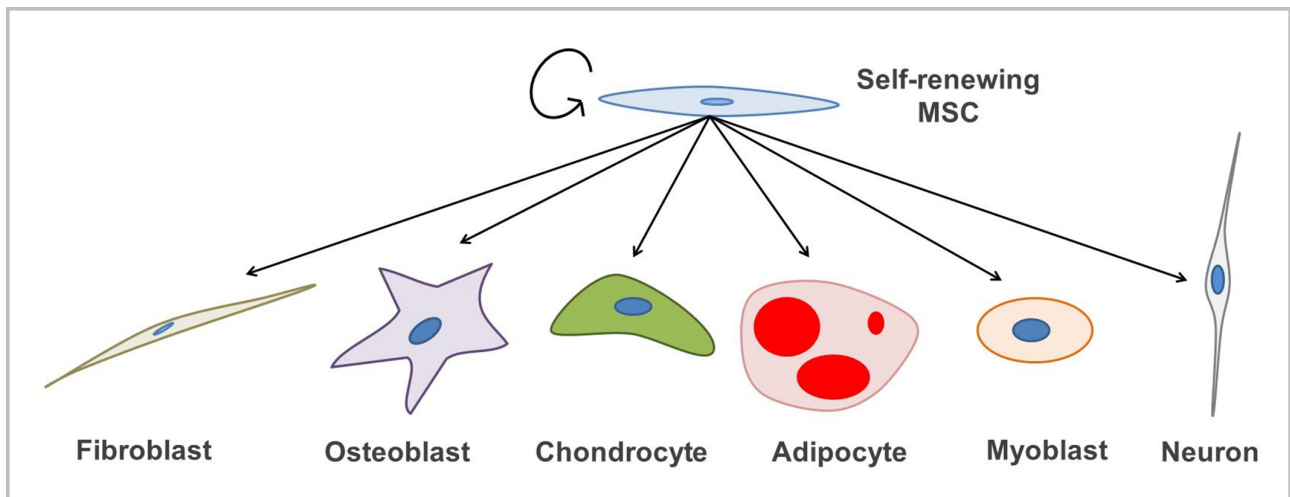


Figure 2: Mesenchymal stem cell. Mesenchymal stem cells are self-renewing cells and are progenitor to many different types of cell lineages such as fibroblast, osteogenic, chondrogenic, adipogenic, myogenic and non-mesodermal neuronal lineage.

Recent studies have shown that MSCs can be isolated from other tissues. In 2006, Kern et al. compared MSCs originated from the bone marrow, umbilical cord blood and adipose tissues [65]. Around the same time da Silva et al. generated long-term cultures of MSCs from a number of tissues of adult mice [66]. Since then MSCs are thought to be present virtually in all connective tissues of an adult organism [66]. Isolating MSCs from sources such as adipose tissues, umbilical cord blood, dental pulp, peripheral blood or Whartons Jelly has provided an advantage as it does not involve invasive procedure and can be carried out under local anaesthesia [65, 67]. In addition, these tissues yield high number of MSCs [65].

Despite the wide popularity of the term Mesenchymal Stem Cells it remains controversial, as the non-skeletal differentiation potential of the MSCs at the single cell level has not been proven *in vivo* [68]. It is also observed that during development the tissues supposed to be developed from post-natal MSCs are actually generated by a set of distinct progenitors [68]. Furthermore, due to a lack of specific markers it is impossible to isolate a single stem cell having stemness properties. The selection of the MSCs based on plastic adherence results into a culture with heterogeneous properties [69]. Hence, the International Society for Cellular Therapy suggested the fibroblast-like plastic adherent cells, regardless of the tissue from which they are isolated, be termed multipotent mesenchymal stromal cells, while the term mesenchymal stem cells to be used only for cells that meet specific criteria (see section 2.3.2). Both of these terms can be denoted with the original acronym MSCs [69].

2.3.2 Criteria used to characterise the MSCs

Due to the range of methods used for isolation and expansion of MSCs from the bone marrow and other tissues, the characteristics defining MSCs are often inconsistent between laboratories. To address these issues and create equivalence International Society for Cellular Therapy proposed three defining criteria of MSCs as [70]:

- i. adherence to plastic

- ii. specific surface antigen expression (presence of CD105, CD73, CD90 on MSC membranes)
- iii. multipotent differentiation potential (*in vitro* trilineage differentiation into osteoblasts, adipocytes and chondrocytes)

Although originally recommended for human mesenchymal stem cells, these criteria are roughly applicable to the MSCs from other species. Therefore, immunophenotype expression analysis is an important step in human and non-human MSC characterisation as it allows rapid identification of MSC cell population and tentatively helps to distinguish them from the other cell types such as haematopoietic and endothelial cells ([70], reviewed by [71]). The antigens expressed (or not expressed) on the surface of MSC population can be determined by flow cytometry analysis [70] or immunofluorescence [72]. Antibodies against typical surface markers expressed on the MSCs are used to perform the flow cytometry experiment. The individual markers expressed on the surface of MSCs can also be observed by direct method such as immunofluorescence (precisely immunocytochemistry) which gives an explicit read-out of the presence or absence of particular surface epitope on a single cell level [72].

According to International Society for Cellular Therapy, hMSCs population must have a level of purity in terms of surface marker expression such that 95% cells should be positive for expression of CD105, CD73, CD90 and 2% can express haematopoietic and endothelial antigens like CD45, CD34, CD14, CD79 α and HLA-DR. However, hMSCs are observed to differ in their surface antigen expression depending on their source tissue. Similarities and differences between surface markers of hMSCs isolated from different tissues have been summarized in Lv et al. (reviewed by [73]). Human mesenchymal stem cells isolated from bone marrow and adipose tissue share defined surface antigens such as CD105, CD73, CD90 but differ in the expression of CD49d, CD54, CD34 and CD106C [57, 74]. Likewise, CD271 (low-affinity nerve growth factor receptor) is differentially expressed on bone marrow, adipose tissue and umbilical cord blood derived MSCs as it is observed to be expressed on bone marrow and adipose tissue MSCs but is absent in umbilical cord blood MSCs ([75], reviewed by [71, 73]). Besides the intra-individual variance observed between different sources of MSCs, the expression of surface markers is also not conserved between species (reviewed by [71]). CD90 and CD105, a part of the antigen panel expressed on hMSCs, are also strongly expressed on murine Mesenchymal Stem Cells (mMSCs) [76], whereas they are absent on MSCs from dog, goat and sheep [77]. Human and murine MSCs differ in the expression level of CD73. This epitope is highly expressed on hMSCs while mMSCs only show very weak (< 5%) expression on their surface. On the other hand, CD80 which is absent on hMSCs is expressed on mMSCs [76]. Interestingly, surface epitope expression also varies between MSCs isolated from different strains of inbred mice. Expression of Sca-1, CD106 and CD34 was found to be different on MSCs from Bl/6, FVB/N, BALB/c and DBA1 mice [78]. Keeping aside the differences of MSC immunophenotype, the isolation of MSCs based on their surface marker expression has a disadvantage in that these antigens are also expressed on other types of cells. For example, human bronchial fibroblasts exhibit expression of CD73, CD90, CD105, and CD166 on their surface and are found to be negative for CD34 and CD 45 [79].

MSCs undergo trilineage differentiation *in vitro* into osteogenic, adipogenic and chondrogenic lineages [56]. MSCs are also shown to also undergo cardiomyogenic [58], smooth muscle cells [19] and neuronal [59] differentiation *in vitro*. Hence, all the MSC cultures are to be tested for their

trilineage differentiation ability (osteogenic, adipogenic and chondrogenic lineages) with *in vitro* staining techniques and this criterion is a must for attesting the validity of a MSC model system. After inducing the MSCs to undergo a given lineage, the presence of differentiated cells in a culture can be tested with various cytochemical stainings. The osteogenic differentiation is usually tested with Alizarin Red, von Kossa or alkaline phosphatase staining. Chondrogenic differentiation is checked with Alcian Blue or immunohistochemical staining for collagen type II whereas adipogenic differentiation is demonstrated by Oil Red O staining [70].

In spite of more than 40 years of research in the MSC field, the actual *in vivo* counterpart of MSCs is yet to be identified as the proof of their trilineage differentiation *in vivo* at a single cell level is still missing. Quite recently two groups [80, 81] have independently shown formation of osteoblasts, chondrocytes and reticular marrow stromal cells/stromal tissues from a single cell *in vivo*. Though, it has been mentioned that these cells do not undergo adipogenic differentiation.

2.3.3 Functional assays to characterise the MSCs

Functional assays can be used to assess the properties of cultured MSCs and help to create equivalency and compare the research made across several laboratories [70].

- Clonogenic assay to assess clonogenicity

Mesenchymal stem cells demonstrate an inherent ability to form colonies *in vitro* [62, 68]. Hence, to assess the clonogenicity cultured MSCs are seeded in a clonal density (limiting dilution) and numbers of colonies formed are counted after several days of *in vitro* culturing. As a colony is usually initiated by a single cell, this assay provides an information about the presence of clonogenic progenitors in the culture [82]. Therefore, the possibility to obtain clones (colony initiated by a single cell) at every MSC passage is a necessary condition to validate the culture of uncommitted, self-renewing progenitor cells [83].

Rosland et al. have observed that the extensive *in vitro* expansion of hMSCs poses the risk of malignant transformation in long-term cultures [84]. Therefore, it is required to examine the cultures for possible malignant transformation by karyotype testing or gene expression analysis. In most transformed cells the enzyme telomerase is reactivated whereas telomere length is shorter compared to the corresponding control cells [85, 86]. Progressive telomere shortening is also observed during ageing (reviewed by [87]). As accelerated telomere shortening causes senescence in nearly all cell types, telomeric length of long-term cultured MSCs should be measured at regular intervals [54]. Senescence is responsible for inducing growth arrest in culture leading to halt in cellular proliferation. Hence, number of senescent cells present in a culture are tested with senescent staining techniques such as Senescence Associated beta-galactosidase staining (SA- β -gal staining) [53, 84, 88]. Use of these different functional assays provides a means to standardize the characterisation of MSCs.

2.3.4 Transcriptional control and phenotypical markers of MSC differentiation

The differentiation process of MSCs is governed by expression of a set of genes and includes various signalling pathways responsible for induction of a certain lineage. The MSC differentiation towards osteogenic or adipogenic lineages appears to be mutually exclusive so that the MSC

can be engaged either in osteoblastic or adipocytic differentiation (reviewed by [89]). An inverse association between MSC adipogenesis and osteogenesis regulation has been found *in vitro* where the culture supplements upregulate persistent osteogenic differentiation of MSCs with related down regulation of adipogenic differentiation, or vice versa (reviewed by [89]). This further implies that the lineage commitment of MSCs to osteoblast or adipocyte takes place at the expense of other as it is brought about by external stimuli and causes changes on genetic and epigenetic level. Therefore, irregularities in the differentiation process can imbalance the tissue homeostasis which may result into diseases such as osteoporosis where simultaneous decrease in bone volume and increase in adipose tissue is seen [90].

The process of osteogenic differentiation of MSCs consists of an interplay between master transcription factors Runt related transcription factor 2 (Runx2), Sp7 transcription factor 7 (Osterix/SP7), SRY (sex determining region Y)-box 9 (Sox9) and morphogens like Transforming Growth Factor Beta (TGFB), Bone Morphogenetic Proteins (BMPs), Fibroblast Growth Factors (FGFs) [91]. Interestingly, the early stages of induction of the chondrogenic lineage of MSCs shares transcription factors with the osteoblastic lineage. Initially, Runx2, Osterix/SP7 and Sox9 expressing cells are still bipotent, and the decision to undergo either osteoblastic or chondrocytic lineage is dependent on the threshold values of these factors [91]. After lineage commitment, during further stages of osteoblast development levels of Runx2 are continuously increased and gradually other factors like Osterix/SP7 come into action [91]. Further development of osteoblasts is characterised by the expression of mature phenotype marker Alkaline Phosphatase (ALPL) [92]. In the case of chondrogenesis the early developmental signalling cascade involving Runx2, Osterix/SP7 and Sox9 along with morphogens results in the expression of fibromodulin, aggrecan, type II and type X collagen, each playing an essential role in later stages of chondrogenesis [93].

Complex interaction among several factors also underlies MSC differentiation towards adipocytes. CCAAT/enhancer-binding protein alpha (CEBPa) and Peroxisome Proliferator-Activated Receptor gamma (PPARg) are transcription factors responsible for promoting adipogenesis and further maturation of adipocytes by activating expression of adipose specific genes [94]. The differentiation of hMSCs to adipocyte is marked by the adipocyte-related gene Lipoprotein Lipase (LPL) [95]. The Sterol Regulatory Element-Binding Protein 1 (SREBP1) is known as a promotor of adipocytic differentiation and plays a role in fat cell gene expression [96]. In contrast to these early differentiation markers, Fatty Acid Binding Protein 4 (FABP4) denotes terminal adipogenic differentiation after pre-adipocytes are committed to adipogenesis [97].

These transcription factors and lineage specific genes mediate lineage induction of MSCs and are responsible for the development of a specialised cell type. Therefore, they can be used as the markers to evaluate early and late stage differentiation of MSCs ([93, 95], reviewed by [89]).

2.3.5 Functions of MSCs

Currently MSCs are the most widely used stem cells in the field of regenerative therapy (reviewed by [98]). Due to their self-renewal, high proliferation and multilineage they are capable to engage in tissue regeneration and thereby maintain the tissue homeostasis [99]. Their ease of isolation from various connective tissue sources makes the process of harvesting patients own MSCs simple and almost non-invasive. This provides an opportunity to isolate patients MSCs and further expand

them in number (*ex vivo* expansion) or differentiate into required cell types. The culture expanded or differentiated cells can be introduced to patients body locally or systemically to help treat variety of diseases or for recovery after tissue damage [67].

MSCs can establish and organize the haematopoietic microenvironment by interaction with host endothelial cells, and by remodelling and maturation of sinusoidal vessels [100]. MSCs provide physical support for formation of haematopoietic microenvironment, and secrete several factors such as growth factors, cytokines necessary for homing and maturation of haematopoietic progenitors [101]. The soluble factors secreted by MSCs are not only important for the establishment of haematopoietic microenvironment but have also shown to modulate the paracrine profiles of surrounding cells [102]. The ability of MSCs to promote angiogenesis is essential for their use in repairing chronic tissue wounds [99].

Mesenchymal stem cells are known to migrate towards the site of inflammation. There they interact with T cells and other immune cells to exert their immune modulatory function by secreting cytoprotective and immune regulatory molecules [103]. Mesenchymal stem cells also secrete chemokines including CXCL12, angiopoietin-1, IL-7, osteopontin to exert immune suppressive effects in their vicinity [104]. In addition, these cells show low inherent immunogenicity, and therefore can escape the immune surveillance *in vivo* [67]. The immunosuppressive effect of MSCs on local immune environment and low immunogenicity grants the possibility of using allogenic MSCs in SC therapy in case patients own cells are not available making them especially beneficial in regenerative therapy [67, 99].

2.3.6 Therapeutic uses and clinical applications of MSCs

Inherent properties of MSCs have been exploited in clinical settings for the treatment of numerous diseases. With 374 clinical trials currently ongoing MSCs are being utilized in the treatment of a range of ailments like GvHD disease, crohns disease, myocardial injury, Ischemic stroke, osteoarthritis and lower back pain, pulmonary disease, liver disease and diabetes (fig. 3)(reviewed by [98]).

MSCs were also successfully used in treating radiation induced skin burns and cutaneous radiation syndrome [105]. Most of the trials involving MSCs are taking place with allogenic cells.

2.3.7 Risks and challenges involved in the use of MSCs for therapeutic purposes

In spite of their tremendous therapeutic potential and diverse use in clinical trials for treating several diseases there are certain concerns with application of MSCs in therapeutic settings. Most of these concerns are related to their short-term and long-term safety and efficacy. Some of the hurdles faced in MSC therapy are related to their own properties upon transplantation.

Like other SCs, MSCs possess the ability of unlimited cell division which is also a characteristic of cancer cells. Having a longer life-span there is always possibility of accumulating genetic instabilities and mutations leading to neoplastic transformation both *in vitro* [54, 84] and *in vivo* after transplantation as observed in neural stem cells [106]. Undesired and inadequate differentiation of MSCs as seen by the formation of ectopic bone within a heart of a mouse which was treated with MSCs for myocardial infarction is also possible [55]. There are also conflicting accounts available for the role of MSCs in promoting [107] or suppressing [108] tumour growth and metastasis. If

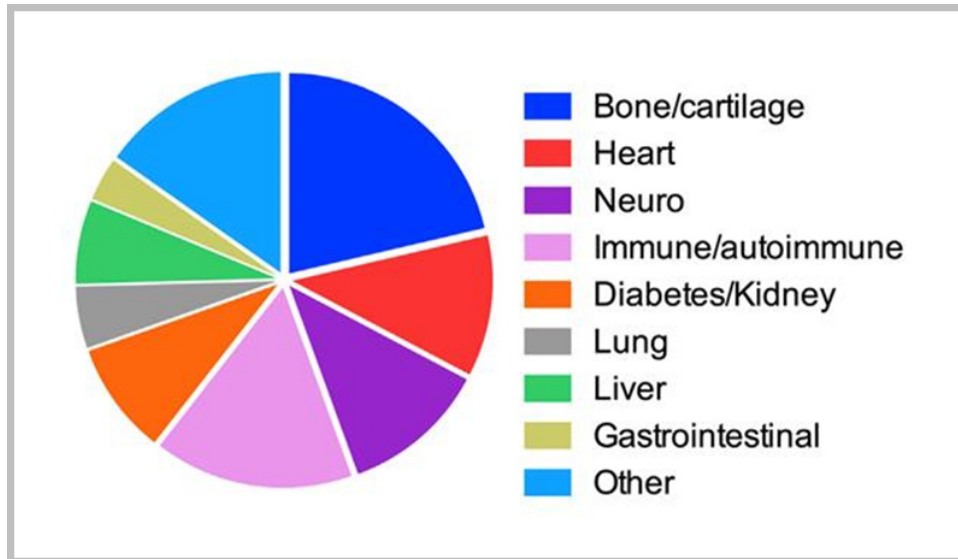


Figure 3: Distribution of MSC clinical trials for treatment of various diseases. A pie chart showing distribution of numbers of clinical trials involving MSCs to treat different indications. Data for 352 registered clinical trials (from Trounson et al. [98])

MSCs indeed favour the tumour growth it needs to be taken into account that they might support the expansion of pre-existing *in vivo* tumours after the transplantation.

The main challenge, however, still lies in the technical aspects of MSC usage due to lack of standard protocols leading to highly heterogeneous culture which contains many different types of cells like genuine SC, progenitors of diverse cell types, precursors and terminally differentiated cells [67].

***In vitro* ageing and malignant transformation of MSCs**

The process of ageing causes impaired biological functioning due to continuous loss of physiological integrity which may ultimately results into death (reviewed by [87]). In 2013, Lopez-Otin et al. proposed 9 cellular and molecular hallmarks of ageing which include genomic instability, telomere attrition, cellular senescence and stem cell exhaustion (reviewed by [87]). Interestingly, changes observed in the hMSC properties after a period of *in vitro* culturing as seen by presence of genetic anomalies [109], continuous replicative senescence [53], rapid telomere loss [110], spontaneous changes of gene expression pattern [111] and decreased maximal life-span [112] are very similar to the cellular and molecular hallmarks of ageing. The cultured induced changes also hold true for murine MSCs as shown by increase in spontaneous malignant transformation and accumulated chromosomal damage with gradual elevation in telomerase activity in aged *in vitro* cultured mMSCs [54, 113]. *in vitro* culturing of mMSCs also weakens their homing ability as reported by Rombouts et al. [114]. These changes in MSC properties raises a possibility that long-term culturing of the MSCs actually leads to their accelerated ageing.

At first the process of ageing and malignant transformation seems to be completely opposite. However, the process of ageing and malignant transformation of the cells often share a common biology [115]. Accumulation of damages in the SC can result into both cancer and ageing. If some of the cells escape the default ageing regulation process and acquire some additional mutations that can

grant them continuous proliferative ability then it may enhance their risk for neoplastic transformation [115]. Hence, the process of ageing can contribute to increase the number of malignant cells.

2.4 Retinoblastoma gene and its haploinsufficiency

The Retinoblastoma (*RB*) gene was the first cloned tumour suppressor gene. It was identified to play a significant role in a rare but malignant childhood cancer of retinoblastoma, a tumour of retinal cells of the eye [116]. Human *RB1* gene encodes the protein pRB. A predominant function of the pRB protein is to act as a signal transducer between the cell cycle progression and the individual transcription molecules [117]. The protein pRB acts at the G1 restriction point (checkpoint) of the cell cycle. It can stop the entry of a cell to S phase when hypo-phosphorylated pRB binds to transcription factor E2F and temporarily inactivates the E2F. This transcription factor is generally responsible for the cell's entry from G1 to S phase [117]. When E2F is inactivated the cell remains in the G1 phase of the cell cycle. As the DNA replication takes place in the S phase this effectively prevents the new DNA synthesis. When *RB1* is phosphorylated by post-translational regulation it can no longer associate with E2F permitting the cell to enter S phase that results into continuation of the cell cycle [117]. This continuation can cause uncontrolled cellular proliferation leading to neoplastic transformation of a cell. The complete loss of pRB due to mutation in both alleles (*RB1*^{-/-}) is absolutely necessary to develop a malignant phenotype and heterozygous mutation (loss of one allele of *RB1*^{+/-}) is not enough for cancer development [118]. However, the heterozygous carriers of *RB1* are pre-disposed to paediatric retinoblastoma and many other second primary tumours, for example, sarcomas where presence of one copy of *RB1* gene was observed in adult sarcomas [119]. Heterozygosity of *RB1* gene also increases the predisposition to radiation induced osteosarcoma [116]. *RB1* heterozygosity was shown to cause replication stress, mitotic defects and aneuploidy in mouse and human fibroblasts [120]. *Rb1* haploinsufficiency was also found to promote telomere attrition and radiation induced genomic instability in mice osteoblastic lineage cells [121].

2.5 Ionizing radiation

Throughout their lifetime all living organisms are continually exposed to ionizing radiation [2, 3]. Ionizing radiation is defined as radiation that has sufficient energy to displace electrons from atoms and molecules [4]. During an interaction between an atom and ionizing radiation, removal of electrons from the atomic orbit by ionizing radiation results into formation of a charged or ionized atom. Ionizing radiation consists of electromagnetic radiation, such as X-rays or gamma rays (γ -rays), or of subatomic particles, such as protons, neutrons, α -particles and β -particles [4].

Ionizing radiation is emitted from both natural and artificial sources. The main natural sources of ionizing radiation are cosmic radiation and natural radionuclides such as radon gas, potassium 40 (K-40) [2]. Artificial sources of exposure include medical diagnosis (not therapy), fallout from atmospheric nuclear testing, occupational exposure etc. Radiation doses are typically expressed in sievert (Sv) or gray (Gy). Annual average doses worldwide from natural sources is estimated to be 2.4 mSv and from artificial sources it is around 0.6 mSv [2]. Medical exposure is the largest source of exposure to ionizing radiation (98% of all artificial sources) and is the second largest contributor

to the population dose worldwide [2]. Annual average dose to the population varies from country to country [2,3]. The distribution of mean effective doses per person in year 2012 in Germany (4.1mSv) is shown in fig. 4. It is clear that nearly 48% of the average annual dose in Germany comes from diagnostic sources (CT and X-ray diagnostics 1.8 mSv, nuclear medical diagnostics 0.1 mSv).

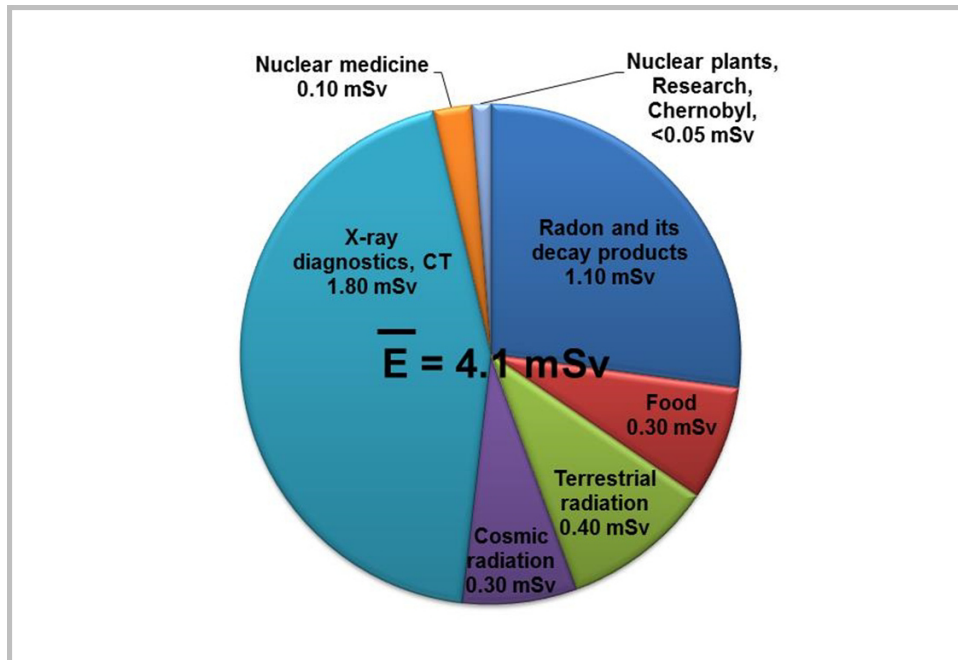


Figure 4: Annual mean effective doses of ionizing radiation per person in Germany. The distribution of mean effective doses per person in year 2012 in Germany is shown. Annual average effective dose per person is 4.1 mSv. Nearly 2.1 mSv of this average dose comes from natural sources of radiation like radon gas, food, terrestrial and cosmic radiation. Remaining 2 mSv is contributed by man-made radiation sources, for example, X-ray, CT, nuclear medicine, nuclear plants, and atomic bomb tests. (source: www.bfs.de).

The medicinal use of ionizing radiation refers to use of X-rays, radionuclides and therapeutic radiation sources [3]. Medical radiation exposure involving diagnostic radiology and nuclear medicine are generally of lower energy and intensity compared to radiation therapy. The ionizing radiation dose range relevant to medical imaging and CT varies between 10 and 100 mSv depending on the organs and body area it is used against. As for the radiography and some nuclear medicine applications this dose is below 10 mSv [4, 122]. Radiation therapy, which is one of the major treatment option routinely exercised for the cancer treatment, is administered with an intention to kill or control the growth of malignant cells while minimizing the damage to surrounding healthy tissues. Usually during the radiation therapy the patients are treated with a very high total dose of ionizing radiation ranging between 40-60 Gy for the cancerous tissues [4]. Hence, human exposure to ionizing radiation by medical means can be of low or high dose based on the type and purpose of radiation treatment used.

2.5.1 Effect of ionizing radiation on biological systems

The effects of ionizing radiation on living matter are the result of physical events set in motion by the ionization and consists of damage to macro molecules [123]. At the molecular level ionizing

radiation causes DNA damage either by direct action that constitutes base damages, DNA single or double strand break, and direct ionization of cellular macromolecules including DNA, RNA, lipids, and proteins, or indirect action generating the free radicals by radiolysis of intracellular water impairing the DNA molecules and the chromosomes [124]. Ionizing radiation can induce a variety of mutations in a cell. These mutations include point mutations in single genes to translocation and deletion resulting in loss of several genes [124]. If not repaired correctly the ionizing radiation-induced damage causes changes in the cell cycle, alterations in cellular functions, loss of proliferation or ultimately cell death [123, 124]. These cellular effects are the preliminary reasons affecting the living tissues which in turn disrupt the normal functioning of an organism and increase their risk of carcinogenesis [123]. Carcinogenesis is the most widely studied adverse late effect of ionizing radiation on biological systems. Strong evidence for ionizing radiation-induced carcinogenesis is mainly available from studies in the cohort of Japanese atomic bomb survivors where increased risk for solid cancer was observed with higher dose consistent with linear association [4].

2.6 Stem cells and ionizing radiation

In addition to their stemness properties SCs have a longer life expectancy and can aggregate the mutations over time ultimately passing it to their progeny and enhancing the cancer risk (fig. 5) (reviewed by [7]). The molecular response of SCs to ionizing radiation is highly relevant for tissue maintenance as the stress induced by ionizing radiation can result into cell killing, depletion of radiosensitive SC or direct damage to SC genome. Hence, ionizing radiation may cause the loss of tissue homeostasis by genotoxic damage to SC and thereby, further increasing the risk of cancer (reviewed by [125]).

The radiosensitivity of a cell can be influenced by various biological factors such as the type of cell, cellular microenvironment, phase of the cell cycle and the expression of distinct damage repair pathways [123]. The physical characteristics of ionizing radiation exposure like the dose (low, medium, high), dose-rate, linear energy transfer all influence the response of differentiated somatic cells (reviewed by [127]). In recent years more and more studies are showing the radio response of different kinds of SCs from different species such as human, mice [8, 9, 43, 128]. Like somatic cells, the different types of stem cells respond differentially to ionizing radiation [8–10]. Several factors like apoptosis, cell cycle analysis, senescence, DNA damage response and repair, transcriptional response, proteomic and metabolomics profiling have been widely investigated after exposure of SCs to low, medium and high doses of ionizing radiation [8, 127, 129]. It is becoming evident that the response of SCs to ionizing radiation indeed varies between the different stem cells in a same species, for example, mice melanocyte stem cells [9] respond differently to ionizing radiation than mice hair follicle bulge SC [130]. Moreover, intensity of the resulting effect can also be dependent on the ionizing radiation dose as seen by dose-dependent response of hESCs to ionizing radiation-induced apoptosis [8]. The dissimilar response of different SC types to ionizing radiation exposure point towards differences in the inherent radiosensitivity of SCs (reviewed by [125, 127]).

Oxygen present in the environment of a cell can play a role in modifying the radiation response by acting as a radiation sensitizer [131]. An increased cellular killing is seen with increased oxygen tension reaching a plateau above 30 mm Hg [123]. In the radiation therapy local tumour hypoxia is

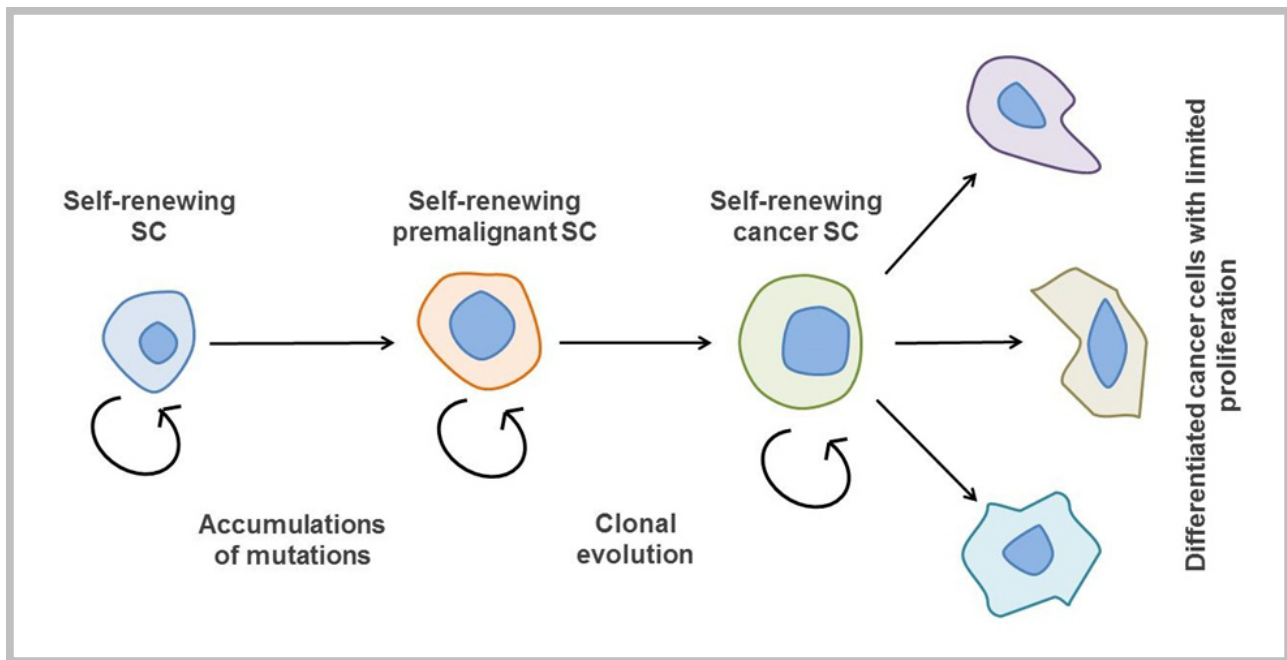


Figure 5: Progression of stem cells to cancer. Hypothetical description for the neoplastic transformation of the stem cells. With its longer life-span stem cell can accumulate mutations turning into a premalignant stem cell and ultimately into the cancer stem cell by clonal evolution (adapted from Pardal et al. [126])

associated with poor prognosis and resistance to the therapy (reviewed by [132]). This suggests that in addition to the effects of ionizing radiation on a SC, an interaction between the microenvironment (commonly referred as niche) where the cell is located and irradiation can considerably influence the cumulative outcome of the stem cell exposure to ionizing radiation.

2.6.1 Possible harmful effects of ionizing radiation on MSCs

Cellular senescence is a feature of mitotic cells *in vitro* where the cells enter irreversible cell cycle arrest and do not divide any longer even in the presence of growth medium. These cells show typical senescent phenotype that includes growth arrest [133, 134], apoptosis resistance [135] and altered gene expression [136]. It is shown that oxidative stress can induce senescence in hMSCs [137]. As ionizing radiation causes oxidative stress in biological system [138] it can be suggested that the *in vitro* culturing conditions such as oxygen tension and genotoxic stress caused by ionizing radiation can affect the life cycle and senescence in MSCs.

If the damage induced by ionizing radiation is not restored correctly and in case it is too great for survival, apoptosis can be triggered by the cell to avoid transmission of fixed damage to the progeny [11] that results in a complete elimination of the affected cell. MSCs inherently possess characteristic longer lifetime in adult organisms but are often limited in numbers [139]. Elimination or loss of these cells due to apoptosis might lead to disruption of tissue regeneration *in vivo* [99]. Therein, detecting the presence or absences of apoptosis in mMSC after radiation treatment can help to elucidate the sensitivity or resistance of MSCs towards ionizing radiation initiated apoptosis.

Assessing the clonogenicity of mMSCs can help to comprehend if ionizing radiation can influence the self-renewal and clonogenic survival of MSC *in vitro*. The colony forming ability of MSCs after

exposure to ionizing radiation can be evaluated with clonogenic assay which is based on the ability of a single cell to grow into a colony and essentially tests every cell in the population to undergo unlimited cell division [140].

The differentiation ability of SCs is essential to maintain the constant turnover of various types of cells *in vivo*. Therefore, complete or partial impairment of the differentiation capacity may compromise the ability of SC to replace the dysfunctional cells *in vivo* affecting the normal organ function (reviewed by [6]). Moreover, if ionizing radiation forces the cells to commit towards a certain lineage this will deprive the stem cells of their characteristic multilineage potential. In case of MSCs this impairment of differentiation will imbalance the regeneration of the connective tissues *in vivo* and affects their therapeutic efficacy *in vitro*. Examining the effects of ionizing radiation on differentiation in MSCs shall help to understand whether MSCs retain their potency even after exposure to stress inducing factors. Furthermore, analysing the expression of genes and transcription factors responsible for maintaining stemness properties and promoting differentiation after ionizing radiation treatment can bring further insights into the response of MSCs towards ionizing radiation.

In vitro culturing of SCs used in the stem cell therapy especially that of hMSCs involve stripping them out of their natural hypoxic milieu and growing the cells in ambient oxygen conditions [141]. This process can make the cells vulnerable towards genotoxic damage induced by ionizing radiation as the usual protective hypoxic environment is absent [123, 131]. Therefore, studying the response of mMSCs to ionizing radiation in hypoxic and normoxic condition could help to elucidate the complex role played by oxygen in the biology of hypoxic niche residing MSCs after their exposure to ionizing radiation.

2.7 Hypothesis

Long lived MSCs present in the body are exposed to natural or medical related ionizing radiation *in vivo*. After their isolation from the donor and during the *ex vivo* expansion these cells are exposed to atmospheric oxygen levels (normoxia). These oxidative stressors (ionizing radiation and non-physiological oxygen concentration) may affect the stability and potency of MSCs for use in cell-based therapy. **Thus in this project we hypothesize that ionizing radiation induces premature ageing in MSCs and affects their inherent properties of self-renewal and multilineage differentiation (fig. 6).**

To test this hypothesis we will:

- i. establish and maintain long-term *in vitro* cultures of MSCs from different mice genotypes
- ii. study the effects of different culture conditions (hypoxia and normoxia) on *in vitro* culturing of mMSCs
- iii. monitor expression of stemness marker genes, mMSC specific genes and identify the genes that change their expression during *in vitro* ageing
- iv. irradiate the mMSCs with low and medium (therapeutically relevant) doses of γ -irradiation and analyse -
 - a. growth, self-renewal and differentiation potential

- b. effect on *in vitro* ageing (senescence) and cell death (apoptosis)
- c. expression of stemness, ageing and lineage specific genes

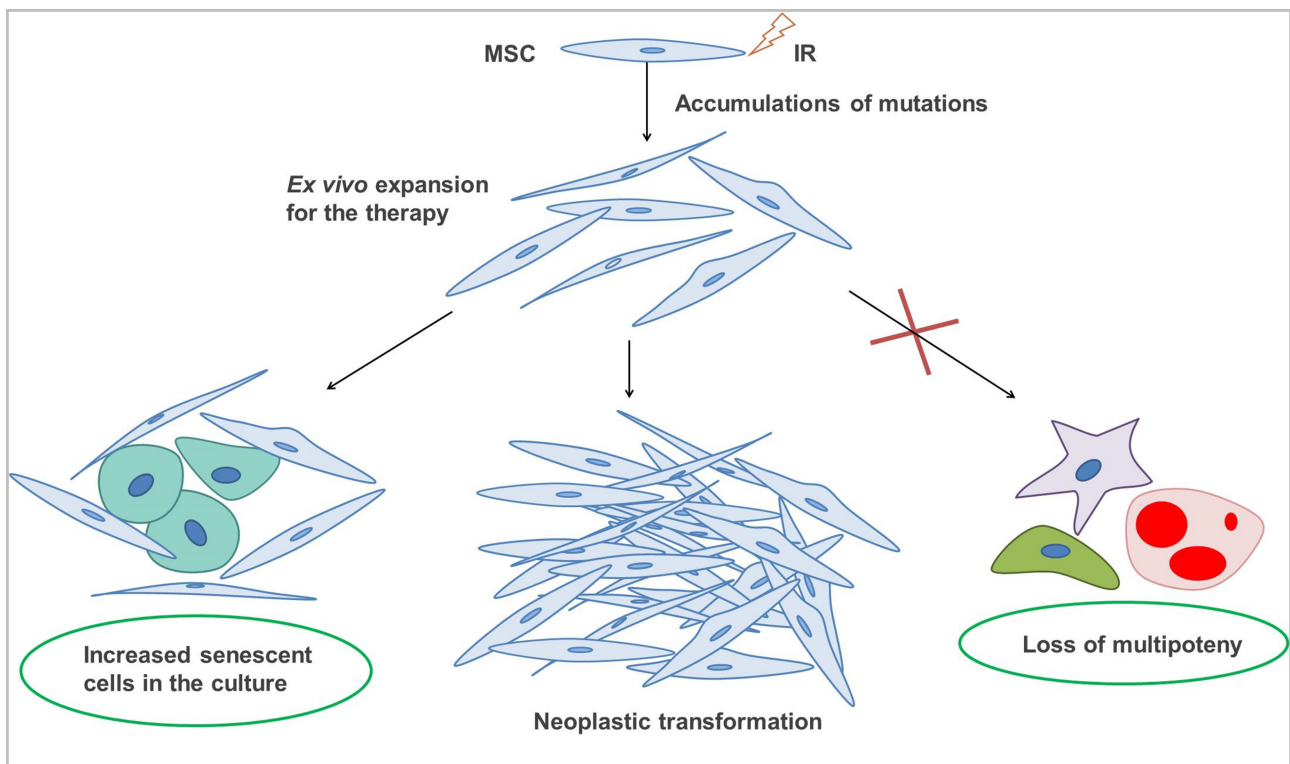


Figure 6: Ionizing radiation-induced damage in MSCs. A schematic representation for the hypothesis of this project. It is hypothesised that the exposure to ionizing radiation can cause accumulation of mutations in self-renewing MSCs resulting into premature ageing (increased number of senescent cells), loss of multipotency and neoplastic transformation in MSC cultures. For this project the entire focus was on *in vitro* ageing and effect on multipotency (encircled in green).

Chapter 3

Materials

3.1 Mice

FVB/N *Rb*^{+/+} mice - Charles River Laboratories, Sulzfeld, Germany.

FVB/N *Rb1*^{+/-} mice - Helmholtz Zentrum Muenchen, Germany.

B6C3F1 mice - Helmholtz Zentrum Muenchen, Germany.

3.2 Cell culture

3.2.1 Standard media and supplements for MSC culturing and differentiation

Cells	Basal medium + Serum	Producer
mMSC	DMEM/F-12, GlutaMAX™ + 10% MSC Qualified Fetal Bovine Serum (FBS)	Gibco™ Thermo Fisher Scientific, Darmstadt, Germany
mMSC differentiation into adipocytes	StemPro® Adipocyte Differentiation Basal Medium + 10% StemPro® Adipogenesis Supplement	Gibco™ Thermo Fisher Scientific, Darmstadt, Germany
mMSC differentiation into chondrocytes	StemPro® Chondrocyte Differentiation Basal Medium + 10% StemPro® Chondrogenesis Supplement	Gibco™ Thermo Fisher Scientific, Darmstadt, Germany
mMSC differentiation into osteoblasts	StemPro® Osteoblast Differentiation Basal Medium + 10% StemPro® Osteogenesis Supplement	Gibco™ Thermo Fisher Scientific, Darmstadt, Germany

3.2.2 Medium and serum mixtures for testing mMSC growth

Cells	Basal medium + Serum	Producer
mMSC	Mesenchymal Stem Cell Growth Medium + 10% Supplement Mix	PromoCell GmbH, Heidelberg, Germany
mMSC	DMEM, low glucose, GlutaMAX™ Supplement, pyruvate + 15% Bio&SELL Fetal Calf Serum (FCS) Gold Plus	Gibco™ Thermo Fisher Scientific, Darmstadt, Germany; Bio&SELL GmbH, Feucht bei Nuernberg, Germany
mMSC	DMEM, low glucose, GlutaMAX™ Supplement, pyruvate; Without FCS	Gibco™ Thermo Fisher Scientific, Darmstadt, Germany

3.2.3 Cell lines

ES-E14TG2A mESC (murine ESC) line passage 27 (kind gift by Dr. Micha Drucker, Institute for Stem Cell Research, Helmholtz Zentrum Muenchen)

HEK293T cell line (kindly provided by Dr. Natasa Anastasov, Institute of Radiation Biology, Helmholtz Zentrum Muenchen)

Primary Osteoblasts FVB/N *Rb1^{+/+}* passage 7 and 9 (kindly provided by Ms. Bahar Sanli-Bonazzi, Institute of Radiation Biology, Helmholtz Zentrum Muenchen)

3.3 Enzymes

Enzyme	Catalogue number	Producer
Accumax™ detachment solution	cell SCR006	Merck, Darmstadt, Germany
Alfazyme	L11-012	PAA Laboratories, Pasching, Austria
Biotase	L2193	Biochrom GmbH, Berlin, Germany
Collagenase CLS TYPE II, CLS II	C 2-28	Biochrom GmbH, Berlin, Germany
Papain	L 2223	Biochrom GmbH, Berlin, Germany
Proteinase K	03115879001	Roche Diagnostics, Basel, Switzerland
RNaseOUT Ribonuclease Inhibitor	10777019	Thermo Fisher Scientific, Darmstadt, Germany
StemPro® Accutase	A1110501	Gibco™ Thermo Fisher Scientific, Darmstadt, Germany

Enzyme	Catalogue number	Producer
SuperScript® II Reverse Transcriptase	18064-022	Thermo Fisher Scientific, Darmstadt, Germany
TrypLE Select (10x)	A12177-01	Gibco™ Thermo Fisher Scientific, Darmstadt, Germany
Trypsin-EDTA 0.05%	25300-054	Gibco™ Thermo Fisher Scientific, Darmstadt, Germany

3.4 Antibodies and Isotype Controls

Antibodies or Isotype Controls	Host	Dilution	Producer and catalogue number
Anti-CD44 antibody [KM201] monoclonal	Rat	1:100	abcam, England ab25340
Anti-Sca1/Ly6A/E antibody	Rat	1:200	abcam, England ab 51317
Anti-Sca-1-PE mouse	Rat	1:10 in 2% FCS in PBS stock solution	Miltenyi Biotec, Bergisch Gladbach, Germany 130-102-832
Anti-CD29-APC-Vio770 mouse	Rat	1:10 in 2% FCS in PBS stock solution	Miltenyi Biotec, Bergisch Gladbach, Germany 130-105-187
Anti-CD44-APC mouse	Rat	1:10 in 2% FCS in PBS stock solution	Miltenyi Biotec, Bergisch Gladbach, Germany 130-102-977
Anti-CD45-PerCP mouse	Rat	1:10 in 2% FCS in PBS stock solution	Miltenyi Biotec, Bergisch Gladbach, Germany 130-102-785
Goat Anti-Rat IgG H&L (Alexa fluor® 488)	Goat	1:500	Abcam, England 982425
Rat IgG2a-PE		1:10 in 2% FCS in PBS stock solution	Miltenyi Biotec, Bergisch Gladbach, Germany 130-103-098
Rat IgG2b-APC		1:10 in 2% FCS in PBS stock solution	Miltenyi Biotec, Bergisch Gladbach, Germany 130-103-085

3.5 Solutions and buffers

Solution or buffers	Reagents
Alcian blue de-staining solution	60 ml 100% Ethanol + 40 ml 96% Acetic acid
Alcian blue staining solution	60 ml Alcian blue stock solution + 40 ml 96% Acetic acid
Alcian blue stock solution	10 mg Alcian blue 8GX + 60 ml 100% Ethanol
Blocking solution for immunocytochemistry	100 ml PBS + 1 g Bovine Serum Albumin + 2.5 ml 20% Triton X-100
Cell cycle solution I	584 mg/ml NaCl + 1 g/l NaCitrate + 0.3 ml/l Nonidet P40 (at RT)
Cell cycle solution II	15 g/l Citric acid + 250 μ l 1 M Saccharose (0.25 M) (1 M Saccharose: 342.3 g/l aqua distilled)
LB agar (pH 7.0)	1 l LB media (pH 7.5) + 20 g Agar
LB media (pH 7.5)	10 g Bacto™ Tryptone + 5 g Bacto™ Yeast extract + 10 g NaCl + 1 l Water
Oil Red O stock solution	0.5 gms Oil Red O + 100 ml 2-Propanol
Oil Red O working solution	60 ml Stock solution + 40 ml Distilled water
Senescence staining solution (pH 6)	1.42 g di-Sodium hydrogen phosphate dehydrate (40 mM) + 200 ml Distilled water + 1.75 g NaCl (150 mM) + 81.32 mg MgCl ₂ (2 mM) + 400 mg Hexacyanoferrat II (5 mM) + 320 mg Hexacyanoferrat III (5 mM) + 100 μ l X-gal (50 mg/ml) to 5ml of Buffer
Stock solution for flow cytometry	2 ml FCS + 100 ml PBS
Substrate solution for alkaline phosphatase staining	1 SIGMA FAST BCIP®/NBT tablet + 10 ml Distilled water
TBE buffer 5x (pH 8.3)	1.1 M Tris + 900 mM Boric acid + 25 mM EDTA

Solution or buffers	Reagents
Tissue (tail-tip) lysis buffer	50 mM Tris pH 8 + 100 mM EDTA + 100 mM NaCl + 1% SDS + 0.5 mg/ml Proteinase K
Washing buffer for alkaline phosphatase staining	0.05% TWEEN® 20 in DPBS without calcium and magnesium

3.6 Chemicals and reagents

Chemical	Catalogue number	Manufacturer
2-Mercapto-ethanol	4227	Carl Roth GmbH + Co. KG, Karlsruhe, Germany
2-Propanol	109634	Merck, Darmstadt, Germany
Acetic acid 96%	100062	Merck, Darmstadt, Germany
Aceton	100014	Merck, Darmstadt, Germany
Agarose	A8963,0500	AppliChem GmbH, Darmstadt, Germany
Agarose (peqGOLD universal)	35-1020	Peqlab Biotechnologie GmbH, Erlangen, Germany
Alcian blue 8GX	A3157-10G	Sigma-Aldrich, Taufkirchen, Germany
Ampicillin	A9393	Sigma-Aldrich, Taufkirchen, Germany
Ampuwa® water	40676.00.00	Fresenius Kabi Deutschland GmbH, Bad Homburg, Germany
Aqua-Poly/Mount	18606	Polysciences, Warrington, USA
Bacto™ Tryptone	211705	BD Biosciences, Heidelberg, Germany
Bacto™ Yeast extract	212750	BD Biosciences, Heidelberg, Germany
Boric acid	100165	Merk, Darmstadt, Germany
Brilliant III Ultra Fast SYBR QPCR master mix	600882	Agilent Technologies Mfg GmbH & Co. KG, Waghäusel-Wiesental, Germany
BSA (Bovine Serum Albumin)	A3059	Sigma-Aldrich, Taufkirchen, Germany

Chemical	Catalogue number	Manufacturer
Chloroform	102445	Merck, Darmstadt, Germany
Citrate acid-monohydrate	1.12014.1000	Merck, Darmstadt, Germany
DAPI (4',6-diamidino-2-phenylindole)	D9542	Sigma-Aldrich, Taufkirchen, Germany
di-Sodiumhydrogen phosphate dehydrate	106576	Merck, Darmstadt, Germany
DMSO (Dimethylsulfoxid)	D2438	Sigma-Aldrich, Taufkirchen, Germany
DNA gel loading dye (6x)	R0611	Thermo Fisher Scientific, Darmstadt, Germany
dNTP	10297-018	Thermo Fisher Scientific, Darmstadt, Germany
DPBS, no calcium, no magnesium	14190-250	Thermo Fisher Scientific, Darmstadt, Germany
DTT 0.1 M	18064-022	Thermo Fisher Scientific, Darmstadt, Germany
EDTA (Ethylenediaminetetraacetic acid)	E5314-500G	Sigma-Aldrich, Taufkirchen, Germany
Ethanol	100983	Merck, Darmstadt, Germany
Ethidium bromide (EtBr)	E1510	Sigma-Aldrich, Taufkirchen, Germany
Glycerol 87%	A0970,1000	AppliChem GmbH, Darmstadt, Germany
GoTaq® Green ,master mix	M7122	Promega GmbH, Mannheim, Germany
Methanol	106009	Merck, Darmstadt, Germany
MgCl ₂	A4425,0250	AppliChem GmbH, Darmstadt, Germany
Na acetate (CH ₃ COONa)	A5268,1000	AppliChem GmbH, Darmstadt, Germany
Na citrate	3580.1	Carl Roth GmbH + Co. KG, Karlsruhe, Germany
NaCl (Sodium chloride)	A2942,5000	AppliChem GmbH, Darmstadt, Germany
NaOH (Sodium hydroxide)	30620	Sigma-Aldrich, Taufkirchen, Germany

Chemical	Catalogue number	Manufacturer
NH ₄ Cl	254134	Sigma-Aldrich, Taufkirchen, Germany
Nonidet P40	21-3277	Sigma-Aldrich, Taufkirchen, Germany
OCT	12351753	Thermo Fisher Scientific, Darmstadt, Germany
Oil Red O	00625-25G	Sigma-Aldrich, Taufkirchen, Germany
Oligo(dT)12-18 primer	18418-012	Thermo Fisher Scientific, Darmstadt, Germany
Paraformaldehyde	A3813, 0250	AppliChem GmbH, Darmstadt, Germany
Potassium hexacyanoferrate II	P9387	Sigma-Aldrich, Taufkirchen, Germany
Potassium hexacyanoferrate III	60299-100G-F	Sigma-Aldrich, Taufkirchen, Germany
PrestoBlue® cell viability reagent	A-13262	Thermo Fisher Scientific, Darmstadt, Germany
Propidium iodide	P3566	Thermo Fisher Scientific, Darmstadt, Germany
Random primers	C1181 P	romega, Mannheim, Germany
Saccharose	S0389	Sigma-Aldrich, Taufkirchen, Germany
SDS (Sodium Dodecyl Sulphate)	17-1313-01	GE Healthcare Biosciences AB, Uppsala, Sweden
SIGMAFAST™ BCIP®/NBT	B5655	Sigma-Aldrich, Taufkirchen, Germany
Staurosporine from Streptomyces sp.	S5921	Sigma-Aldrich, Taufkirchen, Germany
STEM-CELLBANKER®	11890	AMS Biotechnology(Europe) Limited, Oxfordshire, UK
Tris (Tris-(hydroxymethyl)-aminomethane)	A2264,1000	AppliChem GmbH, Darmstadt, Germany
Triton X-100	9002931	Sigma-Aldrich, Taufkirchen, Germany
TWEEN® 20	P9416	Sigma-Aldrich, Taufkirchen, Germany
X-gal	R0401	Thermo Fisher Scientific, Darmstadt, Germany

3.7 Consumables

Product	Manufacturer
96-well plates black	Neolab, Heidelberg, Germany
Adhesive PCR foil seals	Thermo Fisher Scientific, Darmstadt, Germany
Aspiration pipette 2 ml	Sarstedt. Inc., Nuembrecht, Germany
Cell culture flasks T25, T75 (CELLSTAR®)	Greiner Bio-One GmbH, Frickenhausen, Germany
Cell culture plates 6-well, 24-well, 96-well	Falcon™, Corning, United States
Cell scraper 25 cm	Sarstedt. Inc., Nuembrecht, Germany
Combitips advanced 0.1 ml, 0.2 ml	Eppendorf, Hamburg, Germany
Combs for agarose gel electrophoresis	PEQLAB BIOTECHNOLOGIE GmbH, Erlangen, Germany
Cover slips 14 mm	Glaswarenfabrik Karl Hecht GmbH & Co. KG, Sondheim vor der Rhn, Germany
Cryo tubes	Kisker Biotech GmbH & Co. KG, Steinfurt, Germany
FACS tubes BD Falcon™ 5 ml	BD Biosciences, Heidelberg, Germany
Filter paper Whatman 595 125 mm	Whatman GmbH, Dassel, Germany
Filter tips TipOne®	STARLAB GmbH, Hamburg, Germany
Glass slides SuperFrost 76 x 26 mm	Thermo Fisher Scientific, Darmstadt, Germany
MicroAmp® Optical 8-tube strip PCR tubes	Thermo Fisher Scientific, Darmstadt, Germany
MicroAmp® Optical adhesive film	Thermo Fisher Scientific, Darmstadt, Germany
MILLEXGP Filter Unit 0.22 µm	Merck, Darmstadt, Germany
Needle 20 G, 27 G 0.4 mm	Terumo Deutschland GmbH, Eschborn, Germany
Parafilm®	Sigma-Aldrich, Taufkirchen, Germany
PCR 96-Well TW-MT Plate	Biozym, Hessisch Oldendorf, Germany
Petri dishes 10cm	Nunc, Roskilde, Denmark

Product	Manufacturer
Pipettes glass 1, 5, 10, 25, 50 ml (Greiner CELLSTAR®)	Sigma-Aldrich, Taufkirchen, Germany
Reaction tubes 1.5 ml, 2 ml	Eppendorf, Hamburg, Germany
Reaction tubes 15 ml, 50 ml	Greiner Bio-One gmbH, Frickenhausen, Germany
Scalpel, sterile, surgical, disposable	B Braun, Tuttlingen, Germany
Silicone Sealing septa mat	Sigma-Aldrich, Taufkirchen, Germany
Syringe, single-use 1 ml, 5 ml, 10 ml, 50 ml	Henke-Sass Wolf GmbH, Tuttlingen, Deutschland

3.8 Equipment

Device	Manufacturer
¹³⁷ Cs HWM-D 2000 for irradiation	Wlischmiller Engineering, Markdorf, Germany
Alpha Innotech Chemilmager System	Biozym, Hessisch Oldendorf, Germany
Analytical balance	KERN & SOHN GmbH, Balingen, Germany
BD™ LSR II for flow cytometry analysis	BD Biosciences, Heidelberg, Germany
Centrifuge 5415C Rotor: F-45-18-11	Eppendorf, Hamburg, Germany
Centrifuge 5415R Rotor: FA-45-24-11	Eppendorf, Hamburg, Germany
Centrifuge Biofuge pico Rotor: #332513	Heraeus Holding GmbH, Hanau, Germany
Centrifuge MULTIFUGE 3 S-R Rotor: 75006445	Thermo Fisher Scientific, Darmstadt, Germany
Centrifuge Rotina 420 Rotor: 4723	Andreas Hettich GmbH & Co.KG, Tuttlingen, Germany
Centrifuge Rotina 420R Rotor: 4723	Andreas Hettich GmbH & Co.KG, Tuttlingen, Germany
Centrifuge SIGMA 1K15 Rotor: 12024-H	Sigma Laborzentrifugen GmbH, Osterode am Harz, Germany

Device	Manufacturer
Centrifuge SIGMA 3K15 Rotor: 11133	SIGMA Laborzentrifugen GmbH, Osterode am Harz, Germany
Dispenser Multipette® plus	Eppendorf, Hamburg, Germany
Electrophoresis gel system - Horizontal midi gels	PEQLAB BIOTECHNOLOGIE GmbH, Erlangen, Germany
Electrophoresis Power Pac Basic	Bio-Rad Laboratories, Munich, Germany
Heating block Thermomixer compact	Eppendorf, Hamburg, Germany
Incubator 37 °C for bacterial cultures	Heraeus Holding GmbH, Hanau, Germany
Incubator 37 °C, 5% CO ₂ for cell culture	Heraeus Holding GmbH, Hanau, Germany
Incubator 37 °C, 5% CO ₂ , 2% O ₂ for cell culture	Sanyo, ETTEN-LEUR, The Netherlands
Laminar air flow work bench	BDK Luft- u. Reinraumtechnik GmbH, Reutlingen, Germany
Laminar air flow work bench	Thermo Scientific, Schwerte, Germany
Magnetic stirrer	IKA-Werke GmbH & Co. KG, Staufen, Germany
Microscope Axiovert 25	Carl Zeiss, Jena, Germany
Microscope KEYENCE BZ-9000 series	KEYENCE Deutschland GmbH, Neu-Isenburg, Germany
Microscope Laser-Scanning IX81	Olympus, Hamburg, Germany
Microscope Olympus CK2	Olympus, Hamburg, Germany
Microscope Olympus SZX12	Olympus, Hamburg, Germany
Microwave oven TDS M1719N	Samsung, Seoul, South Korea
pH meter Lab850	SI Analytics GmbH, Mainz, Germany
Pipette controller	BRAND GMBH + CO KG, Wertheim, Germany
Pipettes 2, 10, 20, 100, 200, 1000 µl	Gilson, Inc, Limburg, germany
StepOnePlus Real-Time PCR System	Applied Biosystems, Darmstadt, Germany
TECAN Infinity M200 Microplate Reader	Tecan, Mannedorf, Switzerland
Thermal Cycler Veriti® (PCR cycler)	Applied Biosystems, Darmstadt, Germany

Device	Manufacturer
Skylight Super-Blue bluelight LED Transilluminator TFP - 35M 312 nm	Vilber Lourmat Deutschland GmbH, Eberhardzell, Germany
Vortexer Reax top	Heidolph Instruments, Schwabach, Germany
Z Series Coulter Counter - Z1	Beckman Coulter GmbH, Krefeld, Germany

3.9 Commercially available kits

Kit Name	Catalogue number	Producer
BigDye® Terminator v3.1 Cycle Sequencing Kit	4337454	Thermo Fisher Scientific, Darmstadt, Germany
GeneJET Plasmid Miniprep Kit	K0502	Thermo Fisher Scientific, Darmstadt, Germany
Image-iT® LIVE Green Poly Caspases Detection Kit, for microscopy, Molecular Probes®	I35104	Thermo Fisher Scientific, Darmstadt, Germany
QIAamp DNA Blood Mini Kit	51104	Qiagen, Hilden, Germany
QIAquick Gel Extraction Kit	28704	Qiagen, Hilden, Germany
QIAquick PCR Purification Kit	28104	Qiagen, Hilden, Germany
RNase-Free DNase Set	79254	Qiagen, Hilden, Germany
RNeasy Mini Kit 74104	Qiagen,	Hilden, Germany
TOPO® TA Cloning Kit	K4595-40	Thermo Fisher Scientific, Darmstadt, Germany

3.10 Molecular weight and length standards

Marker	Catalogue number	Producer
DNA molecular weight marker VIII Roche	11336045001	Sigma-Aldrich, Taufkirchen, Germany

Marker	Catalogue number	Producer
GeneRuler™ 100bp DNA ladder	SM0241	Thermo Fisher Scientific, Darmstadt, Germany

3.11 PCR array

Product	Catalogue number	Producer
RT ² Profiler PCR Array Mouse Mesenchymal Stem Cells	330231 PAMM-082ZC-2	Qiagen, Hilden, Germany

3.12 Microbiological work

Antibiotic: Ampicillin (50 μ g/ml), Sigma-Aldrich, Taufkirchen, Germany.

Bacteria: One Shot® Top10 chemically competent E.Coli, Thermo Fisher Scientific, Darmstadt, Germany.

Plasmid: pCAG Kosak-td-Tomato vector system (kind gift from Dr. Ingo Burtscher, Institute of Stem Cells Research at Helmholtz Zentrum Muenchen).

3.13 Calibrator cDNA and reference DNA

Pooled DNA from new-born mouse skin as a reference for telomere length assay (kindly provided by Dr. M. Rosemann, Institute of Radiation Biology Helmholtz Zentrum Muenchen).

Pooled embryonic cDNA from BALB/c mice as a calibrator for Real-Time PCR experiments (kindly provided by Dr. M. Rosemann, Institute of Radiation Biology, Helmholtz Zentrum Muenchen.)

3.14 Software

Software	Application	Provider
4Peaks v 1.7	Viewing sequencing files	Nucleobytes, The Netherlands
AxioVisionAC 4.2	Image processing	Carl Zeiss, Germany
BD FACSDiva™ software	Flow cytometry data acquisition	BD Biosciences, Germany
BZ-II Analyzer	Image processing and analysis	KEYENCE Deutschland GmbH, Germany

Software	Application	Provider
Flowing software 2.5.0	Flow cytometry data analysis	University of Turku, Finland
FV10-ASW 2.0	Image processing	Olympus, Germany
GIMP 2.8.4	Image processing and analysis	Open Source
ImageJ - Fiji	Image processing and analysis	Open Source
SPSS statistics client 22	Statistical Analysis	IBM Corp, United States
StepOne software v2.3	Real-Time PCR Data analysis	Applied Biosystems, Germany

3.15 Primers

All the primers were designed using the website http://genscript.com/cgi-bin/tools/primer_genscript.cgi?op=advanced. Annealing temperature for the primers was set at 60 °C. Oligos arrived from the manufacturers in a stock of 100pmol/ μ l and were diluted using RNase-free water to make working concentrations of 1.5, 2.5 or 5 pmol/ μ l.

3.15.1 Genotyping

Gene	Forward primer	Reverse primer	Concentration (pmol)
<i>CreCol</i>	CCTGGAAAATGCTTCTGTCCG TTTGCC	GAGTTGATAGCTGGCTGGTGG CAGATG	5
<i>Rbflox</i>	GGCGTGTGCCATCAATG	AACTCAAGGGAGACCTG	5

3.15.2 Real-Time PCR

For Real-Time PCR reaction to avoid the amplification of genomic DNA ideally the primer should lie on one of the exons or it should span the exon-exon boundaries.

Housekeeping gene

Gene	Forward primer	Reverse primer	Concentration (pmol)
<i>Tbp</i>	ACTTCGTGCAAGAAATGCTG	CTTCACTCTTGGCTCCTGTG	2.5

Stem cell markers

Gene	Forward primer	Reverse primer	Concentration (pmol)
<i>Bmi1</i>	GTCAGCTGATGCTGCCAAT	CCTCTTCTCCTCATCTGCAA	2.5
<i>Klf4</i>	GAACTCACACAGGCGAGAAA	AAAGGCCCTGTCACACTTCT	5
<i>Nanog</i>	TCCAGCAGATGCAAGAACTC	GTGCTGAGCCCTTCTGAATC	5
<i>Nes</i>	CAACTGGCACACCTCAAGAT	GTGTCTGCAAGCGAGAGTTC	2.5
<i>Pou5f1</i>	CGAGTGGAAAGCAACTCAGA	TTTCATGTCCTGGGACTCCT	2.5
<i>Sox2</i>	CCCACCTACAGCATGTCCTA	GTGGGAGGAAGAGGTAACCA	2.5

mMSC specific genes

Gene	Forward primer	Reverse primer	Concentration (pmol)
<i>Abcb1a</i>	CAACATCCACCAGTTCATCG	CTGATGTTGCTTCGTCCAGA	1.5
<i>Bmp2</i>	GAGAACCCAGGTGTCTCCAA	TGACGCTTTTCTCGTTTGTG	5
<i>Bmp6</i>	GAAGGTTGGCTGGAATTTGA	ACCTCGCTCACCTTGAAGAA	5
<i>Csf2</i>	GGCCTTGGAAGCATGTAGAG	CCGTAGACCCTGCTCGAATA	5
<i>Csf3</i>	GTCTCCTGCAGGCTCTATCG	CTGGAAGGCAGAAGTGAAGG	2.5
<i>Eng</i>	GCTGAAGACACTGACGACCA	CCATGTCGATGCACTGTACC	1.5
<i>Fut1</i>	GGCTGCCTACTTAGCTGGTG	GGGGACAAGTCTGCATTGAT	1.5
<i>Fzd9</i>	CCAGCTGTCAAGGTCAGACA	CCTTCTGCCCCTTCTTATCC	1.5
<i>Gdf5</i>	CTGTCCGATGCTGACAGAAA	CGTACCTCTGCTTCCTGACC	5
<i>Gdf6</i>	TGCCAGCTTTTTCCAGTCTT	CCCACCAGCTCTTCTTTGTC	5
<i>Hnf1a</i>	ACCAGTCCCACAGTGTCTC	GCCATCTGGGTGGAGATAAA	1.5
<i>Il6</i>	CCGGAGAGGAGACTTCACAG	CAGAATTGCCATTGCACAAC	1.5
<i>Ins2</i>	TTTGTCAAGCAGCACCTTTG	GGTCTGAAGGTCACCTGCTC	1.5

Gene	Forward primer	Reverse primer	pmol
<i>Itga6</i>	TGAAGATGGGCCCTATGAAG	CTCTTGGAGCACCAGACACA	1.5
<i>Kdr</i>	GGCGGTGGTGACAGTATCTT	GAGGCGATGAATGGTGATCT	5
<i>Mitf</i>	GGACCTTGAAAACCGACAGA	TGATGATCCGATTCACCAGA	5
<i>Ngfr</i>	CTGCTGCTTCTAGGGGTGTC	GTTCACACACGGTCTGGTTG	1.5
<i>Notch1</i>	CCCACTGTGAACTGCCCTAT	CCCCATTCTTGCAGTTGTTT	1.5
<i>Nudt6</i>	GACTCCCGGGATATGCTACA	AACCTCTCGGACTGCTGTGT	1.5
<i>Prom1</i>	TGCGATAGCATCAGACCAAG	TTTGACGAGGCTCTCCAGAT	1.5
<i>Ptprc</i>	GGGTTGTTCTGTGCCTTGTT	GGATAGATGCTGGCGATGAT	2.5
<i>Tbx5</i>	AGGCAGGGAGGAGAATGTTT	GGCTCTGCTTTGCCAGTTAC	2.5
<i>Tert</i>	TGGACCAAGCAAAAACCTTC	AGTGAGCAGGCAGCTGGTAT	5
<i>Tgfb1</i>	TGCGCTTGCCAGAGATTA AAA	CGTCAA AAGACAGCCACTCA	5
<i>Thy1</i>	AACTCTTGGCACCATGAACC	GTTATTCTCATGGCGGCAGT	1.5
<i>Tnf</i>	TATGGCTCAGGGTCCA ACTC	CTCCCTTTGCAGAACTCAGG	1.5
<i>Vwf</i>	CCACTTGCCACAACAACATC	TGGA CT CACAGGAGCAAGTG	1.5
<i>Wnt3a</i>	ATGGCTCCTCTCGGATACCT	GGGCATGATCTCCACGTAGT	2.5
<i>Zfp42</i>	CCCCCTGGAAGTGAGTCATA	TCAGTCTGTGCGAGGGCTCTT	2.5

Lineage specific genes

Gene	Forward primer	Reverse primer	Concentration (pmol)
<i>Cebpa</i>	GAACAGCAACGAGTACCGGGTA	GCCATGGCCTTGACCAAGGAG	5
<i>Fabp4</i>	CCGCAGACGACAGGA	CTCATGCCCTTTCATAAACT	5
<i>Lpl</i>	AGGACCCCTGAAGACAC	GGCACCCAACTCTCATA	5
<i>Pparg</i>	TGCTCAAGTATGGTGTCCATGAG	AGTGCATTGAACTTCACAGCAAA	5
<i>Srebf1</i>	AGCCATGGATTGCACATTT	CACGGACGGGTACATCT	5
<i>Alpl</i>	CGCCAGAGTACGCTCCCGCC	TGTACCCTGAGATTCGT	5
<i>Runx2</i>	CGCCCCTCCCTGAACT	TGCCTGCCTGGGATCTG	5

Telomere length assay

Gene	Forward primer	Reverse primer	Concentration (pmol)
<i>D14Mit224</i>	ATGGCTGTATTTCAATTTTCTGTG	CCTTTAGTGTAGGGACATCTT AGACC	5
<i>Telomere</i>	CGGTTTGTTTGGGTTTGGGTTT GGTTTGGGTTTGGGTT	GGCTTGCCTTACCCTTACCCT TACCCTTACCCTTACCCT	5

Chapter 4

Methods

4.1 Mice

Mice from FVB/N *Rb*^{+/+} and FVB/N *Rb*^{+/-} genotypes were used to isolate primary MSCs from the bone marrow.

4.1.1 FVB/N *Rb*^{+/-} mice

Mice heterozygous for the *Rb1* gene (*Rb1*^{+/-} mice) were obtained by crossing between two transgenic mice lines FVB/N-CreCol x FVB/N-Rb1-LoxP [142] by Dr. M. Rosemann.

4.1.2 B6C3F1 mouse bone marrow

Bone marrow from B6C3F1 background mouse was provided by Dr. M. Rosemann. All the mice were maintained in a breeding colony at the mouse facilities of the Helmholtz Zentrum Muenchen under standard conditions (22 °C, 55% relative humidity and 12 h day/night cycle) by Dr. M. Rosemann and the mouse facility staff. Every cage contained up to 4 mice of the same gender. The mice were fed a normal diet and water ad libidum.

4.2 Cell culture

4.2.1 Cultivation of primary murine mesenchymal stem cells

Primary mMSCs were cultivated and maintained *in vitro* to study the effects of ionizing radiation. MSCs were isolated from the bone marrow of mice sacrificed by CO₂ asphyxiation. To harvest the whole the marrow, both fore- and hind limbs of the mice were dissected, the long bones (femur and humerus) were cleared from adherent soft tissues, and the head of the bone joint was cut with a scalpel (fig. 7). The bone marrow was aspirated with ice-cold DPBS using a 27 gauge needle into a 15 ml Falcon™ tube. The bone marrow aggregate was homogenized into single cells by passing through the needle and then centrifuged at 300 for 5 min. Supernatant was discarded and the cells were resuspended in appropriate amount of DMEM/F-12, GlutaMAX™ media supplemented with 10% MSC Qualified FBS. Total cell number was counted with a coulter counter and the cells were

plated at the density of 3.5×10^5 cells per cm^2 in 6-well plate. The cultures were maintained at 37°C in a humidified atmosphere with 5% CO_2 under 2% O_2 (hypoxia) or 21% O_2 (normoxia). Supernatant containing the non-adherent cells was exchanged with fresh complete media 4 hrs and 16-18 h after mMSCs isolation. This supernatant was cultivated in additional wells to increase the maximum yield of mMSCs by allowing late attaching cells to adhere. For the next 3 days the media were changed 2x a day for original and supernatant mMSC culture (protocol modified from Soleimani and Nadri [143]. After the first 3 days, the cells were continued to grow in the appropriate culture conditions (either in hypoxia or normoxia), and the media was changed 2x a week. All the procedures were performed under aseptic conditions.

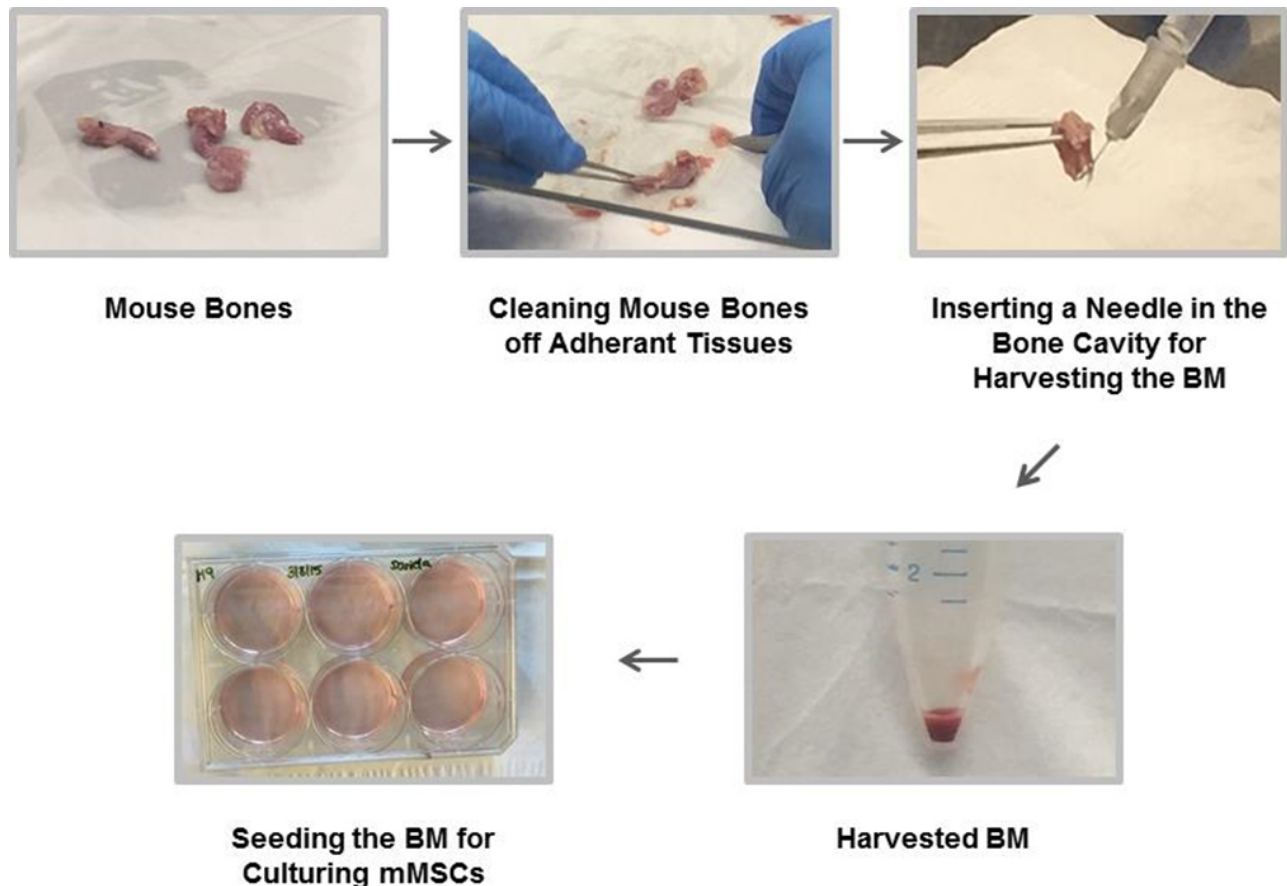


Figure 7: Isolation of murine mesenchymal stem cells from the mouse bone marrow. Graphical representation of the protocol followed for isolating the whole mouse bone marrow and establishment of the mMSC culture *in vitro*.

The age of the mMSCs refers to the period (days) of *in vitro* culturing after the bone marrow isolation or mMSC explantation. Therefore, the terms days of *in vitro* culturing and days after bone marrow isolation or mMSC explantation are used synonymously.

4.2.2 Subculturing of mMSCs

The primary cultures had achieved around 70% - 80% confluency seven days after explantation. For passaging, adherent cells were rinsed with 37°C DPBS and treated with StemPro® Accutase Cell Dissociation Reagent for about 10 minutes (min) at 37°C . 10 ml of StemPro® Accutase was

added per 75 cm² surface area of the cell culture flask. Following incubation, the detached cells were collected, centrifuged at 300 g for 5 min and resuspended in fresh complete MSC media. The resuspended cells were subcultured in new culture flasks. The cultures were continued according to the standard protocol with twice weekly medium change and the cells were passaged when the cultures reached near confluency.

4.2.3 Cell counting

The total cell number was determined using Z1 Series COULTER COUNTER. For cell counting, 200 μ l of cell suspension was diluted with 7.8 ml of 0.9% W/V NaCl solution. Cell plus NaCl mixture was used for automatic counting of cells within a range of 7 μ m to 20 μ m. For the final count the number of cells present per ml was multiplied with the total volume of cell suspension.

4.2.4 Freezing and thawing of mMSCs

Adherent mMSCs were detached using StemPro® Accutase reagent and the cell number was determined. After centrifugation at 300 g for 5 min the cells were resuspended at 1-2*10⁶ cells/ml in STEM-CELLBANKER® reagent. The cell suspension was placed in a 1 ml cryo tube and the tube was immediately transferred to -80 °C for further storage. This reagent is relatively easy to use as it doesnt require controlled rate freezing.

To thaw the frozen cells the cryo tube was warmed in 37 °C water bath for 1-2 min by gentle whirling. The cell mixture was then added drop by drop to a Falcon™ tube containing 10 ml of the fresh MSC medium. After centrifugation at 300 g for 5 min, the supernatant was discarded; the pelleted cells were resuspended with fresh complete growth medium and finally distributed into the new cell culture flasks. The next day medium was replaced to remove the remnants of stem cell banker reagent.

4.3 PrestoBlue® cell viability assay

PrestoBlue® cell viability assay was performed to compare mMSC growth in hypoxic and normoxic culture conditions. PrestoBlue® reagent is a resazurin-based solution which is modified by the reducing environment of the viable living cell and can be used as an indicator to quantify the viable cells present in a culture at a specific time point. It doesnt require cell lysis providing a possibility to monitor the living cells. *Rb1*^{+/-} mMSCs were initially grown in hypoxic atmosphere for 9 days since their explantation from the bone marrow (hypoxia pre-conditioning). On day 9, the cells were passaged into hypoxic and normoxic conditions. For this first passaging, 4000 mMSCs were seeded per well into 96-well plates and continued to grow in either 2% or 21% O₂. Three days after cell seeding PrestoBlue® cell viability assay was performed following manufacturers protocol. To perform the assay, cell medium was replaced with PrestoBlue® cell viability reagent diluted with complete mMSC culture media. The cells were incubated for 30 min. After the incubation, fluorescence was measured with Tecan Infinite M200 microplate reader at 560 nm excitation and 590 nm emission wavelength. Once the readings were taken the PrestoBlue® solution was removed from the wells and fresh complete media was added. The cells were returned to the incubators for continuing the

growth. This procedure was repeated every 2 days till day 13 and final reading was taken on day 14 (after cell seeding). Same procedure was repeated for hypoxia pre-conditioned passage 2 (day 19 after explantation) mMSCs. 4000 cells in mMSC media without PrestoBlue® reagent was used as an internal control. Wells with 100 μ l of mMSC media without cells were used to calculate the background fluorescence. The data collected over two weeks was processed and the values were used to plot the result (days vs. relative fluorescence units) for studying the number of viable mMSCs in hypoxic and normoxic conditions.

4.4 Flow cytometry analysis of the cell cycle

To investigate the effect of oxygen concentration on cell cycle distribution in mMSCs, flow cytometry analysis of the cell cycle was performed. The cell cycle analysis was carried out using the propidium iodide staining technique. Propidium iodide is a fluorescent DNA binding dye that intercalates between the bases without any sequence preference. To perform the analysis, hypoxic and normoxic mMSCs were detached using StemPro® Accutase reagent at the required time points and cell number was assessed by coulter counter. Approximately 3×10^4 cells were used for cell cycle analysis. 500 μ l of solution I, freshly mixed with 0.5 μ l of RNase (1 g/l) and 25 μ l of propidium iodide (1 mg/ml), was added to the pelleted cells. Solution I contains sodium citrate as a buffer to fix the cells and a detergent nonidet P40 to permeabilise the cells and the nuclear membrane for entry of propidium iodide. The mixture of cells and solution I was mixed thoroughly, and the cells were incubated at Room Temperature (RT) for 1 hour (h) in the dark. After an hour the cells were centrifuged at 300 g for 5 min and the supernatant was removed. Pelleted cells were mixed with 500 μ l Solution II containing 25 μ l of propidium iodide (1 mg/ml). Samples were placed on ice until the cell cycle analysis was performed using BD™ LSR II. Alternatively, the samples were stored for up to 10 days at 4 °C in dark. Propidium iodide was excited using standard blue 488-nm laser of the LSR II. For each sample 10^4 events were counted. Data was acquired using BD FACSDiva™ software. Data analysis was carried out with Flowing Software 2.5.0. Cell cycle analysis protocol was adapted from Giaretti et al. [144].

4.5 Irradiation

In this project medium (0.5-5 Gy) and low (0.05-0.5 Gy) doses of ionizing radiation were applied. The dose classification system was used as described by Kadhim et al. [129]. Gamma-irradiation was performed at the irradiation facilities of the Helmholtz Zentrum Muenchen with a ^{137}Cs γ -source HWM D-2000 irradiator. The dose rate delivered was calibrated at 0.5 Gy/min. Doses used was from 0.1 Gy to 4 Gy. Control cells (0 Gy) were sham irradiated by taking the control cultures to the irradiation facility along with the samples but without exposing them to γ -irradiation. Irradiation was carried out at RT. As mMSCs are observed to be oxygen sensitive the gas exchange during irradiation process was minimized by sealing the cell culture flasks with parafilm. After irradiation the cells were incubated in appropriate oxygen condition (2% O_2 or 21% O_2) and 5% CO_2 at 37 °C.

4.6 Molecular biology techniques

4.6.1 Mice genotyping

To establish the retinoblastoma genotype of FVB/N mice allele-specific PCR was carried out. Mouse genotype was identified depending on the presence and location of DNA fragments in comparison with DNA molecular weight marker. Based on their genotypes mice were used to isolate the primary mMSCs. Some of the mice used in this project were genotyped by Dr. M. Rosemann.

4.6.2 DNA isolation

DNA isolation from mouse tail tips

For establishing the *Rb* and *Cre* genotype status about 2 mm long tail tip was cut off from each mouse that has to be genotyped by Dr. M. Rosemann. To extract the DNA from mouse tail tip, initially the tail tip was digested overnight in 750 μ l of tail-tip lysis buffer at 55°C using a thermomixer at 500 rpm. Next day 250 μ l of 6M saturated NaCl was added, mixed thoroughly and the samples were centrifuged at 4 °C and 1300 rpm. The DNA was precipitated from the supernatant by adding 1 ml of 100% ethanol to the reaction tube and centrifuged once again at highest speed for 10 min. The pellet was washed with 500 μ l of 75% ethanol by keeping the reaction tube for 15 min at RT. Then ethanol was removed, pellet was air dried and finally resuspended in 800 μ l double distilled water by mixing with a thermomixer. The DNA concentration was measured with Tecan Infinite M200 microplate reader.

DNA isolation from cells

DNA was extracted from the cells using the QIAamp DNA Blood Mini Kit with manufacturers protocol for cultured cells. At first, cultured mMSCs were harvested using a cell scraper into ice-cold PBS. The cell suspension was centrifuged at 300 g for 5 min and the pelleted cells were resuspended in PBS to a final volume of 200 μ l, and 20 μ l of proteinase K was added to this solution. The solution was mixed with 200 μ l of buffer AL by vortexing to lyse the cells. To yield maximum DNA, the mixture was incubated at 56 °C using a thermomixer for 10 min. 200 μ l of 100% ethanol was added to the reaction tube and it was once again pulse-vortexed. The mixture was applied to QIAamp mini spin columns and centrifuged at 6000 g for a minute. The filtrate was discarded and the column was washed with 500 μ l buffers of AW1 and AW2 respectively. Finally, DNA was eluted from the column with 50 μ l of DNase-free water by centrifugation for a minute at 6000 g. The DNA concentration and purity was measured with Tecan Infinite M200 microplate reader. Eluted DNA was stored at -20 °C.

4.6.3 RNA isolation

RNA isolation from cells

RNA was isolated from the cells using the RNeasy Mini Kit and RNase-Free DNase Set. The manufacturers protocol was slightly modified to make it suitable for mMSCs. Briefly, adherent cells were harvested in a 1.5 ml reaction tube with StemPro® Accutase reagent. Lysis buffer was prepared

beforehand by adding 1 μl of 2-Mercapto-ethanol to 100 μl RLT buffer supplied with the kit. 350 μl of lysis buffer was added to mMSC cell pellet and the tube was slightly vortexed. The mixture was then passed 5-10 times through a 20 gauge needle. 1 volume of 70% ethanol was added and mixed by pipetting. The solution was transferred to an RNeasy spin column and centrifuged at 8000 g for 15 sec. The flow-through was discarded and the column was washed with 700 μl of buffer RW1. To digest any DNA left behind in a column, 10 μl of DNase I in 70 μl of RDD buffer was added to the column and it was incubated for 15 min at 25 °C. Following incubation the column was washed with buffer RW1. One more wash was performed with buffer RPE at 8000 g to wash the column membrane. Finally, the RNA was eluted in 30 μl of RNase-free water. All the reactions were performed on ice to avoid RNA digestion. RNA concentration and purity was measured with Tecan Infinite M200 microplate reader. Purified RNA was stored at -80 °C.

4.6.4 Nucleic acid concentration measurement

Nucleic acid (either DNA or RNA) yield and purity was measured by absorbance method with Tecan Infinite M200 microplate using its NanoQuant plate. 1 μl of nucleic acid is sufficient to calculate the concentration and purity with this instrument. Nucleic acids absorb light most actively at 260 nm. Hence, absorbance readings were taken at A260nm to determine the concentration and at A280nm to confirm the quality. Good-quality nucleic acids have an A260/A280 ratio between 1.7-2.0. Higher or lower ratios may indicate the presence of contaminants such as proteins, salts or lipids.

4.6.5 PCR

PCR for genotyping

DNA extracted from the mouse tail tip was used as a template for a PCR reaction. To execute the PCR, standard reaction mixture was used as given in table 4.1:

Table 4.1: PCR reaction mixture

Reagent	Quantity (μl)
Master mix (GoTaq® Green) 2x	10
Forward primer (5 pmol)	1
Reverse primer (5 pmol)	1
Nuclease free water	7
Template DNA (20 ng/ μl)	1
Total volume	20

GoTaq® Green Master Mix is a premixed ready-to-use solution containing dNTPs, MgCl₂, reaction buffers, and bacterially derived Taq DNA polymerase at optimal concentrations to carry out

the DNA amplification. Primer sequences used for DNA amplification are given in the materials section 3.15.1. PCR reaction was performed with Veriti® Thermal Cycler using a program given in table 4.2.

Table 4.2: PCR reaction program

Cycles	Step (μ l)	Temperature ($^{\circ}$ C)	Time
1x	Initialisation	96	1 min
35x	Denaturation	94	10 sec
	Annealing	60 (for <i>Rb</i>), 64 (for <i>Cre</i>)	15 sec
	Elongation	72	2 min
	Final hold	4	

4.6.6 Agarose gel preparation and electrophoresis

Agarose gel electrophoresis is the most widely used technique for separating DNA and RNA fragments based on their size and length. Nucleic acids have a negatively charged backbone, hence when an electric field is applied they will migrate away from the cathode to the positively charged anode. Due to their uniform mass/charge ratio they are separated by size inside an agarose gel in a pattern such that the distance travelled is inversely proportional to the log of its molecular weight [145].

To prepare 1.5% or 2% agarose gel 1.5 g or 2 g of agar was weighed with an analytical balance. Agar was gently added into 100 ml of electrophoresis buffer (1x TBE) while stirring continuously. The mixture was boiled in a microwave oven to dissolve the agar. This solution was allowed to cool slightly (around 60 $^{\circ}$ C-70 $^{\circ}$ C) whilst stirring on a magnetic rotor and 9 μ l of EtBr (0.5 g/ml working concentration from a stock solution of 10 mg/ml) was added to the mixture. When the EtBr was dissolved the solution was poured into a gel casting tray holding a well-comb. The well-comb was chosen depending on the number and amount of DNA samples to be run. The gel was left to solidify at RT for around 30 - 35 min. When the gel was solidified the well-comb was removed and the gel was immersed in an electrophoresis chamber filled with 1x TBE buffer along with the casting tray. Before loading the samples, both DNA samples (10 μ l for 1.5 mm thick well) and 3 μ l of DNA molecular weight marker VIII were mixed with an appropriate amount (0.2 volume of the sample) of 1x DNA Gel loading dye. Once the samples and the marker were loaded on the gel then the electrophoresis was performed using a Horizontal Midi Gel Electrophoresis system at 90 volts for around 60 min. Separated DNA segments in a gel were detected and visualised under UV light using the Alpha Innotech Chemilmager transilluminator System.

4.6.7 Reverse transcription

The RNA isolated from mMSCs (section 4.6.3) was used for reverse transcription reaction. In reverse transcription reaction, the enzyme SuperScript® II Reverse Transcriptase uses RNA as a template and synthesizes the cDNA. Newly synthesized single stranded cDNA can be used to perform Real-Time PCR reaction and quantify expression of various transcripts. To perform cDNA synthesis around 100ng of RNA was used for every sample. Initially, required volume of RNase-free water was added in the samples to make up the reaction volume to 8 μ l. The samples were further mixed by pipetting with 1.5 μ l of each Oligo dT (0.5 μ g/ μ l) and Random primers (20 ug). The reaction tubes were placed in 70 °C thermomixer for 2 min and then left at RT for 10 min. At this step the primers will start annealing the RNA template. Meanwhile a reverse transcription mixture was prepared as in table 4.3.

Table 4.3: Reverse transcription reaction mixture

Reagent	Quantity (μ l)
F-S-Buffer (5x diluted)	4
DTT (0.1 M)	2
dNTPs (10 μ M)	1
Rnase Out (RNase inhibitor)	1
SuperScript® II Reverse Transcriptase	1
Total volume	9

Following the incubation at RT, the samples were combined with 9 μ l of reverse transcription mixture which makes the final reaction volume to 20 μ l. The mixture was mixed thoroughly and incubated at 42 °C for an hour. Finally, heat inactivation of the elongation reaction and denaturation was performed by exposing the reaction tubes to 95 °C for 5 min. Newly synthesized cDNA can be stored at -20 °C till further use.

4.6.8 Real-Time Polymerase Chain Reaction (Real-Time PCR)

Real-Time Polymerase Chain Reaction (Real-Time PCR) is a technique used to measure the quantity of a DNA template. When combined with a reverse transcription reaction where cDNA is synthesized using RNA as a template this method, also known as Real-Time RT-PCR, is used to quantify RNA and to evaluate gene expression. Therefore, in Real-Time PCR either the DNA extracted directly from the cells or cDNA synthesized in reverse transcription reaction is used as template. Later, this DNA is exponentially amplified using specific primers.

The reaction mixture used to perform Real-Time PCR amplification is as in table 4.4:

20 μ l of Real-Time PCR mix containing the relevant template was added into a well of a StepOnePlus compatible 96-well plate. Every sample was run as technical duplicates. The plate

Table 4.4: Real-Time PCR reaction mixture

Reagent	Quantity (μ l)
Brilliant III Ultra Fast SYBR QPCR master mix	10
Primer mixture [Forward primer (1.5 or 2.5 or 5pmol/ μ l) + Reverse primer (1.5 or 2.5 or 5pmol/ μ l)]	1.5 or 2
Water	5.2 or 5.7
Reference dye	0.3
Template DNA	2 or 3
Total volume	20

was covered with MicroAmp® Optical Adhesive Film to avoid sample evaporation. After a brief centrifugation at 1000 rpm to get the entire sample at the bottom of the well, the plate was placed in StepOnePlus Real-Time PCR System. Real-Time PCR reaction was performed with a pre-designed program that is same for all primers to be quantified and includes following steps as in table 4.5:

Table 4.5: Real-Time PCR reaction program

Steps		Temperature ($^{\circ}$ C)	Time
Holding stage (initial denaturation)		95	10 min
Cycling stages I 40x	Cycling stage (denaturation)	95	15 sec
Cycling stages II 40x	Cycling stage (annealing and elongation)	60	1 min
Melt curve stage I		95	15 sec
Melt curve stage II		60	1 min
Melt curve stage III		95	15 sec

The cycling step was repeated 40x for the amplification of a cDNA template. This method can quantify PCR product produced during each cycle. Once the complete program was run the data was collected from StepOnePlus instrument and analysed using StepOne software v2.3.

Real-Time RT-PCR measurement of mMSC transcript expression

The expression of various transcripts in hypoxic mMSCs at different time points of *in vitro* culturing was measured with the Real-Time RT-PCR method. Here, pooled embryonic cDNA was used as the calibrator for experimental quality control and reference. TBP (TATA Box binding protein) which is stably expressed was employed as a housekeeping gene to control the cDNA quality across different experiments. RNase-free water was used as a NTC to detect unspecific amplification.

Telomere length measurement by Real-Time PCR

For telomere length measurement the DNA was isolated on various time points from *in vitro* cultured mMSCs grown in two different oxygen tensions (as described in section 4.6.2). The extracted DNA was used as a template to determine the telomere length of mMSCs by RT-PCR method [146]. To perform the RT-PCR amplification, forward and reverse telomeric primers each with 5pmol/ μ l concentration annealing to the typical telomeric sequence of (TTAGGG) $_n$ were used. Additionally, forward and reverse primers (each 5 pmol/ μ l) for genomic microsatellite marker, D14Mit224, were used as an internal control to normalize the telomeric length to genomic DNA in separate reactions. Real-Time PCR reactions were carried out as described above. To measure the length to mMSC telomere, pooled DNA from new-born mouse skin was used as a reference. For better estimation, pooled DNA was assigned as 100 Arbitrary Units (AU). RNase-free water was used as a NTC to detect unspecific amplification. The final calculation to determine the telomeric length was performed with the CT method.

Data analysis and quantification of Real-Time RT-PCR target amplification

SYBR green is a fluorescent dye which binds to the double-stranded DNA molecule and upon binding emits a fluorescent signal. This signal can be measured during each cycle. The signal intensity is proportional to the amount of PCR product formed. This allows accurate quantification of the level of starting nucleic acid template. Before calculating the target DNA template concentration, the raw data was analysed using StepOne software v2.3. The baseline and threshold were adjusted separately for each gene to be analysed. The baseline was set in such a way that the amplification plot was considered to start at the cycle number higher than the baseline cycle number. The threshold was set above the background but below the plateau of the amplification plot within a linear region of the curve (fig. 8).

The threshold cycle (C_T) was defined as the PCR cycle value at which the amplification curve crosses a set threshold. To determine the quality and specificity of Real-Time PCR reaction, the cycling program was followed by melting curve analysis. Normally, in the absence of primer-dimers or non-specific amplifications only a single peak for an amplified product of the target gene is visible (fig. 9). If present, primer-dimers or unspecific products appear as several multiple peaks in melting curves of both sample and No Template Control (NTC).

An actual measurement of the quantity of starting nucleic acid template was obtained using a comparative method ($\Delta\Delta C_T$) of relative quantification [147]. The calculation was performed as follows:

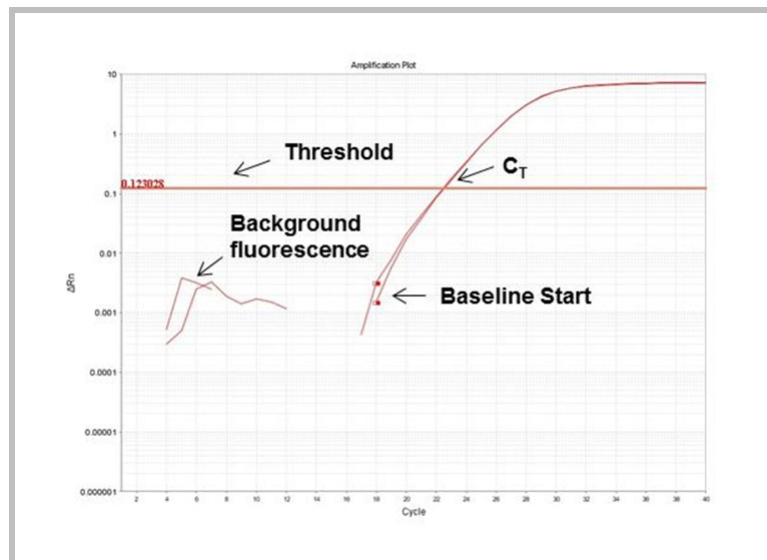


Figure 8: Real-Time PCR amplification plot. A graph showing a set threshold, background fluorescence and a baseline start for the sample after the Real-Time PCR reaction.

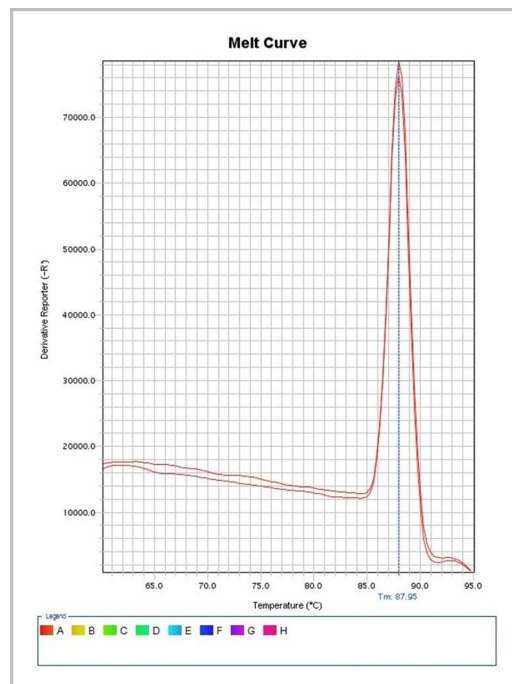


Figure 9: Real-Time PCR melting curve. A graph showing melting curve analysis for a Real-Time PCR reaction. It displays a single peak for the sample run in technical duplicates.

housekeeping gene : TBP (for measurement of mMSC transcript expression) or Genomic microsatellite marker, D14Mit224 (for telomere length measurement).

calibrator : Pooled embryonic cDNA (for measurement of mMSC transcript expression) or Pooled DNA from new-born mouse skin (for telomere length measurement).

$$\Delta C_{T\text{sample}} = \Delta C_{T\text{target gene}} - \Delta C_{T\text{housekeeping gene}}$$

$$\Delta C_{T\text{calibrator}} = \Delta C_{T\text{target gene}} - \Delta C_{T\text{housekeeping gene}}$$

target gene: DNA template expression to be measured

CT is used to normalize for the amount of nucleic acid template or calibrator used.

Now, $\Delta\Delta C_T$ was determined for each sample by:

$$\Delta\Delta C_T = \Delta C_{T\text{sample}} - \Delta C_{T\text{calibrator}}$$

$\Delta\Delta C_T$ describes the difference between the average ΔC_T value of the sample replicates and the average ΔC_T value of the calibrator. For relative quantification all the samples were normalized to the calibrator value.

Finally, the normalized level of target gene/transcript expression (fold change) was calculated by:

$$\text{Fold change} = 2^{\Delta\Delta C_T}$$

Hence, the fold change in the gene expression level of the sample was normalized to the housekeeping gene and was relative to the calibrator.

4.7 Histochemical stainings

4.7.1 Differentiation assays and stainings

To validate the mMSC model system it is necessary to demonstrate the trilineage differentiation of mMSCs *in vitro*. Therefore, mMSCs were seeded in required numbers into the wells of 24- or 96-well plates. The cells were allowed to attach and afterwards induced to differentiate with appropriate differentiation medium. For control purposes the mMSCs were grown in standard mMSC medium for the entire duration without any differentiation medium. All cells used for differentiation assays were cultured at 37 °C with 5% CO₂ under hypoxic atmosphere. The differentiation potential of mMSCs was determined using standard differentiation assays as follows:

Evaluation of osteogenic differentiation with alkaline phosphatase staining

Proliferating osteoblasts show alkaline phosphatase [148] activity which can be detected using BCIP®/NBT as a substrate. This substrate stains the cells undergoing osteoblastic differentiation violet blue in colour due to the presence of enzyme alkaline phosphatase making them easy to identify, while the mMSCs appear colourless.

6×10^3 cells were seeded per well in 24-well plates and grown in standard mMSC media for next 2 days. On day 3, the cells were stimulated with StemPro® Osteocyte/Chondrocyte Differentiation Basal Medium supplemented with StemPro® Osteogenesis Supplement. This culture medium was replaced 3x per week for up to two weeks. On day 14, alkaline phosphatase staining was performed on both induced and control cells according to PromoCells application note for Osteoblast differentiation and mineralization. In brief, the substrate for the detection of alkaline phosphatase activity was prepared by dissolving SIGMA FAST BCIP®/NBT tablet in 10 ml distilled water. Following

a wash with DPBS, the cells were fixed with 500 μ l of 4% paraformaldehyde for 2 min. Longer fixation was avoided as it could inactivate the alkaline phosphatase activity. Fixed cells were washed with 1 ml of washing buffer (0.05% TWEEN® 20 in DPBS w/o calcium and magnesium) and incubated with BCIP®/NBT substrate at RT for 10 min. After a wash cells staining for alkaline phosphatase activity were observed under a microscope.

Evaluation of adipogenic differentiation with Oil Red O staining

To induce adipogenic differentiation, 5×10^4 mMSCs were seeded per well in 24-well plates. The cells were allowed to grow for 2 days in standard mMSC media. On day 3, the cells were incubated with StemPro® Adipocyte Differentiation Basal Medium supplemented with StemPro® Adipogenesis Supplement. The culture medium was changed 3x per week for two weeks. On day 15, Oil Red O staining was performed on both induced and control cells to reveal adipocytes present in the culture. Following a wash with DPBS, the cultures were fixed with 500 μ l of 4% paraformaldehyde for 1 hr. Paraformaldehyde was removed and 1 ml of Oil Red O staining solution was added to cover the well. After 45 min incubation at RT, the staining solution was aspirated and the cells were washed with water. When observed under a microscope the lipid vacuoles present in adipocytes appear bright red in colour due to staining with Oil Red O.

Evaluation of chondrogenic differentiation with alcian blue staining

Murine mesenchymal stem cells undergoing chondrogenic differentiation produce cartilage extracellular matrix that contains the proteoglycan aggrecan. This molecule can be stained an intense blue with the copper-containing dye alcian blue.

To stimulate chondrogenic differentiation a 10 μ l drop containing 8×10^4 mMSCs from MSC cell suspension was seeded as a single spot per well of 96-well plate. For maintaining humidity the plate was sealed with a parafilm around the edges and kept at 37 °C in hypoxic condition. After 2 hrs of incubation, attached cells were stimulated using StemPro® Osteocyte/Chondrocyte Differentiation Basal Medium supplemented with StemPro® Chondrogenesis Supplement. The culture medium was changed 3x per week up to three weeks. On day 21 alcian blue staining was performed on both induced and control cells according to PromoCells application note for Chondrogenic differentiation and analysis of MSC. Following a wash with PBS, the cultures were fixed with 100 μ l of 4% paraformaldehyde for 1 hr. Paraformaldehyde was removed and 100 μ l of alcian blue staining solution was added to the wells. The cultures were incubated with the staining solution overnight in dark at RT. Next day, the staining solution was aspirated and cells were washed twice with 100 μ l of de-staining solution for 20 min at RT. The cells were observed with microscopy after air drying.

4.7.2 Giemsa staining

The giemsa stain is commonly used in histology because it produces high quality staining of the chromatin and nuclear membrane [149]. To stain mMSC colonies with giemsa, the media was aspirated from the culture flasks and the colonies were washed 1x-2x with PBS. The cells were fixed by adding 100% ethanol for minimum 15 - 20 min. Ethanol was removed and the colonies were

allowed to dry for an hour. Giemsa staining solution (5-10% solution of giemsa in PBS) sufficient to entirely cover the cells was added to the colonies. After 15 min the stain was discarded and the cells were washed with a tap water. Following overnight drying the colonies can be observed under a bright-field microscope.

4.7.3 Senescence associated beta-galactosidase staining (SA- β -gal staining)

Senescence staining was performed to study the effects of oxygen tension and ionizing radiation on the onset of senescence in mMSCs. One of the defining characteristic of senescent cells is the expression of SA- β -galactosidase which can be detected due to the formation of an insoluble bluish precipitate by the cleavage of the chromogenic substrate X-Gal [88].

The senescence staining solution was prepared with reagents listed in section 3.5. At first, 1.42 g of di-Sodiumhydrogen Phosphate dihydrate (40 mM) was dissolved in 200 ml of distilled water with the help of a magnetic stirrer and the pH was adjusted immediately at 6 using 1 M Citric acid. To this solution, 1.75 g NaCl (150 mM), 81.32 mg MgCl₂ (2 mM), 400 mg hexacyanoferrat II (5 mM) and 320 mg hexacyanoferrat III was added one after the other and dissolved completely. The addition of hexacyanoferrat III changes the colour of the solution to yellow. Later, 100 μ l X-gal (50 mg/ml) was mixed with 5 ml of the staining solution to prepare the final senescence staining buffer.

To investigate the role of oxygen and irradiation on senescence induction, 6 days-old 1.2×10^3 mMSCs from hypoxic and normoxic conditions were seeded in the wells of a 96-well plate and continued to grow in the same condition. Around 24 h after cell seeding both hypoxic and normoxic cells were exposed to different doses of γ -irradiation (0.1 Gy, 0.2 Gy, 0.5 Gy, 2 Gy and 4 Gy). The control cells were sham-irradiated. When the culture became subconfluent they were washed 2x with 100 μ l of cold PBS and fixed at RT with 100 μ l of 4% formaldehyde for 10 min. After washing 2x with PBS, 100 μ l of staining solution was added to completely cover the cell monolayer and the culture plates were left to stain for 12 hrs in 37 °C incubator. On the following day, the senescent cells were clearly visible under a microscope due to their greenish blue appearance. The senescent cells were counted relative to the total cell number as seen under bright-field microscopy.

4.8 Surface marker expression analysis of mMSCs

Murine mesenchymal stem cells are known to express surface markers such as Sca1, CD44 while they lack hematopoietic and endothelial cell markers on their surface. Investigating the surface marker expression of *in vitro* cultured mMSCs is an important step to validate the mMSC model system. In this project the surface antigen expression of mMSCs was analysed with two methods as described below-

4.8.1 Surface marker analysis by immunocytochemistry

Immunocytochemistry was performed on mMSCs to analyse the expression of antigens CD44 and Sca1 on the surface of *in vitro* cultured mMSCs.

Twenty one days old 2×10^5 mMSCs were seeded on a 14 mm diameter cover slip placed inside a well of the 24-well plate. The well was filled with 1 ml mMSC growth medium and the plate was

incubated for two days at 37 °C in hypoxia to allow the cell proliferation. On day 3, the medium was aspirated and cells growing on a coverslip were washed 2x with 1 ml PBS. After the wash cells were fixed with 500 μ l of 4% paraformaldehyde for around 10 min at RT. Once the cells were fixed, the paraformaldehyde was discarded followed by 3x wash with PBS. After the wash, the coverslip along with adhered mMSCs was carefully lifted from the well and placed in a self-made humidified chamber constructed using a 100mm petri dish.

Treatment with primary antibody and blocking buffer

Primary antibody solution was prepared by diluting the required antibody in 1% blocking buffer (table 4.6). 150 μ l of the appropriate primary antibody solution was added on the coverslips placed in a humidified chamber. The humidified chamber was then transferred either to a refrigerator or a cold room for an overnight incubation in dark at 4 °C taking care that the antibody solution would remain on the top of a coverslip.

Treatment with secondary antibody

Next day, primary antibody solution was aspirated. The cells were then washed with 100 μ l of PBS and 150 μ l of secondary antibody solution was added to the coverslips. Secondary antibody solution was prepared by mixing Goat Anti-Rat IgG H&L (Alexa fluor® 488) antibody with 1% blocking buffer in 1:500 dilution (table 4.6). After 2 h at 4 °C in dark the coverslip was once again washed with PBS. The cells with only secondary antibody were used as experimental controls which allowed excluding auto fluorescence as a cause for the observed signal from the primary antibody.

Table 4.6: Immunocytochemistry antibodies for mMSC surface marker expression

Primary antibody	Concentration in blocking buffer	Secondary antibody
Anti-CD44 antibody [KM291] ab25340 Rat monoclonal	1:100	Goat Anti-Rat IgG H&L (Alexa fluor® 488) 1:500
Anti-Sca1/Ly6A/e antibody [E13 161-7] ab 51317 Rat monoclonal	1:200	Goat Anti-Rat IgG H&L (Alexa fluor® 488) 1:500

DAPI treatment

For counter-staining of nuclei the coverslips of both samples and controls were treated with 150 μ l of DAPI solution (1 μ l DAPI in 10 ml PBS). After 10 min incubation at RT the DAPI solution was removed and cover slips were rinsed 2x with PBS.

Visualisation of immunocytochemistry and image acquisition

To visualise the immunocytochemical staining a drop of Aqua-poly/mount was placed in the middle of the 76 x 26 mm glass slide and the coverslip was gently mounted. The staining was observed under a laser-scanning confocal microscope. Images were acquired at 20x (CD44) or 40x (Sca1) magnification with FV10-ASW 2.0 software and processed using Gimp software version 2.8.4.

4.8.2 Surface marker analysis by flow cytometry

The surface marker expression of mMSCs was also analysed by flow cytometry. To examine the surface antigen expression, antibodies against Sca1, CD44, CD29 and CD45 surface antigens were tested. Murine Embryonic Stem Cell (mESC) line ES-E14TG2A passage 27 was used as a positive control for CD29 expression and a negative control for Sca1 and CD44 expression. These cells lack expression of CD45 which is also absent on mMSCs. In addition, secondary antibody controls for each cell line and one unstained control for mMSCs was used in the experiment.

Cells were harvested using appropriate cell detaching reagent (StemPro® Accutase for mMSCs and 1x Trypsin for mESCs) and counted by coulter counter. After 2x wash with 500 μ l of flow cytometry stock solution, the cells were resuspended in 50 μ l of primary antibody solution. This mixture was incubated in the dark for 10 min in a refrigerator (2-8 °C). Following the incubation, the cells were washed 2x with 500 μ l of flow cytometry stock solution. The supernatant was aspirated after each wash. Finally, the cells were mixed in 500 μ l of flow cytometry stock solution and surface marker expression was immediately measured with a BD™ LSR II flow cytometer. The antibodies used for surface marker expression analysis by flow cytometry were all attached with a fluorophore and can be detected directly by laser excitation making it unnecessary to apply any secondary antibody. These antibodies were excited either by a blue or a red laser depending on the fluorophore. Detailed information of the antibodies is given in table 4.7. Around 5×10^3 events were counted for each sample and control. Data acquisition was done using BD FACSDiva™ software. This experiment was performed with the help from Dr. Wolfgang Beisker. Final data analysis was performed with Flowing Software 2.5.0.

Table 4.7: Flow cytometry antibodies for mMSC surface marker expression

Antibodies	Dilution
CD44-APC mouse	1:10 in 2% FCS in PBS stock solution
CD45-PerCP mouse	1:10 in 2% FCS in PBS stock solution
CD29-APC-Vio770 mouse	1:10 in 2% FCS in PBS stock solution
Anti-Sca-1-PE mouse	1:10 in 2% FCS in PBS stock solution
Rat IgG2b-APC	1:10 in 2% FCS in PBS stock solution
Rat IgG2a-PE	1:10 in 2% FCS in PBS stock solution

4.9 Clonogenic survival assay

The colony forming ability of mMSCs in different oxygen conditions and after ionizing radiation exposure was assessed by the clonogenic survival assay. Usually clonogenic survival assay is performed with higher starting cell number for high doses of irradiation to obtain the same number of colonies after the treatment. However, in this project the clonogenic assay was performed with similar cell number for all doses of irradiation to maintain the biology of mMSC growth.

To study the effect of oxygen concentration on clonogenicity of mMSCs, seven days old 5×10^3 hypoxia pre-conditioned cells (mMSCs grown in hypoxia since their isolation from the bone marrow) were seeded in T75 cell culture flasks. Half of the numbers of culture flasks were then transferred to normoxic condition and remaining half were kept at hypoxic condition. The cultures were continued to grow for two more weeks in their respective oxygen conditions with 2x weekly medium change till the colonies were visible at 10x magnification under a bright-field microscope. On day 21, the colonies were fixed with 100% ethanol and stained with giemsa stain. To assess the clonogenicity of the cells number of colonies was counted under a stereo microscope Olympus SZX12. A group of cell was counted as a colony when minimum 25 cells were present in a colony.

To study the clonogenicity seven days old 5×10^3 hypoxic or normoxic mMSCs were seeded in T75 cell culture flasks and allowed to attach for 24 h. For the radiation experiments, 24 h after cell seeding the cells were exposed to different doses of ionizing radiation (0.1 Gy, 0.2 Gy, 0.5 Gy and 4 Gy) with a dose rate of 0.5 Gy/min using a γ -irradiation source of ^{137}Cs HWM-D 2000. The control cells were sham-irradiated. After the radiation treatment the cells were continued to grow in the same oxygen conditions until the colonies were clearly visible with a bright-field microscope. On day 21 the colonies were stained with giemsa and the number of colonies were counted as described above. The clonogenic survival of mMSCs from each biological replicate after irradiation treatment was assessed by determining the plating efficiencies and survival fractions for different radiation doses [140].

Plating Efficiency (PE) is the ratio of the number of colonies to the number of cells seeded.

$$PE = \frac{\text{Number of colonies formed}}{\text{Number of cells seeded}} \times 100\%$$

When the number of colonies formed after treatment of cells is expressed in terms of PE then it is called as the surviving fraction (SF).

$$SF_D = \frac{\text{Number of colonies formed after treatment}}{\text{Number of cells seeded} \times PE}$$

where, SF_D - survival fraction at dose D

D - ionizing radiation dose

PE - plating efficiency

Survival after ionizing radiation can be fitted by a weighted, stratified, linear regression. The linear-quadratic formula that is used to fit the cell survival after a radiation dose by linear regression is:

$$SF = e^{-\alpha D + \beta D^2}$$

Where, SF - survival fraction at given dose

- α - linear component (constant)
- β - quadratic component (constant)
- e - base of the natural logarithm (constant)

The result of the clonogenic assay of mMSCs was plotted as relative clonogenic survival (log 10) vs. dose of irradiation.

4.10 Apoptosis assay

Apoptosis assay was performed to quantify the effects of ionizing radiation on inducing cell death in hypoxic mMSCs. Image-iT® LIVE Green Poly Caspases Detection Kit for microscopy was used to detect the apoptosis in mMSCs. According to the users manual supplied with the apoptosis detection kit, this assay is based on a fluorescent inhibitor of caspases (FLICA) methodology. The FLICA reagent interacts with the enzymatic reactive centre of an activated caspase. If not bound FLICA molecules diffuse out of the cell and are washed away. Therefore, the remaining green-fluorescent signal coming from FLICA molecule is a direct measure of the amount of active caspase present at the time the inhibitor was added, ultimately informing about the apoptosis status of a cell.

Apoptosis assay was performed on the hypoxic mMSCs and HEK293T cells (used as a control for the kit) growing in a black 96-well plate. To study the ionizing radiation-induced apoptosis in hypoxic mMSCs, 12 days old 5×10^3 cells were seeded in a well of a black 96-well plate. The cells were kept growing in hypoxic condition for 3 days before γ -irradiation with the doses of 0.2 Gy, 0.5 Gy, 2 Gy and 4 Gy. The control cells were sham irradiated. Apoptosis staining was performed 6 h and 24 h post-ionizing radiation. All the reagents required to carry out the apoptosis assay were prepared beforehand as described in table 4.8.

Table 4.8: Reagent preparation for apoptosis assay

Reagent	Quantity (μ l)
FLICA	<p>150x FLICA stock - Add 50 μl DMSO to lyophilised FLICA. Mix by swirling/inverting till dissolved.</p> <p>30x working solution - Mix 1 part stock with 4 parts PBS.</p> <p>Working solution - Dilute 30x working solution to 30x culture medium</p>
1x wash buffer	Add 1 part 10x apoptosis wash buffer to 9 parts of de-ionized water
Hoechst 33342 (3.2 pmol)	Dilute 1 μ l hoechst 33342 (1 mM) in 1000 μ l culture medium
Apoptosis fixative	Mix 1 part 10x apoptosis fixative with 9 parts of 1x wash buffer

To perform the assay, following different treatments (either γ -irradiation or staurosporine which was used as a positive control to induce apoptosis in mMSCs and HEK293T cells) the cultures were washed with 100 μ l cell culture medium. To each well 100 μ l of the working solution of FLICA reagent was added and the plate was incubated for 60 min under appropriate culture condition (hypoxia for mMSCs and normoxia for HEK293T cells) protected from light. After an hour FLICA solution was aspirated and the cells were once again washed with the cell culture medium. For nuclear counter staining the cells were stained with Hoechst 33342 dye. After about 5 min of incubation with similar conditions as before, the cells were washed 3x with 300 μ l wash buffer. The cultures can be analysed immediately to detect the apoptotic cells or can be stored in dark at 2-6 °C up to 24 h after fixation with 30 μ l of apoptosis fixative. Finally, seven representative images were taken with KEYENCE BZ-9000 microscope for every biological replicate to quantify the percentage of cells responding to apoptosis stimuli.

4.11 Differentiation potential of mMSCs after exposure to ionizing radiation

The differentiation ability of mMSCs after ionizing radiation exposure was assessed in two ways. The first one is referred as the induced differentiation potential where mMSCs were forced to undergo osteogenic and adipogenic differentiation by addition of the stimulus (lineage inducing growth medium). For the second one the cells were allowed to grow in appropriate mMSC conditions without any lineage inducing growth medium, and the osteoblasts and adipocytes present in the cultures were examined at a certain time after the radiation exposure.

4.11.1 Differentiation of mMSCs in presence of lineage inducing growth medium after ionizing radiation exposure

To test the induced differentiation ability, 7 days old 1.3×10^4 hypoxic mMSCs were seeded in the wells of 24-well plate. Next day, the cells were exposed to 0.5 Gy of γ -irradiation and the control cells were sham irradiated. After the radiation treatment the cells were continued to grow for the next few days in the same condition as before. On day 19, the cells were seeded in the wells of 96-well plate (0.3×10^4 cells for osteogenesis and 10^4 cells for adipogenesis) to test the osteo- and adipogenic lineage potential. The cells were allowed to grow for 2 more days and then were treated with relevant differentiation medium to induce differentiation. The differentiation conditions used in this experiment were similar to that used in the section 4.7.1. Around 2 weeks after the start of stimulation, the osteogenic and adipogenic differentiation abilities of stress exposed mMSCs were checked with alkaline phosphatase and Oil Red O staining.

4.11.2 Differentiation of mMSCs in absence of lineage inducing growth medium after ionizing radiation exposure

Here, 7 days old 5×10^3 hypoxic and normoxic mMSCs were seeded in the wells of 96-well plate. Next day, the cells were exposed to different doses of γ -irradiation (0.1 Gy, 0.2 Gy, 0.5 Gy, 2 Gy and 4

Gy) and the controls were sham-irradiated. After the treatment the cells were returned to grow in the appropriate oxygen conditions as before. The cells were grown in a complete mMSC media without any lineage inducing trigger. The media was changed 2x per week. On day 14, the osteoblasts and adipocytes present in the cultures of γ -irradiation exposed mMSCs were studied with alkaline phosphatase and Oil Red O staining as described in section 4.7.1.

Quantification of adipocytes in γ -irradiated mMSC cultures

To monitor how γ -irradiation affects the adipogenic differentiation potential of mMSCs, the number of adipocytes present in an mMSC culture were counted after radiation exposure. Briefly, the cells were grown in hypoxia or normoxia, and exposed to the relevant doses of γ -irradiation as described above. To quantify the number of adipocytes after ionizing radiation treatment, on day 14 the cultures were stained with Oil Red O dye. Nuclear counterstaining was achieved by adding 100 μ l of DAPI solution (1 μ l DAPI in 10 ml PBS) for 5 min at RT to visualize the total number of cells present in a single well.

To calculate the percentage of adipocytes present in a well after the radiation treatment, Oil Red O positive adipocytes and DAPI positive total cells were separately counted. Numbers of cells stained with Oil Red O in each well were counted manually under 20x magnifications with Olympus CK2 microscope. To quantify the total numbers of cells present in each well, it was necessary to obtain an image for the entire well of a 96-well plate. With KEYENCE BZ-9000 microscope it is possible to acquire such an image under 10x magnification. In order to do so, location parameters were set in terms of X and Y axis at the four corners of a single well (four points positioned on the edge of a specimen/well). The microscope could take several images between these defined parameters by automatically moving the culture plate along X and Y axis in a single plane. Once all the images were obtained, an entire image of the well can be created using BZ-II-Analyzer software stitching all of the pictures together. This image was used to count total number of cells with ImageJ software.

To estimate total cells present, image acquired with KEYENCE BZ-9000 microscope was opened in an ImageJ program. The colour image showing blue DAPI stained nuclei was converted into a black and white image to make it easier for quantifying the cell number. By adjusting the intensity and threshold, the nuclei can be better differentiated from the background. To achieve finer separation of the clumped nuclei the image was processed using binary and watershed options. Finally, the image was analysed by ImageJ program and total nuclei (cells) were counted automatically by the software. Results showing the total number of cells can be saved in an excel format. As similar settings were applied for all the images, the results obtained for each well are comparable with others.

Counting for both, adipocytes and total cells, was done blind (without knowing the ionizing radiation dose) to avoid bias during the quantification procedure. The percentage of mMSCs undergoing adipogenic differentiation after ionizing radiation exposure was calculated using the number of adipocytes and total numbers of cells present in a well. The complete workflow of this experiment is summarized in fig. 10.

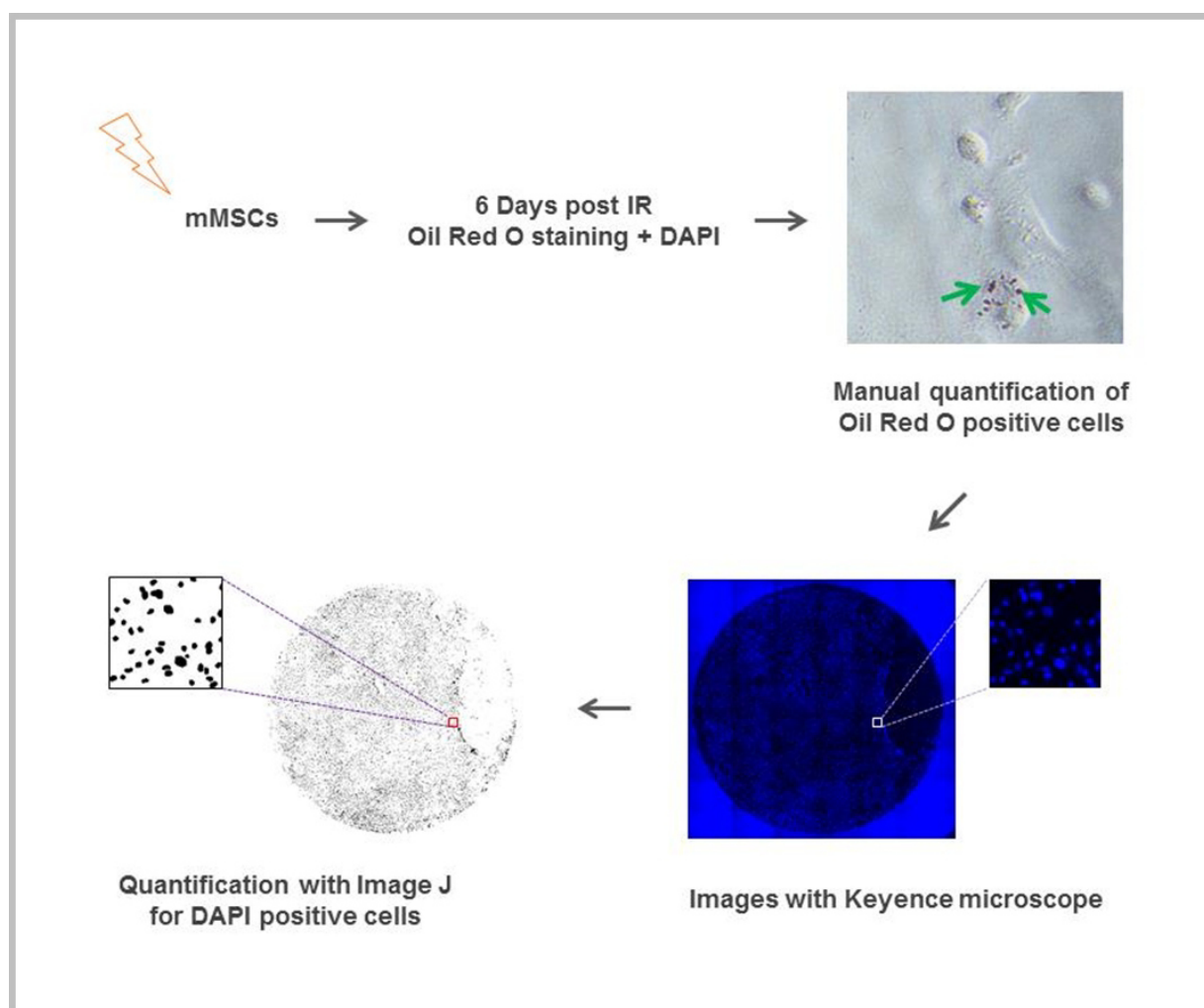


Figure 10: Quantification of *in vitro* differentiated adipocytes. Workflow of the steps performed to quantify adipocytes present in the cultures of γ -irradiation exposed $Rb^{+/+}$ mMSCs in absence of lineage inducing growth medium. Green arrows indicate Oil Red O stained bright red lipid vacuoles present in an adipocyte.

4.12 Quantification of adipocytes in bone marrow tissue sections from whole body irradiated mice

The number of adipocytes present in the bone marrow of irradiated mice can reflect the long term *in vivo* effects of γ -irradiation on the differentiation potential of mMSCs. To count the percentage of adipocytes present in the bone marrow, whole body irradiated (0.125 Gy and 0.5 Gy) mice from B6C3F1 background were sacrificed nearly a year after the irradiation. The bone marrow from irradiated mice was collected in a 1.5 ml reaction tube by pushing it out of the cavity of the long bones (femur and humerus). The collected bone marrow was centrifuged at 300 g and OCT was gently added on the top until the bone marrow was completely immersed. The reaction tube was allowed to stand at RT for a few minutes and was then transferred to -20°C freezer until cryo sectioning was done. The cryo sections were prepared and stained for haematoxylin and Oil Red O by Ms. Elenore Samson. For counting adipocytes, 5 representative images of the bone marrow cryo sections were acquired with KEYENCE BZ-9000 microscope for each mouse (both irradiated and control). The

images were taken under 40x magnification with 1.6x zoom. The bone marrow cryo sections contain all of the different types of cells present in the bone marrow including hematopoietic cells, immune cells, endothelial cells, adipocytes and MSCs. Additionally, many of these cells lie on the top of each other which makes the automatic quantification with a software program highly error prone. Hence, manual quantification was performed to count both total numbers of cells and adipocytes present in a single image. The counting was done as per the instructions from PD Dr. Frauke Neff. By gathering the data of all 5 images from a single mouse together, percentage of adipocytes present in the bone marrow of control and irradiated mice was calculated.

4.13 LB medium and LB agar plates for E. Coli growth

To prepare the liquid LB medium for bacterial growth, 10 g Bacto™-Tryptone, 5 g Yeast extract and 10 g NaCl were added to 900 ml of autoclaved water. The reagents were dissolved completely with a magnetic stirrer and the solution was made up to 1 l by adding remaining amount of water. The pH was adjusted to 7.5 if necessary. To prepare LB agar (pH 7.0), 20 g of Bacto™-Agar was added to a litre of LB medium. The agar can be dissolved using a magnetic stirrer. The pH was checked with a pH meter. Bottles containing LB medium and LB agar were autoclaved and after cooling 7.5 μ l of antibiotic (Ampicillin 50 g/ml) was added. To cast the agar plates, around 15 ml of LB Agar was gently poured into the petri dishes without creating any air bubbles. Once the agar was solidified at RT the plates could be stored in the cold until further use.

4.14 Identification *Pou5f1* transcripts of mMSC

The numbers of products formed in a Real-Time PCR reaction after target gene amplification are visible as separate melting peaks on the melting curve analysis of a sample. To identify the products formed in Real-Time PCR reaction after amplification of the *Pou5f1* transcript of the *Rb^{+/-}* mMSCs various experimental steps had to be carried out.

4.14.1 Purification of Real-Time PCR products

For identifying the *Pou5f1* transcript sequences the first step involves purification of DNA from Real-Time PCR reaction. In order to purify the DNA, QIAquick PCR Purification Kit was used. Manufacturers instructions were followed to purify the DNA. The Real-Time PCR product (10 μ l) was mixed with 5 volumes of buffer PB (50 μ l). This mixture was applied to a QIAquick column placed in a collection tube. After a min of centrifugation at 17,900 g, the flow-through was discarded and the column was washed with 650 μ l of buffer PE. To remove the wash buffer completely the column was centrifuged once again at 17,900 g for 2 min. Following the centrifugation, purified DNA product can be eluted in 30 μ l of DNase-free water and stored at -20 till further use.

4.14.2 Amplification and separation of purified Real-Time PCR products

To exponentially increase the amount of all DNA products present in a purified DNA sample, PCR amplification was performed with *Pou5f1* primers using purified DNA as a template. The reaction

was carried out with standard PCR reaction mixtures as described in table 4.1. The PCR reaction involved following steps as in table 4.9:

Table 4.9: PCR reaction program for amplification of *Pou5f1* transcripts

Cycles	Step	Temperature (°C)	Time
1x	Initialisation	96	3 min
35x	Denaturation	94	1 min
	Annealing	64	40 sec
	Elongation	72	40 sec
1x	Final elongation	72	7 min
	Hold (storage)	4	

To identify the size of different DNA products present in the amplified samples agarose gel electrophoresis was performed with 3% agarose gel. To extract the separated *Pou5f1* gene products first the gel was illuminated under Skylight Super-Blue bluelight LED transilluminator. This helped to mark the position of EtBr stained DNA fragments. The piece of agarose along with a DNA fragment was cut carefully using a scalpel and placed in a 1.5 ml reaction tube. The products were purified from the agarose gel using a QIAquick Gel Extraction Kit with manufacturers protocol. The gel plug was weighed and dissolved by adding 6 volumes of buffer QG. This mixture was incubated at 50 °C thermomixer for about 10 min. Following the incubation 1 volume of isopropanol was added to reaction tube. The tube was briefly vortexed to homogenize the solution. This entire solution was applied to a QIAquick column provided with the kit and centrifuged at 17,900 g for a minute. The flow-through was discarded and the column was washed with 750 μ l of buffer PE. To elute the DNA, 50 μ l of DNase-free water was added to centre of the column and centrifuged once again at 17,900 g for a minute. DNA concentration was measured with Tecan Infinite M200 reader. Purified DNA can be stored at -20 °C.

4.14.3 TOPO® TA cloning

DNA products extracted from the agarose gel are required to be amplified to identify the DNA sequence. Amplification of individual DNA fragment was achieved by performing TOPO® TA cloning on separated fragments. The TOPO® TA cloning reaction was performed as described in the users guide of the cloning kit. The typical cloning reaction is made up of three steps as annealing, ligation (insertion), and E. Coli transformation. pCAG-tdTomato vector plasmid containing an ampicillin resistance gene was used as a transformation positive control and E.Coli cells transformed with an ampicillin resistance plasmid were utilised as an ampicillin plate positive control. To perform the ligation of DNA fragment (separated Real-Time PCR product) to pCR4-TOPO® vector provided with

the kit, DNA insert was gently mixed with pCR4-TOPO® in a reaction tube. The pCR4-TOPO® vector is around 4000 bp long and contains a gene responsible for ampicillin resistance.

The insertion reaction incorporates following reagents as in table 4.10:

Table 4.10: Ligation mixture for TOPO-TA cloning

Reagent	Quantity (μ l)
DNA insert (Real-Time PCR product)	0.5-4 (depending on the DNA concentration)
TOPO®TA vector	1
Salt	1
Sterile water	amount needed to make reaction volume up to 6

The mixture was incubated at RT for about 20 min. After incubation, the tubes were placed immediately on ice and the reaction was continued with the transformation of One Shot® Top10 Chemically Competent E.Coli cells. During transformation the positive control (pCAG-tdTomato vector) was also included in the experiment in addition to the ligated DNA fragments. 5 μ l of ligation product or Tomato plasmid was mixed with 15 μ l of the E.Coli cells. The solution was kept on ice for 30 min and given a heat shock for 30 sec at 42 °C directly after the incubation. This made the ligation product and the plasmid to enter inside the E.Coli cells. The solution was again kept on ice for 5 min and afterwards 200 μ l of S.O.C medium was added to the tube. The cell suspension was incubated at 37 °C for 1 hr with gentle agitation. After an hour, 50 μ l of the suspension was spread with a triangular spreader evenly on an ampicillin containing agar plate. The plates were incubated overnight at 37 °C in a bacterial incubator to grow the transformed colonies. As the agar plates contain ampicillin, only the cells transformed with ligated product are able to grow on the plates.

4.14.4 Colony screening

Colony screening was performed to determine the size and length of an inserted Real-Time PCR product. A part of the single colony was boiled at 95 °C for 15 min in nuclease free water and then used to carry out a PCR reaction using the conditions as in table 4.9. Later, 10 μ l of amplified PCR product was used for electrophoresis with 3% agarose gel and the EtBr stained DNA fragments was visualized with Alpha Innotech Chemilmager System.

4.14.5 Continuing the colony and extraction of Real-Time PCR products

After confirming the size of the inserted product with colony screening, some part of the same colony was continued by streaking on another ampicillin containing agar plate as a back-up. Remaining part of this colony was transferred to 5 ml liquid LB medium and incubated overnight at 37 °C on a 200 rpm shaker. Next day, the LB medium was centrifuged and the cell pellet was collected. The

separated DNA product should be extracted from the cell pellet. Hence, the DNA extraction was performed using GeneJET Plasmid Miniprep Kit with manufacturers instructions. Briefly, transformed cells were resuspended in 250 μ l of resuspension buffer and vortexed. To this, 250 μ l of lysis buffer was added. After mixing by inverting for few times 350 μ l of neutralisation solution was added to the tube. Centrifugation was carried out at 12000 g for 5 min and the supernatant was loaded on GeneJET spin columns. Once again after centrifugation for a minute, the column was washed with 500 μ l of wash solution. The flow through was discarded and 2x the centrifugation was repeated. Finally, the purified DNA was eluted with 50 μ l of elution buffer. DNA concentration and purity was measured with Tecan Infinite M200 reader. The extracted DNA fragment was used for sequencing reaction.

4.14.6 Sequencing

The final experimental step in identifying the *Pou5f1* transcripts of mMSCs is sequencing the extracted Real-Time PCR product. The sequencing reaction was performed using the BigDye® Terminator v3.1 Cycle Sequencing Kit. The template quantity was determined depending on the concentration of DNA as per the instructions given in users manual. All of the transcripts were in a range of 50 to 200 bp lengthwise as visible on the agarose gel. Hence, about 150-300 ng of DNA sample was used as a template. Two separate reactions, one with forward primer and other with reverse primer, were performed for each sample. Hence, the sequencing reaction required two separate master mixes. The reaction mixtures were prepared as in table 4.11:

Table 4.11: Sequencing reaction mixture

Reagent	Quantity (μ l)
Big dye	2
Buffer 5x	1
<i>Pou5f1</i> forward or reverse primer (3.2 pmol)	1
DNA template	required for 150-300 ng of DNA
Water	to make up the volume to 10 μ l
Total volume	10

The reaction mixture was made in a 0.2 ml PCR tube and mixed by pipetting up and down. Reaction conditions for Veriti® thermal cycler are given in table 4.12.

4.14.7 Product purification after cycle sequencing reaction

It is necessary to remove unincorporated dye terminators following the PCR reaction before determining the sequence of a DNA fragment. For purification, 30 μ l of 100% ethanol was added

Table 4.12: Sequencing reaction program

Cycles	Step	Temperature (°C)	Time
1x	Initialisation	96	1 min
25x	Denaturation	96	10 sec
	Annealing	50	5 sec
	Elongation	60	4 min
	Hold (storage)	4	

to the PCR tube. The entire content of the PCR tube was then transferred to the wells of barcode labelled 96-well plate. The plate was covered with aluminium foil and kept in dark for 15 min. After the incubation, the plate was centrifuged at 4500 rpm for 20 min. The cover foil was removed and the plate was briefly centrifuged upside down. 50 μ l of 75% ethanol was added to the reaction mixture and the plate was again covered with an aluminium foil. Centrifugation was repeated as before. The cover foil was removed and the plate was allowed to air dry for minimum 30 min. Finally, 50 μ l of water was added to every well containing the sample and the plate was covered with a Silicone Sealing septa mat required for the sequencing instrument.

Sequencing was carried out at the central sequencing facility of Helmholtz Zentrum Muenchen. For reviewing the sequence files 4Peaks software v 1.7 was used. Once the sequence was determined, BLAST search was done to identify the *Pou5f1* gene products of mMSCs.

4.14.8 Nucleotide blast alignment

Nucleotide BLAST was performed to identify and confirm the sequence of products formed after target amplification of *Pou5f1* gene in mMSCs and to analyse where this sequence belongs in *Pou5f1* gene or in an entire mouse genome. The Blast was performed using online tools on the website: https://blast.ncbi.nlm.nih.gov/Blast.cgi?CMD=Web&PAGE_TYPE=BlastHome.

4.15 Statistical analysis

Statistical analysis of the data was performed using software SPSS Statistics 22. Unless stated all the experiments were performed in technical duplicates with three biological replicates. The data represents mean \pm Standard Error of the Mean (SEM). A statistical significance is assumed when the p-value was < 0.05 . The statistical significance of the data is denoted as * for p-value < 0.05 , ** for p-value < 0.01 and *** for p-value < 0.001 .

The effect of two independent variables (e.g oxygen concentration and irradiation dose) on one continuous dependent variable (e.g percentage of senescent cells) was analysed using two-way ANOVA with Tukey's HSD for post hoc analysis. The one-way ANOVA was used to determine

whether there are any significant differences between the means of three or more independent groups (e.g cells undergoing apoptosis after exposure to 5 different ionizing radiation doses). Comparison between the means of two groups was done with Student's t-test if the data was normally distributed or MannWhitney U test for non-normal distribution of the data.

Chapter 5

Results

5.1 Establishment and long-term maintenance of *in vitro* mesenchymal stem cell culture from mice of different genotypes

5.1.1 Determination of the mouse genotypes

Mouse models provide an ideal source for *in vitro* culturing of MSCs. To obtain the $Rb^{+/+}$ and $Rb^{+/-}$ mMSCs, the genotype of the F1 progeny obtained by a cross between two transgenic mice lines FVB/N-CreCol x FVB/N-Rb1-LoxP was determined using allele-specific PCR as described in section 4.6.5. For *Rb1* genotyping, the presence of two wild type alleles (+/+) showed one strong band around 650 bp, presence of floxed *Rb1* alleles (+/fl) resulted into two narrowly separated bands at around 650 bp and 700 bp, and *Rb1* heterozygous allele (wt/del) showed two widely spaced bands at 650 bp and 235 bp (fig. 11A). As for the Cre gene, one robust band was seen at around 727 bp when the Cre transgene was present (fig. 11B). Based on their genotypes ($Rb1^{+/+}$ or $Rb1^{+/-}$) these mice were later used to isolate the primary mMSCs.

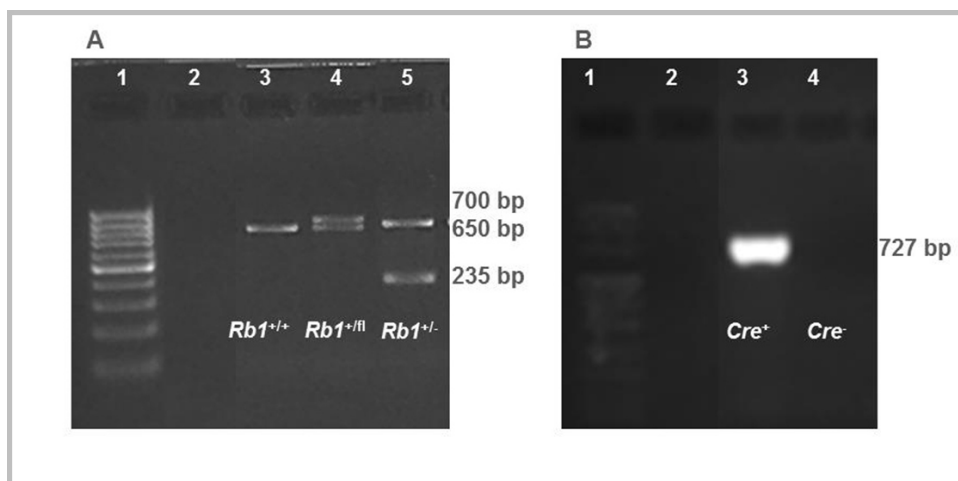


Figure 11: *Rb1* and Cre genotyping using the tail tip DNA of F1 mice progeny. Allele specific PCR products on 2% agarose gel. A) Genotyping for the *Rb1* allele: Lane 1- DNA molecular weight marker VIII, Lane 2- Negative control, Lane 3- $Rb1^{+/+}$ (650 bp), Lane 4- $Rb1^{+/fl}$ (700bp and 650 bp), Lane 5- $Rb1^{+/-}$ (650 bp and 235 bp). B) Genotyping for the Cre allele: Lane 1- DNA molecular weight marker VIII, Lane 2 - Negative control, Lane 3 - Cre^+ (727 bp), Lane 2- Cre^- .

5.1.2 Identification of the optimal environment for long-term *in vitro* culturing of mMSCs

MSC media (DMEM/F-12, GlutaMAX™ with 10% MSC Qualified FBS) was found to be the most optimal nutritional mixture for *in vitro* culturing of mMSCs (Appendix A). However, long-term maintenance of the mMSC culture was still an issue. MSCs are known to be located in a MSC niche where the oxygen concentration is highly regulated [141]. Therefore, in order to find out the optimal culturing environment bone marrow cells were cultured either in hypoxia or normoxia immediately after their explantation. With the culture progression hypoxic cultures found to retain their spindle-shaped morphology while the normoxic cultures appeared heterogeneous as increasing number of cells lost the typical spindle-shaped morphology of mesenchymal stem cells. This difference in the appearance of long-term cultures of 32 days old mMSCs in hypoxic and normoxic condition can be seen in fig. 12.

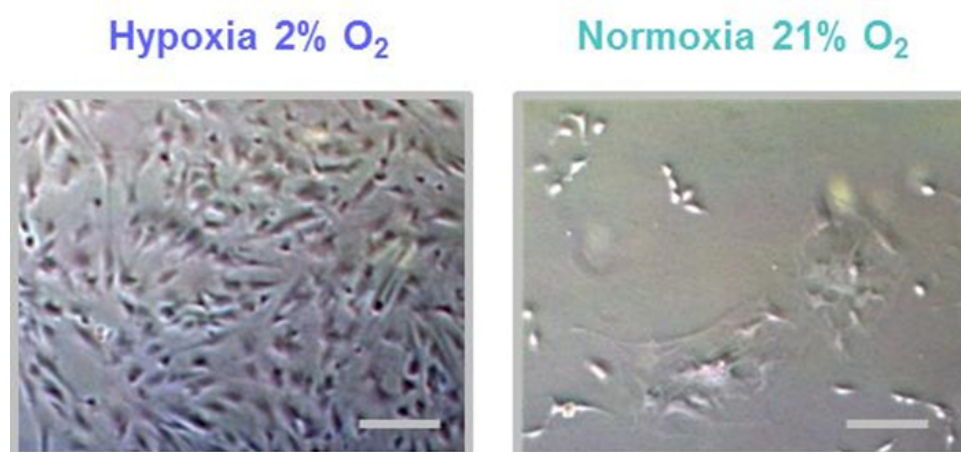


Figure 12: Murine mesenchymal stem cell culture in different oxygen concentrations. $Rb^{+/+}$ murine mesenchymal stem cells as a representative of $Rb^{+/+}$ and $Rb^{+/-}$ cultures growing in hypoxia (left image) and normoxia (right image) on day 32 after the explantation. Scale bar: 50 μm .

When these cultures were observed under a microscope higher numbers of cells were present in hypoxic condition whereas the numbers of cells in normoxic condition were found to be declined over time. Therefore, to investigate the effect of oxygen concentration on mMSC survival and growth, PrestoBlue® Cell Viability Assay was performed on hypoxia pre-conditioned mMSCs as described in section 4.3.

The numbers of viable cells (represented as relative fluorescence units in the graph) obtained from 2 $Rb^{+/-}$ biological replicates did not differ significantly for two weeks after the first passage (fig. 13) between hypoxic and normoxic conditions. For passage 2, however, the oxygen effect was clearly visible. Similar like passage 1, hypoxic and normoxic cultures from passage 2 initially displayed comparable number of living cells, although with culture progression continuous depletion in the number of viable cells was observed in normoxic cultures. The difference between the number of viable cells growing in hypoxia and normoxia was highly significant (Student's t-test, paired, 2-tailed p-value 0.014). This demonstrates that the long-term survival of mMSCs is severely compromised in higher oxygen tension.

Hypoxia was found to be the optimal culturing environment for stable growth and maintenance

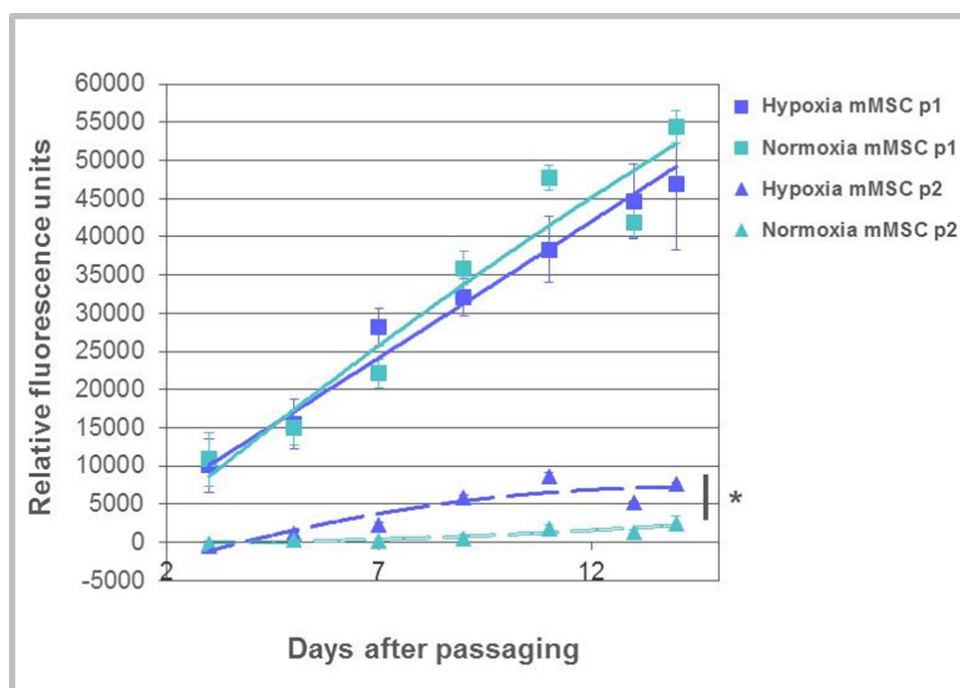


Figure 13: Effect of oxygen concentration on long-term growth of mMSCs. Numbers of viable cells present in hypoxic and normoxic conditions are displayed as relative fluorescence unit in mean values \pm standard error of the mean. The graph shows fluorescence readings for mMSCs from 2 $Rb^{+/+}$ biological replicates for the period of two weeks after passage 1 and passage 2. The difference between the numbers of viable cells growing in two different oxygen conditions was analysed with Student's t-test, paired, 2-tailed; p-value after passage 2 between hypoxia and normoxia was 0.014.

of mMSCs. As the low oxygen concentration (2% hypoxia) was found to promote the *in vitro* growth of mMSCs most of the experiments in the following chapters were performed using hypoxic $Rb^{+/+}$ mMSCs if not stated otherwise.

5.1.3 Selection of an appropriate proteolytic enzyme for subculturing the mMSCs

Culture progression requires subculturing the cells for long-term maintenance *in vitro*. Murine mesenchymal stem cells were resistant towards detachment by Trypsin-EDTA 0.05% with only a low number of cells actually detaching from the culture flasks after extensive trypsin treatment (Table 5.1). Therefore, several proteolytic enzymes were tested to find the most suitable cell detachment reagent for mMSCs (Table 5.1). Assessing the time needed for detachment and growth of the cells after subculturing, StemPro® Accutase was selected as the most suitable enzyme for passaging mMSCs.

5.2 Properties of *in vitro* cultured mMSCs

After establishing the *in vitro* mMSC cultures, the next step involves examining the model system for the inherent MSC characteristics of differentiation ability and surface marker expression.

Table 5.1: List of proteolytic enzymes tested for subculturing the mMSCs

Proteolytic enzymes	Time required for around 80% cells to detach (min)	Temperature (°C)
Accumax™ cell detachment solution	10	RT + 37
Alfazyme	10	RT + 37
Biotase	15-20	RT + 37
Collagenase Cls Type II, Cls II	15-20	RT + 37
Papain	15-20	RT + 37
StemPro® Accutase	10	37
Trypsin-EDTA 0.05%	15	37
TrypLE Select Enzyme (10x)	10	RT + 37

5.2.1 Trilineage differentiation potential of mMSCs

When stimulated with specific growth factors and chemicals MSCs undergo osteogenic, adipogenic, and chondrogenic lineage differentiation *in vitro* [56]. To confirm the potency of mMSCs, 7 days old hypoxic mMSCs obtained from 3 *Rb^{+/+}* biological replicates were seeded in the wells of a culture plate, stimulated with appropriate differentiation (adipogenic, chondrogenic or osteogenic) medium and finally stained with lineage-specific histochemical assays. Equal numbers of MSCs from the same mice were treated as negative control. The trilineage differentiation of mMSCs obtained from 1 mouse as a representative for 3 biological replicates is shown in fig. 14.

Osteogenic differentiation

Nearly two weeks after the induction with osteogenic differentiation cocktail the cultures (both induced and negative control) were stained for alkaline phosphatase activity. Cultures stimulated to undergo osteogenesis appeared violet blue due to the presence of alkaline phosphatase in the cytoplasm of osteoblasts derived from MSCs (fig. 14A upper image). Negative control cells that didnt receive any osteogenic medium were mostly colourless. Sometimes the negative cultures appeared faint purple in colour because of the sporadic osteoblastic differentiation (fig. 14A lower image). Giemsa stain was added to negative control cells for better visualising the individual cells.

Chondrogenic differentiation

Alcian blue treatment of the mMSC aggregates 21 days after the induction revealed positively stained greenish blue coloured deposits for the chondrogenic pellets (fig. 14B upper image) whilst the negative control cells were colourless (fig. 14B lower image).

Adipogenic differentiation

In vitro cultured MSCs after induction with adipogenic medium form mature adipocytes which contain high number of intracellular lipid droplets. The neutral lipid droplets are easily identified by their rich red colour when stained with Oil Red O lysochrome diazo dye. When stimulated with adipogenic medium mMSCs showed existence of adipocytes in their cultures. Nearly 2 weeks after induction these adipocytes were stained bright red with Oil Red O due to the presence of lipid vacuoles (fig. 14C upper image). In contrast, control cells did not exhibit any adipogenic differentiation and were Oil Red O negative (fig. 14C lower image).

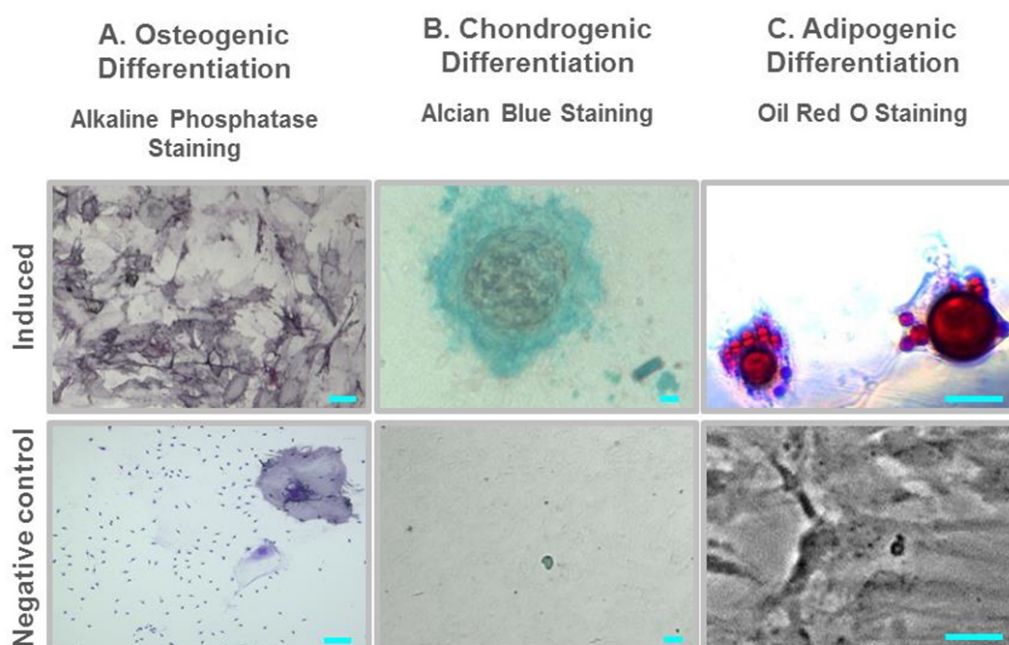


Figure 14: Multilineage differentiation of *in vitro* cultured mMSCs. Representative images showing trilineage differentiation of mMSCs obtained from 3 *Rb*^{+/+} biological replicates. A) Osteogenic differentiation: mMSCs induced to undergo osteogenic differentiation (upper image) and negative control cells (lower image) stained for alkaline phosphatase activity. Scale bar: 100 μm . B) Chondrogenic differentiation: alcian blue staining of mMSCs under induced chondrogenic differentiation (chondrogenic pellets, upper image) and negative control cells (lower image). Scale bar: 25 μm . C) Adipogenic differentiation: mMSCs induced to undergo adipogenic differentiation (upper image) and negative control cells (lower image) stained with Oil red O dye. Scale bar: 25 μm .

5.2.2 Surface marker expression of *in vitro* cultured mMSCs

Mesenchymal stem cells from all species display a typical surface marker expression (immunophenotype) profile. With an extensive literature search [76, 150] and based on the

availability of species specific antibodies CD44, CD29, Sca1 and CD45 were chosen to analyse the immunophenotype of mMSCs used in this study. The analysis of the expression of surface markers was performed by immunocytochemistry and flow cytometry.

Analysis of mMSC surface marker expression by immunocytochemistry

In the first method the expression of CD44 and Sca1 was directly visualized on mMSC surface by immunocytochemistry. Representative images for the expression of CD44 and Sca1 on the surface of hypoxic mMSCs from 1 *Rb*^{+/+} biological replicate are shown in fig. 15 and fig. 16 respectively. The surface marker CD44 was detectable on the cell membrane of mMSCs (fig. 15).

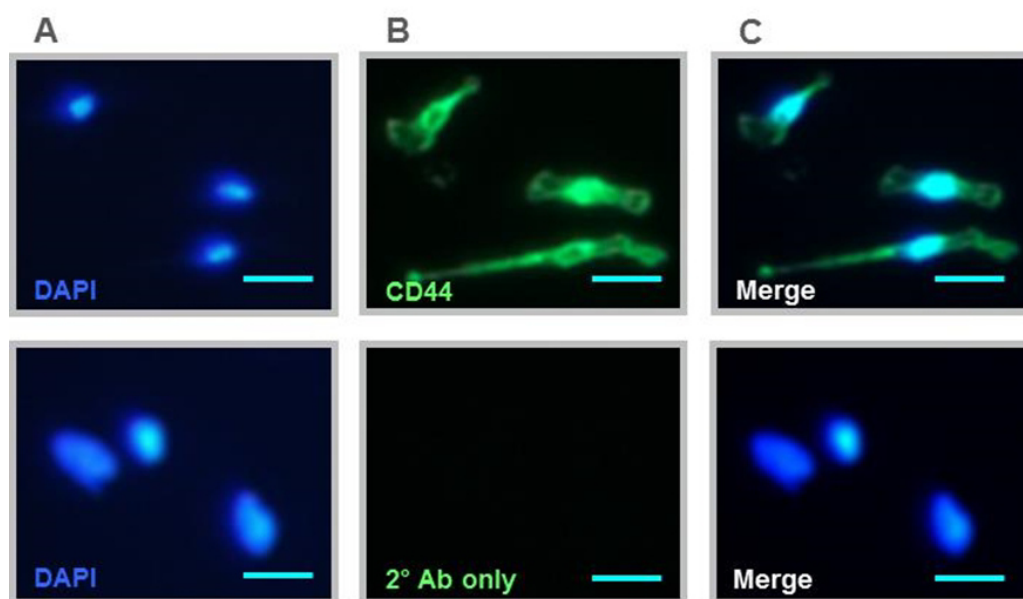


Figure 15: Immunocytochemistry of CD44 expression on mMSC surface. Representative images showing expression of surface marker CD44 on membranes of mMSCs obtained from 1 *Rb*^{+/+} biological replicate. Panel A shows DAPI stained cell nuclei. Panel B displays CD44 positive cells. Panel C is the merged image of panel A and B. Lower row images display signals for the secondary antibody-only control with the same microscope settings. Scale bar: 10 μ m.

In contrast to the equal distribution of CD44, Sca1 antigen showed spotted expression on the membranes (fig. 16).

Analysis of mMSC surface marker expression by flow cytometry

In the second method, the percentage of cells showing presence or absence of CD44, CD29, Sca1 and CD45 was obtained by flow cytometry analysis. Here, hypoxia cultured 21 days old mMSCs from 1 *Rb*^{+/+} biological replicate were treated with mouse specific surface Ab against CD44, CD29, Sca1 and CD45 and murine embryonic stem cell (mESC) line ES-E14TG2A passage 27 was used as a control (fig. 17). Strong expression (99% positive cells) of CD29 and CD44 was observed on mMSCs (fig. 17 upper row). Around 86% mMSCs showed expression of Sca1 on their surface (fig. 17 upper row). Additionally, > 90% of the cells was negative for CD45 (fig. 17 upper row). For mESCs, no expression of the surface antigens CD44, Sca1 and CD45 was observed (fig. 17

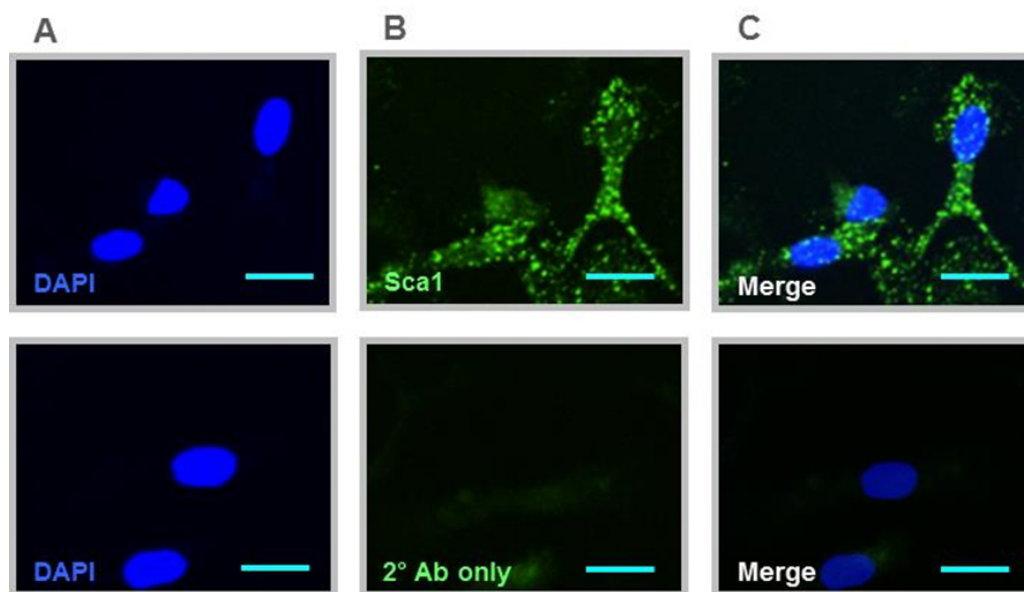


Figure 16: Immunocytochemistry of Sca1 expression on mMSC surface. Representative images showing expression of surface marker Sca1 on membranes of mMSCs obtained from 1 *Rb*^{+/+} biological replicate. Panel A shows DAPI stained cell nuclei. Panel B displays Sca1 positive cells. Panel C is the merged image of panel A and B. Lower row images display signals for the secondary antibody-only control with the same microscope settings. Scale bar: 5 μ m.

lower row). Nearly 99% of the mESC were positive for the CD29 expression (fig. 17 lower row). Therefore, in accordance with the previously published research (reviewed by [71]) mMSCs from this model system express CD44, CD29, Sca1 and lack expression of hematopoietic cell marker CD45 on their surface.

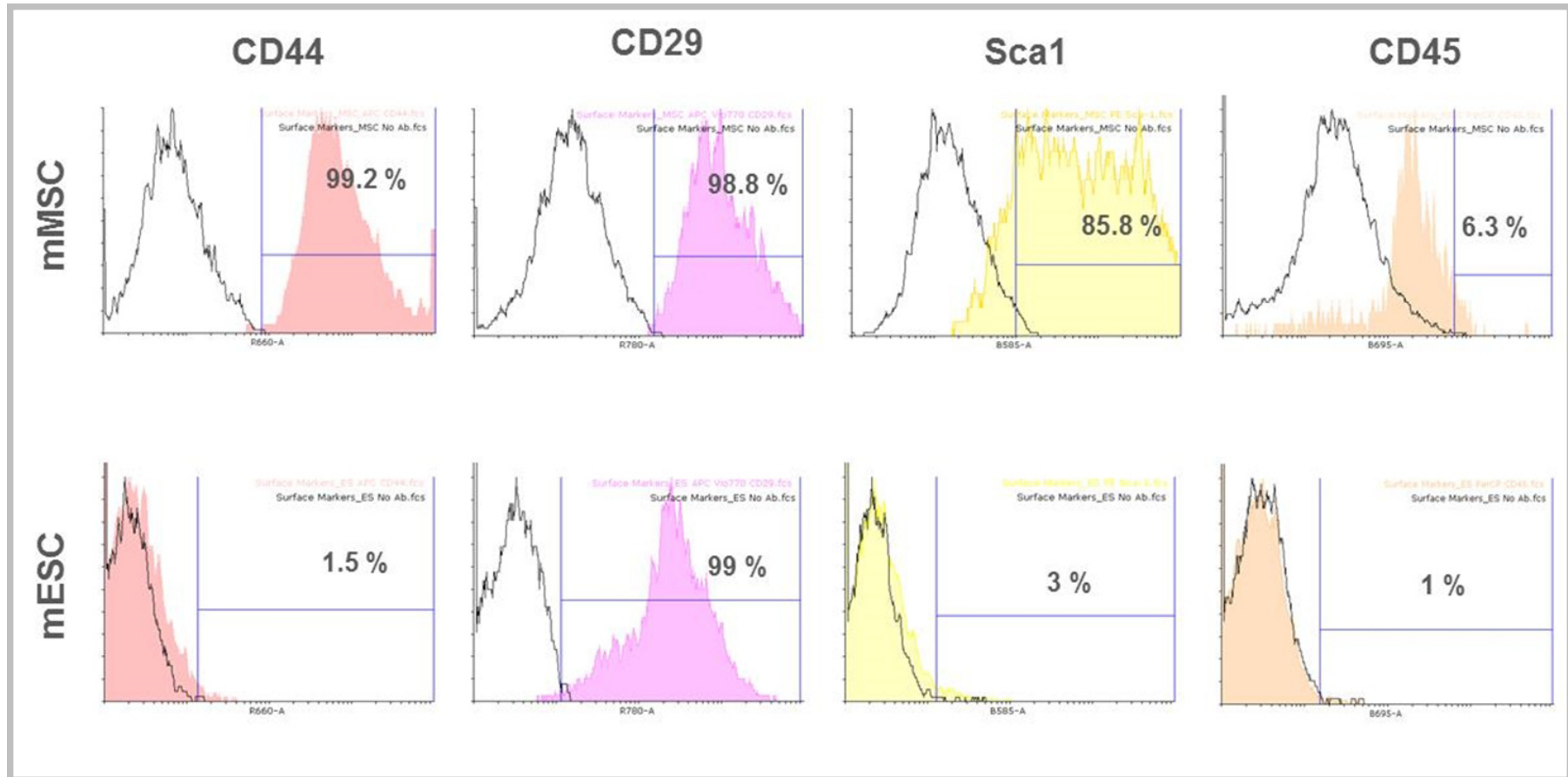


Figure 17: Flow cytometry analysis of mMSC surface marker expression. Expression of surface markers on membranes of mMSCs obtained from 1 *Rb*^{+/+} biological replicate and on the cells from passage 27 of mESC line ES-E14TG2A. Upper row displays histograms for the expression of markers CD44, CD29, Sca1 and CD45 on the surface of 21 days old hypoxic mMSCs. The percentage of cells positive for these markers is mentioned in each histogram. Lower row displays histograms for the expression of markers CD44, CD29, Sca1 and CD45 on the surface of passage 27 mES cell line. The percentage of cells positive for these markers is mentioned in each histogram. Signal from the unstained (no antibody) control samples can be seen as black-lined peaks in the individual panels.

5.3 Effects of oxygen concentration on *in vitro* cultured mMSCs

5.3.1 Colony forming ability of mMSCs under hypoxic and normoxic conditions

To analyse the effect of different oxygen concentrations on the colony forming efficiency of mMSCs, clonogenic assay was performed. For the clonogenic assay, 7 days old 5×10^3 hypoxia pre-conditioned mMSCs obtained from 4 $Rb^{+/+}$ biological replicates were seeded in T75 cell culture flasks and allowed to grow in hypoxic or normoxic condition for two more weeks. On day 21 the colonies were counted. The colony forming efficiency of mMSCs in different oxygen concentration was assessed with Student's t-test, paired, 1-tailed. Oxygen concentration altered the colony forming ability of hypoxia pre-conditioned mMSCs with more colonies in hypoxia and fewer in normoxia (fig. 18).

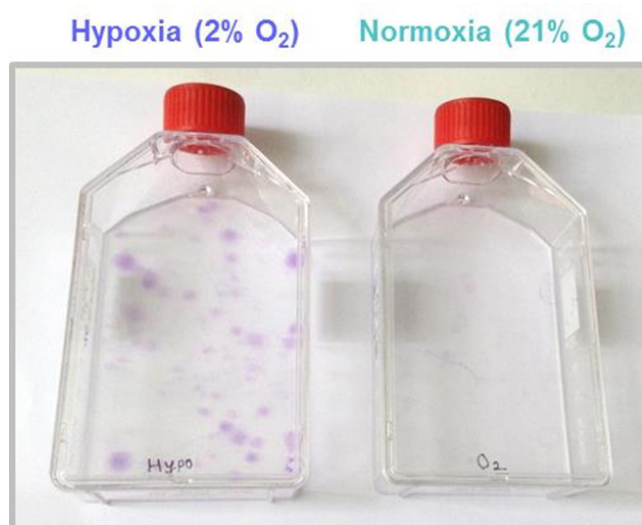


Figure 18: Colony forming ability of mMSCs under hypoxic and normoxic conditions. Representative images of giemsa-stained colonies of hypoxia pre-conditioned mMSCs on day 21. The mMSCs obtained from 4 $Rb^{+/+}$ biological replicates were grown under hypoxia for first 7 days and then subcultured at clonal density into hypoxia (left flask) and normoxia (right flask).

Quantification of four biological replicates revealed 10 fold increase in percentage of colonies formed in hypoxia than in normoxia. Colony forming efficiency of mMSCs in hypoxia and normoxia (fig. 19) differed significantly (p -value 0.03). These results prove that the clonogenicity of mMSCs is impaired in normoxic cultures.

5.3.2 Cell cycle analysis of mMSCs growing in hypoxic and normoxic conditions

Having observed the detrimental effects of high oxygen concentration on growth and clonogenicity of mMSCs the cell cycle distribution of the hypoxic and normoxic mMSCs was analysed to see the oxygen effect on their cell cycle as the culture advances in age. The cell cycle analysis of 7 and 21 days old mMSC from mouse number 81 as a representative of the 2 $Rb^{+/+}$ biological replicates is shown in fig. 20.

The cell cycle distribution of the hypoxic and normoxic mMSCs was analysed using two-way ANOVA with Tukey HSD for post-hoc analysis. The mMSCs from 7 and 21 days old cultures from hypoxia and normoxia did not differ significantly between the number of cells present in Sub-G1

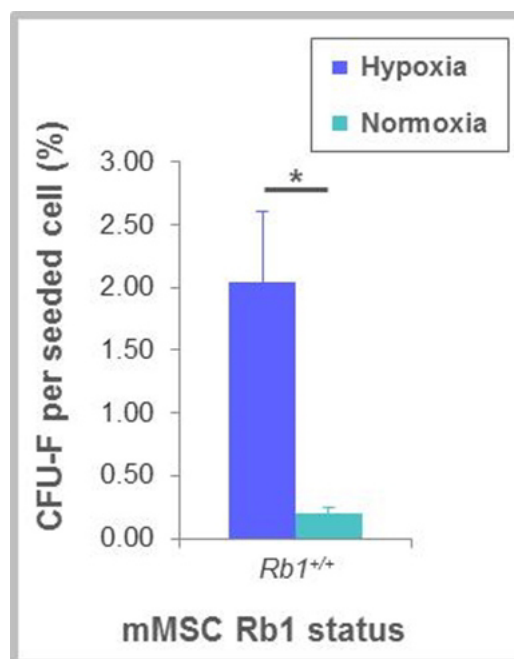


Figure 19: Effect of oxygen concentration on colony forming ability of mMSCs. Colony forming ability of hypoxia pre-conditioned mMSCs in hypoxic and normoxic conditions displayed as plating efficiency in mean values \pm standard error of the mean. Murine mesenchymal stem cells were obtained from 4 *Rb1^{+/+}* biological replicates. The difference between clonogenicity of hypoxic and normoxic mMSCs was analysed with Student's t-test, paired, 1-tailed; p-value 0.03.

(fig. 21A) and G2/M (fig. 21D) cell cycle phases. However, the percentage of cells present in G1 phase was found to be influenced by age and culture condition. These two factors didn't affect the number of cells present in G1 phase (fig. 21B) independently but the interaction effect was statistically meaningful (p-value Oxygen concentration*Age 0.01). In hypoxia, percentage of cells in G1 phase increased with age which indicates G1 cell cycle arrest at 21 days old mMSCs. In contrast, the accumulation of cells in G1 phase was observed in young normoxic mMSCs already by day 7. Therefore, it can be said that the combination of less oxygen and older age induces the G1 phase accumulation in mMSCs. Furthermore, age also appeared to be a critical factor for the percentage of cells present in S phase (fig. 21C). It was obvious that the number of cells undergoing DNA synthesis reduced considerably from day 7 to day 21 independent of the culture condition (p-value Age 0.003). This data indicates that the cell cycle distribution of mMSCs is affected by both age and oxygen concentration.

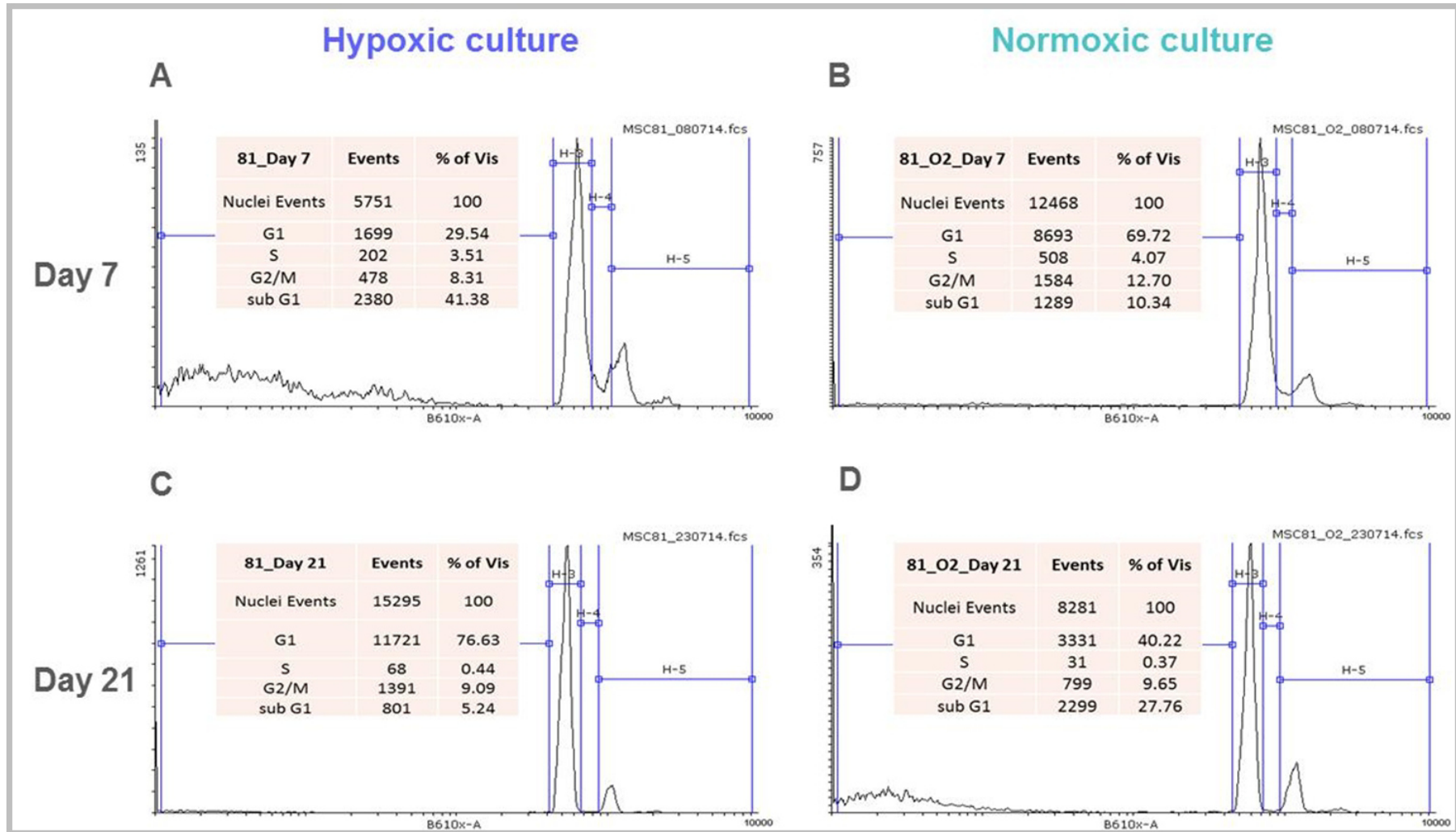


Figure 20: Cell cycle analysis of hypoxic and normoxic mMSCs. Representative histograms showing mMSCs obtained from 2 *Rb*^{+/+} biological replicates in Sub-G1, G0/G1, S, and G2/M phases of the cell cycle. A) Cell cycle analysis of 7 days old hypoxic mMSCs. B) Cell cycle analysis of 7 days old normoxic mMSCs. C) Cell cycle analysis of 21 days old hypoxic mMSCs. D) Cell cycle analysis of 21 days old normoxic mMSCs.

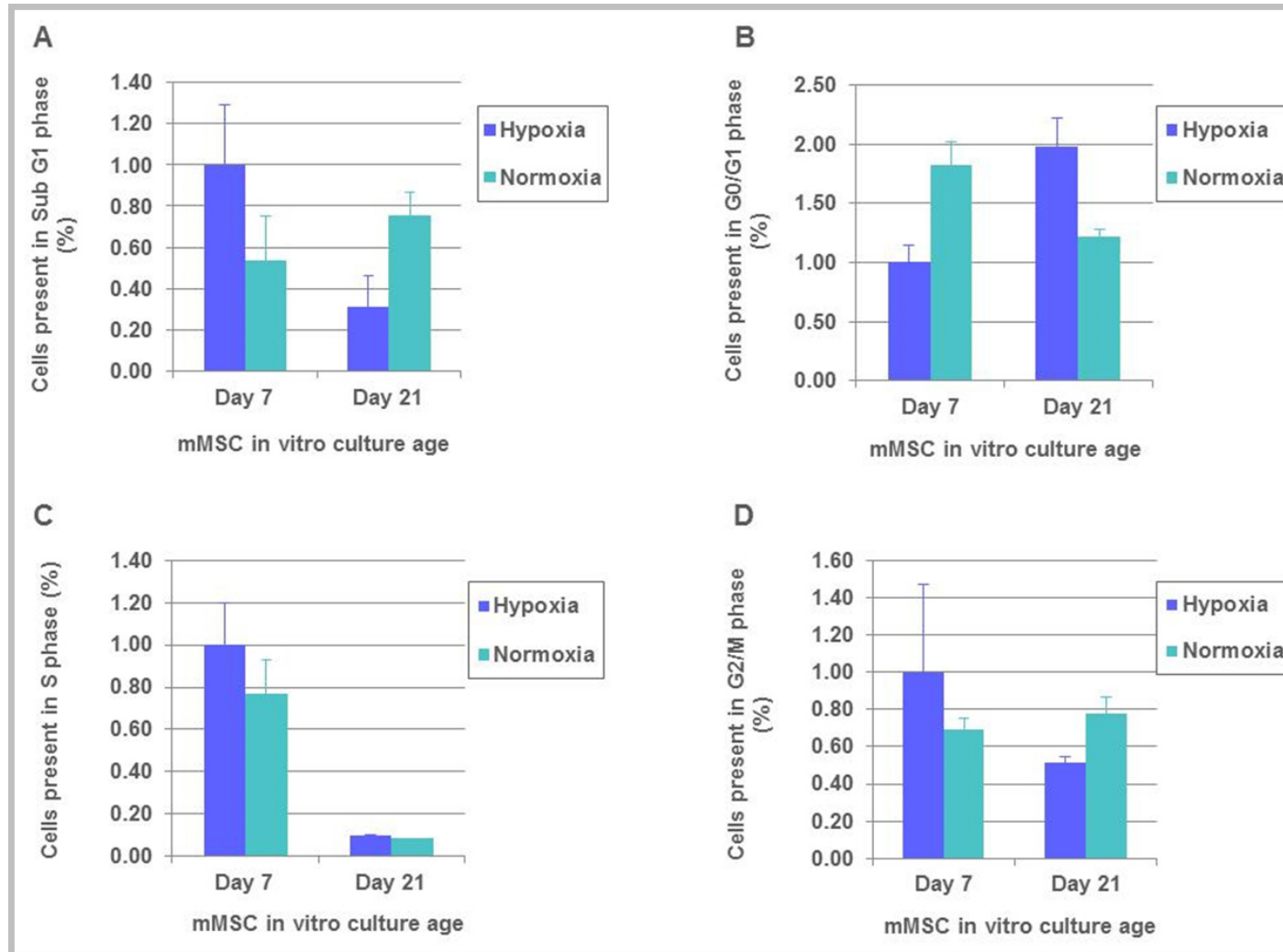


Figure 21: Percentage of mMSCs present in different phases of the cell cycle on day 7 and 21. Bar charts showing percentage of mMSCs from 2 *Rb*^{+/+} biological replicates in mean values \pm standard error of the mean in different phases of the cell cycle A) mMSCs present in Sub-G1 phase. B) mMSCs present in G0/G1 phase (Two-way ANOVA Culture condition* Age p-value 0.01). C) mMSCs present in S phase (Two-way ANOVA Age p-value 0.003). D) mMSCs present in G2/M phase.

5.4 Expression analysis of stemness marker genes in *in vitro* cultured mMSCs

The expression profile of *Sox2*, *Nanog*, *Klf4*, *Nes*, *Bmi1*, *Pou5f1* was monitored over the *in vitro* culture period to test the established mMSC model system for the expression of these stemness and pluripotency markers. Briefly, mMSCs were cultivated under hypoxia after their explantation from the bone marrow. RNA extracted from young (day 7), middle aged (day 17) and old (day 35) cells from 3 *Rb*^{+/+} biological replicates was used for analysis of gene expression using Real-Time PCR. Expression values for every gene on different days of culturing (day 17 and 35) was normalized to its own expression on day 7 and were analysed with Student's t-test, unpaired, 2-tailed.

Throughout the duration of *in vitro* culture mMSCs were positive for *Sox2* expression without any statistically significant difference between day 7, 17 or 35 (fig. 22A). Another embryonic stem cell marker, *Nanog* (fig. 22C), showed nearly 4 times higher mean relative expression in 35 days old cells than 7 days and 17 days old cells. However, the expression difference between cells of different ages was statistically insignificant. The expression of *Bmi1*, a polycomb group protein, was found to increase gradually (fig. 22B). This increase from day 7 vs 35 and day 17 vs 35 was statistically significant (p-value 0.014 and p-value 0.046 respectively). Another important embryonic SC marker, *Pou5f1* (fig. 22D), showed reduced expression at 35 days mMSCs. The fold change was statistically significant between 7 and 35 days old cells (p-value 0.04). *Klf4*, a transcription factor important for stemness property, displayed a trend towards reduced expression as the culture aged (fig. 22F). The decrease in expression values from day 7 to day 17 was significant (p-value 0.04). Expression of *Nes* (Nestin) also declined with culture age (fig. 22E). The loss of its expression in old cells was quite dramatic with fold change from day 7 and day 17 to day 35 being highly significant (p-value 0.004 and p-value 3.07×10^{-5} respectively).

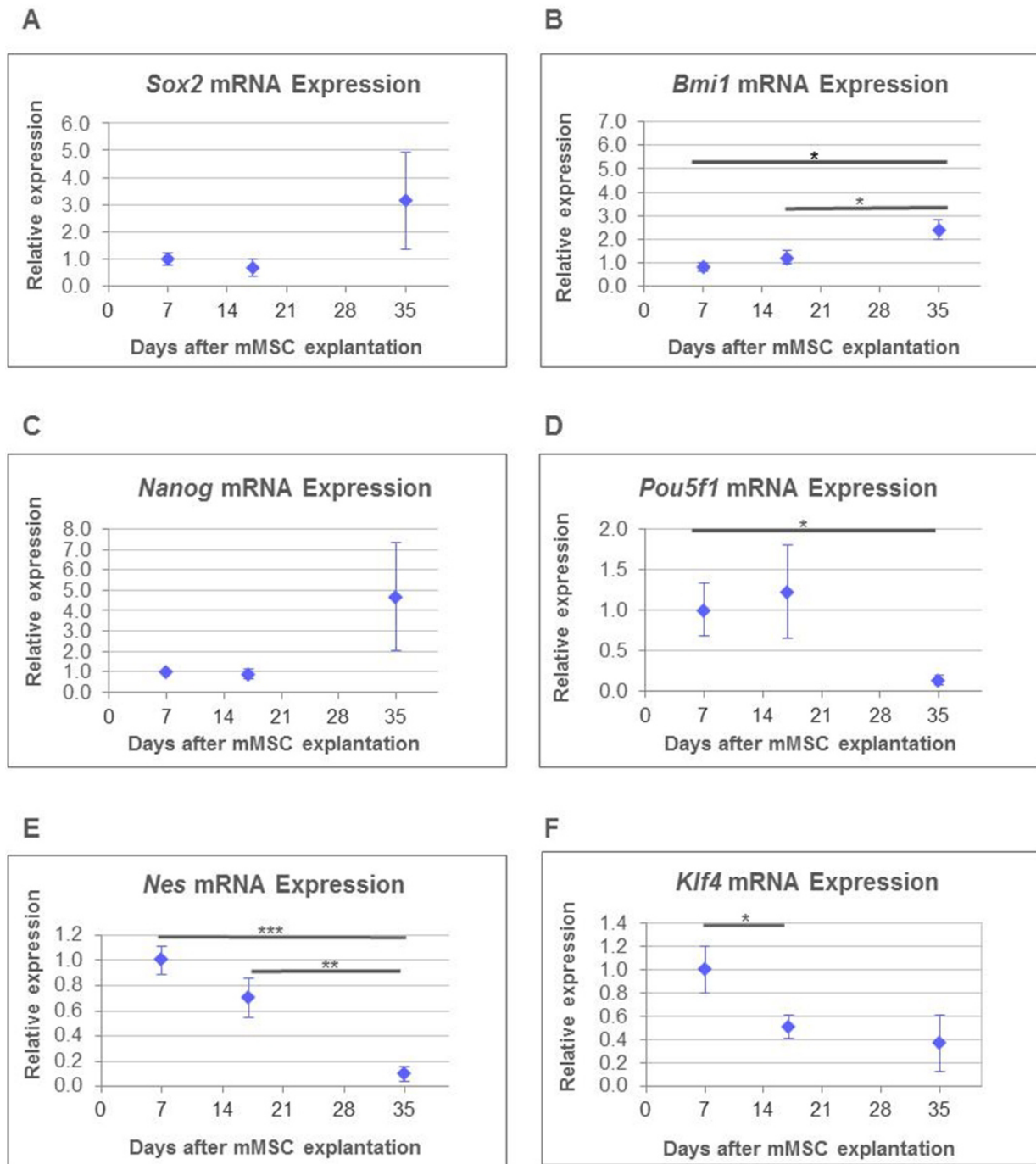


Figure 22: Real-Time PCR expression analysis of stemness and pluripotency marker genes in mMSCs. The plots show relative expression in mean values \pm standard error of the mean. Murine mesenchymal stem cells were obtained from 3 *Rb*^{+/+} biological replicates and the experiment was performed with technical duplicates. The expression values for every gene on different days of the *in vitro* culture were normalized to its own expression on day 7. Difference between the relative expression for day 7, 17 and 35 was statistically evaluated with Student's t-test, unpaired, 2-tailed. TBP was used as a housekeeping gene. A) Expression of *Sox2* in mMSC culture B) Expression of *Bmi1* in mMSC culture (p-value 0.014 for day 7 and day 35; p-value 0.046 for day 17 and day 35) C) Expression of *Nanog* in mMSC culture D) Expression of *Pou5f1* in mMSC culture (p-value 0.04 for day 7 and day 35) E) Expression of *Nes* in mMSC culture (p-value 0.004 for day 7 and day 35; p-value 3.07×10^{-5} for day 17 and day 35) F) Expression of *Klf4* in mMSC culture (p-value 0.04 for day 7 and day 17).

5.5 Telomere length measurement of *in vitro* cultured mMSCs

5.5.1 Effect of oxygen concentration on telomere length in mMSCs

In this study the growth, survival and clonogenicity of the mMSC were found to be severely affected by normoxia. To investigate the effect of oxygen on telomere length in mMSCs, telomere length of 7 and 18 days old hypoxic and normoxic mMSCs from 5 *Rb*^{+/+} biological replicates was compared. The results were analysed with Student's t-test, unpaired, 2-tailed.

On day 7, normoxic mMSCs displayed slightly shorter telomeres than cells grown under hypoxia. (fig. 23). After further culturing, on day 18 telomere length of normoxic mMSCs was further decreased while that in hypoxic mMSCs was increased. However, this difference between the relative telomere lengths of mMSCs grown in two different culture conditions was statistically insignificant. It implies that the telomere length of mMSCs is not critically affected by higher oxygen concentration at least for up to 18 days in culture. It also rules out the possibility of accelerated telomeric shortening resulting into reduced survival of mMSCs in normoxia.

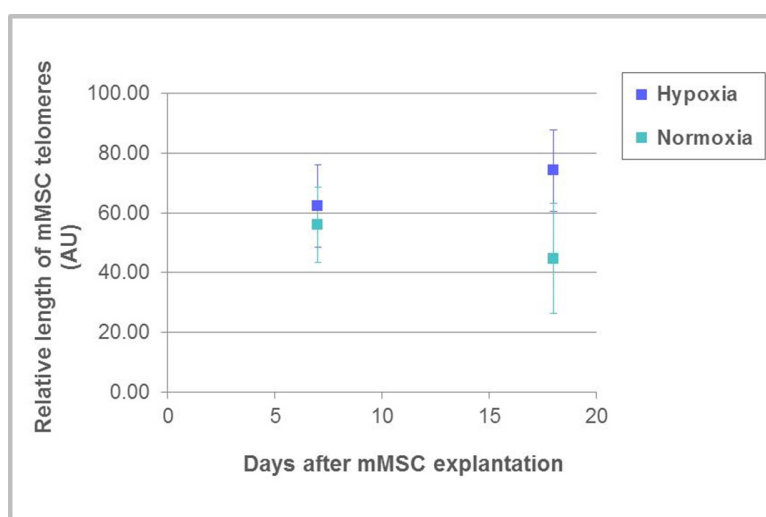


Figure 23: Effect of oxygen concentration on telomere length in mMSCs. Telomeric length of 7 and 18 days old hypoxic and normoxic mMSCs displayed as arbitrary units (AU) in mean values \pm standard error of the mean. The scatter plot shows telomere length values from 5 *Rb*^{+/+} biological replicates with technical duplicates in reference to pooled new-born mouse skin DNA set to 100 AU.

5.5.2 Effect of retinoblastoma gene status on telomere length in mMSCs

The effect of *Rb1* status on telomere length of mMSCs was examined using 7 and 18 days old cells from 3 mice each of *Rb*^{+/+} and *Rb*^{+/-} genotypes respectively. Murine mesenchymal stem cells from both genotypes were grown in optimal culture condition with hypoxia. Telomere length measurement was carried out using pooled new born mouse skin DNA as a reference sample. The results were analysed with Student's t-test, unpaired, 2-tailed.

Initially, *Rb*^{+/-} mMSCs displayed longer telomeres than *Rb*^{+/+} mMSCs (fig. 24). With further culturing *Rb* heterozygous telomeres were shortened contrary to *Rb* wild type telomeres which were slightly lengthened. This difference in the telomere length of *Rb*^{+/-} and *Rb*^{+/+} mMSCs was found

to be statistically insignificant. Therefore, both Rb wild type and heterozygous mMSCs don't show significant changes in their telomeric length for up to 18 days *in vitro*.

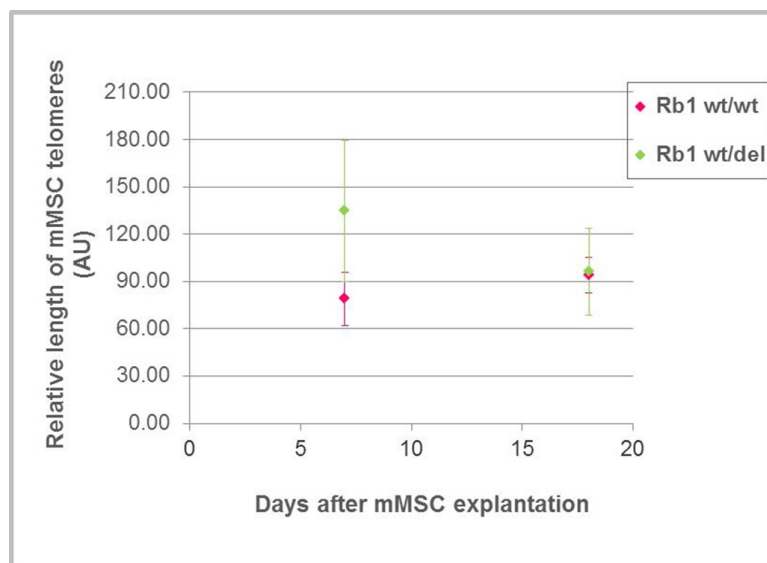


Figure 24: Effect of *Rb1* status on telomere length in mMSCs. Telomeric length of 7 and 18 days old hypoxic *Rb*^{+/+} and *Rb*^{+/-} mMSCs displayed as arbitrary units (AU) in mean values \pm standard error of the mean. The scatter plot shows telomere length values from 3 biological replicates with technical duplicates in reference to pooled new-born mouse skin DNA set to 100 AU.

5.6 Identification of *Pou5f1* Real-Time PCR products in mMSCs

During the Real-Time PCR expression analysis of *Pou5f1* in *Rb*^{+/+} mMSCs multiple melting peaks (at temperature 71.5, 77.5 and 83.5 °C) were observed in a single sample (fig. 25). In the melting curve analysis of a Real-Time PCR experiment having multiple melting peaks in a single sample reflects presence of more than one amplified product. Furthermore, melting temperature of any product is directly proportional to the length of its nucleotide sequence. Hence, it was decided to investigate the probable reasons behind the formation of unspecific products. One of the most plausible hypothesis was the possibility of alternatively spliced mRNA transcripts of *Pou5f1* as previously published [151].

To figure out the identity of unspecific products, Real-Time PCR sample showing 3 different melting peaks was purified and further amplified using PCR conditions as described in section 4.14.2. Agarose gel electrophoresis was performed with amplified products (Fig. 26) and 3 separate *Pou5f1* product bands were extracted, purified and checked for DNA concentration.

These purified DNA samples were cloned separately with TOPO® TA cloning and transformed *E. coli* colonies were continued for each of the individual product. Mini prep was done to isolate different products from the plasmids. Later, sequencing was performed and the sequence files were viewed with 4Peaks software v 1.7.

With sequence analysis the short product (melting peak at 71.5 °C) was found to be 69 bp, middle sized product (melting peak at 77.5 °C) was 134 bp and long product (melting peak at 83.5 °C) was 192 bp in length. Sequence from all the three mMSC *Pou5f1* Real-Time PCR products is given in

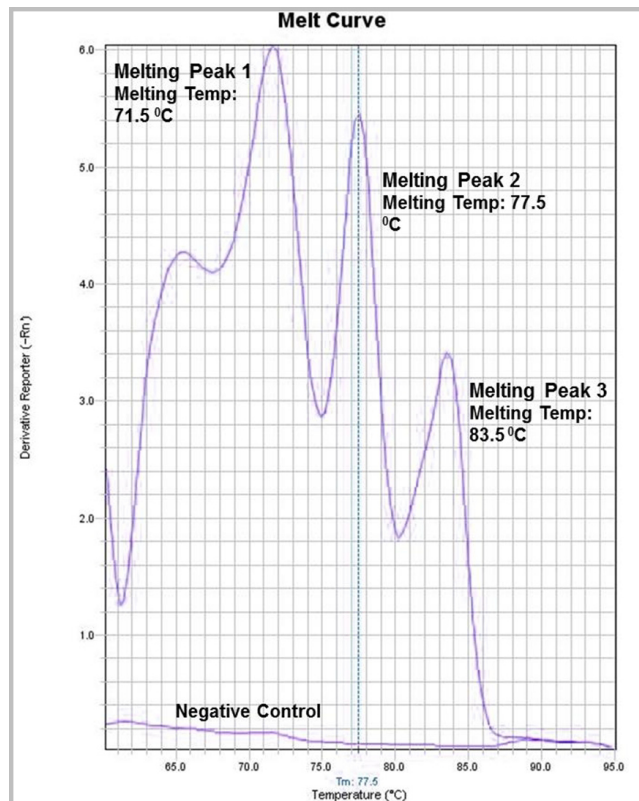


Figure 25: Melting curve analysis of the mMSC sample after Real-Time PCR run with *Pou5f1* primers. Image shows 3 different melting peaks with 3 melting temperatures observed in a single sample of *Rb*^{+/+} mMSC after the Real-Time PCR expression analysis for *Pou5f1* gene.

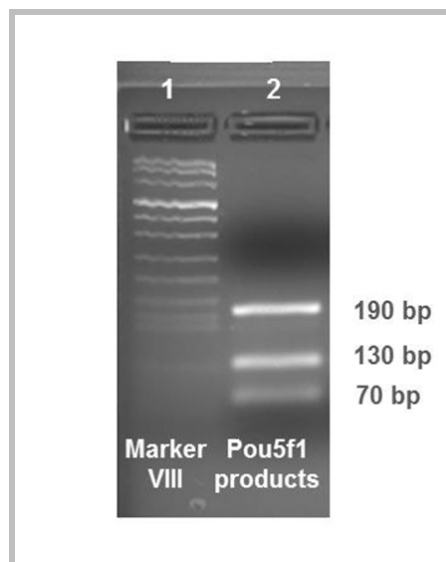


Figure 26: Agarose gel electrophoresis for the *Pou5f1* Real-Time PCR product of mMSCs. PCR amplified *Pou5f1* Real-Time PCR product on 3% agarose gel. Lane 2- Three different bands at 70 bp, 130 bp and 190 bp can be seen in a single sample of the *Rb*^{+/+} mMSCs after Real-Time PCR run with *Pou5f1* primers. Lane 1 displays marker VIII that was used as a DNA molecular length marker.

table 5.2.

Finally, the nucleotide blast for *Mus musculus* was carried out to identify individual products

Table 5.2: Nucleotide sequences for the *Pou5f1* Real-Time PCR products of mMSCs

Product	Melting Temperature (°C)	Length (bp)	Sequence
Short band	71.5	69	GATCACTCACATCGCCAATCA GCTTGGGCTAGAGAAGGATGT GGTTCGAGTATGGTTCTGTAA CCGGCG
Middle sized band	77.5	134	CGCCGGTTACAGAACCATATC CGCAGCAGGTCTCCAAGGTGA ACAGCCTCTGGCATGTTGGAA CAATGTAGGTAAGGGAAGTCG GCAAGCCGGATCCGTAACTTC GGGATAAGGATTGGCGATGTG AGTGATCA
Long band	83.5	192	TCGCCGGTTACAGAACCATAC TGCCTGTGCTCTATGGTTCT GCCAGACTGAAGCCGGCCGGC CTTAGTTCCAGAGTCCTGCCA TGGAATGGAGAGGGTGAAGCC CAGAGGCGGGTTGTTAGCCTT GTTTTATAAACAGATCTAATG CTAGTGCCCATCTCCTGGGGTT GATTGGCGATGTGAGTGATCAA

as described in section 4.14.8. With nucleotide blast the short product was identified as *Mus musculus* POU domain, class 5, transcription factor 1 (*Pou5f1*), transcript variant X1, mRNA (fig. 27A). The product spans the exon 4 and 5 with 40 nucleotides in exon 4 and 29 nucleotides in exon 5 as shown in fig. 27.

Middle sized product was *Mus musculus* mRNA for phosphacan short isoform (RPTP-beta gene), and long product was found to be a Mouse DNA sequence from clone RP23-309H19 on chromosome 11. Both of these products found to share very little sequences with *Pou5f1* transcript (20 nucleotide homology for middle sized product and 21 nucleotide homology for long product). Finally, it was clear that the three Real-Time PCR products amplified with *Pou5f1* primers are in fact the products formed by unspecific binding of the primers to other cDNA species. Therefore, the old primer pair was discontinued and a new one was designed for further use.

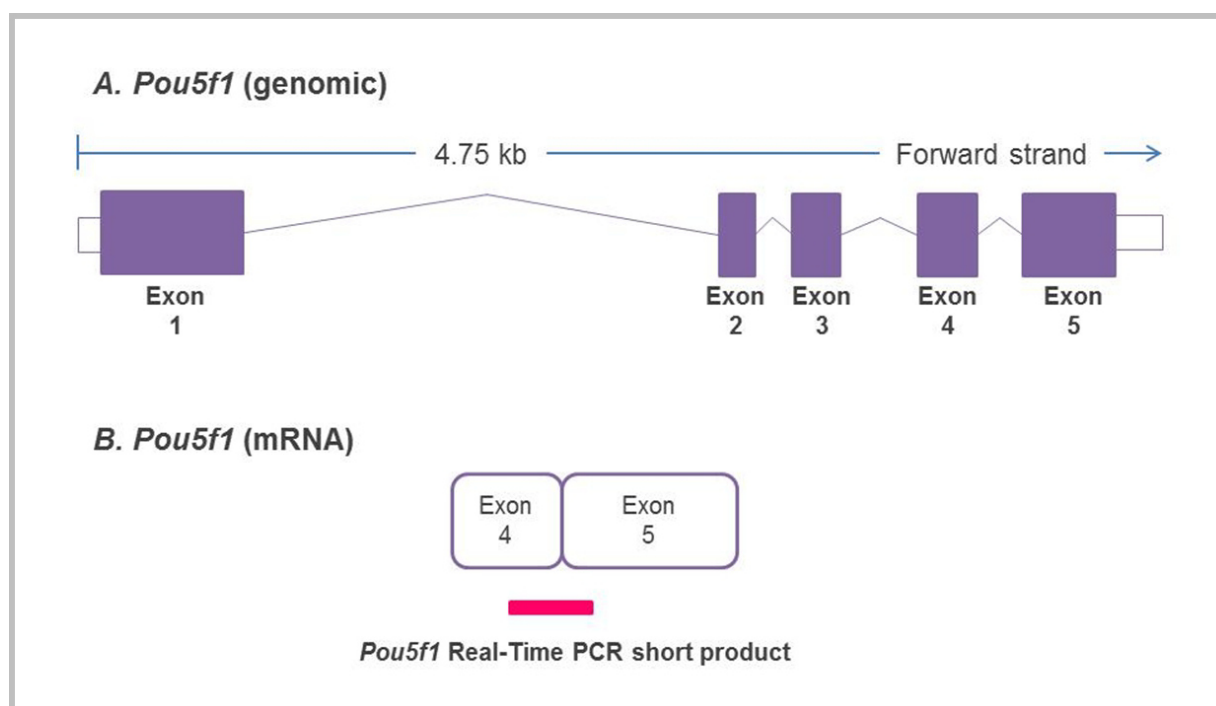


Figure 27: Sequence alignment of *Pou5f1* Real-Time PCR short product on *Pou5f1* gene. A) *Pou5f1* gene with its 5 exons. B) *Pou5f1* Real-Time PCR short product is 69 bp long (displayed in dark pink colour) and spans exon 4 and exon 5 of *Pou5f1* gene.

5.7 *In vitro* ageing of mMSCs

To find out the genes involved in *in vitro* ageing of MSCs, the first step is identification of genes specific to MSCs. In this project, screening approach was adopted for the mMSC specific gene identification using mMSC specific RT² profiler PCR array. To identify the candidate genes specific to mMSCs, pooled sample of 21 days old hypoxic MSCs from 2 *Rb*^{+/+} mice was compared with pooled sample of passage 7 and passage 9 osteoblasts from 2 *Rb*^{+/+} mice. osteoblasts are the terminally differentiated progenies of MSCs. Plus, MSC culture usually displays higher degree of sporadic differentiation towards osteoblastic lineage [152]. Comparing the gene expression pattern of mMSCs against differentiated osteoblasts will identify the genes restricted to mMSCs. Complete list of all genes present in RT² profiler PCR array with their corresponding fold change in mMSCs as compared to osteoblasts is given in Appendix B. To determine the mMSC specific genes, threshold was set at 6 fold expression difference. After the data analysis the genes showing 6 fold expression differences without any technical irregularities such as too low or too high average threshold cycle which may cause erroneous results or presence of more than one melting curves in the sample were considered for further analysis. Hence, 31 differentially regulated (up- and down-regulation) genes in mMSCs compared to osteoblasts were identified. The complete list of these 31 differentially regulated genes with their corresponding fold change is given in table 5.3.

Table 5.3: List of the 31 mMSC specific genes with their corresponding fold change as compared to osteoblasts

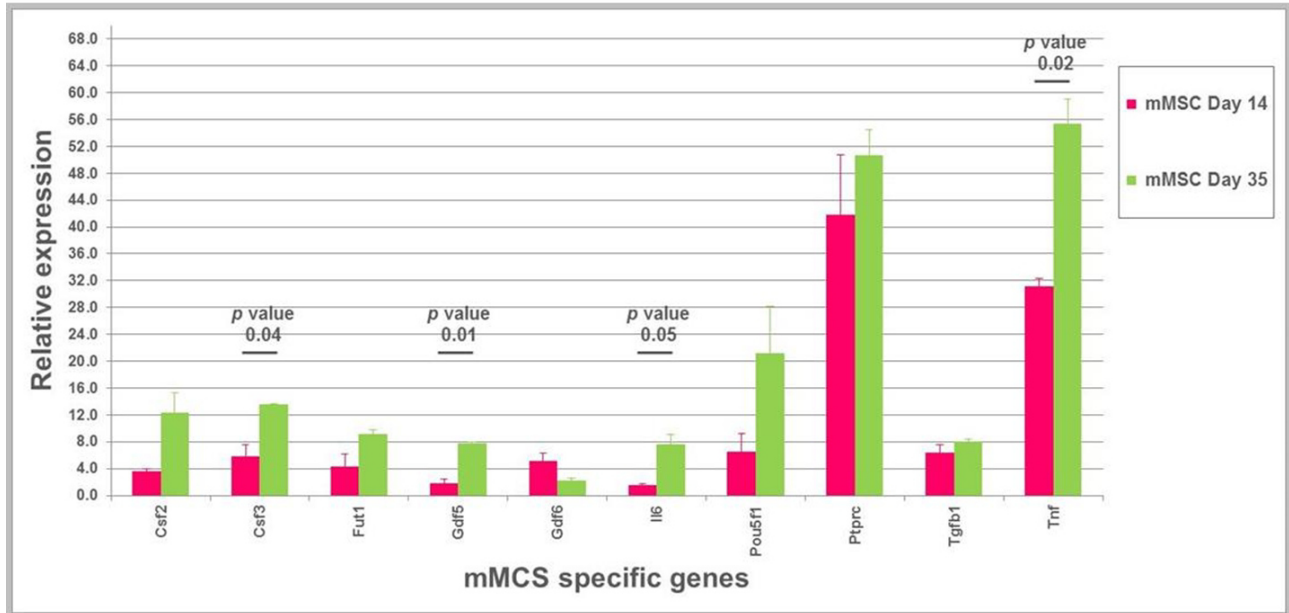
Description	Symbol	Fold change (relative to osteoblasts)
Thymus cell antigen 1, theta	<i>Thy1</i>	-6.38
ATP-binding cassette, sub-family B	<i>Abcb1a</i>	20.1
Bone morphogenetic protein 2	<i>Bmp2</i>	20.09
Bone morphogenetic protein 6	<i>Bmp6</i>	40.39
Colony stimulating factor 2 (granulocyte-macrophage)	<i>Csf2</i>	9.97
Colony stimulating factor 3 (granulocyte)	<i>Csf3</i>	10.04
Endoglin	<i>Eng</i>	39.7
Fucosyltransferase 1	<i>Fut1</i>	159.49
Frizzled homolog 9 (Drosophila)	<i>Fzd9</i>	20.34
Growth differentiation factor 5	<i>Gdf5</i>	39.23
Growth differentiation factor 6	<i>Gdf6</i>	20.28
HNF1 homeobox A	<i>Hnf1a</i>	40.12
Interleukin 6	<i>Il6</i>	20.22
Insulin II	<i>Ins2</i>	19.9
Integrin alpha 6	<i>Itga6</i>	20.13
Kinase insert domain protein receptor	<i>Kdr</i>	19.95

Description	Symbol	Fold change (relative to osteoblasts)
Microphthalmia-associated transcription factor	<i>Mitf</i>	40.07
Nerve growth factor receptor (TNFR superfamily, member 16)	<i>Ngfr</i>	19.96
Notch gene homolog 1 (Drosophila)	<i>Notch1</i>	82.83
Nudix (nucleoside diphosphate linked moiety X)-type motif 6	<i>Nudt6</i>	10.13
POU domain, class 5, transcription factor 1	<i>Pou5f1</i>	20.11
Prominin 1	<i>Prom1</i>	20.06
Protein tyrosine phosphatase, receptor type, C	<i>Ptprc</i>	323.91
SRY-box containing gene 2	<i>Sox2</i>	19.87
T-box 5	<i>Tbx5</i>	40.44
Telomerase reverse transcriptase	<i>Tert</i>	10.04
Transforming growth factor, beta 1	<i>Tgfb1</i>	10.01
Tumor necrosis factor	<i>Tnf</i>	80.74
Von Willebrand factor homolog	<i>Vwf</i>	20.19
Wingless-related MMTV integration site 3A	<i>Wnt3a</i>	169.03
Zinc finger protein 42	<i>Zfp42</i>	39.31

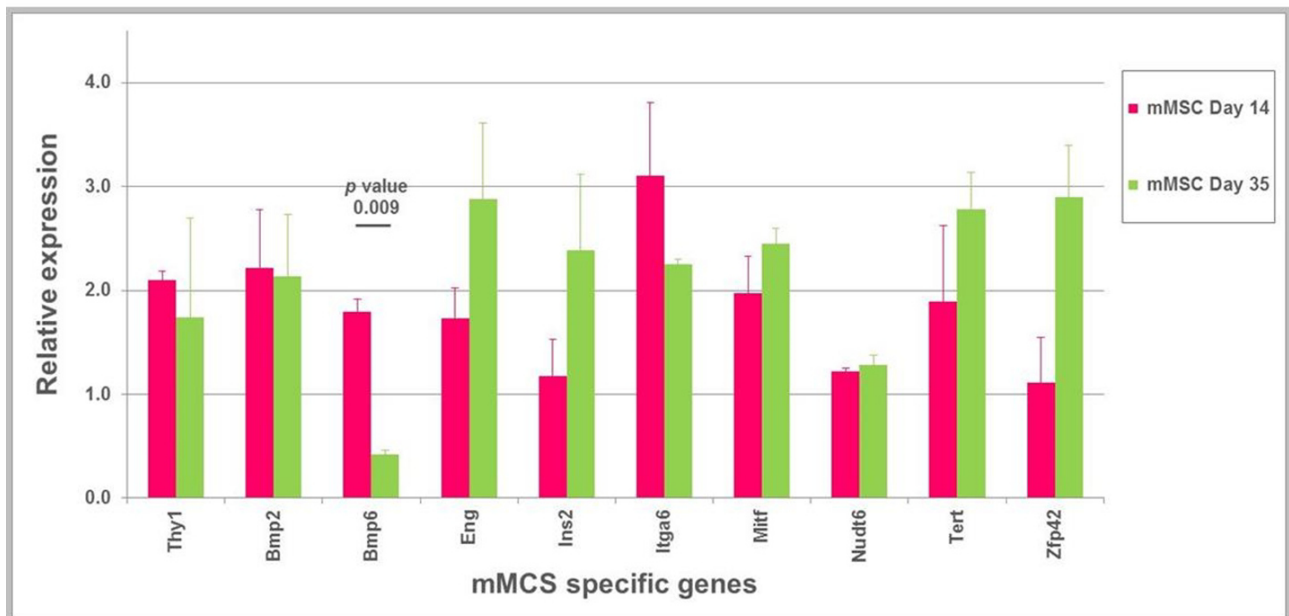
CHAPTER 5. RESULTS

These 31 mMSC specific genes were then analysed in young (day 14) and old (day 35) mMSCs obtained from 2 *Rb*^{+/+} biological replicates to find out the candidate genes that could be implicated in the *in vitro* ageing of the mMSCs as shown in fig. 28.

A



B



C

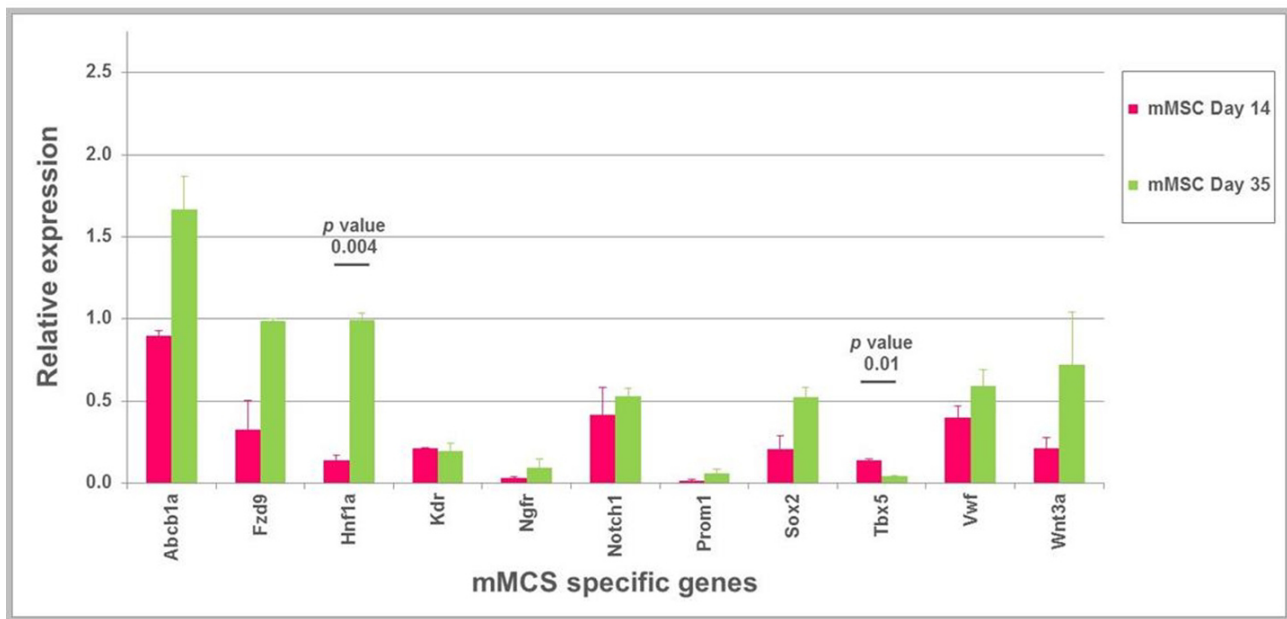


Figure 28: Relative expression of mMSC specific genes. The bar graphs show relative expression of the mMSC specific genes in young (14 days) and old (35 days) mMSCs. Murine mesenchymal stem cells were obtained from 2 *Rb*^{+/+} biological replicates and the experiment was performed with technical duplicates. Expression level of the 31 mMSC specific genes is relative to embryonic cDNA which was used as calibrator. These expression values are the mean values \pm standard error of the mean. Gene expression difference between day 14 and 35 was statistically evaluated with Student's t-test, unpaired, 2-tailed. The p-values for the genes showing statistically significant difference between old and young mMSCs are shown in the figure, A) Relative expression of *Csf2*, *Csf3*, *Fut1*, *Gdf5*, *Gdf6*, *Il6*, *Pou5f1*, *Ptpcr*, *Tgfb1* and *Tnf*. B) Relative expression of *Thy1*, *Bmp2*, *Bmp6*, *Ing*, *Ins2*, *Itga6*, *Mitf*, *Nudf6*, *Tert* and *Zfp42*. C) Relative expression of *Abcb1a*, *Fzd9*, *Hnf1a*, *Kdr*, *Ngfr*, *Notch1*, *Prom1*, *Sox2*, *Tbx5*, *Vwf* and *Wnt3a*.

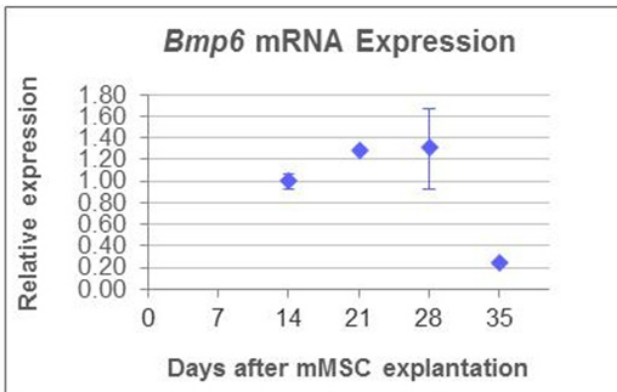
Genes that displayed statistically significant difference in their expression pattern for young and old cells were marked as the genes responsible for *in vitro* ageing of mMSCs. The statistical analysis revealed 7 genes (p -value < 0.05) that are affected when the mMSCs age in culture. The ageing genes with their corresponding expression values on day 14 and day 35 including the p -values obtained by statistical analysis (Student's t-test, unpaired, 2-tailed) are listed in table 5.4.

Table 5.4: List of mMSC ageing genes with their relative expression in young and old *in vitro* cultured mMSCs

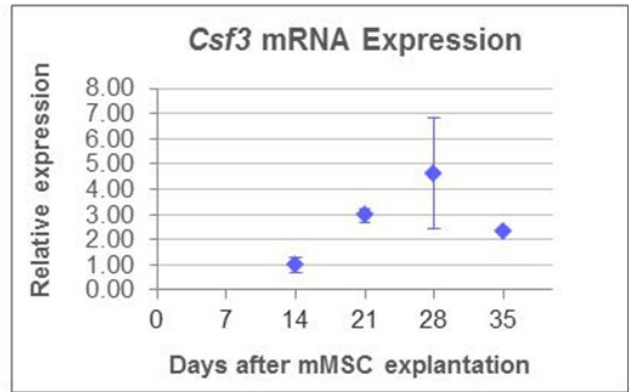
Ageing genes	Relative expression in young mMSCs (14 days)	Relative expression in old mMSCs (35 days)	p-value
<i>Bmp6</i>	1.795	0.426	0.009
<i>Csf3</i>	5.852	13.631	0.042
<i>Gdf5</i>	1.763	7.698	0.015
<i>Hnf1a</i>	0.140	0.992	0.004
<i>Il6</i>	1.511	7.670	0.049
<i>Tbx5</i>	0.135	0.041	0.011
<i>Tnf</i>	31.096	55.323	0.024

The ageing genes were also checked for their expression in middle aged mMSCs of day 21 and day 28. The expression pattern of 7 ageing genes throughout entire culturing from day 14 till day 35, including day 21 and 28 is shown in fig. 29. The fold change values for all the samples were normalized to youngest (14 days old) cells. It was observed that the expression patterns of ageing genes through the period of *in vitro* culturing are rather dynamic and follow a non-linear trend without progressive up- or down-regulation of the gene expression except that of *Hnf1a*.

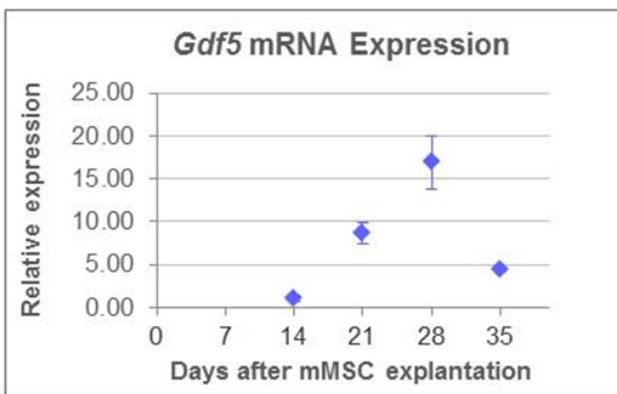
A



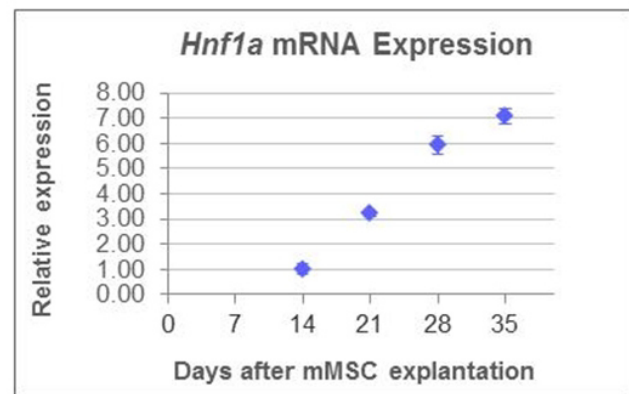
B



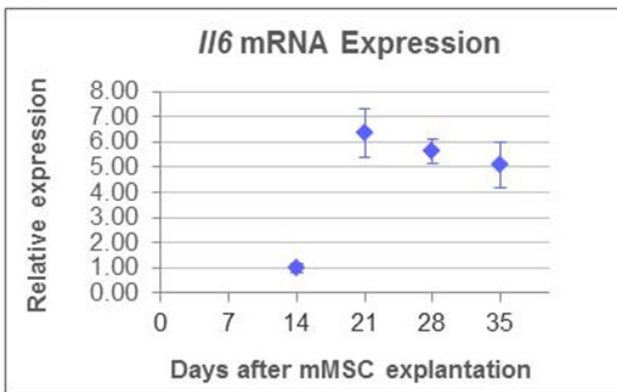
C



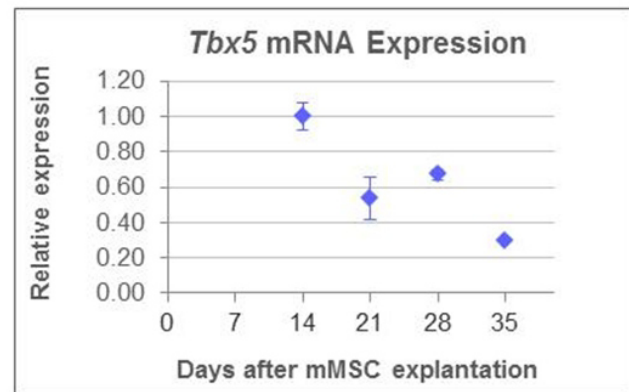
D



E



F



G

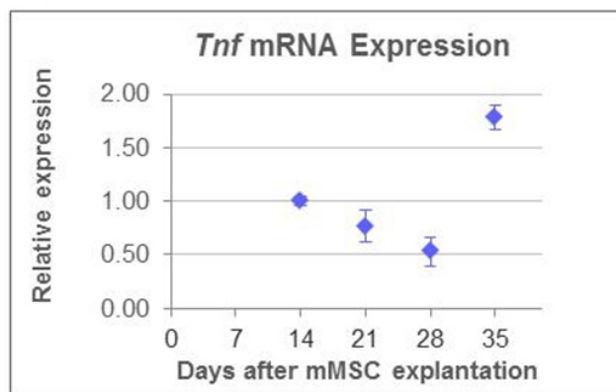


Figure 29: Real-Time PCR expression analysis of the ageing genes in mMSCs of different age. Relative expression of the 7 mMSC ageing genes on different days of the *in vitro* culture was normalized to their own expression on day 14. The plots show expression levels of these genes on day 14, 21, 28 and 35 as the mean values \pm standard error of the mean. Murine mesenchymal stem cells were obtained from 2 *Rb*^{+/+} biological replicates and the experiment was performed with technical duplicates. TBP was used as a housekeeping gene. A) Expression of *Bmp6* in mMSC culture. B) Expression of *Csf3* in mMSC culture. C) Expression of *Gdf5* in mMSC culture. D) Expression of *Hnf1a* in mMSC culture. E) Expression of *Il6* in mMSC culture. F) Expression of *Tbx5* in mMSC culture. G) Expression of *Tnf* in mMSC culture.

5.8 Characterisation of *in vitro* cultured mMSCs after exposure to ionizing radiation

Due to broadening use of MSCs in regenerative therapy and ever increasing exposure to ionizing radiation by means of natural and artificial sources in day-today life, it is of importance to study the interaction between MSCs and ionizing radiation, and the effect of γ -irradiation on the MSC biology.

5.8.1 Effect of ionizing radiation on *in vitro* ageing of mMSCs

To investigate whether ionizing radiation exposure affects the expression of 7 ageing genes and accelerates ageing in mMSCs, young hypoxic mMSCs obtained from 4 *Rb*^{+/+} biological replicates were treated with low (0.1 Gy) and medium (2 Gy) doses of γ -irradiation on day 8. The control cells were sham-irradiated. Expression pattern of the ageing gene was analysed on day 14, 21 and 35 to study the long-term effects of ionizing radiation during the *in vitro* culture progression. The fold change values for all the irradiated samples were normalized to youngest (14 days old) sham irradiated (control) cells. To understand the individual effect of low dose and medium dose γ -irradiation statistical analysis for the two treatments was performed separately. Interaction of ionizing radiation dose and *in vitro* age was assessed using two-way ANOVA with Tukey's HSD for post hoc analysis.

For both, the low dose (0.1 Gy) and medium dose (2 Gy), *Bmp6* (fig. 30A) and *Il6* (fig. 30E) displayed an age-dependent down-regulation from day 14 to day 35 in culture, similar to that of sham-irradiated cells. Medium dose of 2 Gy reduced expression of these genes in 14 days old cells as compared control cells, however, no considerable difference was found for the 21 and 35 days old mMSCs. Statistical analysis revealed that the decreased expression of *Bmp6* and *Il6* is in fact the effect of ageing and ionizing radiation didnt have significant influence on their expression values.

Csf3 (fig. 30B), *Gdf5* (fig. 30C), *Hnf1a* (fig. 30D) and *Tbx5* (fig. 30F) didnt show any significant changes in their expression from day 14 to day 35 both in control and irradiated samples. It indicates that the expression of these genes in mMSCs is independent of the radiation dose.

Interestingly, *Tnf* (fig. 23G) expression was found to be significantly altered with both age (p-value 0.037) and medium dose of 2 Gy (p-value 0.026) independently. Though, the interaction effect of age and radiation was absent. As for the low dose, *Tnf* expression was affected only by age (0.003) without any radiation effect. Hence, medium dose irradiation of young (8 days old) mMSCs induced

persistent changes in the expression of *Tnf*. And the change in the expression pattern of *Tnf* gene is comparable to its expression in sham-irradiated old (35 days old) cells.

The effects of age and low and medium dose ionizing radiation on the expression of mMSC ageing genes are summarized in Table 5.5.

Table 5.5: Effects of *in vitro* age and low and medium dose ionizing radiation on the expression profile of ageing genes in mMSCs (↔ no change in gene expression; ✓ gene expression is affected)

Ageing genes	Effect of ageing	Effect of low dose ionizing radiation	Effect of medium dose ionizing radiation
<i>Bmp6</i>	✓	↔	↔
<i>Csf3</i>	↔	↔	↔
<i>Gdf5</i>	↔	↔	↔
<i>Hnf1a</i>	↔	↔	↔
<i>Il6</i>	✓	↔	↔
<i>Tbx5</i>	↔	↔	↔
<i>Tnf</i>	✓	↔	✓

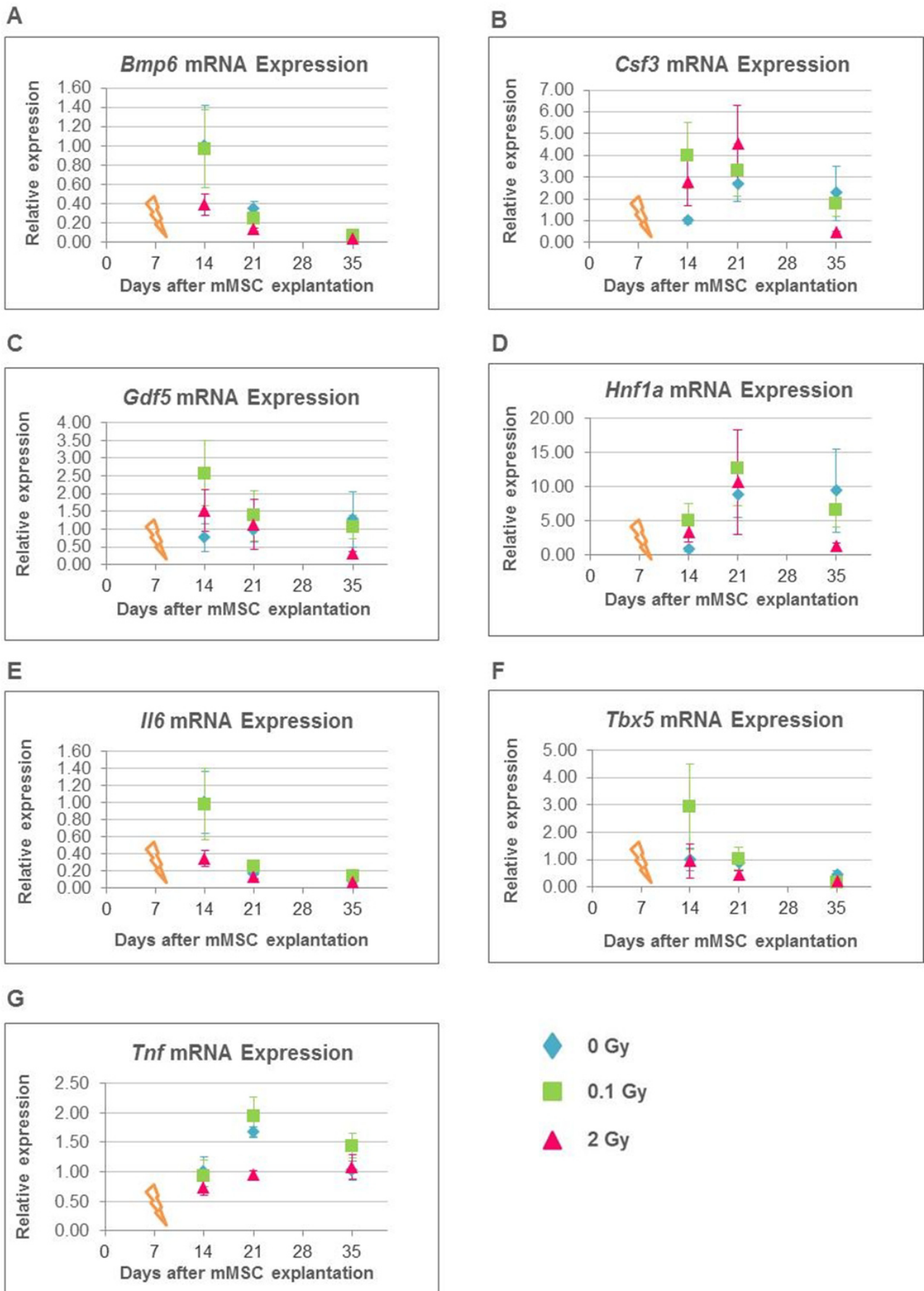


Figure 30: Effect of ionizing radiation on the expression profile of the ageing genes in mMSCs of different age. Relative expression of the 7 mMSC ageing genes on different days after 0 Gy, 0.1 Gy and 2 Gy γ -irradiation treatments. The gene expression level for different days was normalized to its own expression in 14 days old sham irradiated cells. The plots show relative expression values obtained by Real-Time PCR analysis on day 14, 21 and 35 as the mean values \pm standard error of the mean. Murine mesenchymal stem cells were obtained from 4 *Rb*^{+/+} biological replicates and the experiment was performed with technical duplicates. TBP was used as a housekeeping gene. Orange arrow indicates time of radiation exposure (day 8). A) Expression of *Bmp6* in mMSC culture. B) Expression of *Csf3* in mMSC culture. C) Expression of *Gdf5* in mMSC culture. D) Expression of *Hnf1a* in mMSC culture. E) Expression of *Il6* in mMSC culture. F) Expression of *Tbx5* in mMSC culture. G) Expression of *Tnf* in mMSC culture.

5.8.2 Effect of ionizing radiation on clonogenic survival of mMSCs: hypoxic and normoxic conditions

The clonogenic assay is a gold standard for radiation-action on mammalian cells. The colony forming ability of hypoxic and normoxic mMSCs obtained from 3 *Rb*^{+/+} biological replicates after irradiation treatment (0 Gy, 0.1 Gy, 0.2 Gy, 0.5 Gy and 4 Gy) was assessed with clonogenic assay. Images of giemsa stained colonies grown in hypoxia after 0.2 Gy, 0.5 Gy and 4 Gy ionizing radiation treatments along with sham-irradiated colonies as the representative of the hypoxic and normoxic irradiated cultures are shown in fig. 31. Interaction of ionizing radiation dose and oxygen concentration was assessed using two-way ANOVA with Tukey's HSD for post hoc analysis. The

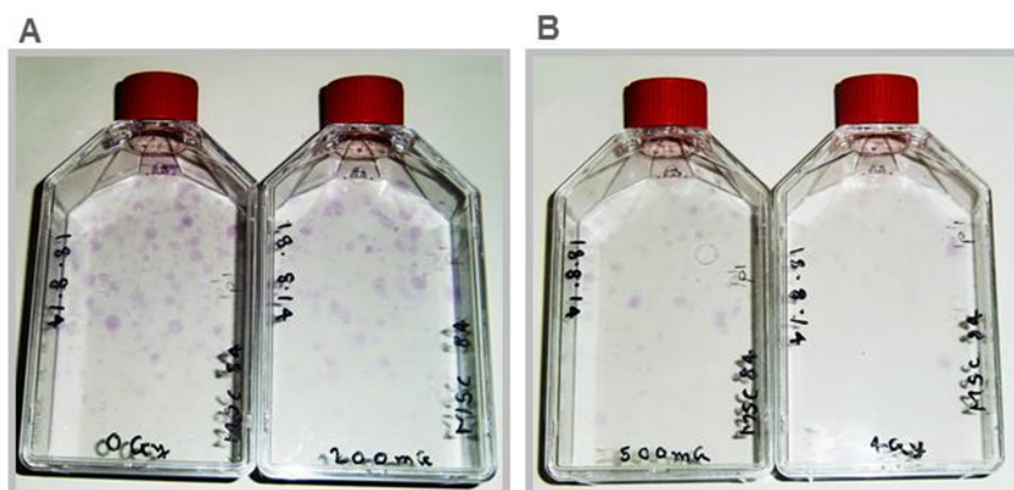


Figure 31: Colony forming ability of mMSCs after exposure to ionizing radiation. Representative images of giemsa-stained colonies of mMSCs obtained from 3 *Rb*^{+/+} biological replicates grown under hypoxia after treatment with 0 Gy, 0.2 Gy, 0.5 Gy and 4 Gy on day 21 of the *in vitro* culturing A) Colonies formed in control and 0.2 Gy irradiated cultures. B) Colonies formed in 0.5 Gy and 4 Gy irradiated cultures.

plating efficiency of mMSCs in hypoxia and normoxia differed considerably with approximately 13 times increase in number of colonies formed in hypoxic condition than in normoxic condition. In hypoxia, a dose-dependent decrease in colony forming ability of mMSCs was observed while there was no clear trend for normoxic mMSCs in the low dose region (fig. 32). Interestingly, low dose

irradiated mMSCs (0.1 Gy, 0.2 Gy, 0.5 Gy) from normoxia displayed higher number of colonies than control cells. Nevertheless, for the medium dose of 4 Gy the clonogenic survival of normoxic mMSCs decreased critically. With statistical analysis it was found that both, oxygen concentration and ionizing radiation have the potential to alter the clonogenicity of mMSCs. Oxygen concentration influences the colony forming ability of mMSCs and this effect is statistically highly significant (p-value 1.45×10^{-9}). Even ionizing radiation has a significant effect on colony formation in mMSCs (p-value ionizing radiation 0.013) which becomes obvious with extensively reduced clonogenicity at the medium dose of 4 Gy. The interaction effect of oxygen concentration and ionizing radiation dose was statistically significant with p-value 0.041. This data clearly suggests that the decreased colony forming ability of mMSCs in normoxia is potentiated by ionizing radiation.

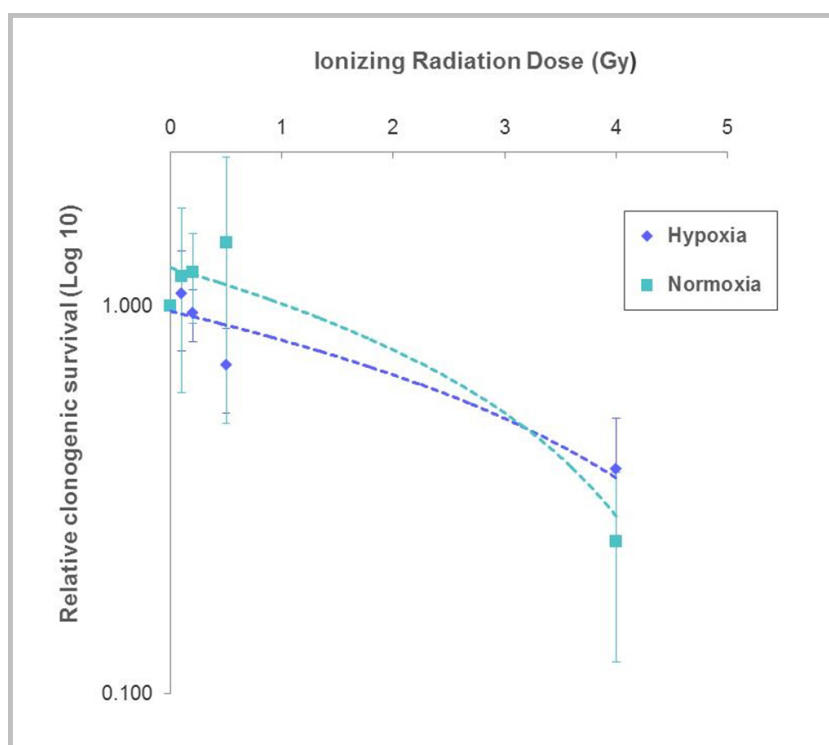


Figure 32: Effect of ionizing radiation on the colony forming ability of mMSCs under hypoxic and normoxic conditions. Number of mMSC colonies formed by 3 *Rb*^{+/+} biological replicates in hypoxic and normoxic conditions after the γ -irradiation treatment with 0 Gy, 0.1 Gy, 0.2 Gy, 0.5 Gy and 4 Gy. The numbers of colonies formed are displayed as relative clonogenic survival (log₁₀) in mean values \pm standard error of the mean. The difference between the clonogenicity of control and ionizing radiation treated cells in hypoxic and normoxic cultures was analysed using two-way ANOVA with Tukey's HSD for post hoc analysis; p-value oxygen concentration*ionizing radiation 0.041, Oxygen concentration 1.45×10^{-9} and ionizing radiation 0.013.

5.8.3 Effect of ionizing radiation on senescence in mMSCs: hypoxic and normoxic conditions

It was observed that ambient oxygen concentration influences the growth and reduces the clonogenicity of mMSCs *in vitro*. This implies that the oxygen concentration may potentially influence the onset of senescence in mMSCs. To investigate the role of oxygen on senescence induction,

mMSCs grown in hypoxic and normoxic conditions obtained from 4 *Rb*^{+/+} biological replicates were assayed for SA- β -Galactosidase activity. The cultures were observed under a microscope when they became subconfluent around 8 days after cell seeding. Visibly no large difference between the numbers of cells growing in hypoxia or normoxia was found as the cells were still in the early stages of *in vitro* culturing. However, normoxic cultures ($53 \pm 9.3\%$) showed remarkable increase in SA- β -Galactosidase positive greenish blue cells over hypoxic cultures ($30 \pm 4.5\%$) (fig. 33 upper row). As the higher oxygen tension increased the number of mMSCs undergoing senescence,

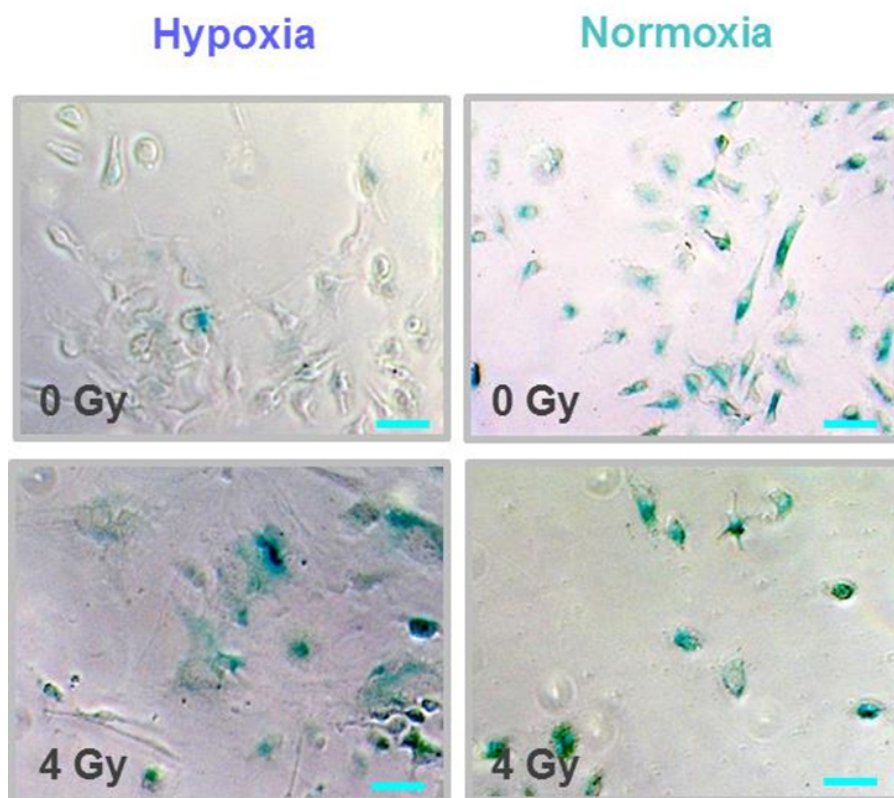


Figure 33: Senescence in mMSCs after exposure to ionizing radiation. Representative images of greenish blue SA- β -Galactosidase positive cells in the cultures obtained from 4 *Rb*^{+/+} biological replicates grown under hypoxia (left panel) and normoxia (right panel) after treatment with 0 Gy (upper row) and 4 Gy (lower row) of the γ -irradiation. Scale bar: 50 μ m.

it was interesting to investigate the effects of ionizing radiation which is known to generate an oxidative stress on biological systems. Therefore, senescent assay was performed on subconfluent irradiated cultures. Low dose treated cells (0.1 Gy, 0.2 Gy and 0.5 Gy) retained their spindle-shaped morphology in both hypoxic and normoxic conditions. Unlike low dose, the cells treated with 4 Gy from both hypoxia and normoxia lacked typical spindle-shaped morphology as seen in fig. 33 (lower row). When observed under a microscope the cell number for 4 Gy irradiated cell was also substantially reduced (fig. 33 lower row). The percentage of hypoxic cells undergoing senescence didnt differ considerably between the control and irradiated cultures (fig. 34). Interestingly, normoxic cells demonstrated increased tendency of senescence even after low dose radiations of 0.1 Gy and 0.2 Gy compared to the control cells. Though, the higher doses of 0.5 Gy, 2 Gy and 4 Gy didnt cause any further increase in senescence than that of 0.2 Gy.

The interaction effect of ionizing radiation and oxygen tension was analysed using two-way ANOVA with Tukey's HSD for post hoc analysis. Interaction of higher oxygen and ionizing radiation significantly increased the senescence in mMSCs (p-value 0.003). Irradiation could independently cause mMSCs to undergo senescence (p-value 0.031). Ambient oxygen concentration on its own was also a crucial factor responsible for increasing senescence in mMSCs (p-value 3.2×10^{-18}). All together this suggests that irradiation increases the sensitivity of mMSCs towards normoxia induced senescence.

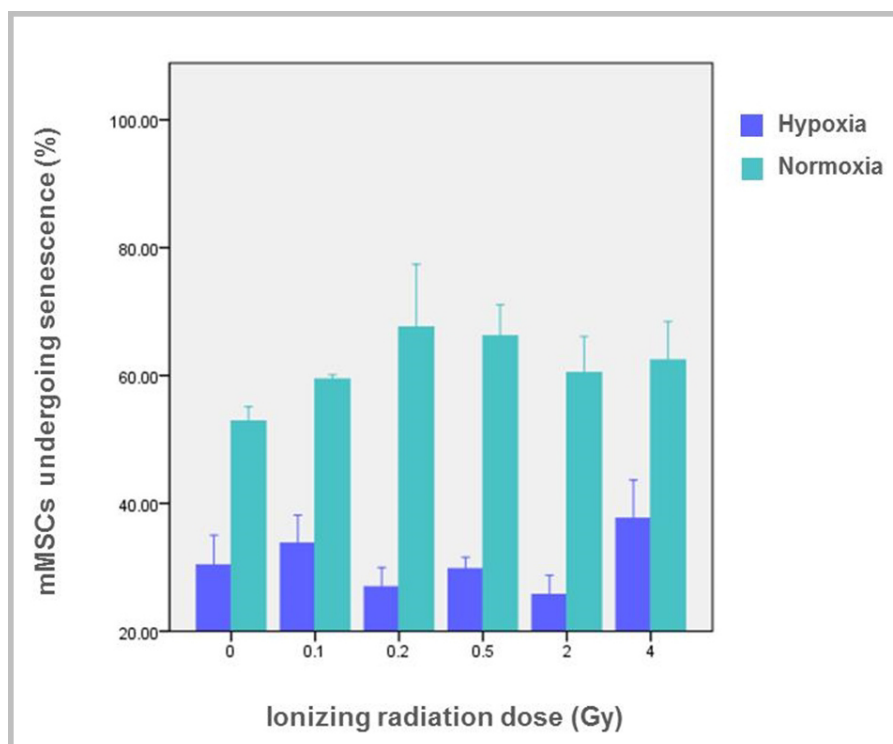


Figure 34: Effect of ionizing radiation on the senescence in mMSCs under hypoxic and normoxic conditions. Percentage of cells undergoing senescence in hypoxic and normoxic conditions after the γ -irradiation treatment with 0 Gy, 0.1 Gy, 0.2 Gy, 0.5 Gy, 2 Gy and 4 Gy. The percentage of senescent cells is depicted as mean values \pm standard error of the mean. Murine mesenchymal stem cells were obtained from 4 *Rb^{+/+}* biological replicates and the experiment was performed in technical duplicates. The difference between the senescent cells of various irradiated cultures was analysed using two-way ANOVA with Tukey's HSD for post hoc analysis; p-value oxygen concentration*ionizing radiation 0.003, Oxygen concentration 3.2×10^{-18} and ionizing radiation 0.031.

5.8.4 Effect of ionizing radiation on apoptosis in mMSCs: hypoxic condition

To find out the response of mMSCs to ionizing radiation-induced apoptosis after treatment with low and medium dose γ -irradiation, Image-iT® LIVE Green Poly Caspases Detection Kit, for microscopy was used.

Staurosporine is known as a robust inducer of apoptosis in various cell lines including mMSC cell lines [128] and HEK293 cell line [153]. To ensure the proper assessment of apoptosis by the preferred method of detection HEK293T cells were treated with 100 nM, 200 nM, 300 nM and 500 nM concentration of staurosporine as an experimental control. At the 6 h time point 100 nM staurosporine

was sufficient to evoke apoptosis in HEK293T cells for the method validation (fig. 35 left image). Additionally, apoptosis was also induced in mMSCs with 300 nM of staurosporine as a positive control for the experiment (fig. 35 right image). To investigate the effect of ionizing radiation on apoptosis

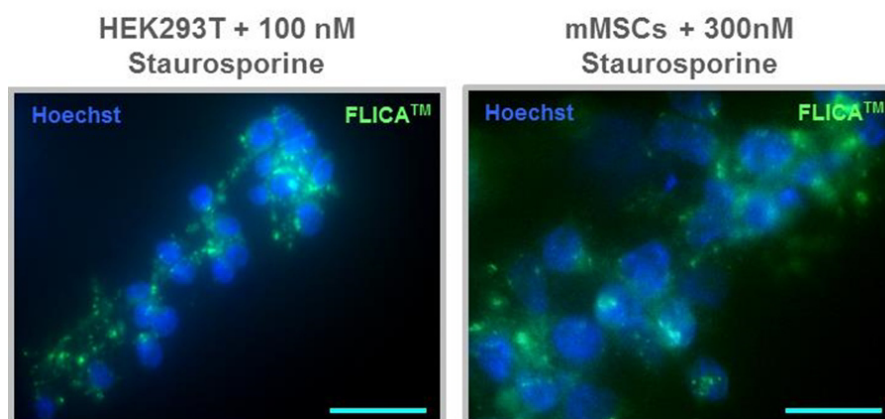


Figure 35: Positive controls used for apoptosis assay with Image-iT® LIVE Green Poly Caspases Detection Kit. Fluorescent green signal is visible in the cells undergoing apoptosis. The cell nuclei are stained with Hoechst dye. HEK293T cells were stimulated to undergo apoptosis by addition of 100nM staurosporine (left image). Apoptosis was induced in mMSCs with 300 nM staurosporine (right image). Scale bar: 25 μm .

induction, hypoxic mMSCs obtained from 4 *Rb*^{+/+} biological replicates were treated with 0 Gy, 0.2 Gy, 0.5 Gy, 2 Gy and 4 Gy of γ -irradiation. The apoptotic response of cells was quantified 6 h and 24 h after irradiation. Images of sham-irradiated and 4 Gy treated cells 24 h post-ionizing radiation as the representatives of 6 and 24 h irradiated cultures are shown in fig. 36. Statistical analysis of the apoptosis data was done using one-way ANOVA with Tukey's HSD for post hoc analysis. In control

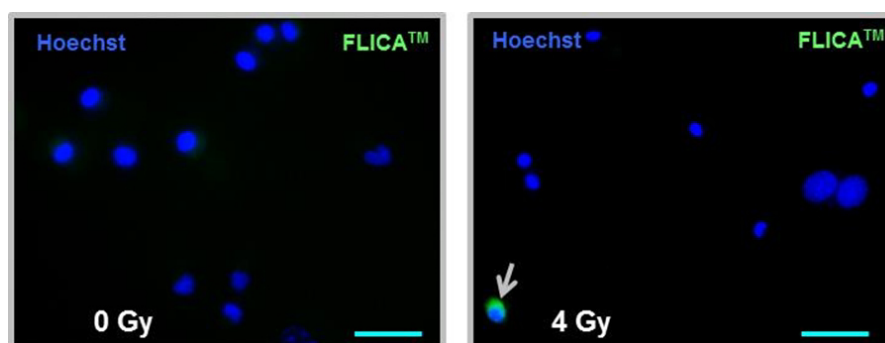


Figure 36: Apoptosis in mMSCs after exposure to ionizing radiation. Apoptosis assay was performed with Image-iT® LIVE Green Poly Caspases Detection Kit on control and γ -irradiation treated hypoxic mMSCs. Representative images of sham (left image) and 4 Gy (right image) treated cells obtained from 4 *Rb*^{+/+} biological replicates 24 h post-irradiation are shown. Grey arrow points towards cell undergoing apoptosis. Scale bar: 50 μm .

cultures, $10 \pm 3\%$ cells were undergoing apoptosis 6 h after irradiation which reduced to $5 \pm 2.5\%$ after 24 h (fig. 37). The number of cells undergoing apoptosis didn't change significantly even after low or medium dose irradiation treatment (fig. 37). This indicates the resistance of young hypoxic mMSCs towards ionizing radiation-induced apoptosis for up to 4 Gy.

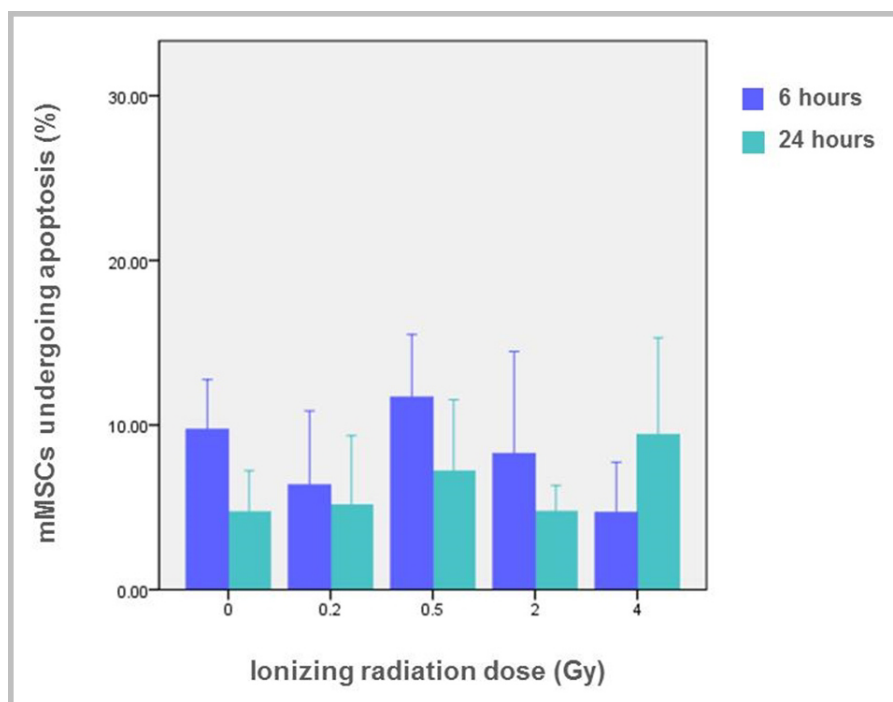


Figure 37: Effect of ionizing radiation on the apoptosis in mMSCs. Percentage of cells undergoing apoptosis 6 h and 24 h after ionizing radiation treatment with 0 Gy, 0.2 Gy, 0.5 Gy, 2 Gy and 4 Gy. The percentage of apoptotic cells is shown as mean values \pm standard error of the mean. Murine mesenchymal stem cells were obtained from 4 *Rb^{+/+}* biological replicates. The difference between the apoptotic cells of various irradiated cultures was analysed using one-way ANOVA with Tukey's HSD for post hoc analysis.

5.8.5 Effect of ionizing radiation on differentiation ability of mMSCs

In this study the differentiation abilities of mMSCs in presence or absence of a lineage inducing medium were assessed after ionizing radiation treatment to investigate the effects of low dose and therapeutically relevant medium dose γ -irradiation on the potency of primary MSCs.

Effect of ionizing radiation on differentiation of mMSCs in presence of lineage inducing growth medium (induced differentiation)

To investigate whether the mMSCs maintain their differentiation ability *in vitro* after the radiation treatment, hypoxic irradiated cells obtained from 3 *Rb^{+/+}* biological replicates were induced to undergo differentiation. Around 2 weeks after the induction osteogenic and adipogenic differentiation abilities of the mMSCs were assessed. This was a qualitative experiment to assess the effect of radiation exposure on characteristic MSC properties; hence, the numbers of differentiated cells was not quantified.

Four weeks after the irradiation induced osteogenic differentiation of primary mMSCs did not differ between control and irradiated cells. Fig. 38 shows sham and 500 mGy irradiated cells with their differentiation along the osteogenic lineage. All of the irradiated cultures showed cells positive for alkaline phosphatase staining. Similarly, for adipogenic differentiation no difference was observed between control or irradiated cells four weeks after irradiation. All the cultures were positive for Oil Red O staining. Fig. 39 shows sham and 500 mGy irradiated cells with their differentiation along

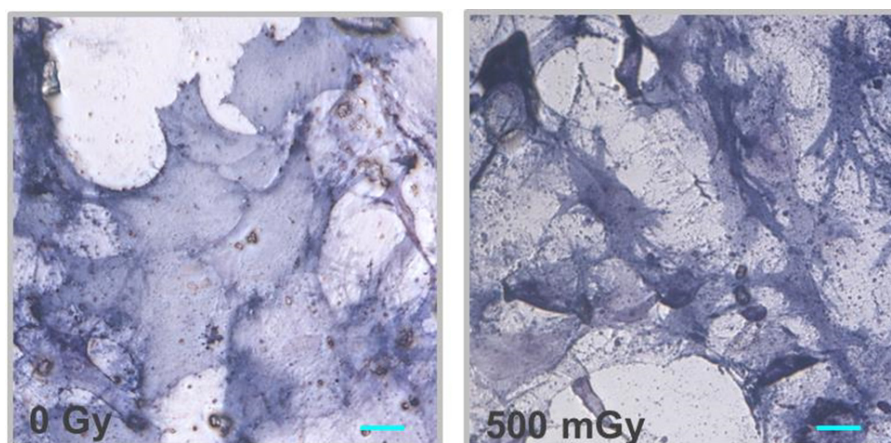


Figure 38: Osteogenic differentiation in mMSCs after exposure to ionizing radiation in presence of lineage inducing growth medium. Representative images of mMSCs obtained from 3 *Rb^{+/+}* biological replicates forced to undergo osteogenic differentiation after ionizing radiation treatment. Appearance of violet blue cells positively stained for the alkaline phosphatase activity 4 weeks post-ionizing radiation after induction of osteogenesis in hypoxic mMSCs treated with 0 Gy (left image) and 500 mGy (right image) γ -irradiation. Scale bar: 50 μ m.

adipogenic lineage. Thus it appears that hypoxic mMSCs retain their osteogenic and adipogenic differentiation potential even after γ -irradiation treatment for up to 500 mGy.

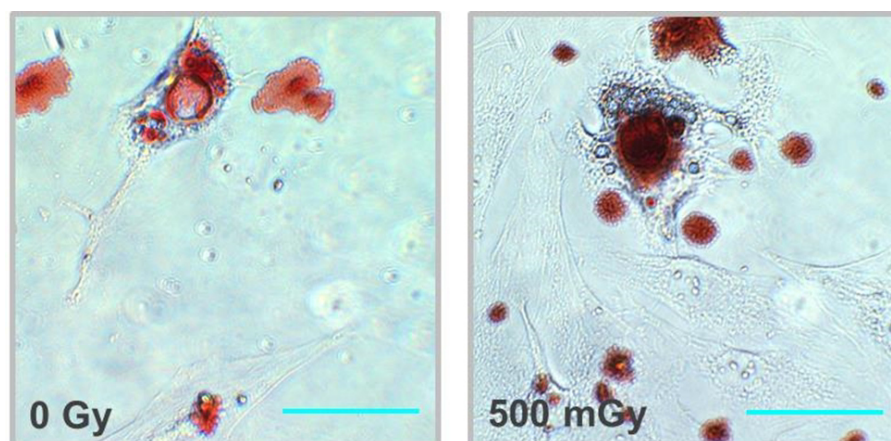


Figure 39: Adipogenic differentiation in mMSCs after exposure to ionizing radiation in presence of lineage inducing growth medium. Representative images of mMSCs obtained from 3 *Rb^{+/+}* biological replicates forced to undergo adipogenic differentiation after ionizing radiation treatment. Presence of rich red coloured lipid vacuoles stained positive for Oil Red O dye 4 weeks post-ionizing radiation after the induction of adipogenesis in hypoxic mMSCs treated with 0 Gy (left image) and 500 mGy (right image) γ -irradiation. Scale bar: 50 μ m.

Effect of ionizing radiation on differentiation of mMSCs in absence of lineage inducing growth medium

The differentiation was also analysed in irradiated mMSC cultures to study if ionizing radiation could induce the mMSCs to undergo differentiation into a certain lineage even in the absence of external

stimuli like lineage inducing growth medium. The analysis was performed in the hypoxic and normoxic cultures obtained from 3 *Rb^{+/+}* biological replicates irradiated with 0 Gy (sham irradiation), 0.1 Gy, 0.2 Gy, 0.5 Gy, 2 Gy and 4 Gy doses of γ -irradiation. Images of control and 500 mGy irradiated hypoxic cells as a representative of irradiated cultures (both conditions) are shown in fig. 40 and fig. 41.

Murine mesenchymal stem cell cultures tend to undergo some spontaneous osteogenesis even in the absence of osteogenic differentiation medium. Thus sham and irradiated cultures from both hypoxic and normoxic conditions displayed cells positive for alkaline phosphatase staining. These violet bluish cells showed typical osteoblastic morphology with flat nucleus and large cytoplasm (fig. 40). No difference was visible between the numbers of cells stained for alkaline phosphatase or between the staining intensity of control and irradiated cultures when observed under the microscope. However, the numbers of cells undergoing osteogenesis in irradiated and non-irradiated cultures (from both oxygen concentrations) were not quantified. In contrast to osteogenic differentiation,

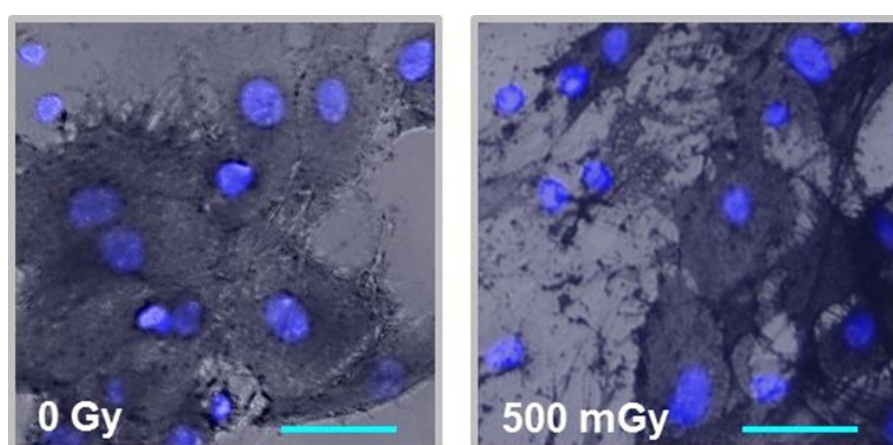


Figure 40: Osteogenic differentiation in mMSCs after exposure to ionizing radiation in absence of lineage inducing growth medium. Representative images of mMSCs obtained from 3 *Rb^{+/+}* biological replicates analysed for osteogenic differentiation 6 days after ionizing radiation treatment. Presence of violet blue cells positively stained for alkaline phosphatase activity after the treatment of hypoxic mMSCs with 0 Gy (left image) and 500 mGy (right image) γ -irradiations. Nuclei are counterstained with DAPI. Scale bar: 50 μ m.

spontaneous adipogenic differentiation in mMSC cultures is a very rare occurrence. To observe if ionizing radiation causes any changes in adipogenic differentiation of mMSCs the numbers of adipocytes and total cells present in irradiated and non-irradiated cultures were quantified as described in section 4.11.2. Six days after ionizing radiation treatment most of the cells undergoing adipogenesis were still at the early stages of differentiation with only one or two small lipid vacuoles visible in their cytoplasm (fig. 41). These early stage adipocytes lacked a typical large and flat cytoplasm, a trademark of terminally differentiated cell, which suggests that mMSC transformation into a fully mature adipocyte was yet to take place. However, due to the presence of one or more Oil Red O stained red lipid vacuoles these cells were counted as adipocytes. Fig. 42 shows the percentage of adipocytes present in sham and irradiated cultures γ from both hypoxic and normoxic atmosphere. Statistical analysis of the data obtained for percentage of mMSCs undergoing ionizing radiation-induced adipogenic differentiation after irradiation treatment was done using two-way ANOVA with Tukey's HSD for post hoc analysis. Ionizing radiation was found to

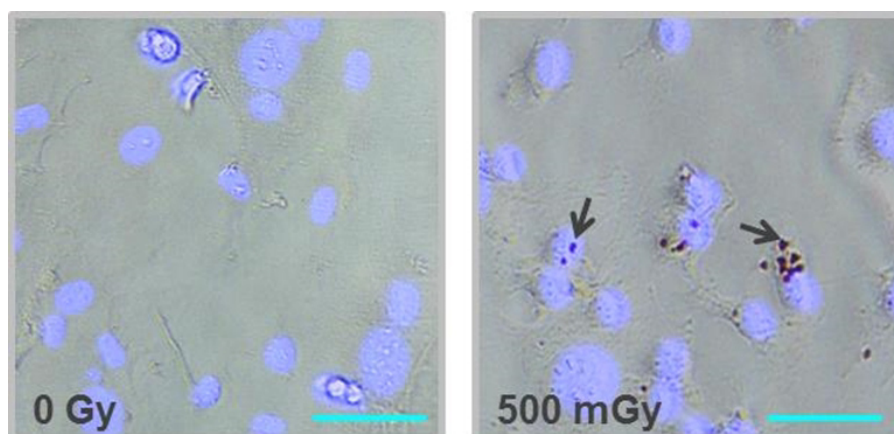


Figure 41: Adipogenic differentiation in mMSCs after exposure to ionizing radiation in absence of lineage inducing growth medium. Representative images of mMSCs obtained from 3 *Rb*^{+/+} biological replicates analysed for adipogenic differentiation 6 days after ionizing radiation treatment. Appearance of bright red coloured lipid vacuoles stained positive for Oil Red O dye after the treatment of hypoxic mMSCs with 0 Gy (left image) and 500 mGy (right image) γ -irradiations. Black arrows point towards Oil Red O stained small lipid vacuoles present in the cytoplasm of the differentiating cells. Nuclei are counterstained with DAPI. Scale bar: 50 μ m.

significantly increase the numbers of adipocytes in mMSC cultures (p-value 0.00002). The interaction effect of ionizing radiation and oxygen concentration was also significant (p-value 0.009). But oxygen concentration by itself did not significantly affect the percentage of adipocytes. This suggests that the oxygen concentration on its own does not induce the differentiation of MSCs but it sensitizes the MSCs exacerbating the already evoked adipogenic differentiation of MSCs after γ -irradiation treatment. Thus ionizing radiation is a primary factor responsible for inducing adipogenesis in mMSC cultures in the absence of lineage inducing growth medium. Conclusively, hypoxic mMSCs undergo ionizing radiation-induced adipogenic differentiation after treatment with γ -irradiation.

5.8.6 Effect of ionizing radiation on the expression of lineage specific genes in MSCs

Increased ionizing radiation-induced adipogenesis was observed in γ -irradiation exposed 14 days old mMSCs (i.e. 6 days after ionizing radiation exposure). Hence, to observe the long-term effects of γ -irradiation on the expression of genes underlying the mMSC differentiation, the expression profile of adipogenic and osteogenic lineage genes was studied in irradiated mMSCs obtained from 4 *Rb*^{+/+} biological replicates. On day 8 the hypoxic mMSCs were treated with 0 Gy, 0.1 Gy and 2 Gy ionizing radiation dose. Real-Time PCR analysis of the marker gene expression was carried out in 14, 21 and 35 days old irradiated mMSCs. The fold change values for all the irradiated samples were normalized to the youngest (14 days old) sham irradiated (control) cell sample. To understand the individual effect of low dose and medium dose γ -irradiation, statistical analysis for the two treatments was done separately using two-way ANOVA with Tukey's HSD for post hoc analysis.

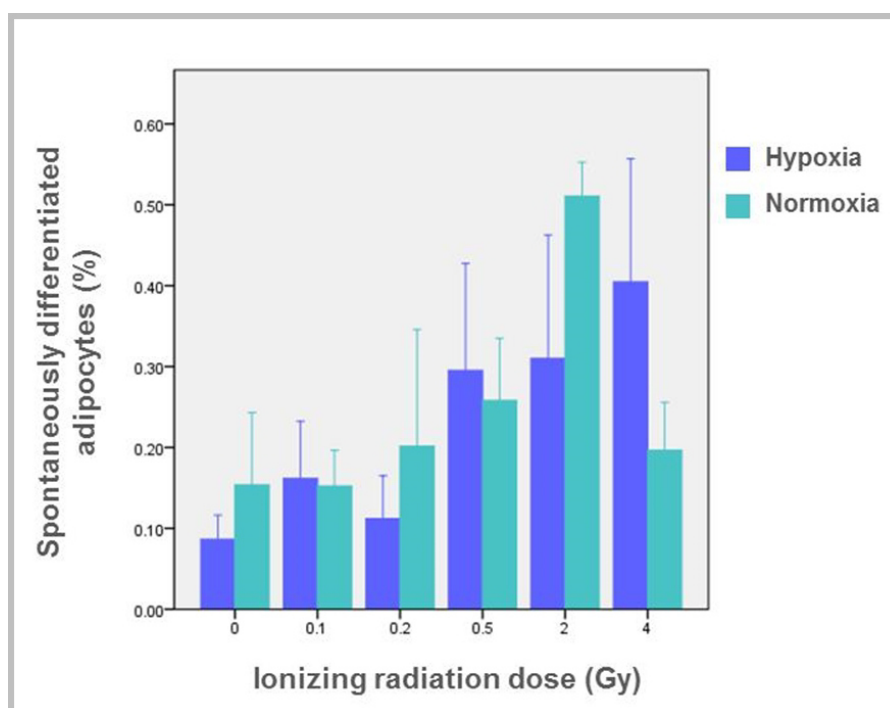


Figure 42: Effect of ionizing radiation on adipogenesis in mMSCs in absence of lineage inducing growth medium. Percentage of cells undergoing adipogenesis in hypoxic and normoxic conditions 6 days after the γ -irradiation treatment with 0 Gy, 0.1 Gy, 0.2 Gy, 0.5 Gy, 2 Gy and 4 Gy. The percentage of differentiated adipocytes is depicted as mean values \pm standard error of the mean. Murine mesenchymal stem cells were obtained from 3 *Rb*^{+/+} biological replicates and the experiment was performed in technical duplicates. The difference between the numbers of ionizing radiation-induced adipocytes in various irradiated cultures was analysed using two-way ANOVA with Tukey's HSD for post hoc analysis; p-value oxygen concentration*ionizing radiation 0.009, ionizing radiation 0.00002.

Ionizing radiation and osteogenic lineage genes

Expression of osteogenic marker *Alpl* (fig. 43A) was greatly reduced with increasing culture age. Irradiation (both low and medium dose) didn't play any significant role influencing *Alpl* expression. Interaction effect of age and ionizing radiation was also absent. Second osteogenic marker, *Runx2* (fig. 43B), showed age related decrease in its expression. Interestingly, a dose of 2 Gy lowered the expression of *Runx2* significantly (p-value 0.05) over the entire period of *in vitro* culturing unlike the low dose of 0.1 Gy which didn't influence its expression. No interaction effect of age and ionizing radiation was observed on its expression.

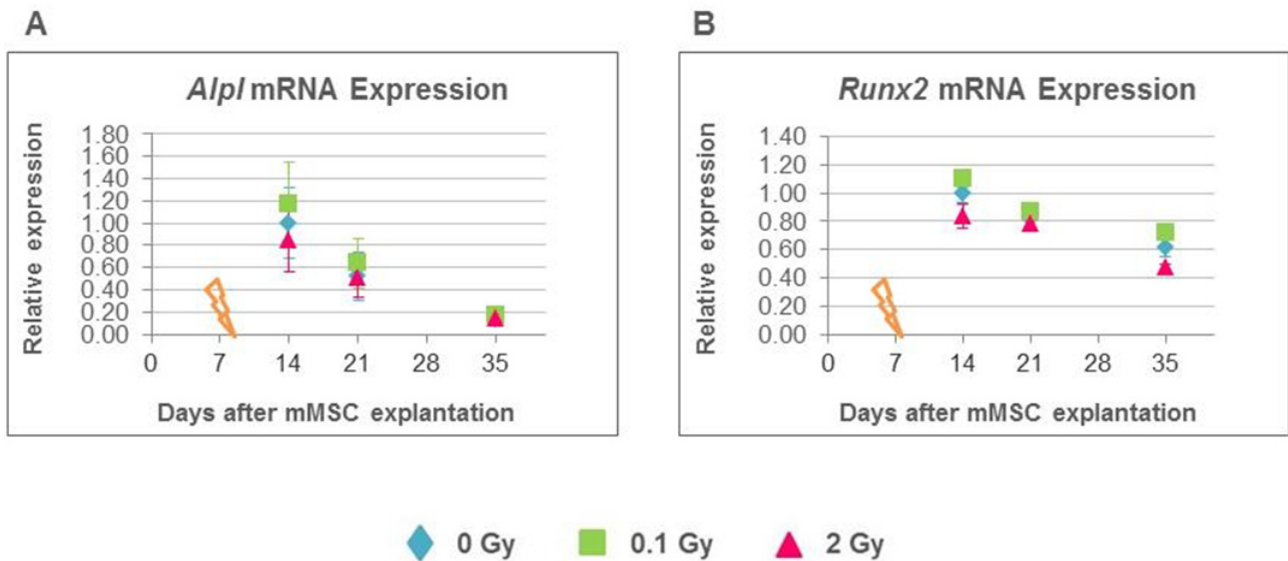


Figure 43: Effect of ionizing radiation on the expression profile of osteogenic lineage marker genes in mMSCs of different age. Relative expression of the osteogenic lineage marker genes on different days after 0 Gy, 0.1 Gy and 2 Gy γ -irradiation treatments. The gene expression level for different days was normalized to its own expression in 14 days old sham irradiated cells. The plots show relative expression values obtained by Real-Time PCR analysis of osteogenic marker genes on day 14, 21 and 35 as the mean values \pm standard error of the mean. Murine mesenchymal stem cells were obtained from 4 *Rb^{+/+}* biological replicates and the experiment was performed with technical duplicates. TBP was used as a housekeeping gene. Orange arrow indicates time of radiation exposure (day 8). A) Expression of *Alpl* in mMSC culture B) Expression of *Runx2* in mMSC culture.

Ionizing radiation and adipogenic lineage genes

Expression of adipogenic lineage markers *Cebpa* (fig. 44A), *Lpl* (fig. 44D) and *Srebf1* (fig. 44E) was altered with increasing age, but no effect of low or medium dose ionizing radiation dose was found. The expression level of *Fabp4* (fig. 44C) and *Pparg* (fig. 44B) decreased with increasing age (p-value below 0.001 for both). For *Fabp4*, medium dose ionizing radiation (2 Gy) treatment didn't evoke any change but the low dose (0.1 Gy) was responsible for significantly enhanced expression (p-value 0.034). *Pparg* showed an impact of ionizing radiation on its expression. Medium dose of 2 Gy significantly reduced the *Pparg* expression (p-value 0.001) while the low dose of 0.1 Gy increased its expression level (p-value 0.013). However, no interaction of age and ionizing radiation significantly influenced the expression of any of these adipogenic markers.

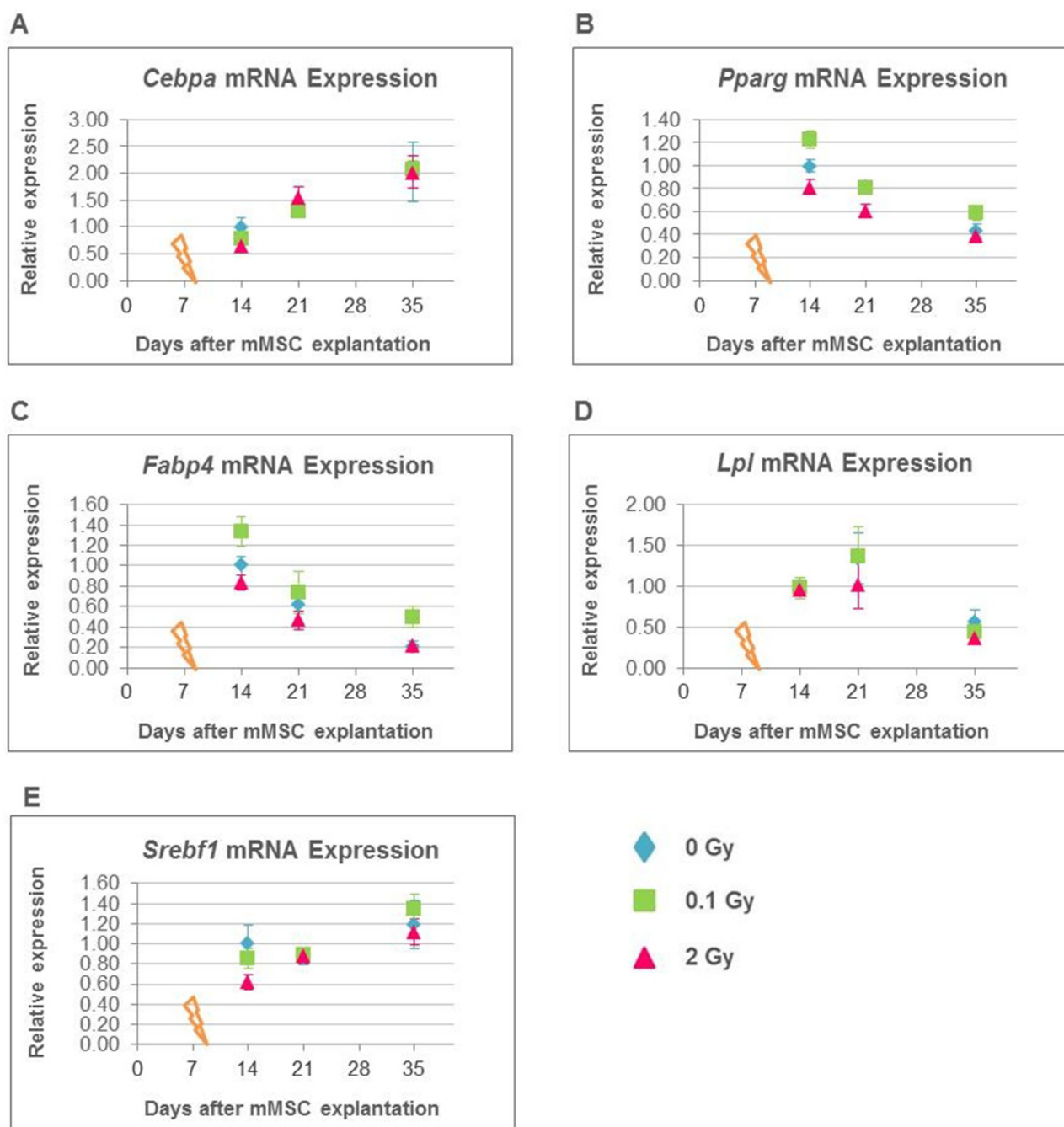


Figure 44: Effect of ionizing radiation on the expression profile of adipogenic lineage marker genes in mMSCs of different age. Relative expression of the adipogenic lineage marker genes on different days after 0 Gy, 0.1 Gy and 2 Gy γ -irradiation treatments. The gene expression level for different days was normalized to its own expression in 14 days old sham irradiated cells. The plots show relative expression values obtained by Real-Time PCR analysis of these genes on day 14, 21 and 35 as the mean values \pm standard error of the mean. Murine mesenchymal stem cells were obtained from 4 *Rb^{+/+}* biological replicates and the experiment was performed with technical duplicates. TBP was used as a housekeeping gene. Orange arrow indicates time of radiation exposure (day 8). A) Expression of *Cebpa* in mMSC culture. B) Expression of *Pparg* in mMSC culture. C) Expression of culture *Fabp4* in mMSC culture. D) Expression of *Lpl* in mMSC culture. E) Expression of *Srebf1* in mMSC culture.

5.8.7 Effect of ionizing radiation on expression profile of stemness and pluripotency marker genes in MSCs

Along with the expression analysis of lineage specific genes, profiling of stemness and pluripotency marker genes was performed on the γ -irradiated (controls, 0.1 Gy and 2 Gy) cultures of hypoxic mMSCs obtained from 2 *Rb*^{+/+} biological replicates. The fold change values for all the irradiated samples were normalized to youngest (14 days old) sham irradiated cells.

Age was found to be a highly significant factor influencing the expression of several genes responsible for maintaining the stemness and pluripotency state of the cells. All the stemness genes displayed considerable down-regulation in the long-term cultured mMSCs from day 14 to day 35. For *Bmi1* (fig. 45B), *Nanog* (fig. 45C) and *Pou5f1* (fig. 45D) the relative expression was found to be affected only by age without any effect of low or medium dose γ -irradiation. Low dose radiation also failed to exert any influence on the expression of *Sox2* (fig. 45A), *Nes* (fig. 45E) and *Klf4* (fig. 45F). In contrast, the expression of *Nes* (p-value 0.015) and *Klf4* (p-value 0.025) was affected by the medium dose (2 Gy) of radiation. No interaction of age and ionizing radiation was observed. The *Sox2* (fig. 45A) expression was found to be changed both with age (p-value 0.0002) and the dose of 2 Gy γ -irradiation (p-value 0.001). The interaction effect of age and radiation dose on *Sox2* expression was statistically significant (p-value 0.015).

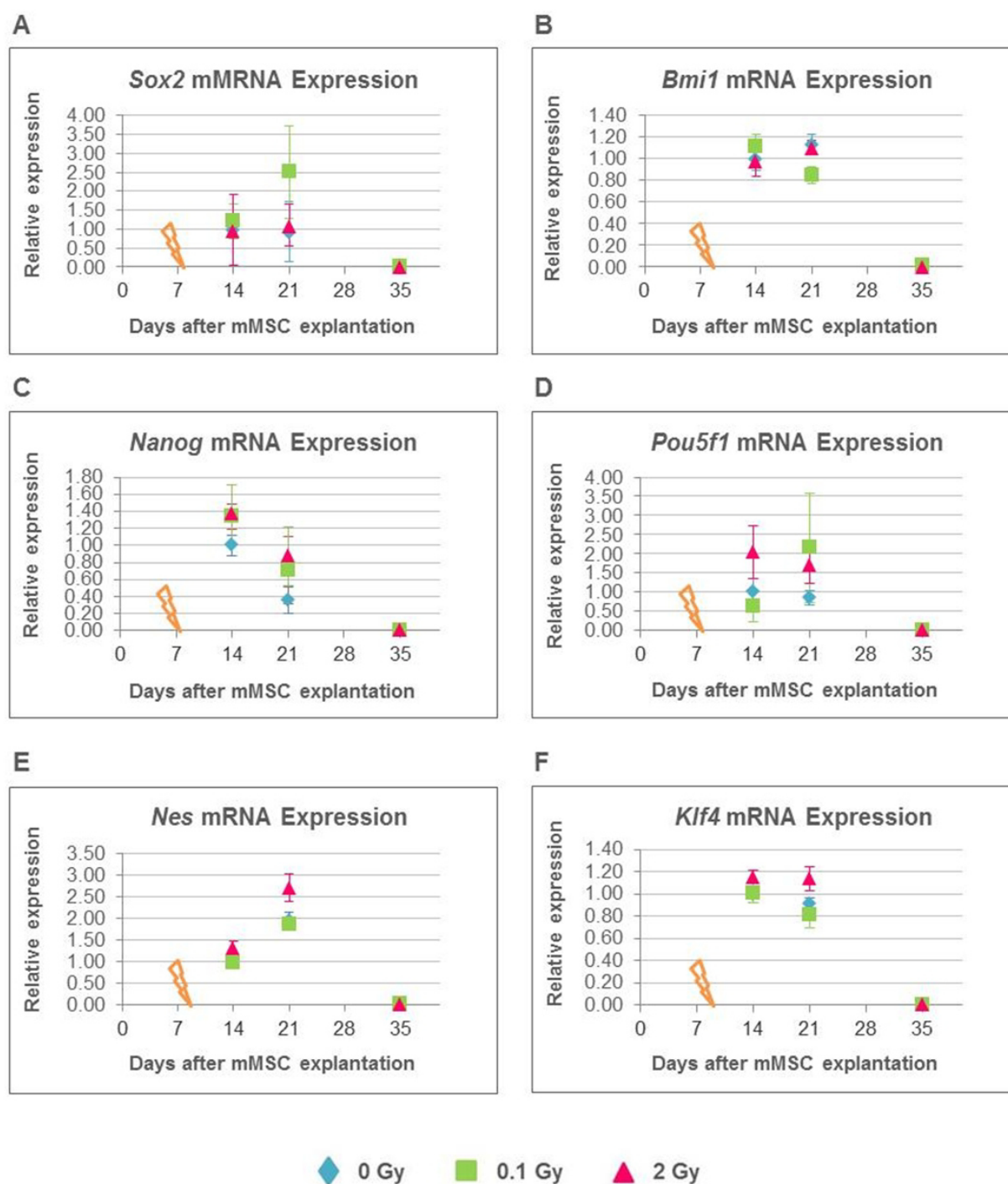


Figure 45: Effect of ionizing radiation on the expression profile of stemness and pluripotency marker genes in mMSCs of different age. Relative expression of the stemness and pluripotency marker genes on different days after 0 Gy, 0.1 Gy and 2 Gy γ -irradiation treatments. The gene expression level for different days was normalized to its own expression in 14 days old sham irradiated cells. The plots show relative expression values obtained by Real-Time PCR analysis of these genes on day 14, 21 and 35 as the mean values \pm standard error of the mean. Murine mesenchymal stem cells were obtained from 2 *Rb*^{+/+} biological replicates and the experiment was performed with technical duplicates. TBP was used as a housekeeping gene. Orange arrow indicates time of radiation exposure (day 8). A) Expression of *Sox2* in mMSC culture. B) Expression of *Bmi1* in mMSC culture. C) Expression of culture *Nanog* in mMSC culture. D) Expression of *Pou5f1* in mMSC culture. E) Expression of *Nes* in mMSC culture. F) Expression of *Klf4* in mMSC culture.

5.8.8 Quantification of adipocytes in the bone marrow sections of whole body irradiated mice

In vitro cultured hypoxic mMSCs exhibit ionizing radiation-induced adipogenesis after the treatment with γ -irradiation. To investigate the effects of low dose γ -irradiation on the number of adipocytes *in vivo*, whole body irradiated B6C3F1 background mice were sacrificed a year after the irradiation and their bone marrow was collected from the long bones (femur and humerus). The bone marrow was obtained from 2 mice irradiated with 0.125 Gy and 2 other mice irradiated with 0.5 Gy and was used to prepare the cryo sections. The cryo sections were stained with haematoxylin and Oil Red O to visualize the hematopoietic cells and adipocytes respectively. Five representative images were taken for each biological replicate and statistical analysis was performed by one-way ANOVA with Tukey's HSD for post hoc analysis.

As visible in the representative images of bone marrow cryo sections from the control and whole body irradiated mice (fig. 46) the hematopoietic cells are smaller in size and appear violet in colour after staining with haematoxylin. In contrast, adipocytes are much bigger and have brownish appearance. Lipid vacuoles present in the adipocytes appear as darker brown spots. Staining artefacts look like larger bright red coloured structure. Hematopoietic cells and adipocytes can be easily distinguished from each other based on their morphology and were counted for the analysis. Sometimes hematopoietic cells lie on the top of the adipocytes making the exact counting difficult. Hence, the colour channels were modified using imageJ software to separate out the adipocytes from overlying hematopoietic cells. From the data analysis no statistically significant difference was

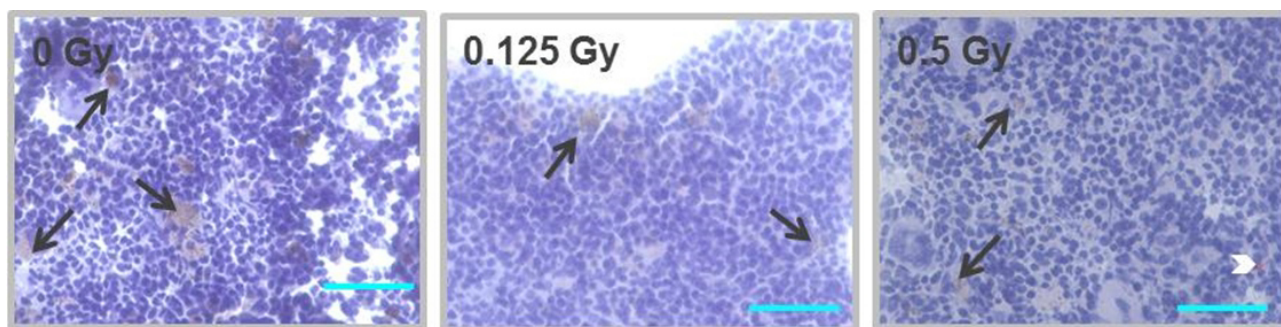


Figure 46: Bone marrow cryo sections of the whole body irradiate mice. Representative images of haematoxylin and Oil Red O stained bone marrow cryo sections obtained from 2 biological replicates of B6C3F1 background mice irradiated with the whole body dose of 0 Gy (left image), 0.125 Gy (middle image) and 0.5 Gy (right image). Hematopoietic and other cells present in the bone marrow appear violet due to haematoxylin staining while adipocytes seem brownish with Oil Red O staining. Black arrows point towards brown coloured adipocytes while the white arrow head indicates the bright red coloured staining artefact. Scale bar: 50 μ m.

observed between the numbers of bone-marrow adipocytes for the whole-body irradiated (0.125 Gy and 0.5 Gy) and control mice (fig. 47). Unlike the *in vitro* observation no increase in percentage of adipocyte was found *in vivo* after ionizing radiation treatment.

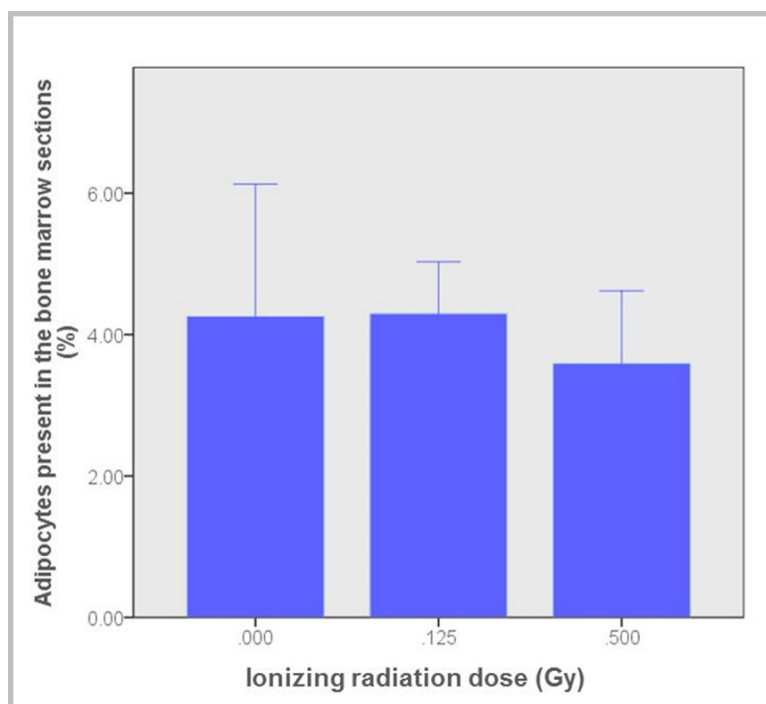


Figure 47: Effect of ionizing radiation on the number of adipocytes present in the bone marrow cryo sections of the whole body irradiated mice. Percentage of adipocytes present in the bone marrow cryo sections a year after the whole body γ -irradiation treatment with the dose of 0 Gy, 0.125 Gy and 0.5 Gy. The percentage of adipocytes present is depicted as mean values \pm standard error of the mean. The bone marrow was obtained from 2 biological replicates of B6C3F1 background mice for each dose. Differences between the numbers of adipocytes observed in the bone marrow sections of various irradiated mice was analysed with one-way ANOVA test.

Chapter 6

Discussion

Stem cells are a fundamental asset for multicellular organisms. They guarantee a continuous supply of specialised cells to replenish damaged or lost cells, thus maintaining long term tissue homeostasis. These properties of stem cells are exploited in a clinical setting. The stem cell therapy entails application of stem cells for the cure of diseases such as macular degeneration, heart failure, amyotrophic lateral sclerosis, and immune disorders (reviewed by [98]). MSCs are the most extensively used adult stem cells for therapeutic purposes (reviewed by [98]). They have been used with varying degree of success to treat indications including myocardial infarction, diabetes, spinal cord injury, liver cirrhosis, systemic lupus, and Parkinsons disease (reviewed by [98]). MSCs can be isolated from different tissue sources, for example bone marrow, adipose tissue, and dental pulp [65, 66]. Despite their wide distribution MSCs are a relatively rare cell population with the number of Colony-forming unit-fibroblastic cells (CFU-Fs) obtained from the bone marrow ranging from 1 in 10000 to 1 in 100000 bone marrow mononuclear cells [139]. Therefore, after isolation of MSCs from a donor tissue it is necessary to expand these cells *in vitro* to obtain therapeutically relevant cell numbers. The *ex vivo* expansion of MSCs requires multiple cell divisions to amplify the number of cells exponentially, with the associated risk of accumulation of genetic damage. For their safe and effective usage in stem cell therapy MSCs should be protected from exogenous DNA damaging agents, such as ionizing radiation that could induce additional genotoxic stress. Ionizing radiation evokes genetic instability intensifying the rates of mutations in the irradiated cells and their progenies [4]. Similar to that of other somatic cells MSCs are vulnerable towards ionizing radiation-induced genotoxic stress. MSCs like other stem cells possess self-renewal ability, longer life-span and differentiation potential [56, 67, 154]. These characteristic stem cell properties increase the risk of transmitting genomic anomalies to their progenies which in turn may disrupt the tissue regeneration process and enhance the risk of carcinogenesis ([12], reviewed by [125]).

The continuous exposure of living organisms to ionizing radiation from both natural and artificial sources has tremendously increased the chances that the donor MSCs have been previously exposed to ionizing radiation. This in turn has increased the probability of using ionizing radiation exposed MSCs in stem cell therapy. The ionizing radiation exposed MSCs may undergo neoplastic transformation due to accumulated mutations [12] making them unsuitable for therapeutic purposes. Thus it is essential to understand the effect of ionizing radiation and oxygen concentration on the stemness properties. In this study mMSCs were obtained from FVB strain mice, *in vitro* cultured in either hypoxic or normoxic environments, and exposed to low and medium doses of γ -irradiation.

Cellular properties of growth, colony forming ability, senescence, apoptosis, and differentiation were assessed in stress exposed MSCs. Marker genes indicating inherent characteristics of self-renewal and differentiation potential were monitored.

6.1 Hypoxia promotes long-term *in vitro* growth and survival of mMSCs

The stem cell niche symbolizes a specific anatomical compartment. Since the first hypothesis of a stem cell niche in 1978 by Schofield [155], the concept of a stem cell niche has been evolved and oxygen is now considered to be a critical factor of the niche (reviewed by [156]). Increasing evidence highlights the role of low oxygen concentration (hypoxia in a range of 1%-9% O₂) in maintaining the stemness properties of proliferation and differentiation state of both ESCs and ASCs (reviewed by [156]). MSCs were shown to be present in perivascular niches in close proximity of the blood vessels irrespective of their source tissues [157, 158]. But despite the perivascular location of MSCs their tissues of origin, for example, bone marrow or adipose tissue display low oxygen tensions of 1%-7% [159] and 2%-8% [160] respectively. Traditionally, MSCs are cultured in non-physiological oxygen environment i.e. normoxia (21% O₂). In this study it was observed that hypoxia (2% O₂) makes a better culturing environment showing sustainable long-term growth and survival of mMSCs as compared to normoxia. With a reduction in the number of viable cells and a lack of homogenous culture over time the effects of ambient oxygen tension on sustainable growth of mMSCs were evident. The beneficial effects of hypoxia over normoxia for *in vitro* proliferation of MSCs have also been observed in MSCs from other species such as rat [161] and humans [162–164].

The difference in the cell viability and long-term growth of hypoxic and normoxic MSCs may arise from altered cell cycle progression. Hypoxia led to an accumulation of 21 days old *in vitro* cultured mMSCs in the G₀/G₁ phase of the cell cycle. This is in accordance with the data from human [165, 166] and equine MSCs [167] where the hypoxic MSCs are shown to accumulate in G₀/G₁ phase of the cell cycle. Accumulation of MSCs in G₀/G₁ phase under hypoxia might actually confer a protective effect on the cells against damage caused during DNA replication in the ensuing S phase. The process of DNA replication is error prone and can give rise to mutations every time a DNA is replicated [168]. Hypoxic MSCs lay dormant in G₀/G₁ phase without undergoing DNA replication, in contrast normoxic MSCs continue with DNA replication and accumulate the damage inflicted by free oxygen radical species present in normoxia [165]. In hypoxic environment the lack of DNA replication process in addition to the absence of free oxygen radical species can reduce the occurrence of DNA damage and protect the genetic integrity of hypoxic mMSCs. The quiescent cells accumulated in G₀ can be activated to reenter the cell cycle during G₁ phase [169]. Thus it seems that the hypoxic mMSCs enter a temporary quiescent state (G₀) that results in the arrest of the cell cycle on the immediate basis; though in presence of favourable growth conditions or external stimuli these cells can once again resume the cell cycle. Therefore, the G₀/G₁ cell cycle arrest of mMSCs in hypoxia can grant them survival advantage over normoxic MSCs resulting into immediate absence of cell cycle but better growth in long-term cultures.

6.2 Reduced clonogenicity of mMSCs in higher oxygen tension is potentiated by ionizing radiation

Besides their intrinsic characteristics like self-renewal, potency and high proliferation capacity adult stem cells exhibit functional properties that include clonogenicity *in vitro* and tissue reconstitution *in vivo* [82]. The *in vitro* clonogenic assay is one of the standard methods used extensively to determine the self-renewal capacity of individual stem cells [170]. In this project in addition to the decline in long-term survival it was observed that the colony forming ability of mMSCs is severely compromised in normoxia. The plating efficiency of hypoxia pre-conditioned mMSCs (mMSCs initially grown in hypoxia before their transfer to either hypoxia or normoxia for the clonogenic assay) was approximately 10 times higher in low oxygen condition (approximately 2.04%) than under normal atmospheric oxygen (approximately 0.21%). Similarly, hypoxic mMSCs displayed higher clonogenicity when the cells were cultured either in hypoxia (approximately 2.3%) or normoxia (approximately 0.18%) immediately after their isolation from the bone marrow. The decreased clonogenicity of the mMSCs under normoxia may suggest lower self-renewal of MSCs. Improved colony forming ability in hypoxia, for both hypoxia pre-conditioned cultures or the cultures grown apart since the MSC isolation, is demonstrated by rat [161] and human [171, 172] MSCs as well. Interestingly, in hMSCs these effects were reversed when the cells were transduced with hypoxia-inducible factor 1- α as shown by comparable (to hypoxia) increase in the frequency of CFU-F under normoxia in the presence of hypoxia-inducible factor 1- α [154]. This positive influence was attributed to the effect of hypoxia-inducible factor 1- α on promoting the self-renewal of mesenchymal progenitors mediating the effects of hypoxia for the subsets of MSCs [154].

Ionizing radiation is known to affect the cell survival by giving rise to variety of cellular lesions [11]. In case of mMSCs, the oxygen concentration was found to influence the colony forming ability of irradiated MSCs. In hypoxia there was a dose-dependent decrease in the number of colonies formed after γ -irradiation treatment compared to sham irradiated control cells, while in normoxia no dose dependence was observed for clonogenicity of mMSCs in low dose region. However, normoxic mMSCs displayed a significant decrease in the number of colonies formed after a medium dose of 4 Gy. Therefore, it can be argued that both oxygen concentration and ionizing radiation have the potential to alter the clonogenicity of the mMSCs individually. The interaction between oxygen tension and irradiation was highly significant, which indicates that the reduced clonogenicity of mMSCs in higher oxygen tension is potentiated by ionizing radiation. The dose-dependent reduction in the number of colonies formed by hypoxic mMSCs after γ -irradiation treatment is in contrast to the behaviour of tumour cells after irradiation of hypoxic tumour areas. In an hypoxic environment the lack of oxygen reduces the production of cytotoxic species such as reactive oxygen species, and prevents the occurrence of irreparable DNA damage after exposure to ionizing radiation, ultimately preventing the cancer cell killing (reviewed by [132]). The differential survival response of hypoxic MSCs and tumour cells in a hypoxic environment after ionizing radiation treatment indicates the paradox in the response of MSCs and tumour cells to ionizing radiation-induced cell killing.

In primary mouse MSCs, atmospheric oxygen has been shown to induce the production of mitochondrial ROS and activate the expression of factors such as p53, Top2A, BCL2-associated X protein resulting into oxidative stress and reduced cell viability [173]. The oxidative stress produced

by normoxic ROS can result into acute damage to DNA, protein, lipids present in the cells triggering various signalling cascades that direct the cell survival or death depending on the severity of the stress [174]. Ionizing radiation is responsible for generating additional oxidative stress in the cells by formation of reactive oxygen species [138]. The additive oxidative stress generated by ionizing radiation may be able to intensify the already existing effects of ambient oxygen concentration on clonogenic survival of mMSCs. Sugrue et. al. have observed that the mouse MSC lines and primary bulk MSCs from passage 6-8 of C57BL/6 background mice show increased radioresistance under hypoxia as seen by the enhanced MSC survival in clonogenic assays post-ionizing radiation treatment [175]. In this project, hypoxic mMSCs exhibited dose-dependent decrease in the clonogenicity after ionizing radiation treatment; however, in normoxic mMSCs the clear detrimental effect of ionizing radiation on the clonogenicity was visible only after the treatment with medium dose of 4 Gy. The doses used in this study differ from that of Sugrue et al. with the use of low dose γ -irradiation. Nevertheless, it is worth mentioning that the effect observed at 4 Gy irradiated hypoxic and normoxic mMSCs were similar in both studies with a greater reduction in number of normoxic colonies compared to that of hypoxia.

6.3 Ionizing radiation sensitises mMSCs towards high oxygen concentration-induced senescence

MSCs are considered to have long *in vivo* life-span; still their *in vitro* life expectancy is limited much alike to other somatic cells [53]. Even though the proliferative capacity of the MSCs can vary from donor to donor [176] all the MSCs, just like any other somatic cells, enter senescent stage after dividing for specific number of times irrespective of their donor species [53, 54]. This replicative senescence is a phase where a cell ceases to proliferate and enter irreversible growth arrest [133, 134]. The process of replicative senescence is shown to share many common features like changes in cell morphology, SA- β -galactosidase activity, cell cycle regulation with the Stress-Induced Premature Senescence (SIPS) phenotype [177]. One of the major causes for SIPS is an occurrence of oxidative stress in the cellular system [177].

In this project, it was observed that higher oxygen tension and ionizing radiation could independently heighten senescence in 14 days old mMSCs cultured *in vitro*. Hypoxia itself did not induce increased senescence in irradiated cultures (up to 4Gy). In contrast, normoxic mMSCs underwent increased senescence after low irradiation doses of ≤ 0.2 Gy and then, the level of senescence plateaued for the remaining doses of ≥ 0.5 Gy as no further increase in the percentage of cells undergoing senescence was observed. Furthermore, the interaction of oxygen tension and ionizing radiation significantly enhanced senescence in the cells. This emphasises the synergistic effect of ionizing radiation and oxygen concentration on senescence induction in mMSCs. Hence, it could be claimed that the MSCs are sensitive towards oxidative stress generated by a combination of normoxia and ionizing radiation; and respond to this unfavourable condition by undergoing senescent phenotype similar to that of stress-induced premature senescence *in vitro*. Indeed, the effect of elevated oxygen tension on enhancing senescence in primary hMSCs has already been shown by Fehrer et al. [162]. High dose γ -irradiation of 20 Gy also generated SIPS in hMSCs from bone marrow and periodontal ligament origin as seen by the presence typical hallmarks of SIPS such as prolonged

upregulation and phosphorylation of p53, increased activity of SA- β -galactosidase and morphologic changes in irradiated cells [178].

The enhanced basal level of senescence (increased senescence in sham irradiated control cells) that was observed in normoxic mMSC cultures as compared to hypoxic mMSC cultures correlates with the data from the cell cycle analysis. It was observed that 7 days old normoxic mMSCs show G0/G1 phase arrest. Usually, the senescent cells are irreversibly arrested in G1 phase of the cell cycle [134]. In the normoxic mMSCs on day 14 increased senescence was observed. Taken together this data suggests that the irreversible arrest of 7 days old mMSCs in G1 phase foreshadows the increased senescence which was observed later. One of the possible reasons for elevated senescence in normoxic mMSCs may be related to culturing the cells in normoxia after their isolation from the bone marrow. Non-physiological normoxic condition can result into immediate oxidative stress and cause DNA damage in normoxic mMSCs [179]. Inability to restore this DNA damage might further drive the cells to undergo senescent phenotype similar to SIPS. Senescent cells no longer proliferate and are under growth arrest which may explain the decreased number of colonies observed in ambient oxygen environment as seen in the clonogenic assay. On other hand, hypoxia seems to confer a protective effect on mMSCs by inducing G0/G1 phase arrest in long-term cultured (21 days) mMSCs as described previously. One of the probable reasons that hypoxic mMSCs were observed to be in G0/G1 cell cycle arrest, but still show better long-term survival is that these cells exhibit similar tendency to cancer cells [180, 181]. Thus hypoxic mMSCs may enter a temporary and reversible quiescent state (G0) which protects them against the DNA damage otherwise caused during DNA replication in case of uninterrupted cell cycle. And when the growth conditions are favourable or external environmental cues are present these dormant cells can resume their proliferation and repair any DNA damage present providing them with longer life cycle as observed in ovarian cancer cells [180] or dormant breast cancer cells [181]. Therefore, hypoxia may safeguard the MSCs by a collective action of preventing the formation of oxidative stress and inducing G0/G1 phase arrest prompting the cells into a quiescent state. The complex interaction between long-term survival, cell cycle arrest, senescence and *in vitro* oxygen conditions that were observed in this study can be illustrated as shown in fig. 48. Recently we have shown that MSCs grown under hypoxia exhibit less spontaneous DNA strand breaks and those under normoxia show higher basal level of DNA damage which further increase after exposure to ionizing radiation [179]. This increased DNA damage after γ -irradiation under normoxia might work as a trigger in evoking higher senescence in normoxic mMSCs after irradiation. It could justify the interaction effect of higher oxygen tension and ionizing radiation for increasing senescence in mMSCs. It can be suggested that already vulnerable normoxic MSCs fail to repair the added DNA damage caused directly by ionizing radiation and associated oxidative stress forcing them to undergo senescent phenotype similar to SIPS. This process of irradiation induced elevated senescence was also present in primary normoxic hMSCs [12, 182].

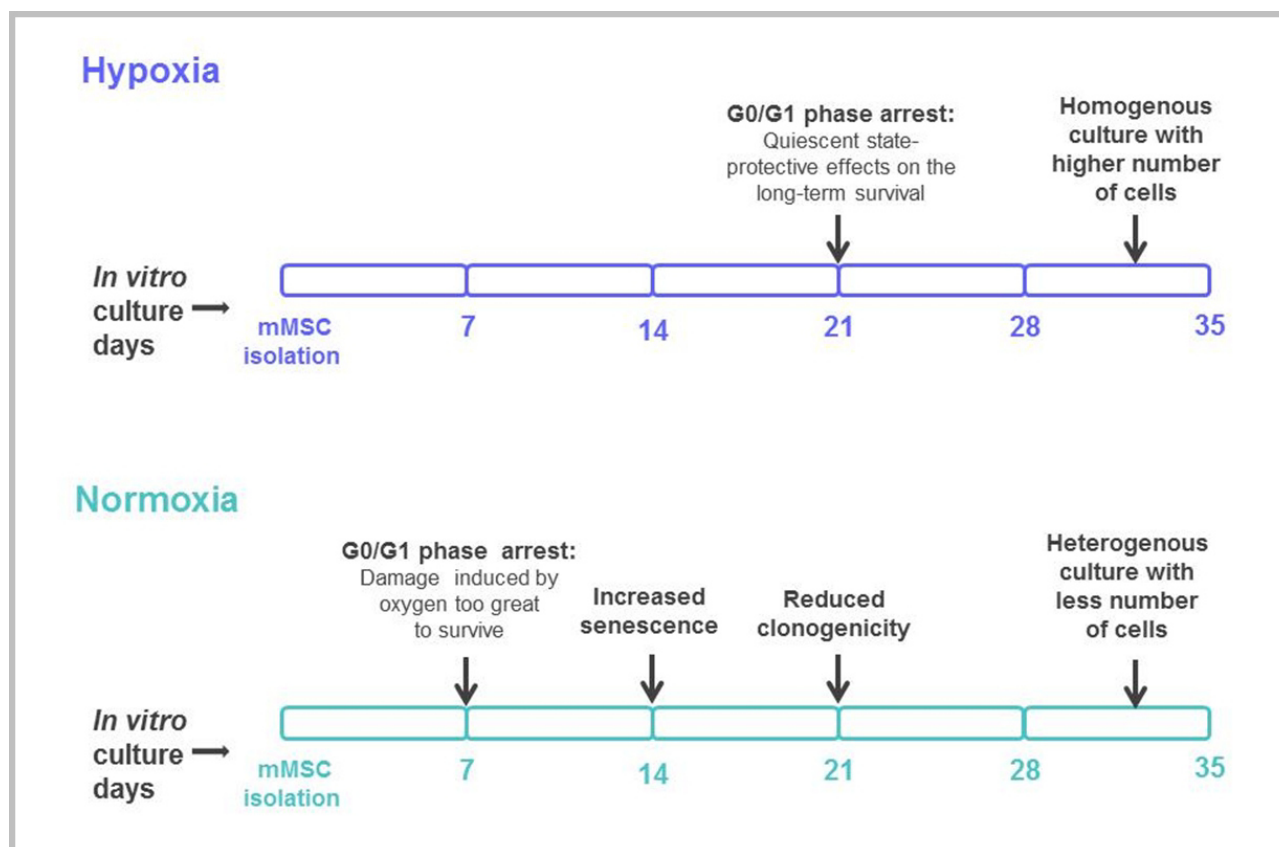


Figure 48: Survival response of mMSCs to *in vitro* hypoxic and normoxic conditions. Murine mesenchymal stem cells growing in hypoxia display G0/G1 cell cycle arrest on day 21 and better long-term survival. In contrast, mMSCs growing in normoxia display G0/G1 cell cycle arrest much earlier on day 7 and low long-term survival. Normoxic mMSCs also undergo increased senescence and show reduced clonogenicity on further culturing.

6.4 Murine mesenchymal stem cells are resistant towards ionizing radiation initiated apoptosis

Apoptosis when initiated by the cell results in complete destruction by activation of caspases to carry out the orderly process of cellular death avoiding inflammation and damage to surrounding cells [11]. The response of stem cells to ionizing radiation initiated apoptosis varies largely among the stem cells of different tissue and species origin. Human haematopoietic stem cells are highly radiosensitive being susceptible to ionizing radiation-induced apoptosis and show a large increase in apoptosis after ionizing radiation exposure (< 3 Gy) [183, 184]. Human mesenchymal stem cells, in contrast, are relatively radioresistant to the ionizing radiation activated apoptosis. Human mesenchymal stem cells isolated from the bone marrow exhibited nominal apoptosis after high doses of ionizing radiation exposure [10, 185, 186]. Sugrue et al. have shown that the clonal mouse MSC lines are radioresistant with a minimal response to ionizing radiation-induced apoptosis even after irradiation with 10 Gy [128]. In this project the primary mMSCs growing in hypoxia showed resistance towards ionizing radiation-induced apoptosis for the γ -irradiation doses up to 4 Gy. For hMSCs, this resistance was shown to be related to their efficient reactive oxygen species scavenging capacity and high double strand break repair ability [185, 187] after the ionizing radiation treatment. These properties endowed

the cells with an ability to better repair the DNA damage caused by ionizing radiation [185, 187]. Nevertheless, up-regulation of both pro- and anti-apoptotic gene expressions after irradiation (3-12 Gy) was also found in mMSCs [188]. Taken together with the results obtained from the senescence assay this data suggests that MSCs preferably go through senescent phenotype similar to stress induced premature senescence over apoptosis after γ -irradiation treatment to avoid the transmission of an impaired genome to the daughter cell.

6.5 Murine mesenchymal stem cells retain their induced multilineage differentiation ability but undergo ionizing radiation-induced adipogenesis after γ -irradiation treatment

For stem cells, the effects of genotoxic stress could modify their innate ability to differentiate into one or more lineages that could impair tissue homeostasis and normal organ development ([9], reviewed by [6]). Human embryonic stem cells were shown to retain their pluripotency even after irradiation with 4 Gy dose when the cells were able to form teratomas by differentiating into three germ layers [8]. Human mesenchymal stem cells are also known to maintain their multilineage differentiation capacity after exposure to doses of up to 10 Gy [185, 186]. Indeed, primary mMSCs from this study retained their osteo- and adipogenic differentiation ability when the cells were induced to differentiate after exposure to the γ -irradiation dose of up to 500 mGy. Supporting evidence for mouse MSCs sustaining their *in vitro* potency is available from the work of Sugrue et al. where they have successfully demonstrated the osteo and adipo lineage differentiation of mouse MSC cell lines irradiated up to 10 Gy [128]. This suggests that even after irradiation MSCs are able to preserve their potency and can undergo multilineage differentiation if permissive external and environmental cues are present.

Interestingly, compared to sham-irradiated cells, the irradiated cultures (from 0.5 Gy to 4 Gy) showed significantly increased numbers of differentiated adipocytes even without any lineage inducing growth medium 6 days after ionizing radiation treatment. Oxygen levels on their own did not significantly influence the transformation of mMSCs towards the adipogenic lineage, but an interaction between oxygen level and γ -irradiation in influencing adipogenesis was observed. This implies that oxygen concentration plays a supplementary role, intensifying the adipogenesis induced by irradiation. Differentiation of MSCs *in vitro* after irradiation was also observed by Havelek et. al. when they found that the dental pulp stem cells differentiate into odonto/osteoblast lineage prematurely after treatment with 6 Gy γ -irradiation dose [189]. Mouse melanocyte stem cells were shown to terminally differentiate into mature melanocyte at the expense of self-renewal after a dose of 5 Gy to the skin [9]. In contrast, differentiation of hair follicle bulge stem cells, which share the same niche with melanocyte stem cells, was unaffected after 5 Gy irradiation treatment [130].

Studies on the possible effects of ionizing radiation on differentiation ability of different kinds of stem cells have demonstrated that these effects could play out in different ways; either the stem cell could resist any effect by ionizing radiation on their potency and preserve their multipotent differentiation capacity [8] or it may result in loss of multipotency by propelling the cells to undergo premature differentiation into one lineage at the expense of others [9, 189]. The spontaneous

differentiation of stem cell after exposure to stress factors may imply the loss of its stemness properties affecting both self-renewal and multipotency. As previously described, osteogenic and adipogenic lineages of MSCs are mutually exclusive and lineage commitment of MSCs is virtually irreversible (reviewed by [89]). Favouring the bone marrow mesenchymal stem cell differentiation into adipocytes at the expense of osteoblasts could accelerate the formation of yellow marrow. Yellow (fatty) marrow consists predominantly of fat cells and is continuously increased with age [190]. It is haematopoietically inactive [190] thereby displacing the normal haematopoiesis. Increased bone marrow fat could also have serious health consequences like escalated risk of osteoporosis [90, 191] and diabetes mellitus [192]. If indeed hMSCs respond to γ -irradiation in a similar way to mMSCs then ionizing radiation-induced adipogenesis after a treatment with γ -irradiation could result into a serious health concern. Radiation therapy with high doses of ionizing radiation, and medical and occupational radiation exposure, involving accumulation of low doses of ionizing radiation, may create a cohort of people at higher risk of unforeseen secondary illnesses resulting due to the after effects of irradiation much later in their life.

The variable effects of ionizing radiation on the potency and other properties of the stem cells are the result of their innate radio response which depends on the reaction to ionizing radiation-induced DNA damage [9, 128, 187]. In addition, various factors present in a SC niche like oxygen is known to modulate the cellular response to ionizing radiation [131, 175]. Therefore, our observations of the preserved ability of irradiated primary mMSCs to be able to undergo osteo- and adipogenic lineage when stimulated, occurrence of ionizing radiation-induced adipogenesis and enhanced senescence following γ -irradiation can be suggested to relate with the DNA damage induced by ionizing radiation in primary mMSCs, and their ensuing response which is fine tuned by microenvironment and intrinsic cellular factors. As the mechanism of DNA damage response is of fundamental importance to regulate how the cells react towards the genotoxic stress (reviewed by [127]) it would be indeed worth investigating whether DNA damage response also determines the response of primary mMSCs to ionizing radiation and to other stress inducing factors such as non-physiological high oxygen.

6.6 Ionizing radiation affects the gene expression profile of mMSCs

To identify the genes involved in *in vitro* ageing of mMSCs the genes specific to mMSCs were quantified by reverse transcription PCR array. The 31 differentially regulated candidate genes as compared to osteoblasts were further studied in young and old mMSCs, and 7 genes were identified that could be implicated in the *in vitro* ageing of the cells. The expression pattern of these 7 ageing genes was studied after irradiation and *Tnf* was found to be significantly down regulated after the medium dose (2 Gy) γ -irradiation treatment.

The pro-inflammatory cytokine *Tnf* plays an important role in regulating anti-inflammatory effects of MSCs in case of tissue injuries such as corneal injury [193] and myocardial infarction [194]. *Tnf* also found to enhance the transmigration properties of hMSCs and rat MSCs [195, 196]. In hMSCs that are undergoing replicative senescence *in vitro* Wagner et al. has observed significant down-regulation of mRNA for the tumour necrosis factor (ligand) superfamily member 11 [53]. In this study *in vitro* ageing was found to affect the *Tnf* expression for both low dose and medium dose irradiated cells. However, the gene expression was dynamic and a clear trend of either up-

or down-regulation was absent. Although no effect of low dose (0.1 Gy) was observed on *Tnf* expression, medium ionizing radiation dose of 2 Gy significantly influenced its expression in long-term cultured mMSCs. The decreased expression of *Tnf* mRNA in mMSCs after 2 Gy γ -irradiation is in contrast to other human [197] and cancer cells [198] that show augmented levels of the same gene TNF-alpha after ionizing radiation exposure. The expression pattern of the ageing genes that were studied in this project can serve as a starting point to be able to comprehend the molecular and genetic changes in the MSC specific properties after stress exposure. The small number of genes that were evaluated represents a subset of candidate regulators but do not include all potentially relevant genes. The response of MSCs to stress is a very complex process which might involve many more genes, and therefore a global transcriptome approach to provide more comprehensive picture of molecular changes caused by ionizing radiation and oxygen during ageing will be informative.

As stated previously, mMSCs showed an ionizing radiation-induced adipogenesis 6 days after exposure to γ -irradiation starting as low as 0.5 Gy. In stem cells the process of differentiation is accompanied by changes in the expression pattern of genes necessary for maintaining stemness and for driving differentiation. For example, in the case of hESCs the stemness genes SOX2, NANOG, POU5F1 etc. are all down-regulated in differentiated embryoid bodies [43]. Therefore, the expression pattern of different stemness and differentiation markers were analysed in mMSCs starting 6 days after ionizing radiation treatment. However, no downregulation of the mRNA expression level of the stemness and pluripotency markers (*Sox2*, *Bmi1*, *Nanog*, *Pou5f1*, *Nes* and *Klf4*) were detected after γ -irradiation treatment. A possible reason for these observations is the detection limits due to the extremely low adipogenic differentiation rate of mMSCs (approximately 0.1% in 0 Gy and 0.4% in 4 Gy hypoxic mMSCs). The expression of stemness genes from highly abundant, undifferentiated mMSCs is possibly masking the expression alterations in the few differentiated cells.

The expression pattern of osteogenic and adipogenic marker genes in sham-irradiated (control) mMSC cultures throughout the period of *in vitro* expansion is shown in fig. 49. In contrast to control cells downregulation of the osteogenic marker *Runx2* was observed in 2 Gy irradiated mMSCs. *Runx2* is a master regulator of osteogenesis and plays a decisive role in differentiation of hMSCs to the osteogenic lineage [199]. Therefore, reduced *Runx2* expression after irradiation may indicate a switch in differentiation in irradiated mMSCs, away from the osteogenic lineage towards increased adipogenesis. Interestingly, despite the ionizing radiation-induced adipogenesis the expression level of key adipogenic regulator *Pparg* was significantly reduced after a dose of 2 Gy but the expression of other adipogenic marker *Fabp4* was not significantly affected. At the same time the lower dose of 0.1 Gy significantly increased the levels of *Pparg* and *Fabp4*. One probable reason behind these discrepancies between elevated adipogenesis and variable expression of adipogenic markers in irradiated mMSCs is perhaps the mechanisms involved in the activation of different pathways of differentiation. The process of MSC differentiation is a multistep process and is characterised by a temporarily and spatially orchestrated expression of the genes involved in the differentiation process. Those genes are often expressed in a transient manner [91, 94]. This can explain the observed non-linear expression patterns of differentiation markers over time and makes it challenging to find informative differentiation markers for irradiated MSCs at different developmental stages. In addition, the role played by post-transcriptional, post-translational, and epigenetic modifications like histone modifications which can regulate the gene expression must also be taken into account for osteogenic

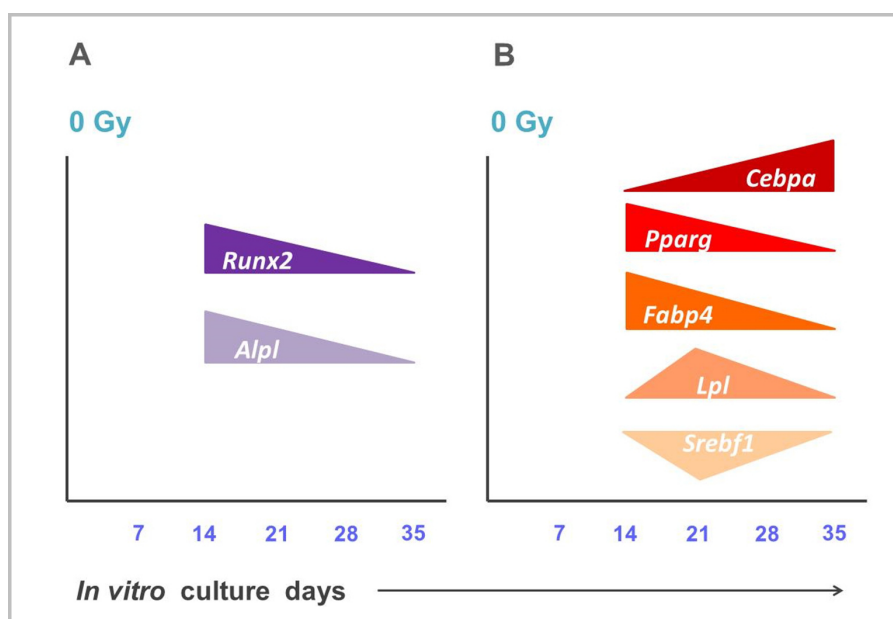


Figure 49: A schematic representation of the alterations in gene expression during *in vitro* mMSC culture. Panel A displays expression of osteogenic markers *Runx2* and *Alpl* from day 14 till day 35 in sham-irradiated *Rb*^{+/+} mMSC cultures. Panel B displays expression of adipogenic markers *Cebpa*, *Pparg*, *Fabp4*, *Lpl* and *Srebf1* from day 14 till day 35 in sham-irradiated *Rb*^{+/+} mMSC cultures.

and adipogenic differentiation of MSCs [200].

Finally, one of the very important facts that have to be considered is in a clinical situation there is extremely low possibility that the MSCs are treated with ionizing radiation during actual *ex vivo* expansion after their isolation from a donor tissue. Nonetheless, with continuous ionizing radiation exposure by means of natural and artificial sources in daily life greater likelihood is that the donor has been previously exposed to γ -irradiation. This prior *in vivo* exposure to ionizing radiation raises the probability that the MSCs have already accumulated ionizing radiation associated molecular and cytogenetic changes. Afterwards, if these cells are expanded in non-physiological O₂ levels synergistic negative effects might arise in ionizing radiation primed MSCs.

6.7 Conclusions

In this project we have demonstrated that the stress inflicted by non-physiologically high oxygen concentration and ionizing radiation can affect the innate stemness characteristics of *ex vivo* expanded murine MSCs. This implies that the usage of inadvertently stress exposed MSCs in stem cell therapy can be a risk factor potentially affecting the final therapeutic outcome.

In the initial hypothesis it was assumed that ionizing radiation induces premature ageing in MSCs and affects their inherent properties of self-renewal and multilineage differentiation. Findings from this study show that mMSCs are in fact sensitive towards oxidative stress generated by both γ -irradiation and higher oxygen level *in vitro*. Sustainable growth and efficient colony forming ability of mMSCs in hypoxia rather than normoxia illustrate the protective effects conferred by low oxygen concentration on self-renewal ability of mMSCs. The impaired growth of mMSCs in higher oxygen tension was correlated with increased basal level of senescence which itself was potentiated by

ionizing radiation. In the long-term the combined effects of high oxygen during *ex vivo* expansion and possible exposure to radiation leads to considerable reduction in the number of clonogenic cells and increased senescence in mMSCs. Nevertheless, despite the lower long-term survival of mMSCs in higher oxygen tension both hypoxic and normoxic mMSCs were observed to maintain their telomeric length for up to 18 days *in vitro*. It implies that accelerated telomeric shortening may not be the direct cause behind reduced survival of mMSCs in normoxia.

Hypoxic mMSCs were found to be resistant towards ionizing radiation-induced apoptosis for doses up to 4 Gy; meaning ionizing radiation is unable to cause the decline in mMSC number by direct cell killing. On the other hand, though the irradiated MSCs maintained their osteo- and adipogenic differentiation after stimulation, occurrence of ionizing radiation-induced adipogenesis in hypoxic mMSCs after γ -irradiation dose signify changes in the *in vitro* differentiation program of the mMSCs. The ionizing radiation-induced adipogenesis displayed by irradiated hypoxic mMSCs, even in the absence of any lineage inducing trigger, could disrupt tissue homeostasis and cellular reconstitution. Together this data suggests that normoxia and ionizing radiation can synergistically act to induce genotoxic stress in mMSCs which leads to the loss of their clonogenic ability and potency. This work helps to recognize the consequences of lifetime MSC exposure to stressors for future stem cell therapy procedures. This understanding of the biology underlying the MSC response to stress will improve the safety and efficacy of the MSC therapy by raising awareness of potential interaction between oxygen status and ionizing radiation exposure.

Bibliography

- [1] Mary Helen Barcellos-Hoff, Catherine Park, and Eric G Wright. Radiation and the microenvironment - tumorigenesis and therapy. *Nature reviews. Cancer*, 5(11):867–75, dec 2005.
- [2] United Nations Scientific Committee on the Effects of Atomic Radiation. SOURCES AND EFFECTS OF IONIZING RADIATION: Report to the General Assembly with Scientific Annexes. Technical report, United Nations Publications, 2008.
- [3] United Nations Scientific Committee on the Effects of Atomic Radiation. SOURCES AND EFFECTS OF IONIZING RADIATION: Annex A. Technical report, 2008.
- [4] National Research Council. *Health Risks from Exposure to Low Levels of Ionizing Radiation: BEIR VII Phase 2*. National Academies Press, 2006.
- [5] Detlef Weigel and Gerd Jürgens. Stem cells that make stems. *Nature*, 415(6873):751–4, feb 2002.
- [6] Robert Passier and Christine Mummery. Origin and use of embryonic and adult stem cells in differentiation and tissue repair. *Cardiovascular research*, 58(2):324–35, may 2003.
- [7] T Reya, S J Morrison, M F Clarke, and I L Weissman. Stem cells, cancer, and cancer stem cells. *Nature*, 414(6859):105–11, nov 2001.
- [8] Kitchener D Wilson, Ning Sun, Mei Huang, Wendy Y Zhang, Andrew S Lee, Zongjin Li, Shan X Wang, and Joseph C Wu. Effects of Ionizing Radiation on Self Renewal and Pluripotency of Human Embryonic Stem Cells. *Cancer Research*, 70(13):5539–48, 2010.
- [9] Ken Inomata, Takahiro Aoto, Nguyen Thanh Binh, Natsuko Okamoto, Shintaro Tanimura, Tomohiko Wakayama, Shoichi Iseki, Eiji Hara, Takuji Masunaga, Hiroshi Shimizu, and Emi K. Nishimura. Genotoxic Stress Abrogates Renewal of Melanocyte Stem Cells by Triggering Their Differentiation. *Cell*, 137(6):1088–1099, 2009.
- [10] Monika Damek-poprawa, Derek Stefanik, Lawrence M Levin, and SO Akintoye. Human bone marrow stromal cells display variable anatomic site-dependent response and recovery from irradiation. *Archives of Oral Biology*, 55(5):358–64, 2010.
- [11] D Watters. Molecular mechanisms of ionizing radiation-induced apoptosis. *Immunology and Cell Biology*, 77:263–271, 1999.
- [12] R Christensen, J Alsner, F Brandt Sorensen, F Dagnaes-Hansen, S Kolvraa, and N Serakinci. Transformation of human mesenchymal stem cells in radiation carcinogenesis: long-term effect of ionizing radiation. *Regenerative medicine*, 3(6):849–861, 2008.
- [13] National Academy of Sciences. *Understanding Stem Cells: An Overview of the Science and Issues from the National Academics*. The National Academics of Sciences, Engineering, Medicine, 2006.

BIBLIOGRAPHY

- [14] Sean J Morrison and Judith Kimble. Asymmetric and symmetric stem-cell divisions in development and cancer. *Nature*, 441(7097):1068–74, jun 2006.
- [15] M J Evans and M H Kaufman. Establishment in culture of pluripotential cells from mouse embryos., 1981.
- [16] Mark E. Levenstein, Tenneille E Ludwig, Ren-He Xu, Rachel A Llanas, Kaitlyn VanDenHeuvel-Kramer, Daisy Manning, and James A Thomson. Basic fibroblast growth factor support of human embryonic stem cell self-renewal. *Stem cells*, 24(3):568–74, 2006.
- [17] S J Bruce, B B Gardiner, L J Burke, M M Gongora, S M Grimmond, and A C Perkins. Dynamic transcription programs during ES cell differentiation towards mesoderm in serum versus serum-freeBMP4 culture. *BMC Genomics*, 8:365, 2007.
- [18] Pengbo Zhang, Jian Li, Zhijia Tan, Chengyan Wang, Ting Liu, Lin Chen, Jun Yong, Wei Jiang, and Xiaomeng Sun. Short-term BMP-4 treatment initiates mesoderm induction in human embryonic stem cells. *Blood*, 111(4):1933–1941, 2008.
- [19] Eun Su Jeon, Hyun Jung Moon, Mi Jeong Lee, Hae Young Song, Young Mi Kim, Yong Chan Bae, Jin Sup Jung, and Jae Ho Kim. Sphingosylphosphorylcholine induces differentiation of human mesenchymal stem cells into smooth-muscle-like cells through a TGF-beta-dependent mechanism. *Journal of cell science*, 119(Pt 23):4994–5005, 2006.
- [20] Noboru Sato, Laurent Meijer, Leandros Skaltsounis, Paul Greengard, and Ali H Brivanlou. Maintenance of pluripotency in human and mouse embryonic stem cells through activation of Wnt signaling by a pharmacological GSK-3-specific inhibitor. *Nature Medicine*, 10(1):55–63, 2004.
- [21] Roel Nusse. Wnt signaling and stem cell control. *Cell research*, 18(5):523–27, may 2008.
- [22] Tong Ihn Lee, Richard G Jenner, Laurie A Boyer, Matthew G Guenther, Stuart S Levine, Roshan M Kumar, Brett Chevalier, Sarah E Johnstone, Megan F Cole, Kyo-ichi Isono, Haruhiko Koseki, Takuya Fuchikami, Kuniya Abe, Heather L Murray, Jacob P Zucker, Bingbing Yuan, George W Bell, Elizabeth Herbolsheimer, Nancy M Hannett, Kaiming Sun, Duncan T Odom, Arie P Otte, Thomas L Volkert, David P Bartel, Douglas A Melton, David K Gifford, Rudolf Jaenisch, and Richard A Young. Control of developmental regulators by Polycomb in human embryonic stem cells. *Cell*, 125(2):301–13, apr 2006.
- [23] Paul Delgado-Olguín, Yu Huang, Xue Li, Danos Christodoulou, Christine E Seidman, J G Seidman, Alexander Tarakhovsky, and Benoit G Bruneau. Epigenetic repression of cardiac progenitor gene expression by Ezh2 is required for postnatal cardiac homeostasis. *Nature genetics*, 44(3):343–7, mar 2012.
- [24] N S Christophersen and K Helin. Epigenetic control of embryonic stem cell fate. *J Exp Med*, 207(11):2287–2295, 2010.
- [25] Jessica Segales, Eusebio Perdiguero, and Pura Munoz-Canoves. Epigenetic control of adult skeletal muscle stem cell functions. *FEBS Journal*, 282(9):1571–1588, 2015.
- [26] Kazutoshi Takahashi and Shinya Yamanaka. Induction of Pluripotent Stem Cells from Mouse Embryonic and Adult Fibroblast Cultures by Defined Factors. *Cell*, 126(4):663–676, 2006.
- [27] Keisuke Okita, Tomoko Ichisaka, and Shinya Yamanaka. Generation of germline-competent induced pluripotent stem cells. *Nature*, 448(7151):313–317, 2007.

BIBLIOGRAPHY

- [28] M Wernig, A Meissner, R Foreman, T Brambrink, M Ku, K Hochedlinger, B E Bernstein, and R Jaenisch. In vitro reprogramming of fibroblasts into a pluripotent ES-cell-like state. *Nature*, 448:318–324, 2007.
- [29] Nimet Maherali, Rupa Sridharan, Wei Xie, Jochen Utikal, Sarah Eminli, Katrin Arnold, Matthias Stadtfeld, Robin Yachechko, Jason Tchieu, Rudolf Jaenisch, Kathrin Plath, and Konrad Hochedlinger. Directly reprogrammed fibroblasts show global epigenetic remodeling and widespread tissue contribution. *Cell Stem Cell*, 1(1):55–70, 2007.
- [30] L A Boyer, T I Lee, M F Cole, S E Johnstone, S S Levine, J P Zucker, M G Guenther, R M Kumar, H L Murray, R G Jenner, D K Gifford, D A Melton, R Jaenisch, and R A Young. Core transcriptional regulatory circuitry in human embryonic stem cells. *Cell*, 122(6):947–956, 2005.
- [31] Yui-Han Loh, Qiang Wu, Joon-Lin Chew, Vinsensius B Vega, Weiwei Zhang, Xi Chen, Guillaume Bourque, Joshy George, Bernard Leong, Jun Liu, Kee-Yew Wong, Ken W Sung, Charlie W H Lee, Xiao-Dong Zhao, Kuo-Ping Chiu, Leonard Lipovich, Vladimir a Kuznetsov, Paul Robson, Lawrence W Stanton, Chia-Lin Wei, Yijun Ruan, Bing Lim, and Huck-Hui Ng. The Oct4 and Nanog transcription network regulates pluripotency in mouse embryonic stem cells. *Nature genetics*, 38(4):431–440, 2006.
- [32] L Liu and R M Roberts. Silencing of the gene for the beta subunit of human chorionic gonadotropin by the embryonic transcription factor Oct-3/4. *The Journal of biological chemistry*, 271(28):16683–9, jul 1996.
- [33] Guang Jin Pan, Zeng Yi Chang, Hans R Schöler, and Duanqing Pei. Stem cell pluripotency and transcription factor Oct4. *Cell Research*, 12(5-6):321–329, 2002.
- [34] Mei-Hui Tai, Chia-Cheng Chang, Matti Kiupel, Joshua D Webster, L Karl Olson, and James E Trosko. Oct4 expression in adult human stem cells: evidence in support of the stem cell theory of carcinogenesis. *Carcinogenesis*, 26(2):495–502, 2005.
- [35] A A Avilion, S K Nicolis, L H Pevny, L Perez, N Vivian, and R Lovell-Badge. Multipotent cell lineages in early mouse development on SOX2 function. *Genes Dev.*, 17:126–140, 2003.
- [36] Katrin Arnold, Abby Sarkar, Mary Anna Yram, Jose M. Polo, Rod Bronson, Sumitra Sengupta, Marco Seandel, Niels Geijsen, and Konrad Hochedlinger. Sox2 + adult stem and progenitor cells are important for tissue regeneration and survival of mice. *Cell Stem Cell*, 9(4):317–329, 2011.
- [37] Chih Chien Tsai, Pei Fen Su, Yi Feng Huang, Tu Lai Yew, and Shih Chieh Hung. Oct4 and Nanog Directly Regulate Dnmt1 to Maintain Self-Renewal and Undifferentiated State in Mesenchymal Stem Cells. *Molecular Cell*, 47(2):169–82, 2012.
- [38] Peilin Zhang, Rose Andrianakos, Yang Yang, Chunming Liu, and Wange Lu. Kruppel-like factor 4 (Klf4) prevents embryonic stem (ES) cell differentiation by regulating Nanog gene expression. *The Journal of Biological Chemistry*, 285(12):9180–9189, 2010.
- [39] Donghyun Park, Andy Peng Xiang, Frank Fuxiang Mao, Li Zhang, Chun Guang Di, Xiao Mei Liu, Yuan Shao, Bao Feng Ma, Jae Hyun Lee, Kwon Soo Ha, Noah Walton, and Bruce T. Lahn. Nestin is required for the proper self-renewal of neural stem cells. *Stem Cells*, 28(12):2162–2171, 2010.
- [40] Henryk Zulewski, Elizabeth J Abraham, Melissa J Gerlach, Philip B Daniel, Wolfgang Moritz, Mario Vallejo, Melissa K Thomas, and Joel F Habener. Multipotential nestin-positive stem cells isolated from adult pancreatic islets differentiate ex vivo into pancreatic endocrine, exocrine, and hepatic phenotypes. *Diabetes*, 50(March 2001):521–533, 2001.

- [41] Jakub Neradil and Renata Veselska. Nestin as a marker of cancer stem cells. *Cancer Science*, 106(2015):803–811, 2015.
- [42] In Kyung Park, Sean J. Morrison, and Michael F. Clarke. Bmi1, stem cells, and senescence regulation. *Journal of Clinical Investigation*, 113(2):175–179, 2004.
- [43] Jingli Cai, Jia Chen, Ying Liu, Takumi Miura, Yongquan Luo, Jeanne F Loring, William J Freed, Mahendra S Rao, and Xianmin Zeng. Assessing self-renewal and differentiation in human embryonic stem cell lines. *Stem Cells*, 24(3):516–30, mar 2006.
- [44] Maria P De Miguel, Sherezade Fuentes-Julián, and Yago Alcaina. Pluripotent stem cells: origin, maintenance and induction. *Stem cell reviews*, 6(4):633–49, 2010.
- [45] Frederick R Appelbaum. Hematopoietic-cell transplantation at 50. *The New England journal of medicine*, 357(15):1472–1475, 2007.
- [46] James A Thomson, J Itskovitz-Eldor, Sander S Shapiro, Michelle A Waknitz, Jennifer J Swiergiel, Vivienne S Marshall, and Jeffrey M Jones. Embryonic stem cell lines derived from human blastocysts. *Science*, 282(5391):1145–47, 1998.
- [47] G J Annas, A Caplan, and S Elias. Stem cell politics, ethics and medical progress. *Nature medicine*, 5(12):1339–41, dec 1999.
- [48] K H Campbell, J McWhir, W A Ritchie, and I Wilmut. Sheep cloned by nuclear transfer from a cultured cell line., 1996.
- [49] Jack T Mosher, Trevor J Pemberton, Kristina Harter, Chaolong Wang, Erkan O Buzbas, Petr Dvorak, Carlos Simón, Sean J Morrison, and Noah A Rosenberg. Lack of population diversity in commonly used human embryonic stem-cell lines. *The New England journal of medicine*, 362(2):183–5, jan 2010.
- [50] Daisy.A. a. Robinton and Gq George Q. Daley. The promise of induced pluripotent stem cells in research and therapy. *Nature*, 481(7381):295–305, 2012.
- [51] Jesse K Biehl and Brenda Russell. Introduction to stem cell therapy. *The Journal of cardiovascular nursing*, 24(2):98–105, 2009.
- [52] Song-Yan Liao and Hung-Fat Tse. Multipotent (adult) and pluripotent stem cells for heart regeneration: what are the pros and cons? *Stem cell research & therapy*, 4(6):151, jan 2013.
- [53] Wolfgang Wagner, Patrick Horn, Mirco Castoldi, Anke Diehlmann, Simone Bork, Rainer Saffrich, Vladimir Benes, Jonathon Blake, Stefan Pfister, Volker Eckstein, and Anthony D. Ho. Replicative senescence of mesenchymal stem cells: A continuous and organized process. *PLoS ONE*, 3(5):e2213, 2008.
- [54] Masako Miura, Yasuo Miura, Hesed M Padilla-Nash, Alfredo a Molinolo, Baojin Fu, Vyomesh Patel, Byoung-Moo Seo, Wataru Sonoyama, Jenny J Zheng, Carl C Baker, Wanjun Chen, Thomas Ried, and Songtao Shi. Accumulated chromosomal instability in murine bone marrow mesenchymal stem cells leads to malignant transformation. *Stem cells*, 24:1095–1103, 2006.
- [55] Martin Breitbach, Toktam Bostani, Wilhelm Roell, Ying Xia, Oliver Dewald, Jens M Nygren, Jochen W U Fries, Klaus Tiemann, Heribert Bohlen, Juergen Hescheler, Armin Welz, Wilhelm Bloch, and Sten Eirik W Jacobsen. Potential risks of bone marrow cell transplantation into infarcted hearts. *Blood*, 110(4):1362–1369, 2007.

- [56] Mark F Pittenger, Alastair M Mackay, Stephen C Beck, Rama K Jaiswal, Robin Douglas, Joseph D Mosca, Mark A Moorman, Donald W Simonetti, Stewart Craig, and Daniel R Marshak. Multilineage potential of adult human mesenchymal stem cells. *Science*, 284(5411):143–47, 1999.
- [57] Patricia A Zuk, Min Zhu, Peter Ashjian, Daniel A De Ugarte, Jerry I Huang, Hiroshi Mizuno, Zeni C Alfonso, John K Fraser, Prosper Benhaim, and Marc H Hedrick. Human adipose tissue is a source of multipotent stem cells. *Molecular Biology of the Cell*, 13(12):4279–95, dec 2002.
- [58] Shinji Makino, Keiichi Fukuda, Shunichirou Miyoshi, Fusako Konishi, Hiroaki Kodama, Jing Pan, Motoaki Sano, Toshiyuki Takahashi, Shingo Hori, Hitoshi Abe, Jun-ichi Hata, Akihiro Umezawa, and Satoshi Ogawa. Cardiomyocytes can be generated from marrow stromal cells in vitro. *The Journal of Clinical Investigation*, 103(5):697–705, 1999.
- [59] Philippe Tropel, Nadine Platet, Jean-Claude Platel, Danièle Noël, Mireille Albrieux, Alim-Louis Benabid, and François Berger. Functional neuronal differentiation of bone marrow-derived mesenchymal stem cells. *Stem Cells*, 24(12):2868–2876, 2006.
- [60] A Friedenstein and A I Kuralesova. Osteogenic precursor cells of bone marrow in radiation chimeras. *Transplantation*, 12(2):99–108, aug 1971.
- [61] A J Friedenstein, R K Chailakhyan, and U V Gerasimov. Bone marrow osteogenic stem cells: in vitro cultivation and transplantation in diffusion chambers. *Cell and tissue kinetics*, 20(3):263–72, may 1987.
- [62] A J Friedenstein, N V Latzinik, Gorskaya YuF, E A Luria, and I L Moskvina. Bone marrow stromal colony formation requires stimulation by haemopoietic cells. *Bone and mineral*, 18(3):199–213, sep 1992.
- [63] M Owen and A J Friedenstein. Stromal stem cells: marrow-derived osteogenic precursors. *Ciba Foundation symposium*, 136:42–60, jan 1988.
- [64] Arnold I Caplan. Mesenchymal stem cells., 1991.
- [65] Susanne Kern, Hermann Eichler, Johannes Stoeve, Harald Klüter, and Karen Bieback. Comparative analysis of mesenchymal stem cells from bone marrow, umbilical cord blood, or adipose tissue. *Stem cells*, 24(5):1294–301, 2006.
- [66] Lindolfo da Silva Meirelles, Pedro Cesar Chagastelles, and Nance Beyer Nardi. Mesenchymal stem cells reside in virtually all post-natal organs and tissues. *Journal of cell science*, 119(Pt 11):2204–13, 2006.
- [67] R Rodriguez, J Garcia-Castro, C Trigueros, M Garcia Arranz, and P Menendez. Multipotent mesenchymal stromal cells: clinical applications and cancer modeling. *Advances in Experimental Medicine and Biology*, 741:187–205, 2012.
- [68] Paolo Bianco, Pamela Gehron Robey, and Paul J Simmons. Mesenchymal stem cells: revisiting history, concepts, and assays. *Cell stem cell*, 2(4):313–9, apr 2008.
- [69] E M Horwitz, K Le Blanc, M Dominici, I Mueller, I Slaper-Cortenbach, F C Marini, R J Deans, D S Krause, and a Keating. Clarification of the nomenclature for MSC: The International Society for Cellular Therapy position statement. *Cytotherapy*, 7(5):393–395, 2005.
- [70] M Dominici, K Le Blanc, I Mueller, I Slaper-Cortenbach, Fc Marini, Ds Krause, Rj Deans, A Keating, Dj Prockop, and Em Horwitz. Minimal criteria for defining multipotent mesenchymal stromal cells. The International Society for Cellular Therapy position statement. *Cytotherapy*, 8(4):315–17, 2006.

- [71] Sally A Boxall and Elena Jones. Markers for characterization of bone marrow multipotential stromal cells. *Stem cells international*, 2012:975871, jan 2012.
- [72] C Pautke, F Haasters, A Kolk, H Gülkan, W Mutschler, S Milz, and M Schieker. Characterization of human mesenchymal stem cells by six-color immunofluorescence. *International Journal of Oral and Maxillofacial Surgery*, 34(1):43–44, apr 2005.
- [73] Feng-Juan Lv, Rocky S Tuan, Kenneth M C Cheung, and Victor Y L Leung. Consise review: the surface markers and identity of human mesenchymal stem cells. *Stem cells*, 32(6):1408–19, jun 2014.
- [74] Daniel A. De Ugarte, Zeni Alfonso, Patricia A. Zuk, Amir Elbarbary, Min Zhu, Peter Ashjian, Prosper Benhaim, Mare H. Hedrick, and John K. Fraser. Differential expression of stem cell mobilization-associated molecules on multi-lineage cells from adipose tissue and bone marrow. *Immunology Letters*, 89(2-3):267–270, 2003.
- [75] Mustapha Zeddou, Alexandra Briquet, Biserka Relic, Claire Josse, Michel G Malaise, André Gothot, Chantal Lechanteur, and Yves Beguin. The umbilical cord matrix is a better source of mesenchymal stem cells (MSC) than the umbilical cord blood. *Cell biology international*, 34(7):693–701, jul 2010.
- [76] Rebecca A. Pelekanos, Joan Li, Milena Gongora, Vashe Chandrakanthan, Janelle Scown, Norseha Suhaimi, Gary Brooke, Melinda E. Christensen, Tram Doan, Alison M. Rice, Geoffrey W. Osborne, Sean M. Grimmond, Richard P. Harvey, Kerry Atkinson, and Melissa H. Little. Comprehensive transcriptome and immunophenotype analysis of renal and cardiac MSC-like populations supports strong congruence with bone marrow MSC despite maintenance of distinct identities. *Stem Cell Research*, 8(1):58–73, 2012.
- [77] Henk Rozemuller, Henk-Jan Prins, Benno Naaijken, Jojet Staal, Hans-Jörg Bühring, and Anton C Martens. Prospective isolation of mesenchymal stem cells from multiple mammalian species using cross-reacting anti-human monoclonal antibodies. *Stem Cells and Development*, 19(12):1911–1921, 2010.
- [78] Alexandra Peister, Jason A. Mellad, Benjamin L. Larson, Brett M. Hall, Laura F. Gibson, and Darwin J. Prockop. Adult stem cells from bone marrow (MSCs) isolated from different strains of inbred mice vary in surface epitopes, rates of proliferation, and differentiation potential. *Blood*, 103(5):1662–1668, 2004.
- [79] Federica Sabatini, Loredana Petecchia, Manuela Tavian, Vanina Jodon de Villeroché, Giovanni a Rossi, and Danièle Brouty-Boyé. Human bronchial fibroblasts exhibit a mesenchymal stem cell phenotype and multilineage differentiating potentialities. *Laboratory Investigation*, 85(8):962–971, 2005.
- [80] Charles K F Chan, Eun Young Seo, James Y. Chen, David Lo, Adrian McArdle, Rahul Sinha, Ruth Tevlin, Jun Seit, Justin Vincent-Tompkins, Taylor Wearda, Wan Jin Lu, Kshemendra Senarath-Yapa, Michael T. Chung, Owen Marecic, Misha Tran, Kelley S. Yan, Rosalynd Upton, Graham G. Walmsley, Andrew S. Lee, Debashis Sahoo, Calvin J. Kuo, Irving L. Weissman, and Michael T. Longaker. Identification and specification of the mouse skeletal stem cell. *Cell*, 160(1-2):285–298, 2015.
- [81] Daniel L Worthley, Michael Churchill, Jocelyn T Compton, Yagnesh Tailor, Meenakshi Rao, Yiling Si, Daniel Levin, Matthew G Schwartz, Aysu Uygur, Yoku Hayakawa, Stefanie Gross, Bernhard W Renz, Wanda Setlik, Ashley N Martinez, Xiaowei Chen, Saqib Nizami, Heon Goo Lee, H Paco Kang, Jon-Michael Caldwell, Samuel Asfaha, C Benedikt Westphalen, Trevor Graham, Guangchun Jin, Karan Nagar, Hongshan Wang, Mazen A Kheirbek, Alka Kolhe,

- Jared Carpenter, Mark Glaire, Abhinav Nair, Simon Renders, Nicholas Manieri, Sureshkumar Muthupalani, James G Fox, Maximilian Reichert, Andrew S Giraud, Robert F Schwabe, Jean-Phillipe Pradere, Katherine Walton, Ajay Prakash, Deborah Gumucio, Anil K Rustgi, Thaddeus S Stappenbeck, Richard A Friedman, Michael D Gershon, Peter Sims, Tracy Grikscheit, Francis Y Lee, Gerard Karsenty, Siddhartha Mukherjee, and Timothy C Wang. Gremlin 1 identifies a skeletal stem cell with bone, cartilage, and reticular stromal potential. *Cell*, 160(1-2):269–84, jan 2015.
- [82] C E Gargett. Uterine stem cells: What is the evidence? *Human reproduction update*, 13(1):87–101, jan 2007.
- [83] Federico Mosna and Luc Sensebe. Human Bone Marrow and Adipose Tissue Mesenchymal Stem Cells : A User ' s Guide. *Stem Cells and Development*, 19(10):1–53, 2010.
- [84] Gro Vatne Rosland, Agnete Svendsen, Anja Torsvik, Ewa Sobala, Emmet McCormack, Heike Immervoll, Josef Mysliwietz, Joerg Christian Tonn, Roland Goldbrunner, Per Eystein Lønning, Rolf Bjerkvig, and Christian Schichor. Long-term cultures of bone marrow-derived human mesenchymal stem cells frequently undergo spontaneous malignant transformation. *Cancer Research*, 69(13):5331–5339, 2009.
- [85] Masood A Shammas, Aamer Qazi, Ramesh B Batchu, Robert C Bertheau, Jason Y Y Wong, Manjula Y Rao, Madhu Prasad, Diptiman Chanda, Selvarangan Ponnazhagan, Kenneth C Anderson, Christopher P Steffes, Nikhil C Munshi, Immaculata De Vivo, David G Beer, Sergei Gryaznov, Donald W Weaver, and Raj K Goyal. Telomere maintenance in laser capture microdissection-purified Barrett's adenocarcinoma cells and effect of telomerase inhibition in vivo. *Clinical cancer research : an official journal of the American Association for Cancer Research*, 14(15):4971–80, aug 2008.
- [86] Masood A Shammas. Telomeres, lifestyle, cancer, and aging. *Current Opinion in Clinical Nutrition and Metabolic Care*, 14(1):28–34, 2011.
- [87] Carlos López-Otín, Maria A. Blasco, Linda Partridge, Manuel Serrano, and Guido Kroemer. The hallmarks of aging. *Cell*, 153(6):1194–217, 2013.
- [88] G P Dimri, X Lee, G Basile, M Acosta, G Scott, C Roskelley, E E Medrano, M Linskens, I Rubelj, and O Pereira-Smith. A biomarker that identifies senescent human cells in culture and in aging skin in vivo. *Proceedings of the National Academy of Sciences of the United States of America*, 92(20):9363–67, sep 1995.
- [89] Aaron W James. Review of Signaling Pathways Governing MSC Osteogenic and Adipogenic Differentiation. *Scientifica*, 2013:684736, 2013.
- [90] R K Jaiswal, N Jaiswal, S P Bruder, G Mbalaviele, D R Marshak, and M F Pittenger. Adult human mesenchymal stem cell differentiation to the osteogenic or adipogenic lineage is regulated by mitogen-activated protein kinase. *The Journal of biological chemistry*, 275(13):9645–52, mar 2000.
- [91] Amjad Javed, Haiyan Chen, and Farah Y Ghori. Genetic and transcriptional control of bone formation. *Oral and maxillofacial surgery clinics of North America*, 22(3):283–93, aug 2010.
- [92] C Kasperk, J Wergedal, D Strong, J Farley, K Wangerin, H Gropp, R Ziegler, and D J Baylink. Human bone cell phenotypes differ depending on their skeletal site of origin. *The Journal of clinical endocrinology and metabolism*, 80(8):2511–7, aug 1995.
- [93] F Barry, R E Boynton, B Liu, and J M Murphy. Chondrogenic differentiation of mesenchymal stem cells from bone marrow: differentiation-dependent gene expression of matrix components. *Experimental cell research*, 268(2):189–200, 2001.

- [94] Evan D Rosen. The transcriptional basis of adipocyte development. *Prostaglandins, Leukotrienes, and Essential Fatty Acids*, 73(1):31–4, jul 2005.
- [95] Shih-Chieh Hung, Ching-Fang Chang, Hsiao-Li Ma, Tain-Hsiung Chen, and Larry Low-Tone Ho. Gene expression profiles of early adipogenesis in human mesenchymal stem cells. *Gene*, 340(1):141–50, 2004.
- [96] J B Kim and B M Spiegelman. ADD 1/SREBP1 promotes adipocyte differentiation and gene expression linked to fatty acid metabolism. *Genes and Development*, 10:1096–1107, 1996.
- [97] T. Shan, W. Liu, and S. Kuang. Fatty acid binding protein 4 expression marks a population of adipocyte progenitors in white and brown adipose tissues. *The FASEB Journal*, 27(1):277–287, oct 2012.
- [98] Alan Trounson and Courtney McDonald. Stem Cell Therapies in Clinical Trials: Progress and Challenges. *Cell Stem Cell*, 17(1):11–22, 2015.
- [99] Amy M Dimarino, Arnold I Caplan, and Tracey L Bonfield. Mesenchymal stem cells in tissue repair. *Frontiers in immunology*, 4:201, jan 2013.
- [100] Benedetto Sacchetti, Alessia Funari, Stefano Michienzi, Silvia Di Cesare, Stefania Piersanti, Isabella Saggio, Enrico Tagliafico, Stefano Ferrari, Pamela Gehron Robey, Mara Riminucci, and Paolo Bianco. Self-Renewing Osteoprogenitors in Bone Marrow Sinusoids Can Organize a Hematopoietic Microenvironment. *Cell*, 131(2):324–336, 2007.
- [101] Chae Woon Park, Keun-Soo Kim, Sohyun Bae, Hye Kyeong Son, Pyung-Keun Myung, Hyo Jeong Hong, and Hyeon Kim. Cytokine secretion profiling of human mesenchymal stem cells by antibody array. *International Journal of Stem Cells*, 2(1):59–68, 2009.
- [102] Yan Yao, Ji Huang, Yongjian Geng, Haiyan Qian, Fan Wang, Xiaohui Liu, Meisheng Shang, Shaoping Nie, Nian Liu, Xin Du, Jianzeng Dong, and Changsheng Ma. Paracrine Action of Mesenchymal Stem Cells Revealed by Single Cell Gene Profiling in Infarcted Murine Hearts. *Plos One*, 10(6):e0129164, 2015.
- [103] Günter Lepperdinger. Inflammation and mesenchymal stem cell aging. *Current opinion in immunology*, 23(4):518–24, aug 2011.
- [104] Simón Méndez-Ferrer, Tatyana V Michurina, Francesca Ferraro, Amin R Mazloom, Ben D Macarthur, Sergio a Lira, David T Scadden, Avi Ma’ayan, Grigori N Enikolopov, and Paul S Frenette. Mesenchymal and haematopoietic stem cells form a unique bone marrow niche. *Nature*, 466(7308):829–834, 2010.
- [105] Eric Bey, Marie Prat, Patrick Duhamel, Marc Benderitter, Michel Brachet, François Trompier, Pierre Battaglini, Isabelle Ernou, Laetitia Boutin, Muriel Gourven, Frédérique Tissedre, Sandrine Créa, Cédric Ait Mansour, Thierry De Revel, Hervé Carsin, Patrick Gourmelon, and Jean Jacques Lataillade. Emerging therapy for improving wound repair of severe radiation burns using local bone marrow-derived stem cell administrations. *Wound Repair and Regeneration*, 18(1):50–58, 2010.
- [106] T Shane Johnson, Anne C O’Neill, Pejman M Motarjem, Jamal Nazzal, Mark Randolph, and Jonathan M Winograd. Tumor formation following murine neural precursor cell transplantation in a rat peripheral nerve injury model. *Journal of reconstructive microsurgery*, 24(8):545–50, nov 2008.

BIBLIOGRAPHY

- [107] Antoine E Karnoub, Ajeeta B Dash, Annie P Vo, Andrew Sullivan, Mary W Brooks, George W Bell, Andrea L Richardson, Kornelia Polyak, Ross Tubo, and Robert a Weinberg. Mesenchymal stem cells within tumour stroma promote breast cancer metastasis. *Nature*, 449(7162):557–563, 2007.
- [108] Makiko Ono, Nobuyoshi Kosaka, Naoomi Tominaga, Yusuke Yoshioka, Fumitaka Takeshita, Ryou-U Takahashi, Masayuki Yoshida, Hitoshi Tsuda, Kenji Tamura, and Takahiro Ochiya. Exosomes from bone marrow mesenchymal stem cells contain a microRNA that promotes dormancy in metastatic breast cancer cells. *Science Signaling*, 7(332):ra63, 2014.
- [109] J C Estrada, Y Torres, A Benguría, A Dopazo, E Roche, L Carrera-Quintanar, R A Pérez, J A Enríquez, R Torres, J C Ramírez, E Samper, and A Bernad. Human mesenchymal stem cell-replicative senescence and oxidative stress are closely linked to aneuploidy. *Cell death & disease*, 4(e691), 2013.
- [110] Melissa A Baxter, Robert F Wynn, Simon N Jowitt, J Ed Wraith, Leslie J Fairbairn, and Ilaria Bellantuono. Study of telomere length reveals rapid aging of human marrow stromal cells following in vitro expansion. *Stem cells*, 22(5):675–682, 2004.
- [111] A Banfi, G Bianchi, R Notaro, L Luzzatto, R Cancedda, and R Quarto. Replicative aging and gene expression in long-term cultures of human bone marrow stromal cells. *Tissue Eng*, 8(6):901–910, 2002.
- [112] Karin Stenderup, Jeannette Justesen, Christian Clausen, and Moustapha Kassem. Aging is associated with decreased maximal life span and accelerated senescence of bone marrow stromal cells. *Bone*, 33:919–926, 2003.
- [113] Hanchen Li, Xueli Fan, Ramesh C. Kovi, Yunju Jo, Brian Moquin, Richard Konz, Calin Stoicov, Evelyn Kurt-Jones, Steven R. Grossman, Steven Lyle, Arlin B. Rogers, Marshall Montrose, and JeanMarie Houghton. Spontaneous expression of embryonic factors and p53 point mutations in aged mesenchymal stem cells: A model of age-related tumorigenesis in mice. *Cancer Research*, 67(22):10889–10898, 2007.
- [114] W J C Rombouts and R E Ploemacher. Primary murine MSC show highly efficient homing to the bone marrow but lose homing ability following culture. *Leukemia*, 17(1):160–70, 2003.
- [115] Toren Finkel, Manuel Serrano, and Maria Blasco. The common biology of cancer and ageing. *Nature*, 448(7155):767–74, 2007.
- [116] C Eng, F P Li, D H Abramson, R M Ellsworth, F L Wong, M B Goldman, J Seddon, N Tarbell, and J D Boice. Mortality from 2nd Tumors among Long-Term Survivors of Retinoblastoma. *Journal of the National Cancer Institute*, 85(14):1121–28, 1993.
- [117] S P Chellappan, S Hiebert, M Mudryj, J M Horowitz, and J R Nevins. The E2F transcription factor is a cellular target for the RB protein. *Cell*, 65(6):1053–61, jun 1991.
- [118] X Zhu, J M Dunn, A D Goddard, J A Squire, A Becker, R A Phillips, and B L Gallie. Mechanisms of loss of heterozygosity in retinoblastoma. *Cytogenetics and cell genetics*, 59(4):248–52, jan 1992.
- [119] Kyung In Woo and J William Harbour. Review of 676 second primary tumors in patients with retinoblastoma: association between age at onset and tumor type. *Archives of Ophthalmology*, 128(7):865–70, jul 2010.

BIBLIOGRAPHY

- [120] Courtney H Coschi, Charles A Ishak, David Gallo, Aren Marshall, Srikanth Talluri, Jianxin Wang, Matthew J Cecchini, Alison L Martens, Vanessa Percy, Ian Welch, Paul C Boutros, Grant W Brown, and Frederick A Dick. Haploinsufficiency of an RB-E2F1-Condensin II complex leads to aberrant replication and aneuploidy. *Cancer discovery*, 4(7):840–53, jul 2014.
- [121] Iria Gonzalez-Vasconcellos, Natasa Anastasov, Bahar Sanli-Bonazzi, Olena Klymenko, Michael J. Atkinson, and Michael Rosemann. Rb1 haploinsufficiency promotes telomere attrition and radiation-induced genomic instability. *Cancer Research*, 73(14):4247–4255, 2013.
- [122] Eugene C Lin. Radiation risk from medical imaging. *Mayo Clinic Proceedings*, 85(12):1142–46, 2010.
- [123] Maurice Tubiana, Jean Dutrix, Andre Wambersie, and D.R. Bewley. *Introduction to Radiobiology*. Taylor & Francis Ltd, UK, 1 edition edition, 1990.
- [124] Eric J Hall. *Radiobiology for the Radiologist*. Harper & Row publishers, second edi edition, 1978.
- [125] Kevin M. Prise and Anna Saran. Concise review: Stem cell effects in radiation risk. *Stem Cells*, 29(9):1315–1321, 2011.
- [126] Ricardo Pardal, Michael F Clarke, and Sean J Morrison. Applying the principles of stem-cell biology to cancer. *Nature Reviews Cancer*, 3(12):895–902, 2003.
- [127] Mykyta Sokolov and Ronald Neumann. Lessons learned about human stem cell responses to ionizing radiation exposures: A long road still ahead of us. *International Journal of Molecular Sciences*, 14:15695–15723, 2013.
- [128] Tara Sugrue, James A L Brown, Noel F. Lowndes, and Rhodri Ceredig. Multiple facets of the DNA damage response contribute to the radioresistance of mouse mesenchymal stromal cell lines. *Stem Cells*, 31(1):137–145, 2013.
- [129] Munira Kadhim, Sisko Salomaa, Eric Wright, Guido Hildebrandt, Oleg V Belyakov, Kevin M Prise, and Mark P Little. Non-targeted effects of ionising radiation-implications for low dose risk. *Mutation Research*, 752(1):84–98, 2013.
- [130] P A Sotiropoulou, A Candi, G Mascré, S De Clercq, K K Youssef, G Lapouge, E Dahl, C Semeraro, G Denecker, J C Marine, and C Blanpain. Bcl-2 and accelerated DNA repair mediates resistance of hair follicle bulge stem cells to DNA-damage-induced cell death. *Nature Cell Biology*, 12(6):572–582, 2010.
- [131] J B Little. Cellular effects of ionizing radiation. *The New England journal of medicine*, 278(7):369–76 concl, feb 1968.
- [132] Adrian L. Harris. Hypoxia a Key Regulatory Factor in Tumour Growth. *Nature Reviews Cancer*, 2(1):38–47, 2002.
- [133] A Di Leonardo, S P Linke, K Clarkin, and G M Wahl. DNA damage triggers a prolonged p53-dependent G1 arrest and long-term induction of Cip1 in normal human fibroblasts. *Genes & development*, 8(21):2540–51, nov 1994.
- [134] Zhiyong Mao, Zhonghe Ke, Vera Gorbunova, and Andrei Seluanov. Replicatively senescent cells are arrested in G1 and G2 phases. *Aging*, 4(6):431–435, 2012.
- [135] Barbara Hampel, Florence Malisan, Harald Niederegger, Roberto Testi, and Pidder Jansen-Dürr. Differential regulation of apoptotic cell death in senescent human cells. *Experimental gerontology*, 39(11-12):1713–21, jan 2004.

- [136] D N Shelton, E Chang, P S Whittier, D Choi, and W D Funk. Microarray analysis of replicative senescence. *Current biology : CB*, 9(17):939–45, sep 1999.
- [137] Anita Brandl, Matthias Meyer, Volker Bechmann, Michael Nerlich, and Peter Angele. Oxidative stress induces senescence in human mesenchymal stem cells. *Experimental Cell Research*, 317(11):1541–1547, 2011.
- [138] P A Riley. Free radicals in biology: oxidative stress and the effects of ionizing radiation. *International Journal of Radiation Biology*, 65(1):27–33, 1994.
- [139] H Castro-Malaspina, R E Gay, G Resnick, N Kapoor, P Meyers, D Chiarieri, S McKenzie, H E Broxmeyer, and M A Moore. Characterization of human bone marrow fibroblast colony-forming cells (CFU-F) and their progeny. *Blood*, 56(2):289–301, aug 1980.
- [140] Nicolaas A P Franken, Hans M Rodermond, Jan Stap, Jaap Haveman, and Chris van Bree. Clonogenic assay of cells in vitro. *Nature Protocols*, 1(5):2315–19, 2006.
- [141] Ivana Rosova, Mo Dao, Ben Capoccia, Daniel Link, and Jan a. Nolte. Hypoxic Preconditioning Results in Increased Motility and Improved Therapeutic Potential of Human Mesenchymal Stem Cells. *Stem Cells*, 26(8):2173–2182, 2008.
- [142] Iria Gonzalez-Vasconcellos, Tanja Domke, Virginija Kuosaite, Irene Esposito, Bahar Sanli-Bonazzi, Michaela Nathrath, Michael J Atkinson, and Michael Rosemann. Differential effects of genes of the Rb1 signalling pathway on osteosarcoma incidence and latency in alpha-particle irradiated mice. *Radiation and environmental biophysics*, 50(1):135–41, mar 2011.
- [143] Masoud Soleimani and Samad Nadri. A protocol for isolation and culture of mesenchymal stem cells from mouse bone marrow. *Nature protocols*, 4(1):102–6, jan 2009.
- [144] W Giaretti and M Nüsse. Light scatter of isolated cell nuclei as a parameter discriminating the cell-cycle subcompartments. *Methods in cell biology*, 41:389–400, jan 1994.
- [145] R B Helling, H M Goodman, and H W Boyer. Analysis of endonuclease R-EcoRI fragments of DNA from lambdaoid bacteriophages and other viruses by agarose-gel electrophoresis. *Journal of virology*, 14(5):1235–44, nov 1974.
- [146] Nathan O'Callaghan, Varinderpal Dhillon, Philip Thomas, and Michael Fenech. A quantitative real-time PCR method for absolute telomere length. *BioTechniques*, 44(6):807–9, may 2008.
- [147] K J Livak and T D Schmittgen. Analysis of relative gene expression data using real-time quantitative PCR and the 2(-Delta Delta C(T)) Method. *Methods*, 25(4):402–8, dec 2001.
- [148] R S SIFFERT. The role of alkaline phosphatase in osteogenesis. *The Journal of experimental medicine*, 93(5):415–26, may 1951.
- [149] Juan José Barcia. The Giemsa stain: its history and applications. *International journal of surgical pathology*, 15(3):292–6, jul 2007.
- [150] Shengkun Sun, Zikuan Guo, Xuren Xiao, Bing Liu, Xiaodan Liu, Pei-Hsien Tang, and Ning Mao. Isolation of mouse marrow mesenchymal progenitors by a novel and reliable method. *Stem Cells*, 21(5):527–35, jan 2003.
- [151] J Takeda, S Seino, and G I Bell. Human Oct3 gene family: cDNA sequences, alternative splicing, gene organization, chromosomal location, and expression at low levels in adult tissues. *Nucleic acids research*, 20(17):4613–20, sep 1992.

- [152] Zhilong Li, Chenxiong Liu, Zhenhua Xie, Pengyue Song, Robert C H Zhao, Ling Guo, Zhigang Liu, and Yaojiong Wu. Epigenetic dysregulation in mesenchymal stem cell aging and spontaneous differentiation. *PloS one*, 6(6):e20526, jan 2011.
- [153] Eiichiro Nagata, Hongbo R Luo, Adolfo Saiardi, Byoung-Il Bae, Norihiro Suzuki, and Solomon H Snyder. Inositol hexakisphosphate kinase-2, a physiologic mediator of cell death. *The Journal of Biological Chemistry*, 280(2):1634–40, jan 2005.
- [154] I H Park, K H Kim, H K Choi, J S Shim, S Y Whang, S J Hahn, O J Kwon, and I H Oh. Constitutive stabilization of hypoxia-inducible factor alpha selectively promotes the self-renewal of mesenchymal progenitors and maintains mesenchymal stromal cells in an undifferentiated state. *Experimental & Molecular Medicine*, 45(9):e44, 2013.
- [155] R Schofield. The relationship between the spleen colony-forming cell and the haemopoietic stem cell. *Blood cells*, 4(1-2):7–25, jan 1978.
- [156] Ahmed Mohyeldin, Tomás Garzón-Muvdi, and Alfredo Quiñones-Hinojosa. Oxygen in stem cell biology: a critical component of the stem cell niche. *Cell Stem Cell*, 7(2):150–61, aug 2010.
- [157] Songtao Shi and Stan Gronthos. Perivascular niche of postnatal mesenchymal stem cells in human bone marrow and dental pulp. *Journal of Bone and Mineral Research*, 18(4):696–704, 2003.
- [158] Mihaela Crisan, Solomon Yap, Louis Casteilla, Chien Wen Chen, Mirko Corselli, Tea Soon Park, Gabriella Andriolo, Bin Sun, Bo Zheng, Li Zhang, Cyrille Norotte, Pang Ning Teng, Jeremy Traas, Rebecca Schugar, Bridget M. Deasy, Stephen Badylak, Hans J??rg Buhning, Jean Paul Giacobino, Lorenza Lazzari, Johnny Huard, and Bruno Peault. A Perivascular Origin for Mesenchymal Stem Cells in Multiple Human Organs. *Cell Stem Cell*, 3(3):301–313, 2008.
- [159] Jonathan S Harrison, Pranela Rameshwar, Vicotr Chang, and Persis Bandari. Oxygen saturation in the bone marrow of healthy volunteers. *Blood*, 99(1):394, jan 2002.
- [160] M. Pasarica, O. R. Sereda, L. M. Redman, D. C. Albarado, D. T. Hymel, L. E. Roan, J. C. Rood, D. H. Burk, and S. R. Smith. Reduced Adipose Tissue Oxygenation in Human Obesity: Evidence for Rarefaction, Macrophage Chemotaxis, and Inflammation Without an Angiogenic Response. *Diabetes*, 58(3):718–725, dec 2008.
- [161] D P Lennon, J M Edmison, and a I Caplan. Cultivation of rat marrow-derived mesenchymal stem cells in reduced oxygen tension: effects on in vitro and in vivo osteochondrogenesis. *Journal of cellular physiology*, 187(3):345–355, 2001.
- [162] Christine Fehrer, Regina Brunauer, Gerhard Laschober, Hermann Unterluggauer, Stephan Reitingner, Frank Kloss, Christian G?lly, Robert Gaßner, and G?nter Lepperdinger. Reduced oxygen tension attenuates differentiation capacity of human mesenchymal stem cells and prolongs their lifespan. *Aging Cell*, 6(6):745–757, 2007.
- [163] J C Estrada, C Albo, A Benguría, A Dopazo, P López-Romero, L Carrera-Quintanar, E Roche, E P Clemente, J A Enríquez, A Bernad, and E Samper. Culture of human mesenchymal stem cells at low oxygen tension improves growth and genetic stability by activating glycolysis. *Cell death and differentiation*, 19(5):743–55, 2012.
- [164] Maximilian Michael Saller, Wolf Christian Prall, Denitsa Docheva, Veronika Schoenitzer, Tzvetan Popov, David Anz, Hauke Clausen-Schaumann, Wolf Mutschler, Elias Volkmer, Matthias Schieker, and Hans Polzer. Increased stemness and migration of human mesenchymal stem cells in hypoxia is associated with altered integrin expression. *Biochemical and Biophysical Research Communications*, 423(2):379–85, 2012.

- [165] C Holzwarth, M Vaegler, F Gieseke, S M Pfister, R Handgretinger, G Kerst, and I Muller. Low physiologic oxygen tensions reduce proliferation and differentiation of human multipotent mesenchymal stromal cells. *BMC Cell Biol*, 11(11), 2010.
- [166] Eun Kyoung Jun, Qiankun Zhang, Byung Sun Yoon, Jai Hee Moon, Gilju Lee, Gyuman Park, Phil Jun Kang, Jung Han Lee, Aree Kim, and Seungkwon You. Hypoxic conditioned medium from human amniotic fluid-derived mesenchymal stem cells accelerates skin wound healing through TGF- β /SMAD2 and PI3K/Akt pathways. *International Journal of Molecular Sciences*, 15(1):605–628, 2014.
- [167] B Ranera, A R Remacha, S Alvarez-Arguedas, A Romero, F J Vazquez, P Zaragoza, I Martin-Burriel, and C Rodellar. Effect of hypoxia on equine mesenchymal stem cells derived from bone marrow and adipose tissue. *BMC Vet Res*, 8(1):142, 2012.
- [168] A L Jackson and L A Loeb. The contribution of endogenous sources of DNA damage to the multiple mutations in cancer. *Mutation research*, 477(1-2):7–21, jun 2001.
- [169] A B Pardee. G1 events and regulation of cell proliferation. *Science*, 246(4930):603–8, nov 1989.
- [170] Hongjuan Cui, Jun Ma, Jane Ding, Tai Li, Goleeta Alam, and Han Fei Ding. Bmi-1 regulates the differentiation and clonogenic self-renewal of I-type neuroblastoma cells in a concentration-dependent manner. *Journal of Biological Chemistry*, 281(45):34696–34704, 2006.
- [171] Francisco Dos Santos, Pedro Z. Andrade, Joana S. Boura, Manuel M. Abecasis, Cláudia Lobato Da Silva, and Joaquim M S Cabral. Ex vivo expansion of human mesenchymal stem cells: A more effective cell proliferation kinetics and metabolism under hypoxia. *Journal of Cellular Physiology*, 223(1):27–35, 2010.
- [172] Lisa B Boyette, Olivia A Creasey, Lynda Guzik, Thomas Lozito, and Rocky S Tuan. Human bone marrow-derived mesenchymal stem cells display enhanced clonogenicity but impaired differentiation with hypoxic preconditioning. *Stem cells translational medicine*, 3(2):241–54, 2014.
- [173] Siddaraju Boregowda, Veena Krishnappa, Jeremy Chambers, Phillip V Lograsso, Wen-tzu Lai, Luis a Ortiz, and Donald G Phinney. Atmospheric oxygen inhibits growth and differentiation of marrow-derived mouse mesenchymal stem cells via a p53 dependent mechanism: implications for long-term culture expansion. *Stem Cells*, 30(5):975–987, 2012.
- [174] Martin Ott, Vladimir Gogvadze, Sten Orrenius, and Boris Zhivotovsky. Mitochondria, oxidative stress and cell death. *Apoptosis : an international journal on programmed cell death*, 12(5):913–22, may 2007.
- [175] Tara Sugrue, Noel F Lowndes, and Rhodri Ceredig. Hypoxia enhances the radioresistance of mouse mesenchymal stromal cells. *Stem Cells*, 32(8):2188–200, aug 2014.
- [176] Maria Ester Bernardo, Nadia Zaffaroni, Francesca Novara, Angela Maria Cometa, Maria Antonietta Avanzini, Antonia Moretta, Daniela Montagna, Rita Maccario, Raffaella Villa, Maria Grazia Daidone, Orsetta Zuffardi, and Franco Locatelli. Human bone marrow-derived mesenchymal stem cells do not undergo transformation after long-term in vitro culture and do not exhibit telomere maintenance mechanisms. *Cancer Research*, 67(19):9142–49, 2007.
- [177] O. Toussaint, E. E. Medrano, and T. Von Zglinicki. Cellular and molecular mechanisms of stress-induced premature senescence (SIPS) of human diploid fibroblasts and melanocytes. *Experimental Gerontology*, 35(8):927–945, 2000.

- [178] Jana Cmielova, Radim Havelek, Tomas Soukup, Alena Jiroutová, Benjamin Visek, Jakub Suchánek, Jirina Vavrova, Jaroslav Mokry, Darina Muthna, Lenka Bruckova, Stanislav Filip, Denis English, and Martina Rezacova. Gamma radiation induces senescence in human adult mesenchymal stem cells from bone marrow and periodontal ligaments. *International Journal of Radiation Biology*, 88(5):393–404, 2012.
- [179] Ines Höfig, Yashodhara Ingawale, Michael J Atkinson, Heidi Hertlein, Peter J Nelson, and Michael Rosemann. p53-Dependent Senescence in Mesenchymal Stem Cells under Chronic Normoxia Is Potentiated by Low-Dose γ -Irradiation. *Stem cells international*, 2016:6429853, 2016.
- [180] Jing Hu, Hassan Nakhla, and Eileen Friedman. Transient arrest in a quiescent state allows ovarian cancer cells to survive suboptimal growth conditions and is mediated by both Mirk/dyrk1b and p130/RB2. *International Journal of Cancer*, 129(2):307–318, 2011.
- [181] Pranela Rameshwar. Breast cancer cell dormancy in bone marrow: potential therapeutic targets within the marrow microenvironment. *Expert Review of Anticancer Therapy*, 10(2):129–32, 2010.
- [182] Nedime Serakinci, Rikke Christensen, Jesper Graakjaer, Claire J. Cairney, W. Nicol Keith, Jan Alsner, Gabriele Saretzki, and Steen Kolvraa. Ectopically hTERT expressing adult human mesenchymal stem cells are less radiosensitive than their telomerase negative counterpart. *Experimental Cell Research*, 313(5):1056–1067, 2007.
- [183] O Katoh, H Tauchi, K Kawaishi, A Kimura, and Y Satow. Expression of the vascular endothelial growth factor (VEGF) receptor gene, KDR, in hematopoietic cells and inhibitory effect of VEGF on apoptotic cell death caused by ionizing radiation. *Cancer Research*, 55(23):5687–5692, 1995.
- [184] Aimin Meng, Yong Wang, Gary Van Zant, and Daohong Zhou. Ionizing Radiation and Busulfan Induce Premature Senescence in Murine Bone Marrow Hematopoietic Cells. *Cancer Research*, 63(17):5414–5419, 2003.
- [185] Miao-Fen Chen, Ching-Tai Lin, Wen-Cheng Chen, Cheng-Ta Yang, Chih-Cheng Chen, Shuen-Kuei Liao, Jacqueline Ming Liu, Chang-Hsien Lu, and Kuan-Der Lee. The sensitivity of human mesenchymal stem cells to ionizing radiation. *International journal of radiation oncology, biology, physics*, 66(1):244–53, sep 2006.
- [186] Nils H. Nicolay, Eva Sommer, Ramon Lopez, Ute Wirkner, Thuy Trinh, Sonevisay Sisombath, Jürgen Debus, Anthony D. Ho, Rainer Saffrich, and Peter E. Huber. Mesenchymal stem cells retain their defining stem cell characteristics after exposure to ionizing radiation. *International Journal of Radiation Oncology Biology Physics*, 87(5):1171–1178, 2013.
- [187] Áine M. Prendergast, Séverine Cruet-Hennequart, Georgina Shaw, Frank P. Barry, and Michael P. Carty. Activation of DNA damage response pathways in human mesenchymal stem cells exposed to cisplatin or γ -irradiation. *Cell Cycle*, 10(21):3768–3777, 2011.
- [188] Federico Mussano, Kenneth J Lee, Patricia Zuk, Lisa Tran, Nicholas A Cacalano, Anahid Jewett, Stefano Carossa, and Ichiro Nishimura. Differential effect of ionizing radiation exposure on multipotent and differentiation-restricted bone marrow mesenchymal stem cells. *Journal of Cellular Biochemistry*, 111(2):322–32, oct 2010.
- [189] R Havelek, T Soukup, J Čmielová, M Seifrtová, J Suchánek, J Vávrová, J Mokrý, D Muthná, and M ezáčová. Ionizing Radiation Induces Senescence and Differentiation of Human Dental Pulp Stem Cells. *Folia Biologica (Praha)*, 59(5):188–97, 2013.

- [190] Agata Małkiewicz and Magdalena Dzedzic. Bone marrow reconversion - imaging of physiological changes in bone marrow. *Polish journal of radiology / Polish Medical Society of Radiology*, 77(4):45–50, 2012.
- [191] David K W Yeung, James F Griffith, Gregory E Antonio, Francis K H Lee, Jean Woo, and Ping C Leung. Osteoporosis is associated with increased marrow fat content and decreased marrow fat unsaturation: a proton MR spectroscopy study. *Journal of Magnetic Resonance Imaging: JMRI*, 22(2):279–85, aug 2005.
- [192] Sergiu Botolin and Laura R. McCabe. Bone loss and increased bone adiposity in spontaneous and pharmacologically induced diabetic mice. *Endocrinology*, 148(1):198–205, 2007.
- [193] Gavin W Roddy, Joo Youn Oh, Ryang Hwa Lee, Thomas J Bartosh, Joni Ylostalo, Katie Coble, Robert H Rosa, and Darwin J Prockop. Action at a distance: systemically administered adult stem/progenitor cells (MSCs) reduce inflammatory damage to the cornea without engraftment and primarily by secretion of TNF- α stimulated gene/protein 6. *Stem cells (Dayton, Ohio)*, 29(10):1572–9, oct 2011.
- [194] Ryang Hwa Lee, Andrey A Pulin, Min Jeong Seo, Daniel J Kota, Joni Ylostalo, Benjamin L Larson, Laura Semprun-Prieto, Patrice Delafontaine, and Darwin J Prockop. Intravenous hMSCs improve myocardial infarction in mice because cells embolized in lung are activated to secrete the anti-inflammatory protein TSG-6. *Cell stem cell*, 5(1):54–63, jul 2009.
- [195] Xiaobing Fu, Bing Han, Sa Cai, Yonghong Lei, Tongzhu Sun, and Zhiyong Sheng. Migration of bone marrow-derived mesenchymal stem cells induced by tumor necrosis factor- α and its possible role in wound healing. *Wound Repair and Regeneration*, 17(2):185–191, 2009.
- [196] Yahaira Naaldijk, Adiv A. Johnson, Stefan Ishak, Hans Jörg Meisel, Christian Hohaus, and Alexandra Stolzing. Migrational changes of mesenchymal stem cells in response to cytokines, growth factors, hypoxia, and aging. *Experimental Cell Research*, 338(1):97–104, 2015.
- [197] A O'Brien-Ladner, M E Nelson, B F Kimler, and L J Wesselius. Release of interleukin-1 by human alveolar macrophages after in vitro irradiation. *Radiation research*, 136(1):37–41, oct 1993.
- [198] Jamunarani Veeraraghavan, Mohan Natarajan, Sheeja Aravindan, Terence S Herman, and Natarajan Aravindan. Radiation-triggered tumor necrosis factor (TNF) alpha-NFkappaB cross-signaling favors survival advantage in human neuroblastoma cells. *The Journal of biological chemistry*, 286(24):21588–600, jun 2011.
- [199] Anne-Mari Håkelién, Jan Christian Bryne, Kristine G Harstad, Susanne Lorenz, Jonas Paulsen, Jinchang Sun, Tarjei S Mikkelsen, Ola Myklebost, and Leonardo A Meza-Zepeda. The regulatory landscape of osteogenic differentiation. *Stem cells*, 32(10):2780–93, oct 2014.
- [200] Chad M Teven, Xing Liu, Ning Hu, Ni Tang, Stephanie H Kim, Enyi Huang, Ke Yang, Mi Li, Jian-Li Gao, Hong Liu, Ryan B Natale, Gaurav Luther, Qing Luo, Linyuan Wang, Richard Rames, Yang Bi, Jinyong Luo, Hue H Luu, Rex C Haydon, Russell R Reid, and Tong-Chuan He. Epigenetic regulation of mesenchymal stem cells: a focus on osteogenic and adipogenic differentiation. *Stem Cells International*, 2011:201371, 2011.

Abbreviations

°C	Degree Celsius
γ-rays	Gamma rays
μg	Microgram
μl	Microlitre
Alpl	Alkaline phosphatase
ASC	Adult stem cell
AU	Arbitrary units
Bmi1	Bmi1 polycomb ring finger oncogene
Cebpa	CCAAT/enhancer-binding protein alpha
cDNA	Complementary DNA
CFU-F	Colony-forming unit-fibroblastic
C _T	Threshold cycle
DNA	Deoxyribonucleic acid
ESC	Embryonic stem cell
Fabp4	Fatty acid binding protein 4
FBS	Fetal bovine serum
FCS	Fetal calf serum
FLICA	Fluorescent inhibitor of caspases
g	Gram
Gy	Gray
h	Hour
hESC	Human embryonic stem cell

hMSC	Human mesenchymal stem cell
iPSC	Induced pluripotent Stem Cell
Klf4	Kruppel-like factor 4
l	Litre
Lpl	Lipoprotein lipase
M	Molar
mESC	Murine embryonic stem cell
mg	Milligram
mGy	Milligray
Min	minute
ml	Millilitre
mM	Millimolar
mMSC	Murine mesenchymal stem cell
MSC	Mesenchymal stem cell
mSV	Millisievert
Nanog	Nanog homeobox
Nes	Nestin
ng	Nanogram
NTC	No template control
PCR	Polymerase chain reaction
pmol	Picomolar
Pou5f1	POU class 5 homeobox 1
Pparg	Peroxisome proliferator-activated receptor gamma
RB	Retinoblastoma
Real-Time PCR	Real-time polymerase chain reaction
RNA	Ribonucleic acid
RT	Room temperature
RT-PCR	Reverse transcription-polymerase chain reaction

NTC	No template control
Runx2	Runt related transcription factor 2
SA- β -gal	Senescent associated- β -galactosidase
SC	Stem cell
SEM	Standard error of the mean
SIPS	Stress-induced premature senescence
Sox2	Sex determining region Y-box 2
Srebf1	Sterol regulatory element binding transcription factor 1
Sv	Sievert
TBP	TATA box binding protein

Appendices

Appendix A

Identification of the suitable nutrient mixture for *in vitro* culturing of mMSCs

The bone marrow obtained from $Rb^{+/+}$ and $Rb^{+/-}$ mice was cultured in different media and serum combinations to find out the most suitable nutritional mixture for establishing and maintaining the mMSC culture. Four different kinds of basal medium and supplement mixtures used for examining the mMSC growth *in vitro* are listed in the following table. Seven days after the bone marrow isolation,

Table A.1: List of nutrient mixtures tested for *in vitro* culturing of mMSCs

List of nutrient mixtures tested for <i>in vitro</i> culturing of mMSCs (Basal Medium + FBS/FCS)
DMEM/F-12, GlutaMAX™ + 10% MSC Qualified FBS
Mesenchymal Stem Cell Growth Medium + 10% Supplement Mix
DMEM, low glucose, GlutaMAX™ Supplement, pyruvate + 15% Bio&SELL FCS Gold Plus
DMEM, low glucose, GlutaMAX™ Supplement, pyruvate without FCS

cells cultured in DMEM, low glucose, GlutaMAX™ pyruvate supplemented with 15% FCS lacked a typical spindle-shaped morphology and the culture appeared to be highly heterogeneous with a presence of many round shaped cells floating around (fig. C). In contrast, the cultures from both Mesenchymal Stem Cell Growth Medium (fig. B) and DMEM/F-12, GlutaMAX™ (fig. A) displayed cells with typical fibroblast like morphology and a homogenous culture without many non-adherent cells. The cells growing in DMEM/F-12, GlutaMAX™ displayed higher proliferation and growth on the long-term (around 3-4 weeks after isolation) as compared to Mesenchymal Stem Cell Growth Medium when observed under the microscope. The basal medium DMEM, low glucose, GlutaMAX™ Supplement, pyruvate without any FCS was also tested for mMSC growth. However, the cells failed to grow in the absence of a serum. Therefore, DMEM/F-12, GlutaMAX™ with 10% MSC Qualified

APPENDIX A. IDENTIFICATION OF THE SUITABLE NUTRIENT MIXTURE FOR *IN VITRO*
CULTURING OF MMSCS

FBS (together referred as MSC media) was found to be the most suitable nutrient mixture for further cultivation of mMSCs *in vitro*.

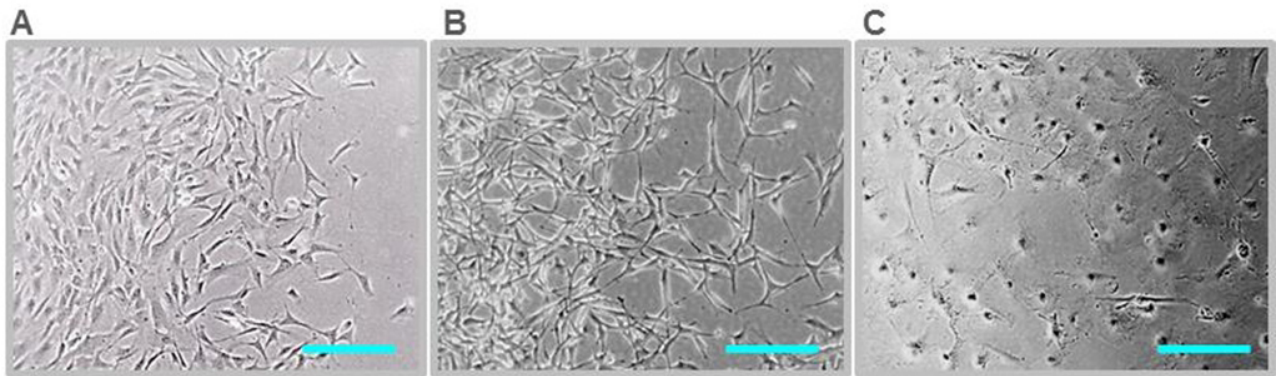


Figure 50: Murine mesenchymal stem cell (mMSCs) culture in different media and serum combinations on day 7 after the explantation. A) mMSCs growing in DMEM/F-12, GlutaMAX™ with 10% MSC Qualified FBS. B) mMSCs growing in Mesenchymal Stem Cell Growth Medium with 10% supplement mix. C) mMSCs growing in DMEM, low glucose, GlutaMAX™ Supplement, pyruvate with 15% FCS Gold Plus. Scale bar: 50 μ m.

Appendix B

List of RT² profiler genes with their corresponding fold change in mMSCs as compared to osteoblasts

Description	Symbol	Fold Up- or Down-Regulation Test MSC /Control Osteoblasts
ATP-binding cassette, sub-family B (MDR/TAP), member 1A	<i>Abcb1a</i>	20.10329845
Activated leukocyte cell adhesion molecule	<i>Alcam</i>	5.027831655
Alanyl (membrane) aminopeptidase	<i>Anpep</i>	4.979916041
Annexin A5	<i>Anxa5</i>	1.237890394
Brain derived neurotrophic factor	<i>Bdnf</i>	1.244315868
Bone gamma carboxyglutamate protein	<i>Bglap</i>	40.32520322
Bone morphogenetic protein 2	<i>Bmp2</i>	20.09054504
Bone morphogenetic protein 4	<i>Bmp4</i>	1.253587344
Bone morphogenetic protein 6	<i>Bmp6</i>	40.38928285
Bone morphogenetic protein 7	<i>Bmp7</i>	40.01986933
Caspase 3	<i>Casp3</i>	-1.619353594
CD44 antigen	<i>Cd44</i>	1.254092933
Collagen, type I, alpha 1	<i>Col1a1</i>	-1.603586028

APPENDIX B. LIST OF RT² PROFILER GENES WITH THEIR CORRESPONDING FOLD CHANGE IN MMSCS AS COMPARED TO OSTEOBLASTS

Description	Symbol	Fold Up- or Down-Regulation Test MSC /Control Osteoblasts
Colony stimulating factor 2 (granulocyte-macrophage)	<i>Csf2</i>	9.966062317
Colony stimulating factor 3 (granulocyte)	<i>Csf3</i>	10.04381176
Catenin (cadherin associated protein), beta 1	<i>Ctnnb1</i>	1.247912258
Epidermal growth factor	<i>Egf</i>	160.7668638
Endoglin	<i>Eng</i>	39.70487721
V-erb-b2 erythroblastic leukemia viral oncogene homolog 2, neuro/glioblastoma derived oncogene homolog (avian)	<i>ErbB2</i>	1.255757013
Fibroblast growth factor 10	<i>Fgf10</i>	1.275932782
Fibroblast growth factor 2	<i>Fgf2</i>	5.007486085
Fucosyltransferase 1	<i>Fut1</i>	159.4945264
Fucosyltransferase 4	<i>Fut4</i>	20.00281964
Frizzled homolog 9 (Drosophila)	<i>Fzd9</i>	20.33849722
Growth differentiation factor 15	<i>Gdf15</i>	2.493018081
Growth differentiation factor 5	<i>Gdf5</i>	39.22787682
Growth differentiation factor 6	<i>Gdf6</i>	20.28226955
Growth differentiation factor 7	<i>Gdf7</i>	20.18895538
General transcription factor III A	<i>Gtf3a</i>	1.272550025
Histone aminotransferase 1	<i>Hat1</i>	-3.210205173
Histone deacetylase 1	<i>Hdac1</i>	2.496841018
Hepatocyte growth factor	<i>Hgf</i>	2.484440323
HNF1 homeobox A	<i>Hnf1a</i>	40.12025797
Intercellular adhesion molecule 1	<i>Icam1</i>	5.064718467
Interferon gamma	<i>Ifng</i>	39.66704796
Insulin-like growth factor 1	<i>Igf1</i>	4.982062827
Interleukin 10	<i>Il10</i>	40.20521487

APPENDIX B. LIST OF RT² PROFILER GENES WITH THEIR CORRESPONDING FOLD CHANGE IN MMSCS AS COMPARED TO OSTEOBLASTS

Description	Symbol	Fold Up- or Down-Regulation Test MSC /Control Osteoblasts
Interleukin 1 beta	<i>Il1b</i>	1367.704521
Interleukin 6	<i>Il6</i>	20.21978062
Insulin II	<i>Ins2</i>	19.89710763
Integrin alpha 6	<i>Itga6</i>	20.12584926
Integrin alpha V	<i>Itgav</i>	2.499113144
Integrin alpha X	<i>Itgax</i>	40.84977251
Integrin beta 1 (fibronectin receptor beta)	<i>Itgb1</i>	1.252442649
Jagged 1	<i>Jag1</i>	2.541734105
K(lysine) acetyltransferase 2B	<i>Kat2b</i>	1.245451488
Kinase insert domain protein receptor	<i>Kdr</i>	19.95443067
Kit ligand	<i>Kitl</i>	2.51846993
Leukemia inhibitory factor	<i>Lif</i>	2.494824917
Melanoma cell adhesion molecule	<i>Mcam</i>	-1.58304602
Microphthalmia-associated transcription factor	<i>Mitf</i>	40.07154204
Matrix metalloproteinase 2	<i>Mmp2</i>	-1.595438213
Nestin	<i>Nes</i>	5.018268847
Nerve growth factor receptor (TNFR superfamily, member 16)	<i>Ngfr</i>	19.95780775
Notch gene homolog 1 (Drosophila)	<i>Notch1</i>	82.82527049
5' nucleotidase, ecto	<i>Nt5e</i>	-1.600908512
Nudix (nucleoside diphosphate linked moiety X)-type motif 6	<i>Nudt6</i>	10.13009316
Platelet derived growth factor receptor, beta polypeptide	<i>Pdgfrb</i>	2.512520311
Phosphatidylinositol glycan anchor biosynthesis, class S	<i>Pigs</i>	2.501050045

APPENDIX B. LIST OF RT² PROFILER GENES WITH THEIR CORRESPONDING FOLD CHANGE IN MMSCS AS COMPARED TO OSTEOBLASTS

Description	Symbol	Fold Up- or Down-Regulation Test MSC /Control Osteoblasts
POU domain, class 5, transcription factor 1	<i>Pou5f1</i>	20.10821599
Peroxisome proliferator activated receptor gamma	<i>Pparg</i>	2.512639896
Prominin 1	<i>Prom1</i>	20.05681414
PTK2 protein tyrosine kinase 2	<i>Ptk2</i>	2.524256757
Protein tyrosine phosphatase, receptor type, C	<i>Ptprc</i>	323.9063708
Ras homolog gene family, member A	<i>Rhoa</i>	-1.586054283
Runt related transcription factor 2	<i>Runx2</i>	1.258000288
Solute carrier family 17 (anion/sugar transporter), member 5	<i>Slc17a5</i>	2.535659127
MAD homolog 4 (Drosophila)	<i>Smad4</i>	-1.596375012
SMAD specific E3 ubiquitin protein ligase 1	<i>Smurf1</i>	2.500874803
SMAD specific E3 ubiquitin protein ligase 2	<i>Smurf2</i>	2.527980538
SRY-box containing gene 2	<i>Sox2</i>	19.87321035
SRY-box containing gene 9	<i>Sox9</i>	-3.116291675
T-box 5	<i>Tbx5</i>	40.43581894
Telomerase reverse transcriptase	<i>Tert</i>	10.04483427
Transforming growth factor, beta 1	<i>Tgfb1</i>	10.01127874
Transforming growth factor, beta 3	<i>Tgfb3</i>	-3.230505084
Thymus cell antigen 1, theta	<i>Thy1</i>	-6.381339447
Tumor necrosis factor	<i>Tnf</i>	80.74044881
Vascular cell adhesion molecule 1	<i>Vcam1</i>	-1.601960768
Vascular endothelial growth factor A	<i>Vegfa</i>	2.490017275
Vimentin	<i>Vim</i>	-1.592073237

APPENDIX B. LIST OF RT² PROFILER GENES WITH THEIR CORRESPONDING FOLD CHANGE IN MMSCS AS COMPARED TO OSTEOLASTS

Description	Symbol	Fold Up- or Down-Regulation Test MSC /Control Osteoblasts
Von Willebrand factor homolog	<i>Vwf</i>	20.19012983
Wingless-related MMTV integration site 3A	<i>Wnt3a</i>	169.0304761
Zinc finger protein 42	<i>Zfp42</i>	39.30902114

Appendix C

List of Genes

Official name	Symbol	Application
5' nucleotidase, ecto	<i>Nt5e</i>	RT ² Profiler PCR Arrays
Activated leukocyte cell adhesion molecule	<i>Alcam</i>	RT ² Profiler PCR Arrays
Alanyl (membrane) aminopeptidase	<i>Anpep</i>	RT ² Profiler PCR Arrays
Alkaline Phosphatase	<i>Alpl</i>	Osteogenic differentiation marker
Annexin A5	<i>Anxa5</i>	RT ² Profiler PCR Arrays
ATP-binding cassette, sub-family B (MDR/TAP), member 1A	<i>Abcb1a</i>	RT ² Profiler PCR Arrays
<i>Bmi1</i> polycomb ring finger oncogene	<i>Bmi1</i>	Stemness and pluripotency marker
Bone gamma carboxyglutamate protein	<i>Bglap</i>	RT ² Profiler PCR Arrays
Bone morphogenetic protein 2	<i>Bmp2</i>	RT ² Profiler PCR Arrays
Bone morphogenetic protein 4	<i>Bmp4</i>	RT ² Profiler PCR Arrays
Bone morphogenetic protein 6	<i>Bmp6</i>	RT ² Profiler PCR Arrays
Bone morphogenetic protein 7	<i>Bmp7</i>	RT ² Profiler PCR Arrays
Brain derived neurotrophic factor	<i>Bdnf</i>	RT ² Profiler PCR Arrays
Caspase 3	<i>Casp3</i>	RT ² Profiler PCR Arrays
Catenin (cadherin associated protein), beta 1	<i>Ctnnb1</i>	RT ² Profiler PCR Arrays
CCAAT/enhancer-binding proteins	<i>Cebpa</i>	Adipogenic differentiation marker
CD44 antigen	<i>Cd44</i>	RT ² Profiler PCR Arrays
Collagen, type I, alpha 1	<i>Col1a1</i>	RT ² Profiler PCR Arrays

APPENDIX C. LIST OF GENES

Official name	Symbol	Application
Colony stimulating factor 2 (granulocyte-macrophage)	<i>Csf2</i>	RT ² Profiler PCR Arrays
Colony stimulating factor 3 (granulocyte)	<i>Csf3</i>	RT ² Profiler PCR Arrays
Endoglin	<i>Eng</i>	RT ² Profiler PCR Arrays
Epidermal growth factor	<i>Egf</i>	RT ² Profiler PCR Arrays
Fatty Acid Binding Protein 4	<i>Fabp4</i>	Adipogenic differentiation marker
Fibroblast growth factor 10	<i>Fgf10</i>	RT ² Profiler PCR Arrays
Fibroblast growth factor 2	<i>Fgf2</i>	RT ² Profiler PCR Arrays
Frizzled homolog 9 (Drosophila)	<i>Fzd9</i>	RT ² Profiler PCR Arrays
Fucosyltransferase 1	<i>Fut1</i>	RT ² Profiler PCR Arrays
Fucosyltransferase 4	<i>Fut4</i>	RT ² Profiler PCR Arrays
General transcription factor III A	<i>Gtf3a</i>	RT ² Profiler PCR Arrays
Growth differentiation factor 15	<i>Gdf15</i>	RT ² Profiler PCR Arrays
Growth differentiation factor5	<i>Gdf5</i>	RT ² Profiler PCR Arrays
Growth differentiation factor 6	<i>Gdf6</i>	RT ² Profiler PCR Arrays
Growth differentiation factor 7	<i>Gdf7</i>	RT ² Profiler PCR Arrays
Hepatocyte growth factor	<i>Hgf</i>	RT ² Profiler PCR Arrays
Histone aminotransferase 1	<i>Hat1</i>	RT ² Profiler PCR Arrays
Histone deacetylase 1	<i>Hdac1</i>	RT ² Profiler PCR Arrays
HNF1 homeobox A	<i>Hnf1a</i>	RT ² Profiler PCR Arrays
Insulin II	<i>Ins2</i>	RT ² Profiler PCR Arrays
Insulin-like growth factor 1	<i>Igf1</i>	RT ² Profiler PCR Arrays
Integrin alpha 6	<i>Itga6</i>	RT ² Profiler PCR Arrays
Integrin alpha V	<i>Itgav</i>	RT ² Profiler PCR Arrays
Integrin alpha X	<i>Itgax</i>	RT ² Profiler PCR Arrays
Integrin beta 1 (fibronectin receptor beta)	<i>Itgb1</i>	RT ² Profiler PCR Arrays
Intercellular adhesion molecule 1	<i>Icam1</i>	RT ² Profiler PCR Arrays

APPENDIX C. LIST OF GENES

Official name	Symbol	Application
Interferon gamma	<i>Ifng</i>	RT ² Profiler PCR Arrays
Interleukin 1 beta	<i>Il1b</i>	RT ² Profiler PCR Arrays
Interleukin 10	<i>Il10</i>	RT ² Profiler PCR Arrays
Interleukin 6	<i>Il6</i>	RT ² Profiler PCR Arrays
Jagged 1	<i>Jag1</i>	RT ² Profiler PCR Arrays
K(lysine) acetyltransferase 2B	<i>Kat2b</i>	RT ² Profiler PCR Arrays
Kinase insert domain protein receptor	<i>Kdr</i>	RT ² Profiler PCR Arrays
Kit ligand	<i>Kitl</i>	RT ² Profiler PCR Arrays
Kruppel-like factor 4	<i>Klf4</i>	Stemness and pluripotency marker
Leukemia inhibitory factor	<i>Lif</i>	RT ² Profiler PCR Arrays
Lipoprotein Lipase	<i>LPI</i>	Adipogenic differentiation marker
MAD homolog 4 (Drosophila)	<i>Smad4</i>	RT ² Profiler PCR Arrays
Matrix metalloproteinase 2	<i>Mmp2</i>	RT ² Profiler PCR Arrays
Melanoma cell adhesion molecule	<i>Mcam</i>	RT ² Profiler PCR Arrays
Microphthalmia-associated transcription factor	<i>Mitf</i>	RT ² Profiler PCR Arrays
<i>Nanog</i> homeobox	<i>Nanog</i>	Stemness and pluripotency marker
Nerve growth factor receptor (TNFR superfamily, member 16)	<i>Ngfr</i>	RT ² Profiler PCR Arrays
Nestin	<i>Nes</i>	RT ² Profiler PCR Arrays, Stemness and pluripotency marker
Notch gene homolog 1 (Drosophila)	<i>Notch1</i>	RT ² Profiler PCR Arrays
Nudix (nucleoside diphosphate linked moiety X)-type motif 6	<i>Nudt6</i>	RT ² Profiler PCR Arrays
Peroxisome proliferator activated receptor gamma	<i>Pparg</i>	RT ² Profiler PCR Arrays, Adipogenic differentiation marker
Phosphatidylinositol glycan anchor biosynthesis, class S	<i>Pigs</i>	RT ² Profiler PCR Arrays
Platelet derived growth factor receptor, beta polypeptide	<i>Pdgfrb</i>	RT ² Profiler PCR Arrays

APPENDIX C. LIST OF GENES

Official name	Symbol	Application
POU domain, class 5, transcription factor 1	<i>Pou5f1</i>	RT ² Profiler PCR Arrays, Stemness and pluripotency marker
Prominin 1	<i>Prom1</i>	RT ² Profiler PCR Arrays
Protein tyrosine phosphatase, receptor type, C	<i>Ptprc</i>	RT ² Profiler PCR Arrays
PTK2 protein tyrosine kinase 2	<i>Ptk2</i>	RT ² Profiler PCR Arrays
Ras homolog gene family, member A	<i>Rhoa</i>	RT ² Profiler PCR Arrays
Runt related transcription factor 2	<i>Runx2</i>	RT ² Profiler PCR Arrays, Osteogenic differentiation marker
SMAD specific E3 ubiquitin protein ligase 1	<i>Smurf1</i>	RT ² Profiler PCR Arrays
SMAD specific E3 ubiquitin protein ligase 2	<i>Smurf2</i>	RT ² Profiler PCR Arrays
Solute carrier family 17 (anion/sugar transporter), member 5	<i>Slc17a5</i>	RT ² Profiler PCR Arrays
SRY-box containing gene 2	<i>Sox2</i>	RT ² Profiler PCR Arrays, Stemness and pluripotency marker
SRY-box containing gene 9	<i>Sox9</i>	RT ² Profiler PCR Arrays
Sterol Regulatory Element-Binding Protein 1	<i>Srebf1</i>	Adipogenic differentiation marker
T-box 5	<i>Tbx5</i>	RT ² Profiler PCR Arrays
Telomerase reverse transcriptase	<i>Tert</i>	RT ² Profiler PCR Arrays
Thymus cell antigen 1, theta	<i>Thy1</i>	RT ² Profiler PCR Arrays
Transforming growth factor, beta 1	<i>Tgfb1</i>	RT ² Profiler PCR Arrays
Transforming growth factor, beta 3	<i>Tgfb3</i>	RT ² Profiler PCR Arrays
Tumor necrosis factor	<i>Tnf</i>	RT ² Profiler PCR Arrays
Vascular cell adhesion molecule 1	<i>Vcam1</i>	RT ² Profiler PCR Arrays
Vascular endothelial growth factor A	<i>Vegfa</i>	RT ² Profiler PCR Arrays
V-erb-b2 erythroblastic leukemia viral oncogene homolog 2, neuro/glioblastoma derived oncogene homolog (avian)	<i>ErbB2</i>	RT ² Profiler PCR Arrays
Vimentin	<i>Vim</i>	RT ² Profiler PCR Arrays
Von Willebrand factor homolog	<i>Vwf</i>	RT ² Profiler PCR Arrays

APPENDIX C. LIST OF GENES

Official name	Symbol	Application
Wingless-related MMTV integration site 3A	<i>Wnt3a</i>	RT ² Profiler PCR Arrays
Zinc finger protein 42	<i>Zfp42</i>	RT ² Profiler PCR Arrays

List of Figures

1	Stem cell	8
2	Mesenchymal stem cell	12
3	Distribution of MSC clinical trials for treatment of various diseases	17
4	Annual mean effective doses of ionizing radiation per person in Germany	19
5	Progression of stem cells to cancer	21
6	Ionizing radiation-induced damage in MSCs	23
7	Isolation of murine mesenchymal stem cells from the mouse bone marrow	41
8	Real-Time PCR amplification plot	50
9	Real-Time PCR melting curve	50
10	Quantification of <i>in vitro</i> differentiated adipocytes	60
11	<i>Rb1</i> and Cre genotyping using the tail tip DNA of F1 mice progeny	67
12	Murine mesenchymal stem cell culture in different oxygen concentrations	68
13	Effect of oxygen concentration on long-term growth of mMSCs	69
14	Multilineage differentiation of <i>in vitro</i> cultured mMSCs	71
15	Immunocytochemistry of CD44 expression on mMSC surface	72
16	Immunocytochemistry of Sca1 expression on mMSC surface	73
17	Flow cytometry analysis of mMSC surface marker expression	74
18	Colony forming ability of mMSCs under hypoxic and normoxic conditions	75
19	Effect of oxygen concentration on colony forming ability of mMSCs	76
20	Cell cycle analysis of hypoxic and normoxic mMSCs	77
21	Percentage of mMSCs present in different phases of the cell cycle on day 7 and 21	78
22	Real-Time PCR expression analysis of stemness and pluripotency marker genes in mMSCs	80
23	Effect of oxygen concentration on telomere length in mMSCs	81
24	Effect of <i>Rb1</i> status on telomere length in mMSCs	82
25	Melting curve analysis of the mMSC sample after Real-Time PCR run with <i>Pou5f1</i> primers	83
26	Agarose gel electrophoresis for the <i>Pou5f1</i> Real-Time PCR product of mMSCs	83
27	Sequence alignment of <i>Pou5f1</i> Real-Time PCR short product on <i>Pou5f1</i> gene	85
28	Relative expression of mMSC specific genes	89
29	Real-Time PCR expression analysis of the ageing genes in mMSCs of different age	92

LIST OF FIGURES

30	Effect of ionizing radiation on the expression profile of the ageing genes in mMSCs of different age	95
31	Colony forming ability of mMSCs after exposure to ionizing radiation	95
32	Effect of ionizing radiation on the colony forming ability of mMSCs under hypoxic and normoxic conditions	96
33	Senescence in mMSCs after exposure to ionizing radiation	97
34	Effect of ionizing radiation on the senescence in mMSCs under hypoxic and normoxic conditions	98
35	Positive controls used for apoptosis assay with Image-iT® LIVE Green Poly Caspases Detection Kit	99
36	Apoptosis in mMSCs after exposure to ionizing radiation	99
37	Effect of ionizing radiation on the apoptosis in mMSCs	100
38	Osteogenic differentiation in mMSCs after exposure to ionizing radiation in presence of lineage inducing growth medium	101
39	Adipogenic differentiation in mMSCs after exposure to ionizing radiation in presence of lineage inducing growth medium	101
40	Osteogenic differentiation in mMSCs after exposure to ionizing radiation in absence of lineage inducing growth medium	102
41	Adipogenic differentiation in mMSCs after exposure to ionizing radiation in absence of lineage inducing growth medium	103
42	Effect of ionizing radiation on adipogenesis in mMSCs in absence of lineage inducing growth medium	104
43	Effect of ionizing radiation on the expression profile of osteogenic lineage marker genes in mMSCs of different age	105
44	Effect of ionizing radiation on the expression profile of adipogenic lineage marker genes in mMSCs of different age	106
45	Effect of ionizing radiation on the expression profile of stemness and pluripotency marker genes in mMSCs of different age	108
46	Bone marrow cryo sections of the whole body irradiate mice	109
47	Effect of ionizing radiation on the number of adipocytes present in the bone marrow cryo sections of the whole body irradiated mice	110
48	Survival response of mMSCs to <i>in vitro</i> hypoxic and normoxic conditions	116
49	A schematic representation of the alterations in gene expression during <i>in vitro</i> mMSC culture	120
50	Murine mesenchymal stem cell (mMSCs) culture in different media and serum combinations on day 7 after the explantation	142

List of Tables

4.1	PCR reaction mixture	45
4.2	PCR reaction program	46
4.3	Reverse transcription reaction mixture	47
4.4	Real-Time PCR reaction mixture	48
4.5	Real-Time PCR reaction program	48
4.6	Immunocytochemistry antibodies for mMSC surface marker expression	54
4.7	Flow cytometry antibodies for mMSC surface marker expression	55
4.8	Reagent preparation for apoptosis assay	57
4.9	PCR reaction program for amplification of <i>Pou5f1</i> transcripts	62
4.10	Ligation mixture for TOPO-TA cloning	63
4.11	Sequencing reaction mixture	64
4.12	Sequencing reaction program	65
5.1	List of proteolytic enzymes tested for subculturing the mMSCs	70
5.2	Nucleotide sequences for the <i>Pou5f1</i> Real-Time PCR products of mMSCs	84
5.3	List of the 31 mMSC specific genes with their corresponding fold change as compared to osteoblasts	86
5.4	List of mMSC ageing genes with their relative expression in young and old <i>in vitro</i> cultured mMSCs	90
5.5	Effects of <i>in vitro</i> age and low and medium dose ionizing radiation on the expression profile of ageing genes in mMSCs (↔ no change in gene expression; ✓ gene expression is affected)	93
A.1	List of nutrient mixtures tested for <i>in vitro</i> culturing of mMSCs	141

Acknowledgments

At first I would like to thank Prof. Dr. Michael J. Atkinson for his guidance throughout the duration of the thesis. Without his support and advice this project would not have been successfully completed, I am very much grateful for his mentoring!

I want to extend my gratitude towards Dr. Michael Rosemann for believing in me and giving me an opportunity to perform my thesis in his group on such an interesting topic. I have learnt a lot under his supervision. I appreciate his ideas and the helpful discussions.

I am also thankful to my thesis committee members Prof. Dr. Peter Nelson and PD Dr. Natalia Pellegata. Their feedback contributed substantially to the progress of this project.

I would like to thank Dr. Sebastian Götz for his constant help. His scientific suggestions and advices were definitely useful for performing the experiments and for writing the thesis. I am grateful to Dr. Ines Höfig for her support with the MSC project. I also appreciate her efforts in our publication. In addition, I would like to thank all the past and present members of Rosemann group. All of them helped me throughout this learning process.

I thank Dr. Omid Azimzadeh for critically reading my thesis. His critics and encouragement helped with the writing of this thesis.

I thank all my colleagues at the Institute of Radiation Biology for giving me such a wonderful time and memories at ISB. Especially the lovely ladies, Ms. Solvejg Schröder and Ms. Silvia Köhn. Thank you very much for all your care! And for the fun time and laughs I want to thank the members of office 143.

I am obliged to Dr. Wolfgang Beisker for his assistance with the flow cytometry experiments. I am thankful also to PD Dr. Frauke Neff and Ms. Elenore Samson for their help with the bone marrow cryo section experiment.

I am pleased to thank MLST PhD program managing director Dr. Katrin Offe and co-coordinator Ms. Desislava Zlatanova for their support. I also thank DINI members and HELENA-RS2 people for the great time at the Helmholtz campus.

Finally and importantly, our handsome FVB/N mice and my beloved Mesenchymal Stem Cells, You deserve the credit for this project. It was of course not easy working with you. But I am glad that I got to work with you!!

And my family Aai-Pappa, Didi-Jiju, Dada-Bhabhi and the Pillus, nothing would have been possible without you. Thank you for always being there!!! माझ काम आणि हा प्रबंध तुम्हासगळ्यांसाठी.

Curriculum Vitae

Yashodhara Ingawale

Address: Richildenstrasse 8

80639 Munich, Germany

Nationality: Indian

Phone: +49 (0) 15163865216

Email: yashodhara.ingawale@yahoo.com

Educational Qualification

- 10/2012 – 09/2016 Doctoral studies Medical Life Sciences and Technology (MLST) program
TUM School of Medicine, Technical University Munich, Germany
Characterisation of murine mesenchymal stem cells during ageing and radiation exposure
- 09/2007 – 08/2011 MSc Medicinal and Industrial Pharmaceutical Sciences
Institute of Pharmaceutical Sciences, ETH Zurich, Switzerland
Main Subjects: Quality Management, Regulatory Affairs, Process and Project Management
- 08/2003 – 07/2006 BSc Biotechnology
Bangalore University, Bangalore, India
Main Subjects: Animal, Plant and Environmental Biotechnology, Genetics, Biochemistry

Work Experience

- 10/2012 – 01/2016 Institute of Radiation Biology, Helmholtz Center Munich, Germany
PhD Student
- Member of Helmholtz Graduate School of Environmental Health (HELENA)
 - Member of The Helmholtz Research School of Radiation Sciences (RS2)

Publication

Ines Hoefig*, **Yashodhara Ingawale***, Michael J Atkinson, Heidi Hertlein, Peter J Nelson, and Michael Rosemann. p53-Dependent Senescence in Mesenchymal Stem Cells under Chronic Normoxia Is Potentiated by Low-Dose γ -Irradiation. *Stem cells international*, 2016:6429853, 2016.

* Shared first authorship

Research Projects

- 07/2010 – 02/2011 Master thesis at the Hubrecht Institute, Utrecht, The Netherlands
Epigenetics: Detection of chromatin modification changes in Zebrafish embryos
- 11/2008 – 01/2009 Research project in the Institute of Pharmaceutical Sciences, ETH Zurich, Switzerland
Cancer Biology: Identification of miR-326 target genes

Language Proficiency

- English (fluent)
- Marathi (native speaker)
- Hindi (native speaker)
- German (intermediate)

Computer Proficiency

- Microsoft office: Word, Excel and PowerPoint
- Image processing software: ImageJ, Gimp, AxioVision
- Statistical Software: SPSS (basic)
- Document preparation system: LaTeX